INFORMATION TO USERS

This material was produced from a microfilm copy of the original document. While the most advanced technological means to photograph and reproduce this document have been used, the quality is heavily dependent upon the quality of the original submitted.

The following explanation of techniques is provided to help you understand markings or patterns which may appear on this reproduction.

1. The sign or "target" for pages apparently lacking from the document photographed is "Missing Page(s)". If it was possible to obtain the missing page(s) or section, they are spliced into the film along with adjacent pages. This may have necessitated cutting thru an image and duplicating adjacent pages to insure you complete continuity.

2. When an image on the film is obliterated with a large round black mark, it is an indication that the photographer suspected that the copy may have moved during exposure and thus cause a blurred image. You will find a good image of the page in the adjacent frame.

3. When a map, drawing or chart, etc., was part of the material being photographed the photographer followed a definite method in "sectioning" the material. It is customary to begin photoing at the upper left hand corner of a large sheet and to continue photoing from left to right in equal sections with a small overlap. If necessary, sectioning is continued again — beginning below the first row and continuing on until complete.

4. The majority of users indicate that the textual content is of greatest value, however, a somewhat higher quality reproduction could be made from "photographs" if essential to the understanding of the dissertation. Silver prints of "photographs" may be ordered at additional charge by writing the Order Department, giving the catalog number, title, author and specific pages you wish reproduced.

5. PLEASE NOTE: Some pages may have indistinct print. Filmed as received.

75-19,608

LEIBRECHT, Robert John, 1948-
AN URBAN AIRSHED MODEL FOR PREDICTING CARBON
MONOXIDE CONCENTRATIONS IN TUCSON, ARIZONA.

The University of Arizona, Ph.D., 1975
Engineering, mechanical

Xerox University Microfilms, Ann Arbor, Michigan 48106

AN URBAN AIRSHED MODEL FOR

PREDICTING CARBON MONOXIDE CONCENTRATIONS

IN TUCSON, ARIZONA

by

Robert John Leibrecht

A Dissertation Submitted to the Faculty of the

AEROSPACE AND MECHANICAL ENGINEERING DEPARTMENT

In Partial Fulfillment of the Requirements
For the Degree of

DOCTOR OF PHILOSOPHY
WITH A MAJOR IN MECHANICAL ENGINEERING

In the Graduate College

THE UNIVERSITY OF ARIZONA

1 9 7 5

THE UNIVERSITY OF ARIZONA

GRADUATE COLLEGE

I hereby recommend that this dissertation prepared under my

direction by _____ ROBERT JOHN LEIBRECHT _____.

entitled ___AN URBAN AIRSHED MODEL FOR PREDICTING CARBON MONOXIDE___

___CONCENTRATIONS IN TUCSON, ARIZONA_____

be accepted as fulfilling the dissertation requirement of the

degree of ___DOCTOR OF PHILOSOPHY_____

_____H. C. Perkins_____   ___March 31, 1975___
Dissertation Director   Date

After inspection of the final copy of the dissertation, the

following members of the Final Examination Committee concur in

its approval and recommend its acceptance:*

H C Perkins	3/31/75
R. B. Kinney	3/31/75
Thomas Cromwell	4-3-75
M. Coxon	4-4-75

*This approval and acceptance is contingent on the candidate's
adequate performance and defense of this dissertation at the
final oral examination. The inclusion of this sheet bound into
the library copy of the dissertation is evidence of satisfactory
performance at the final examination.

STATEMENT BY AUTHOR

This dissertation has been submitted in partial fulfillment of requirements for an advanced degree at The University of Arizona and is deposited in the University Library to be made available to borrowers under rules of the Library.

Brief quotations from this dissertation are allowable without special permission, provided that accurate acknowledgment of source is made. Requests for permission for extended quotation from or reproduction of this manuscript in whole or in part may be granted by the head of the major department or the Dean of the Graduate College when in his judgment the proposed use of the material is in the interests of scholarship. In all other instances, however, permission must be obtained from the author.

SIGNED: *Robert John Leibrecht*

DEDICATION

I dedicate this dissertation to my wife Julie and my parents. My wife was very understanding and patient during the writing and final preparation of this manuscript. The support of my parents for undergraduate training was quite instrumental in building my engineering foundation for graduate work at the University.

ACKNOWLEDGMENTS

TABLE OF CONTENTS

TABLE OF CONTENTS--Continued

LIST OF ILLUSTRATIONS

LIST OF ILLUSTRATIONS--<u>Continued</u>

Figure   Page

LIST OF TABLES

LIST OF TABLES--Continued

ABSTRACT

This study is an analysis of the carbon monoxide problem existing in Tucson, Arizona. The analysis includes the development of a multi-box model for predicting the levels of carbon monoxide to which the average population is exposed. The study also includes monitoring of carbon monoxide in areas of high traffic density. The results of this effort should help develop a data base for Tucson so that the Pima County Air Pollution Control District can initiate a locally based plan for controlling carbon monoxide.

The predictive model uses a fixed coordinate approach so that the Tucson airshed is divided into a grid of cells (boxes) each having a height equal to the mixing layer of the atmosphere. The conservation of mass principle is applied to each box in the grid accounting for the mechanisms of advection and diffusion, the sources of carbon monoxide, and the change of storage of mass all as functions of time. The chemical reaction mechanism is neglected since carbon monoxide is relatively inert. A set of algebraic equations are obtained when a finite difference approximation is applied to each derivative in the continuity equation. A Crank-Nicholson implicit technique is used to obtain the final form of the equations which are then solved numerically to obtain the carbon monoxide concentration in each box as a function of time. The mixing height, wind speed, wind direction, and source strength are the time dependent input parameters.

The multi-box model assumes that the predicted concentration for each box is the same at any height from the ground up to the height of the mixing height. A pseudo three dimensional dependency is obtained by assuming a logarithmic distribution for the concentration in the vertical direction so that a ground level concentration can be calculated for each box. These predicted ground level concentrations can be compared to ambient measurements of carbon monoxide taken throughout the Tucson basin. The ambient air levels are determined using a non-dispersive infrared analyzer.

The comparison between predicted results and measured data is good when the sampling location is in an area of low traffic density, i.e., residential area. In areas of high traffic density measurements of carbon monoxide show in general that the 1-hour average ambient standard is not being exceeded.

The multi-box model for the entire airshed predicts average concentrations for 4 square mile boxes. Since this macro-model distributes the sources of carbon monoxide uniformly over each box, the predicted levels can not represent measured data in areas of high traffic density. In order to predict levels in regions of moderate sources a single 4 square mile macro-box is subdivided into 64 smaller boxes. This micro-model accounts for the sources locally in each box, but still predicts levels for a finite size box. The grid refinement is limited by the multi-box assumption of homogeneous vertical mixing. However, the micro-model is able to predict concentrations in areas of higher source strength than the macro-model.

The models are useful in predicting area-wide increased levels due to large transient sources, i.e., stadiums and shopping centers. Of special interest is the model's availability for prediction of levels during possible episode periods and in regulating and controlling land-use in order to achieve and maintain the ambient air quality standards.

CHAPTER 1

INTRODUCTION

In passing the Clean Air Act of 1970 Congress established mechanisms for setting certain minimum standards for air quality, that would ensure clean air nationwide, and for enforcing and maintaining those standards. Following the instructions in the Act, national air quality standards were set using the best medical and technical evidence available at that time. The primary standards, to be met by mid-1975, were set at levels calculated to prevent any damage to human health from air pollution, including an adequate margin of safety. The secondary standards, to be met in a "reasonable time," were set to avoid any known effects of air pollution on public welfare. Decreased visability and plant damage are examples of such effects.

The Act instructed the States to prepare implementation plans due in January 1972 to meet those standards (Federal Register, April 1971a). It quickly became apparent that some States would need land-use and transportation controls in order to meet the carbon monoxide and photochemical oxidant standards in certain urban areas. The Environmental Protection Agency therefore gave these States until February 1973 to submit their plans and permitted an extension to mid-1977 for meeting the air quality standards involved (Federal Register, May 1972).

The National Resources Defense Council sued EPA on the grounds that the States should not be allowed either a longer time period to prepare their plans or an extension of the 1975 deadline for meeting the standards. So on January 31, 1973, the United States Court of Appeals for the District of Columbia Circuit ruled that EPA did not conform to the strict requirements of the Clean Air Act of 1970, and therefore, the Appeals Court established a new timetable for the plans (Federal Register, March 1973a). The States were required to submit the plans to EPA by April 15, 1973, whereafter EPA had until June 15, 1973, to either approve or disapprove. If disapproved, the deadline for EPA to promulgate substitute regulations was October 15, 1973. In the second major part of the ruling, the Appeals Court agreed with EPA that extensions could and should be given if control technology was not yet available (Federal Register, April 1973b).

Phoenix-Tucson Air Quality Control Region

A transportation control plan was required for the Phoenix-Tucson Intrastate Air Quality Control Region in order to attain the photochemical oxidant and carbon monoxide standards. This AQCR includes the five counties of Maricopa, Pima, Pinal, Gila, and Santa Cruz, encompassing some 29,753 square miles, 1.5 million people, and 800,000 motor vehicles. The State of Arizona submitted a control plan for the Phoenix-Tucson region on April 11, 1973 (Federal Register, April 1973b). The State plan for controlling photochemical oxidant was fully approved by EPA. However, the portion of the plan dealing with the control of carbon monoxide was disapproved because of (1) doubts that the proposed strategies would in fact

lead to the attainment of the standards and (2) the lack of interim and alternative measures required in order for an extension beyond mid-1975 to be granted (Federal Register, June 1973c).

The State plan (as related to carbon monoxide emissions) basically consisted of (1) increased air quality surveillance, (2) mandatory vehicle testing, inspection, and maintenance for all light duty vehicles, i.e., those less than 6000 pounds, (3) a retrofit of all pre-1975 light-duty vehicles with additional emission control devices, (4) conversion of the fuel systems of some 10,000 government vehicles to liquefied petroleum gas, and (5) a re-evaluation of the effects of these control strategies after one year based on extensive air quality monitoring conducted by the State, Maricopa County, and Pima County air pollution control agencies.

EPA Control Plan for Carbon Monoxide

After rejecting the portion of the Arizona Implementation Plan (Federal Register, June 1973c) for controlling carbon monoxide emissions, EPA was required under the Clean Air Act to propose substitute regulations. On July 7, 1973, EPA (Federal Register, July 1973d) proposed the following control strategies which would be used in addition to the strategies proposed in the State plan, and which would allow Arizona to qualify for the two-year extension:

1. 20% reduction in off-street publicly owned parking spaces.

2. Limitation on new privately owned parking spaces.

3. Formation of bus/carpool lanes for freeways and major streets.

4. Voluntary formation of employee carpools with use of a State operated computer.

5. Limitation of the total quantities of gasoline available at service stations.

6. Limited motorcycle registration.

The preceding control strategies were designed to make driving conditions so difficult for the commuter that he would voluntarily seek other means for getting to work. The EPA calculated that these controls would reduce the total vehicle miles traveled (VMT) by about 32%, compared to 1977 projections for VMT.

The EPA plan for the Phoenix-Tucson Air Quality Control Region was based on 1971 data obtained from only one point within the five-county region, that point being the Maricopa County Health Department site in Phoenix. The highest 8-hour average reading of carbon monoxide at this site was 31 milligrams per cubic meter, recorded on November 10, 1971. Comparing this with the national standard of 10 milligrams per cubic meter, for an 8-hour average, it was calculated that by 1977 a reduction of 44.5% would be required in the concentration of carbon monoxide in the air. A rollback model was used to determine the needed reduction in emissions to attain the national standards. The model calculates the maximum allowable emissions for carbon monoxide using the following expression:

$$\frac{\text{National CO Standard}}{\text{Second Highest Air Quality Level}} \times \frac{\text{Emissions in}}{\text{Base Year}} = \frac{\text{Maximum}}{\text{Allowable Emissions}}$$

A percent reduction in emissions can then be obtained using the maximum allowable emissions with the actual emission for the base year. The roll-back model uses the second highest air quality level since the national standard can be exceeded once a year. The excess emissions were to be reduced by a decrease in vehicle miles traveled. Assuming that only light duty vehicles are amenable to VMT reductions, it was determined that a 32% reduction in VMT would be required by 1977. According to EPA, the control strategies in their plan should provide the needed reduction.

Pima County Plan

On September 10, 1973, a public hearing on the EPA Transportation Control Plan for the Phoenix-Tucson Intrastate AQCR was held in Tucson (Federal Register, Oct. 1973e). At that time the general public had an opportunity to comment on the proposed regulations set forth by EPA. The Pima County Air Pollution Control District presented their proposal for meeting the national standards for carbon monoxide. In the plan, Pima County recommended being considered as a subregion separate from the other four counties in the Phoenix-Tucson Region. On September 12, 1973, the hearing moved to Phoenix after which the EPA studied the written comments and testimony presented at the public hearings before reaching a final decision on what control measures were to be promulgated.

On December 3, 1973, EPA finally accepted the Arizona Implementation Plan for controlling carbon monoxide and also gave the state a two-year extension to May 31, 1977, to meet the national air quality standard (Federal Register, Dec. 1973f). Tucson is to be included in the Phoenix-Tucson AQCR until the Pima County Health Department is able to obtain its

own data base to show a difference in the air quality between Tucson and Phoenix. A data base of at least one year is required before EPA will consider the possibility of Pima County being a subregion in the Phoenix-Tucson AQCR. However, the Pima County Health Department is optimistic that upon presentation of their own data base for Tucson, EPA will allow Pima County to become a subregion of its own in controlling carbon monoxide emissions. If and when this should occur the Pima County Plan would then become effective in the Tucson area for controlling carbon monoxide emissions.

In determining the control strategies needed for the Pima County Plan, several inputs were required. These included:

1. Approximately 3-1/2 months of carbon monoxide sampling near the intersection of 22nd Street and Craycroft, and 1-1/2 months of sampling in downtown Tucson at 151 West Congress, with traffic densities, wind speeds and direction measured simultaneously at both locations,

2. Use of the data obtained at the two locations for calibration of a mathematical model which was subsequently used, together with traffic densities, for calculating concentrations of carbon monoxide at locations of maximum traffic densities during "worst" winter-time meteorological conditions, and

3. An emission inventory of carbon monoxide from stationary and mobile sources for the entire County, using EPA approved

emission factors and calculation methods and the latest traffic data provided by the Pima Association of Governments Transportation Planning Agency.

These three items were presented in "Controlling Emissions of Carbon Monoxide within Pima County, Arizona," (1973) which was prepared by the Pima County Air Pollution Control District. It is not clear in the report how the mathematical model was calibrated as stated in item 2. The model used the standard Gaussian diffusion approach, treating an intersection as a line source as explained by Turner (1969). The model assumes the wind is blowing perpendicular to the street and directly towards the monitor. Further, a minimal wind speed is chosen to predict a worst case situation. The model predicts the pollutant concentration at only one location and neglects horizontal diffusion of the pollutant. This is only a good approximation when the convection is large, but during conditions of high winds the pollutant levels are usually low. Although the model is not too sophisticated it can be calibrated by varying the vertical diffusion coefficient until the calculated results match the data. The results from the model and data did show that a potential air pollution problem for carbon monoxide does exist within Pima County—particularly in the Tucson urban area. However, the problem is not necessarily the same as in Phoenix since Tucson has less than one-half the population of that city, is 1500 feet higher in altitude, and has 30% higher average wind speeds. The emissions, meteorology and land area involved are all different.

The Pima County Plan basically consists of implementation within Pima County of those portions of the State plan which were approved by the EPA, plus interim control strategies specifically for Pima County. These new proposals would replace for Pima County those interim controls proposed by the EPA for the entire Phoenix-Tucson Air Quality Control Region. The alternate strategies proposed by Pima County for the Tucson urban area consist of the following:

1. Increased voluntary use of carpools for work and school oriented commuters.

2. An improved and expanded bus system which would attract more work and school commuters as well as shoppers.

3. A computerized traffic system in the Tucson area which would decrease emissions through increased average traffic speeds.

4. A public education program to aid successful implementation of the strategies.

5. Continuous monitoring of air quality and progress made in attaining the objectives of the plan.

These control strategies would not be stringent enough to attain the national standard by 1975 if the standard is presently being exceeded. However, according to the Pima County Air Pollution Control District, the standard could be achieved in 1977 with only a 9% reduction in VMT, and the plan should yield a 20% reduction. The evidence presented in the plan shows how the national standards for carbon monoxide can be achieved

in Pima County by 1977 without economically and socially disruptive legis-
lation.

Objectives of the Present Study

During the several months in which the Pima County Air Pollution
Control District has monitored carbon monoxide (May to September, 1973) at
two locations in Tucson, the national ambient air quality standards have
not been exceeded. However, results from the use of an EPA-approved dif-
fusion model for calculating concentrations of carbon monoxide from a
line source during adverse winter-time meteorological and climatological
conditions indicate that the national standards may be exceeded in the
Tucson urban area during the periods between November and March, with the
most frequent excesses occurring during January.

From all of the above history it is clear that there is a need
for measuring levels of carbon monoxide at locations of suspected high
concentrations, particularly in the winter. There is also a need for a
more sophisticated predictive model for carbon monoxide. The model
should be able to predict levels throughout Tucson accounting for turbu-
lent diffusion and treating the case of low wind (near-calm) conditions.
This dissertation will be devoted to developing a more comprehensive
data base to account for the deficiencies in the data base used to develop
the Pima County Plan for controlling carbon monoxide emissions. This
data base will include:

1. Approximately six months of carbon monoxide sampling at vari-
   ous locations where concentrations are expected to be highest

along with data obtained from the Pima County Air Pollution

Control District at two locations within the city,

2. A predictive model for average concentrations of carbon monoxide throughout the Tucson urban area under any meteorological conditions,

3. An emission inventory of carbon monoxide from stationary and mobile sources for the Tucson area.

In order to analyze the carbon monoxide concentrations in Tucson, the urban area is divided into many boxes whose height, as a function of time, is equal to the mixing height in the atmosphere. The mass continuity equation is applied to each box. This equation accounts for convection and diffusion of the pollutant as well as the sources of carbon monoxide in each box. An emissions inventory is obtained so that the emissions of carbon monoxide due to mobile and stationary sources can be used as an input to the predictive model. A set of algebraic equations is obtained when a finite difference approximation is applied to each derivative in the mass continuity equation. These equations are solved numerically on the computer to obtain the carbon monoxide concentration in each box as a function of time. These numerical results are compared with data taken at several locations in Tucson. The data are obtained with a non-dispersive infrared analyzer.

The predictive model can be used as an important aid in urban and regional planning if the model's validity can be shown. This model can:

(1) simulate the effects of alternate air pollution control strategies on pollutant concentrations in the airshed,

(2) plan for land use so that projected freeways and indus-

trial sites may be located where their air pollution poten-

tial is minimized,

(3) determine the long-term air pollution control strategy

which accomplishes desired air quality objectives at least

cost, and

(4) make real-time predictions so that an impending air pol-

lution episode may be anticipated and proper preventive

action taken.

Health Effects of Carbon Monoxide

Carbon monoxide is relatively inert and, therefore, is a good

tracer gas to use for verification of the predictive model. EPA is

concerned about carbon monoxide because in moderate concentrations it can

have serious health effects. An important health property of carbon

monoxide stems from its reversible reaction with hemoglobin to form car-

boxyhemoglobin. The carboxyhemoglobin level is dependent on the carbon

monoxide (CO) concentration in the air, the duration of exposure, and the

level of physical and metabolic activity. An 8-hour CO concentration of

$10mg/m^3$ (9ppm) will result in a 1.3 to 1.4 percent carboxyhemoglobin

level and a 1-hour CO concentration of $40mg/m^3$ (35 ppm) will result in a

carboxyhemoglobin level of from 1.3 to 2.9 percent depending on the level

of activity. These two CO concentration levels are those adopted as the

national primary ambient air quality standards.

Recent studies (Dinman, 1968; Cohen, Deane, and Goldsmith, 1969;

"Effects of Chronic Exposure ...," 1969) indicate a significant proportion

of the population, those with coronary artery disease, are extremely sus-
ceptible to the effects of carbon monoxide. Increases in average car-
boxyhemoglobin levels from a background of 1.3 percent to a level of 2.9
percent have been shown to produce significant electrocardiographic changes
and increased severity of angina pain for subjects engaged in very mild
physical activity. A study in Los Angeles (Hexter and Goldsmith, 1971) has
generally confirmed these results by demonstrating that men with heart
disease, exposed to levels of carbon monoxide found in freeway traffic,
experienced decreased exercise tolerance and shortened time before the
development of angina pain while exercising. In addition, exposure to
carbon monoxide resulting in carboxyhemoglobin levels of 2 percent has
been shown to have effects upon the ability to discriminate time inter-
vals between auditory signals (Beard and Wertheim, 1967). Accordingly,
the current standards afford a relatively small margin of safety for
individuals with heart disease, some of whom are adversely affected at
equilibrium carboxyhemoglobin levels of 3 percent.

Summary of Content

Since there is a small margin of safety in the national stan-
dard for the air quality of carbon monoxide, the present work is of
importance in determining the extent to which the residents of Tucson
could be susceptible to the health effects related to carbon monoxide
exposure. This is of importance for Tucson since there are many elderly
retired people living here with some type of heart problem.

The dissertation contains in Chapter 2 a review of previous
models in an attempt to find an accurate but not overly complicated model

to be applied to the Tucson area. A mathematical analysis of the physics involved in the predictive model is the subject of Chapter 3. An emission inventory for carbon monoxide which is an input for the airshed model is contained in Chapter 4. Chapter 5 presents the numerical model along with the procedures to obtain the solution. The numerical results are in Chapter 6, while the experimental data are presented in Chapter 7. Chapter 8 discusses the comparison between the numerical and experimental results. The conclusions obtained from the study on carbon monoxide in Tucson are discussed in Chapter 9 along with some recommendations for future work.

CHAPTER 2

SURVEY OF PREVIOUS DIFFUSION MODELS

Since it is impossible to measure the carbon monoxide levels at

every location in a large urban area, it is necessary to have a model

to predict the approximate levels that might be expected at any time.

The model does not necessarily have to predict the maximum levels

obtained since these values can be measured in the areas of largest

source strength, i.e., highest traffic density. Such a model would be

of importance both in predicting the levels of carbon monoxide under

adverse meteorological conditions and for land-use planning.

Several types of models are used to describe the dispersion of

atmospheric contaminants. Among these are the box, plume, and puff

models. They differ in the way that the mechanisms of dispersion are

treated. A model represents mathematically the atmospheric convection,

dispersion, and chemical reaction processes which occur. For the prob-

lem of predicting carbon monoxide concentrations, the chemical reaction

mechanism can be neglected since carbon monoxide is relatively inert in

the atmosphere.

Box Model

The simplest type of model is the so-called box model. Within

the box the pollutant concentrations are assumed to be homogeneous. The

vertical dimension of the box is the height of the mixing layer of the

atmosphere. The box model assumes that the emitted pollutants are instantaneously and uniformly mixed, and the transport mechanism is characterized by a uniform wind. This idea was applied by Reiquam (1970, 1971). An airshed was divided into a two dimensional network of interconnected boxes or well-mixed cells. The cell volume and wind were allowed to vary with time. Reiquam used this model to estimate monthly average pollutant concentrations for the Willamette Valley of Western Oregon. In addition, the model was evaluated in a modified form in a small Norwegian valley in which a single point source was present.

Gaussian Plume and Puff Models

The Gaussian plume and puff models characterize the next level of complexity. These models describe the concentration distribution of a species downwind of a point, line or area source. The Gaussian (binormal) distribution is assumed for the concentration of the pollutant in the vertical and cross-wind directions about the plume centerline downwind from the source. In the usual applications of these models, the wind shear is neglected. A sink term can be included. The measures of plume and puff spread are based on experimental studies, are independent of the height, and are a function of atmospheric stability class.

The Gaussian model was applied by Frenkiel (1956), who is considered to be a pioneer in mathematical modeling of urban air pollution, for his analysis of atmospheric pollution in the Los Angeles basin. The effluent from a number of large area sources was assumed to emanate from a point at the center of each source. The effluent emitted from the continuous point source during an hour was treated as a single puff. The

elementary Gaussian diffusion model was used superimposing the concentration arising from each point source. Estimates were made of the diurnal variation of the pollutant concentrations at various locations in the Los Angeles basin.

In 1959, Neiburger developed a model accounting for the meteorological influences of light winds and thermal inversions in Los Angeles. The Gaussian diffusion model was used, but the pollutants in the area source could only diffuse up to an impenetrable inversion lid. Further, the pollutants were assumed to disperse instantaneously and uniformly all the way up to the inversion lid. Horizontal spread was limited to that caused by the advective transport of the mean wind since horizontal turbulent diffusion was neglected. The model was applicable only for predicting average concentrations for large regions.

Following these early studies a series of simple urban air pollution models were described in papers by Leavitt (1960), Pooler (1961), Clarke (1964), Turner (1964), Miller and Holzworth (1967), and Koogler et al. (1967). These studies have much in common. They each approach the urban area-source concentration problem by way of the usual Gaussian point source diffusion model. Differences occur only in the details of how the area source summation is carried out and in how various meteorological parameters are included.

In the study by Miller and Holzworth (1967), a more realistic approach to the treatment of diffusion in the mixing layer was considered than had been done by Neiburger (1959). The model assumed that vertical diffusion followed the Gaussian distribution in the mixing layer until the plume intersected the inversion lid, whereas Neiburger assumed

immediate vertical mixing and uniform distribution in the mixing layer.
The Miller and Holzworth model also assumed that the sources emit contin-
uously at the surface and are uniformly distributed over the urban area.
The model is limited to estimating mean concentrations for an entire
urban area and cannot predict pollutant concentrations on a small scale.

A group at the Travelers Research Center developed a receptor-
oriented mesoscale air pollution model for the State of Connecticut.
This study was published by Bowne (1969). The model used a grid of 5600
area cells having multiple sources in each cell. The mean ground level
concentration averaged over a 2-hour interval was predicted for each grid
area.

The TRC model determines the pollutant concentration within the
volume of air over a given grid square at a given time by following the
volume backward in time along its trajectory. The amount of material
injected into the volume by the sources that can contribute along the
trajectory is then computed. This computation is made by using the emis-
sion rate of the source during the time period that the volume of air was
over that source. The large-scale wind fields which determine the trajec-
tories are analytically represented by stream functions. As the pollu-
tants move along their trajectories, diffusion from each area or point
source was represented by the binormal distribution. However, within
each volume the concentrations were assumed to be uniform; this assump-
tion is consistent with the spatial resolution of the model. The stan-
dard deviations used in the model were empirical values based upon the
atmospheric stability and the travel distance for the appropriate trajec-
tory from a contributing source to the area of interest. The loss of

a pollutant due to reaction or deposition was accounted for by a simple exponential decay term. The model was first reported on by Hilst (1967). The model was extensively validated in the study by Hilst (1970).

Argonne National Laboratory (ANL) began developing a computerized, transient, urban air pollution dispersion model in 1968. The model was developed for operational use in an air resources management system and has been reported in various stages of evolution by Croke et al. (1968) and Croke and Roberts (1971). The report was completed in February 1971. Meteorological parameters used in the model are varied at hourly intervals so this is the time interval used in averaging the predicted concentrations of pollutants.

The model accounts for the diffusion and convective transport mechanisms by considering individual puffs of effluent instead of plumes. The puff results from an instantaneous release of a discrete amount of effluent from point or area sources. The puffs are assumed to diffuse with a Gaussian distribution and the standard deviations for each of the three directions of diffusion were obtained from two sources of empirical curves; these were the Pasquill-Gifford curves in Turner (1969) and the Turner curves in Roberts, Croke, and Kennedy (1970). The transport of the puffs is obtained from the piecewise - constant hourly wind vectors. The Gaussian puff formula is treated as a mathematical kernel. The concentration resulting from a continuous-source plume is then obtained by integrating the puff result over time with a convolution integral. Since all puff formulas must be integrated over time for continuous pollutant sources, this type of dispersion model is often referred to as an "integrated puff" model.

The integrated puff model has the advantage of being able to evaluate the effect of a sub-area source on locations within the area as well as external to the area. The model is capable of simulating near-zero wind speed conditions. The model was applied to Chicago where a large data base was available for validation studies. The Chicago tele-metered air-monitoring network has collected over three years of data consisting of 15 minute averages from eight stations for SO_2 concentrations, wind speed, and wind direction. The model as applied to Chicago is presented in Proceeding of the Second International Clean Air Congress by Roberts et al. (1971).

A mathematical diffusion model was developed at New York University (NYU) only a few months before Argonne National Laboratory started their work using a very similar approach. The NYU model was a very sophisticated source-oriented model based upon the three-dimensional Gaussian puff diffusion assumption with piecewise-constant input quantities in time and required a digital computer for solution. The NYU model was less general than ANL model since the standard deviations of the diffusing Gaussian puffs were obtained using empirical formulas whose parameters were evaluated using New York City data, whereas the ANL model employed the widely used empirical curves. The NYU model was presented at the Symposium on Multiple-Source Urban Diffusion Models by Shieh, Davidson, and Friend (1970).

Model Using Numerical Solution of Mass
Continuity Equation

The models thus far discussed have employed either a homogeneous or a Gaussian distribution for the pollutant in the three directions of dispersion. These models can treat only non-reacting species and usually cannot account for variations in meteorological parameters. The models are steady state or at most quasi-steady state solutions for pollutant concentrations. The limitations of these models can be partially removed by use of a dynamical model involving the solution of the partial differential equation for the conservation of mass. This approach permits the inclusion of chemical reactions, time-varying meteorological conditions, and complex source emission patterns. The solution can simulate the concentrations in time throughout a computational grid representing the urban area.

The mass conservation equation can be solved using either a moving cell or fixed coordinate approach as pointed out by Seinfeld, Reynolds, and Roth (1972). In the moving cell model a hypothetical column of air is followed through the airshed as it is advected by the wind. The air column may or may not be well mixed vertically. The pollutants are injected at the base of the column, and chemical reactions can take place within the column. In the fixed coordinate model the airshed is divided into a three dimensional grid of stacked cells. A set of coupled equations is solved numerically after applying the mass continuity equation to each cell. From a fluid mechanical standpoint the moving cell approach is Lagrangian while the fixed coordinate approach is Eulerian.

In the moving cell model the concentration changes in the hypothetical parcel of air are computed as the parcel traverses the airshed. The model assumes no horizontal transport of material across the boundaries of the air column, no horizontal wind change with height, and neglects vertical advection. Additionally, the parcel of air is assumed to maintain its integrity while traversing the airshed.

The moving cell technique is used basically for computing concentration histories along a given air trajectory. Eschenroeder and Martinez (1972) used this approach assuming a nonuniform distribution for the concentration of pollutants in the vertical direction. Their model accounted for chemical reactions due to the interaction of the pollutants in the air. They showed that the histories of reactive hydrocarbons, oxides of nitrogen, and ozone were consistent with the variations observed at air monitoring stations in the Los Angeles basin. The moving cell approach was also employed by Wayne et al. (1971) for the Los Angeles basin. In their model the column of air was assumed to be mixed homogeneously so the equations to be solved reduced to a set of ordinary differential equations. The moving cell approach is not feasible for use as an airshed model since a large number of trajectory calculations would be required to predict concentrations as a function of time and location throughout the airshed.

In the fixed coordinate approach a set of N equations is solved numerically with time to obtain the pollutant concentration for each cell in the airshed grid. The numerical solution can be obtained by the conventional finite difference method, the particle in cell (PIC) method, or the variational method. The variational method involves assuming the form

of the concentration distribution which usually is an expansion of known functions, and then evaluating the coefficients in the expansion. As pointed out by Seinfeld et al. (1972), this is a relatively new method for solving the three dimensional time-dependent partial differential equation for conservation of mass.

The particle in cell (PIC) technique treats the continuous concentration field as a collection of mass points or particles, each representing a given amount of pollutant and each located at the center of mass of the volume it represents. The mass particles are moved by advection and diffusion. The particles are located within a fixed three dimensional grid according to the mass distribution of the material. During a time step in the numerical solution, the particles move a distance equal to the product of the mean wind and the time step. New particles are emitted during the time step from the sources in each cell, and then the particles in each cell are allowed to react chemically. At the end of the time step the average concentration in each cell is determined by totalling the mass of particles occupying the cell and then dividing by the cell volume. This procedure is continued to get the concentrations in each cell as a function of time. The PIC technique has been applied by Sklarew, Fabrick, and Prager (1972) to model air pollution in Los Angeles.

The most common method for solution of the set of continuity equations, obtained from the airshed grid for the fixed coordinate model, is the finite difference technique. The finite difference approximation transforms the partial differential equations into a set of algebraic equations which are then solved to give the pollutant

concentration in each cell. This method is repeated for subsequent time steps to obtain the distribution of the pollutant concentration with time in the airshed. The finite difference technique has been widely used.

Mahoney and Egan (1971) employ this approach in developing a mesoscale air pollution model. They developed a model to investigate the effects of short term changes in emission strengths and meteorological parameters. Their model is based on the solution to an advective-diffusion equation representing the transport and dispersion of one or more pollutants. A two-dimensional "driven" approach is assumed. The calculated concentrations are considered to be "driven" or forced by the external parameters. The distribution of the pertinent meteorological parameters is considered to be imposed externally, with known values, and the pollutant source distribution is also assumed to be known.

In the two-dimensional model the vertical advection term is neglected in comparison to the horizontal advection, and the horizontal diffusion is neglected in comparison to the vertical diffusion. The solution is obtained using a finite difference formulation employing a "lock" method. By the "lock" method is meant that the material (pollutant) is retained in a single grid cell for several time steps, until the pollutant has had sufficient time to traverse the entire width of the grid cell due to advection, and then the material is entirely transported into the next cell. The impulsive error due to this method is overcome by averaging the concentration distributions over a few sequential time steps.

Another air pollution model using a finite difference approach to the solution of the mass continuity equation was developed for the San

Francisco Bay area by MacCracken et al. (1972). The model uses the simple box approach where the cells are considered as well-mixed. The pollutants in each box are assumed to be homogeneously mixed up to the top of the box, which is the mixing height of the atmosphere. The conservation of mass equation is applied to a chemically conservative pollutant in each box of the airshed. This reduces the problem to solving a set of two-dimensional time dependent partial differential equations. A finite difference approximation is then applied to the spatial derivatives, and the equations are transformed to ordinary differential equations where time is in the independent variable. The set of ordinary differential equations is solved using a relatively new mathematical method developed at Lawrence Livermore Laboratory.

The MacCracken model predicts concentrations of carbon monoxide (CO) for the airshed of the San Francisco Bay area as a function of time. The results of the numerical solution give only an average concentration for each box. A logarithmic distribution is assumed for the concentration of CO in the vertical direction so a ground level value for CO can be calculated. From sparse meteorological data for the complicated topographical region time-varying inversion heights and horizontal wind fields are determined for use in the airshed model. An extensive emission inventory for CO was obtained for inputting time and spatially varying pollutant sources. The observed and calculation CO concentrations for a 1-hour average seem to agree fairly well.

Tucson Model

The models discussed have developed to a rather sophisticated level of complexity. The simplest model assumed the pollutant distribution was uniform. The next level yielded the concentration according to the Gaussian distribution which is a specialized solution of the transient diffusion equation. The most fundamental model involves a numerical solution of the time dependent mass continuity equation. The latter approach is needed in order to simulate time varying concentrations as for the Tucson airshed.

In the model to be developed here, the Tucson airshed is divided into a network of interconnected boxes each with a square base and a height equal to the mixing layer in the atmosphere. The model treats carbon monoxide which is relatively inert and assumes the pollutant is homogeneously mixed in each box. This assumption reduces the problem to solving the two dimensional time dependent mass conservation equation. This is similar to the approach employed in the Lawrence Livermore Laboratory (LLL) – MacCracken model. The differences arise in the method used to perform the numerical analysis. The mass continuity equation is applied to each box in the grid. A finite difference approximation is applied to each derivative in the equation leaving a set of algebraic equations to be solved. The LLL model applies the finite difference approximation to the spatial derivatives only and instead obtains a set of time dependent ordinary differential equations for solution. The resulting solution in either case gives the average concentration of carbon monoxide in each box as a function of time. A ground level

concentration for each box can be calculated assuming some distribution for the pollutant in the vertical distribution. The "driven" approach is incorporated into the Tucson model, that is, the meteorological parameters are externally put into the model. The mathematical analysis in developing the physics of the pollutant dispersion is presented in the next chapter.

CHAPTER 3

ANALYSIS

In developing the urban airshed model, a mathematical representation for the unsteady motion of the air pollutant concentration is required. In the atmosphere the air pollutant is transported both by the mean motion of the wind and by turbulent and molecular diffusion towards areas where its concentration is small. The pollutant is emitted by stationary and mobile sources and may be produced by chemical reactions.

Basic Governing Equation

The conservation of mass principle is used to obtain the basic partial differential equation governing the time evolution of the air pollutant concentration. The mass conservation equation for $C_a(x,y,z,t)$, the concentration of pollutant a, is written as

$$\frac{\partial C_a}{\partial t} + u \frac{\partial C_a}{\partial x} + v \frac{\partial C_a}{\partial y} + w \frac{\partial C_a}{\partial z} = \frac{\partial}{\partial x} (K_x \frac{\partial C_a}{\partial x}) \qquad (3.1)$$

$$+ \frac{\partial}{\partial y} (K_y \frac{\partial C_a}{\partial y}) + \frac{\partial}{\partial z} (K_z \frac{\partial C_a}{\partial z}) + S_a(x,y,z,t)$$

$$+ P_a(C_a, C_b, \ldots, C_n, t)$$

where u, v, and w are the three velocity components which are functions of x, y, z, and t; K_x, K_y, and K_z are the three eddy diffusion coefficients and can be a function of x, y, z, and t. $S_a(x,y,z,t)$ is the

source field for pollutant a . $P_a(C_a, C_b, \ldots, C_n, t)$ is the chemical reaction expression for pollutant a . S_a and P_a both have units of $gm/hour-m^3$.

Numerous assumptions are involved in obtaining equation (3.1). Most importantly, the continuity equation is uncoupled from the equations of momentum and energy. This is done by assuming that the presence of pollutants in the atmosphere do not cause variations to occur in temperature and velocity. The molecular diffusion is negligible in comparison to the turbulent diffusion. Another assumption is that the atmospheric flow approximates that of an incompressible fluid. Since the wind velocities and concentrations are fluctuating variables, their magnitudes are treated as mean values averaged over a certain time interval which is small compared to the time scale for pollutant source which is measured in hours. And finally, it is assumed that the turbulent fluxes are linearly related to the gradients in the mean concentration.

The solution of equation (3.1) gives the mean concentration of the air pollutant a as a function of time at any point (x,y,z). A source emissions inventory and pertinent meteorological data are needed as inputs to the equation. The magnitudes of the turbulent eddy diffusivities and any chemical reaction mechanism are also needed before the solution of (3.1) can be obtained. The general differential equation is very difficult to solve, and to date, some simplifications have been needed to achieve a workable model.

Fixed Coordinate Approach

A basic and extremely simplified approach to solving (3.1) is to
apply the equation to a chemically conservative pollutant in a single
large box so that spatial variations in the terms can be ignored. This
approach was employed by Smith (1961) and a two part solution is obtained
for the pollutant concentration. There is an unsteady term based on an
exponential decay of the initial concentration. A corresponding steady
state term is included where the concentration is equal to S/HLU. This
assumes a zero background concentration. S is the source strength, H is
the height of the box, and L is the width perpendicular to the uniform
wind velocity U. The use of this approach has been mainly limited to
calculations of spatial and long term temporal averages and is completely
inadequate for air pollution episodes and for calculating local air pol-
lution concentrations.

A more sophisticated fixed coordinate approach, to account for
local conditions, is to divide the urban area into a grid of square boxes
with a base area of L^2 and a height H. The height H can represent the
vertical extent of the mixing layer of the atmosphere. This approach is
used by MacCracken et al. (1972). There the pollutant treated was inert
and assumed to be homogeneously and uniformly mixed in each box. This
approach is sometimes referred to as a multi-box model. This idea of the
multiple box model can be envisioned in Fig. 3.1.

Using the box structure with the idea that the pollutant in each
box is homogeneously mixed to the top of the box, i.e., through the mixing
layer, the z dependence can be eliminated from (3.1). The mass conserva-
tion for an inert pollutant using the multi-box approach becomes

MASS TRANSFER BETWEEN BOXES
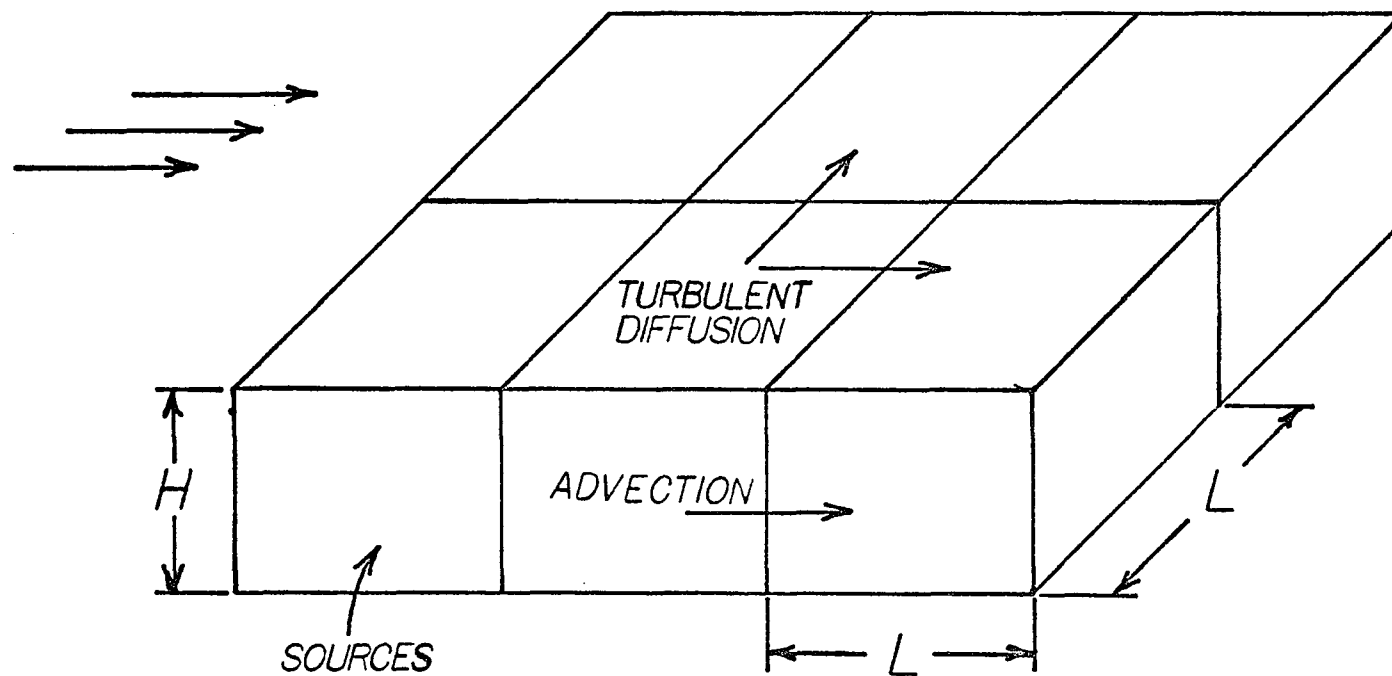
Fig. 3.1 Conceptual Picture of Multi-box Model

$$\frac{\partial C}{\partial t} + u \frac{\partial C}{\partial x} + v \frac{\partial C}{\partial y} =$$

$$\frac{\partial}{\partial x} (K_x \frac{\partial C}{\partial x}) + \frac{\partial}{\partial y} (K_y \frac{\partial C}{\partial y}) + \frac{S(x,y,t)}{V} \qquad (3.2)$$

C is the concentration for an inert species, u and v are the two mean horizontal velocity components which will be a function of time only. S(x,y,t) is the source field, and V is the volume of each box so that $V = L^2 H$.

If in addition we assume that the horizontal turbulent diffusivities are a constant and equal in both the x and y directions, such that $K_x = K_y = K_H$, equation (3.2) reduces to

$$\frac{\partial C}{\partial t} + u \frac{\partial C}{\partial x} + v \frac{\partial C}{\partial y} =$$

$$K_H (\frac{\partial^2 C}{\partial x^2} + \frac{\partial^2 C}{\partial y^2}) + \frac{S(x,y,t)}{V} \qquad (3.3)$$

The idea of treating each box as a well mixed cell reduces the mass conservation equation from a three dimensional time dependent problem to a two dimensional time dependent problem. The solution of (3.3) can be obtained by applying a finite difference approximation to each derivative in the equation. By externally inputting the velocity components along with the horizontal eddy diffusivity and source field, the concentration of an inert species can be calculated as a function of time at any location (x,y). At that location (x,y) the calculated concentration is by assumption the same for any height z from the ground up to the top of the mixing layer H. Since the concentration is not really

uniform in the vertical direction, a distribution for the concentration in the z direction is needed so that an actual ground level concentration can be determined. This will be discussed later in the chapter. An initial condition is needed at zero time and four boundary conditions are required in order to obtain the solution to (3.3). These conditions will also be presented in the latter part of this chapter.

Mass Balance

The concentration of the air pollutant can be obtained by finite differencing equation (3.3) and applying the results to each box. A more basic approach is to apply the conservation of mass principle to each box, that is, a mass (concentration) balance is made on each control volume. Each control volume is centered about a node (i,j) in space with its neighboring nodes. This idea is visualized in Fig. 3.2. Each control volume represents a box of volume L^2H. Note that each control volume has only four adjacent nodes since this problem has been reduced to two spatial dimensions using the multi-box approach. The node point value of the concentration C is the average over the control volume.

Using the control volume approach, the conservation of mass principle can be written as

$$\begin{matrix} \text{INCREASE IN} \\ \text{STORAGE} \\ \text{OF MASS} \end{matrix} = \begin{matrix} \text{INFLOW} \\ \text{OF} \\ \text{MASS} \end{matrix} - \begin{matrix} \text{OUTFLOW} \\ \text{OF} \\ \text{MASS} \end{matrix} \qquad (3.4)$$

The mechanisms for inflow and outflow of mass are advection and diffusion. The advection is the transport due to the wind velocity U which has components u and v in the x and y directions, respectively. The pollutant
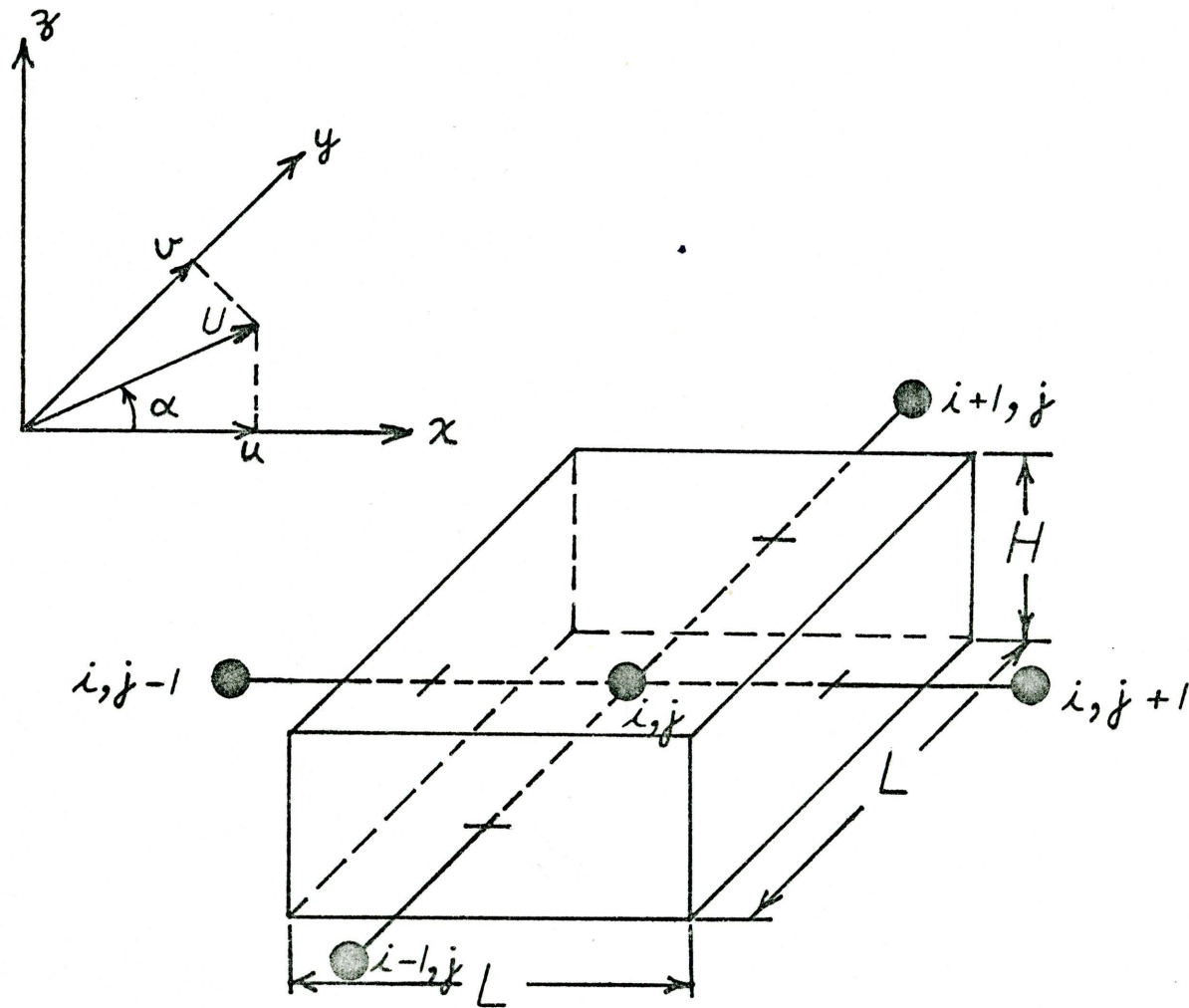
Fig. 3.2 Control Volume for Node (i,j)

sources emitted from the surface can also account for an inflow. The mass balance is written for the control volume for a time interval Δt and all terms are evaluated at $t+\Delta t/2$. This gives an average between the previous time t and the new time $t+\Delta t$. This approach is called the Crank-Nicholson method (Carson and Emery, 1969).

The increase of storage of mass at node (i,j) is

$$\frac{\partial C}{\partial t}\bigg|_{i,j}^{t+\Delta t/2} (L^2 H)$$

The inflow of mass due to advection in the x and y direction is

$$[u(C_{i,j-1})^{t+\Delta t/2} + v(C_{i-1,j})^{t+\Delta t/2}] \ (LH)$$

Likewise, the outflow advection from the control volume is

$$[u(C_{i,j})^{t+\Delta t/2} + v(C_{i,j})^{t+\Delta t/2}] \ (LH)$$

In writing the advection terms, the u and v velocity components are taken as constant for the time step Δt and also are assumed to not vary spatially throughout the grid. In the advection terms the concentration C advected into the node is not the value at the boundary, but the value of C at the upwind node. In the outflow by advection, the value of C at the node (i,j) is transported to the adjacent downwind nodes. This approach gives the same results as would be obtained by treating the convection terms in equation (3.3) using an upwind finite difference (i.e., backward difference).

To calculate the flow of mass due to diffusion, a diffusion rate law is needed. The simplest diffusion law is the linear law that says the diffusion flux rate of C, which is called $\dot{m}$, is proportional to the gradient of the concentration C(i.e., Fick's law).

$$\dot{m} = - K \frac{\partial C}{\partial x}$$

The minus sign indicates that a C which increases in x causes diffusion in the negative x direction. K is the turbulent eddy diffusion coefficient with molecular diffusion neglected.

The inflow of mass due to diffusion in the x and y direction is

$$[-K_H \frac{\partial C}{\partial x} \Big|_{i,j-\frac{1}{2}}^{t+\Delta t/2} - K_H \frac{\partial C}{\partial y} \Big|_{i-\frac{1}{2},j}^{t+\frac{\Delta t}{2}}] \; (LH)$$

Similarly, the outflow of mass due to the diffusion from the node (i,j) is

$$[-K_H \frac{\partial C}{\partial x} \Big|_{i,j+\frac{1}{2}}^{t+\frac{\Delta t}{2}} - K_H \frac{\partial C}{\partial y} \Big|_{i+\frac{1}{2},j}^{t+\Delta t/2}] \; (LH)$$

In obtaining the diffusion terms the gradients of C are evaluated at the boundaries between the nodes. K_H is the horizontal eddy diffusion coefficient.

The inflow of mass due to the pollutant sources at the surface is $S_{i,j}$. This is the mass per unit time obtained by summing all the sources emitted from a surface of area L^2 for the node (i,j). The information needed to obtain S for each box will be presented in

Chapter 4. That chapter deals with determining the emissions inventory for carbon monoxide from all sources.

Using the above expressions in equation (3.4), the relation for the conservation of mass for the control volume becomes

$$\frac{\partial C}{\partial t}\bigg|_{i,j}^{t+\Delta t/2} (L^2 H) = u(C_{i,j-1} - C_{i,j})^{t+\Delta t/2} (LH)$$

$$+ v(C_{i-1,j} - C_{i,j})^{t+\frac{\Delta t}{2}} (LH) \tag{3.5}$$

$$+ K_H \left(\frac{\partial C}{\partial x}\bigg|_{i,j+\frac{1}{2}}^{t+\Delta t/2} - \frac{\partial C}{\partial x}\bigg|_{i,j-\frac{1}{2}}^{t+\Delta t/2}\right) (LH)$$

$$+ K_H \left(\frac{\partial C}{\partial y}\bigg|_{i+\frac{1}{2},j}^{t+\Delta t/2} - \frac{\partial C}{\partial y}\bigg|_{i-\frac{1}{2},j}^{t+\frac{\Delta t}{2}}\right) (LH) + S_{i,j}$$

A Taylor series expansion can be used to approximate the partial derivative terms remaining in equation (3.5). The mathematics of this analysis is carried out in Appendix A and the results are presented here.

$$\frac{\partial C}{\partial t}\bigg|_{i,j}^{t+\Delta t/2} = \frac{C_{i,j}^{t+\Delta t} - C_{i,j}^{t}}{\Delta t}$$

and

$$\frac{\partial C}{\partial x}\bigg|_{i,j+\frac{1}{2}}^{t+\frac{\Delta t}{2}} = \frac{(C_{i,j+1} - C_{i,j})^{t+\frac{\Delta t}{2}}}{L}$$

The other three remaining spatial derivative approximations are similar to the latter equation above. These above results have the same form as a forward finite difference (Roache, 1972). The concentration C at each

node is evaluated at t+(Δt/2) so an approximation must be made in order to integrate and obtain a value for C at the end of the time step Δt. A Crank-Nicholson approximation is used as discussed in a paper by Carson and Emery (1969). The assumption involves a simple averaging which gives

$$C_{i,j}^{t+\Delta t/2} = \frac{1}{2} (C_{i,j}^t + C_{i,j}^{t+\Delta t}) \tag{3.6}$$

The concentration at the mid-time step is the average of C at the previous time t and the new time t+Δt. Using equation (3.6) along with the approximations for the partial derivatives in equation (3.5), a final expression is obtained.

$$C_{i,j}^{t+\Delta t} (\frac{1}{\theta} + 8\beta + 2\cos\alpha + 2\sin\alpha)$$

$$- C_{i,j-1}^{t+\Delta t} (2\beta + 2\cos\alpha) - C_{i-1,j}^{t+\Delta t}(2\beta + 2\sin\alpha)$$

$$- C_{i,j+1}^{t+\Delta t} (2\beta) - C_{i+1,j}^{t+\Delta t} (2\beta)$$

$$= C_{i,j}^t (\frac{1}{\theta} - 8\beta - 2\cos\alpha - 2\sin\alpha)$$

$$+ C_{i,j-1}^t (2\beta + 2\cos\alpha) + C_{i-1,j}^t (2\beta + 2\sin\alpha) \tag{3.7}$$

$$+ C_{i,j+1}^t (2\beta) + C_{i+1,j}^t (2\beta) + 4C_{SS,ij}$$

The algebra involved to obtain (3.7) is presented in detail in Appendix A. Equation (3.7) relates the concentrations at the new time t+Δt to

their value at the previous time t. The terms in parentheses are all non-dimensional.

A non-dimensional time θ is defined which relates the wind speed U to the numerical time step Δt and the width of the square box L. The parameter is given by

$$\theta = \frac{U\Delta t}{4L} \tag{3.8}$$

The criterion used in determining the magnitude of θ will be discussed in Chapter 5. The number 4 is added only to simplify the final form of equation (3.7). Another non-dimensional parameter is defined which gives the order of magnitude relationship between the advection and diffusion mechanisms involved in the problem. This relation is given by

$$\beta = \frac{V_D}{U} \tag{3.9}$$

where

$$V_D = \frac{K_H}{L} \tag{3.10}$$

V_D is defined as the diffusion velocity and is equal to the eddy diffusivity divided by the width of the box L. The parameter β usually has a magnitude less than one for the simulation of atmospheric motion.

The wind velocity U can be divided into two components which are parallel to the x and y directions. The angle α is defined such that the wind velocity U is parallel to the x direction when $\alpha = 0^o$. The value of α is positive counterclockwise as can be seen from Fig. 3.2. The velocity components are then defined as

$$u = U \cos\alpha$$
$$\text{and}$$
$$v = U \sin\alpha$$

where u and v are the components in the x and y directions, respec-

tively.

A final term to be defined in equation (3.7) is $C_{SS,ij}$. This is

the steady state concentration of a control volume centered at node

(i,j) having a source strength S under the assumption that the control

volumes surrounding (i,j) all have a zero concentration. The horizontal

diffusion is also neglected in obtaining the result. The control volume

has a height H, and L is the width of the square base of the control

volume having a uniform wind velocity U. This steady state concentration

was obtained by Smith (1961) for a single box. The expression for that

case is given by

$$C_{SS} = \frac{S}{LUH} \tag{3.11}$$

Equation (3.7) is written for each control volume (box) in the

grid. A set of algebraic equations is then obtained which must be solved

simultaneously to get the concentration in each box at the end of one

time step Δt. This procedure is repeated to obtain the concentration in

each box as a function of time. Once an initial distribution for the

concentration field and the distribution for the source strength in the

grid are determined, the solution for the first time step can be obtained.

These new concentrations calculated from the set of simultaneous equa-

tions are now used as the initial concentration distribution for the next

step. The procedure is continued to get the concentration distribution

for each successive time step. The numerical procedure involved in cal-

culating the concentration distribution from the set of simultaneous

algebraic equations is discussed in Chapter 5.

Zero Advection Case

There are certain meteorological conditions under which air pol-
lution concentrations are usually high. These cases are of interest for
predicting the possible local maximum levels that could be observed.
When the wind is relatively calm, the mechanism of advection due to the
wind becomes small and diffusion is the only mechanism for motion of an
inert air pollutant. Due to the motionless state of the wind the air
pollutant emissions can accumulate. This zero wind (calm condition)
problem cannot be handled, as pointed out by MacCracken et al. (1972),
using the Gaussian plume model. The Gaussian model predicts an infinite
value for the concentration at the source and zero everywhere else as
the wind speed approaches zero. The zero advection case can be handled
by the method used in this study, that is, the numerical solution of the
mass continuity equation.

To handle this calm condition, the wind speed U is set equal
to zero. If this is done, β becomes infinite and θ goes to zero;
therefore, equation (3.7) cannot be used. The analyses must start back
at equation (3.5) which is the mass balance obtained for the control vol-
ume in Fig. 3.2. Starting with this equation and setting u and v equal
to zero, the following result is obtained

$$\frac{\partial C}{\partial t}\bigg|_{i,j}^{t+\Delta t/2} (L^2 H) = K_H \left(\frac{\partial C}{\partial x}\bigg|_{i,j+\frac{1}{2}}^{t+\frac{\Delta t}{2}} - \frac{\partial C}{\partial x}\bigg|_{i,j-\frac{1}{2}}^{t+\frac{\Delta t}{2}}\right) (LH)$$

$$+ K_H \left(\frac{\partial C}{\partial y}\bigg|_{i+\frac{1}{2},j}^{t+\Delta t/2} - \frac{\partial C}{\partial y}\bigg|_{i-\frac{1}{2},j}^{t+\Delta t/2}\right) (LH) \qquad (3.12)$$

$$+ S_{i,j}$$

This equation (3.12) can now be used to obtain the concentration for the case of zero wind speed U. The simplification of (3.12) proceeds in the same manner as did equation (3.5). The partial derivatives are approximated as before using a Taylor series expansion with the results presented in Appendix A. The value of the concentration at $t + \frac{\Delta t}{2}$ is the average between its values at t and at $t+\Delta t$. Following this line of analysis a final expression is obtained for the case of no advection. The algebra involved in obtaining this equation appears in Appendix A and the equation is presented below as

$$
\begin{aligned}
C_{i,j}^{t+\Delta t}(1 + 4\phi) &- \phi(C_{i,j-1} + C_{i-1,j} + C_{i,j+1} + C_{i+1,j})^{t+\Delta t} \\
&= C_{i,j}^{t}(1 - 4\phi) + C_{zw,ij} \\
&+ \phi(C_{i,j-1} + C_{i-1,j} + C_{i,j+1} + C_{i+1,j})^{t}
\end{aligned}
\tag{3.13}
$$

Equation (3.13) contains the concentrations at $t+\Delta t$ on the left side with their corresponding values at t on the right side. A non-dimensional time parameter ϕ is defined such that

$$
\phi = \frac{K_H \Delta t}{2L^2} = \frac{V_D \Delta t}{2L}
\tag{3.14}
$$

where

$$
V_D = \frac{K_H}{L}
\tag{3.10}
$$

ϕ relates the diffusion speed V_D to the numerical time step Δt and the width of the square box L. The factor of 1/2 in equation (3.14) is included only to simplify the final form of equation (3.13).

Another term appearing in equation (3.13) is $C_{zw,ij}$. This is the resulting concentration for a time interval Δt for the case of no advection. The expression is given by

$$C_{zw} = \frac{S\Delta t}{L^2 H} \qquad .$$

(3.15)

Equation (3.15) says that the concentration for a node (i,j) is equal to the source strength for that node multiplied by the time of its emission Δt, divided by the volume of the box. This again assumes that the surrounding boxes have a zero concentration. This result (3.15) gives the concentration density for a time of emission Δt for the case of zero advection and diffusion for a box of volume $L^2 H$ having a source strength S.

Equation (3.13) can be solved in a similar fashion to equation (3.7) to obtain the concentration distribution for the grid as a function of time. The resulting distribution should contain higher levels than would be obtained using equation (3.7) since equation (3.13) now accounts for the zero wind condition.

By applying a backward finite difference to each partial derivative in equation (3.3), the same result is obtained as equation (3.7) which was developed using a mass balance on a control volume. The same is true for the case of no convection; in this case the final result by either approach is equation (3.13).

Boundary Conditions

In order to solve any differential equation, certain initial and/or boundary conditions are needed. To obtain a solution to the mass continuity equation (3.3) using the multi-box approach, four boundary

conditions and one initial condition are needed. Equation (3.3) is a parabolic partial differential equation in the independent variable-time. An initial condition is required since the equation is of order one in the variable time. The initial condition is represented by the initial distribution for the concentration field. This distribution contains the concentration in each box at the start of time, i.e., t = 0. To start the analysis, a distribution is assumed such that the concentration in each box at t = 0 is the same and equal to a background concentration C_o. However, other initial distributions could be chosen. The concentration field can then be obtained after each time step Δt once the boundary conditions are known.

The conservation of mass equation (3.3) is an elliptic partial differential equation in the independent space variables. The equation is second order in the variables x and y so four boundary conditions are needed. The boundary conditions are the values of the dependent variable at the spatial boundaries. The dependent variable is the air pollutant concentration C, and the values of C are needed at the four boundaries of the airshed grid.

Since the air pollutant C is transported through the grid by the wind velocity U, there are two boundary conditions needed upwind of the grid and two required downwind of the grid. The wind velocity U can rotate by changing its angle orientation α. The wind can be in any of the four 90° wind quadrants making up a 360° circle. Due to the rotation of the wind velocity, the upwind boundary conditions can become the downwind conditions and vice versa. The wind rotation is accounted for

in the analysis of this study since to simulate the concentration field time-history, the variation in the meteorological parameters are required.

The boundary conditions are represented by specifying the concentration C for a fictitious set of boxes surrounding the airshed grid. In starting the analysis with the initial distribution C_o at t = 0, the wind velocity U is in some initial wind quadrant. The upwind boundary conditions, one each in the x and y direction, are represented by the set of boxes in both directions upwind of the grid having a concentration equal to the background concentration C_o. The downwind boundary conditions are not so easy to handle. Their values are not the background level since the larger concentrations from inside the airshed are convected out of the grid in the downwind direction.

The downwind conditions can be handled by first expanding the airshed grid by adding a couple of rows of boxes surrounding the actual grid. In these additional boxes the pollutant source S is taken as zero. In these outer rows of boxes, β is set equal to zero which means that the diffusion is neglected, i.e., the equation becomes parabolic. Since the advection terms are handled using an upwind finite difference, no outflow (downwind) boundary conditions are needed. This approach is similar to the method pointed out by Roache (1972) in his Computational Fluid Dynamics text. In solving the vorticity transport equation, as the Reynolds number approaches infinity, no boundary condition on the vorticity is necessary at outflow. The Reynolds number can be thought of as representing the ratio of the convection to the viscous diffusion. If the Reynolds number approaches infinity, this means that the viscous

diffusion is small and approaches zero. This is analogous to β approaching zero since β is the ratio of turbulent diffusion to convection for the mass continuity equation. For the case where convection is accounted for, β is usually about 0.10 or so which gives a Reynolds number (based on the cell length, L) of 10.

Using this approach, only the inflow boundary conditions are needed. The outflow boundary conditions are suppressed by neglecting the diffusion out of the downwind boxes which are adjacent to the grid boundary. The mass continuity equation solved for these boxes adjacent to the boundary is either equation (3.7) with β = 0 or equation (3.13) with φ = 0 depending on whether the advection is zero or not. This is the same as setting the horizontal eddy diffusion coefficient equal to zero in the initial mass balance, equation (3.5) or equation (3.12).

In obtaining the concentration field after each time step Δt, the wind velocity can change quadrants from its initial quadrant. When this occurs, one or both of the outflow-boundary conditions can now become inflow boundary conditions. This new inflow boundary condition is probably no longer equal to the background concentration since the air pollutant concentration has had time to accumulate downwind just outside of the grid boundary. The new inflow boundary conditions for the time t+Δt can be approximated from the concentration field at time t. Using a set of fictitious boxes surrounding the grid, the concentrations for each of these boxes can be approximated using a linear interpolation with the two adjacent upwind boxes in the same direction as shown in Fig. 3.3. So the concentration at the fictitious node I+1 is

$$C_{I+1} = 2C_I - C_{I-1} \qquad\qquad (3.16)$$
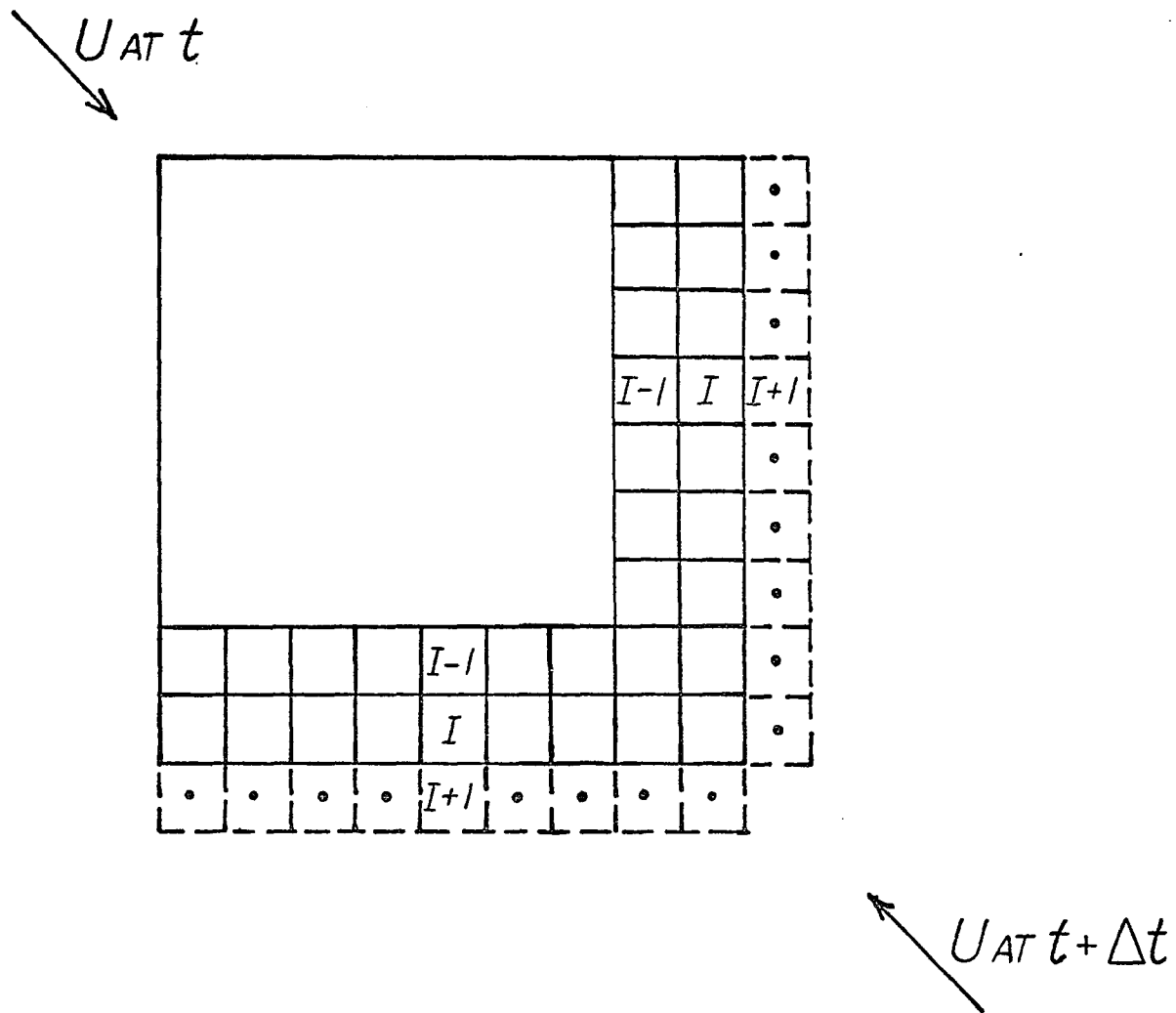
Fig. 3.3 Node Configuration Including Change in Wind Direction

The value for the new upwind boundary condition for time t+Δt is twice the concentration at the nearest adjacent node minus the concentration at the node which is two node lengths away. The values C_I and C_{I-1} are part of the concentration field determined at time t. This approach of using a fictitious node approximated by a linear interpolation was used by Briley (1970). This process is continued for as many time steps as necessary until initial background is reached. A restriction is set on equation (3.16) such that the value of C_{I+1} can not be less than the background concentration C_o. The new outflow boundary condition again is handled as before, with zero diffusion in the boxes adjacent to the outflow boundaries.

Input Data

Having obtained the set of algebraic equations, representing the mass balance for each box in the grid, along with the appropriate initial and boundary conditions, the input data must now be developed so that the time history of the carbon monoxide concentration field for the Tucson airshed can be calculated. There are three important pieces of information needed as input. They are the meteorological parameters, the source field for carbon monoxide, and the turbulent eddy diffusivity coefficients in the horizontal and vertical directions.

Meteorology

The meteorological parameters needed are the wind speed U, wind direction α, and the mixing height of the atmosphere H. The wind direction and speed are obtained from the National Weather Service located at the Tucson International Airport. These parameters are recorded on an

hourly basis by the Weather Service. It is assumed that this location is representative of the city as a whole. It would, of course, be better to have local data. The morning and afternoon mixing heights can also be obtained using the radiosonde data from the airport. The morning mixing height is calculated as the height above the ground at which the dry adiabatic extension of the morning minimum surface temperature plus $5^{\circ}C$ intersects the vertical temperature profile observed at 1200 Greenwich Median Time (GMT). The minimum temperature is determined from the regular hourly airway reports from 0200 through 0600 Local Standard Time (LST). The afternoon mixing height is less complicated than the morning, but is calculated in the same way, except that instead of the minimum temperature plus $5^{\circ}C$, the maximum surface temperature observed from 1200 through 1600 LST is used. This procedure for calculating the mixing heights is described in AP-101 (Holzworth 1972, hereafter cited as AP-101).

To simulate the time history for the concentration field, the morning and afternoon mixing height levels are not sufficient information, but they are useful in determining the needed mixing height as a function of time. A linear interpolation between the morning and afternoon mixing heights can be made using the surface temperature variation to calculate the mixing height variation with time. After sunset the mixing height used is the morning mixing height of the second day since after sunset in Tucson an inversion usually starts at the ground. The inversion remains until it is burnt off by the morning sun of the next day. The expressions used are

$$H(t) = H_{m_1} + \frac{T(t) - T_{min_1}}{T_{max} - T_{min_1}} (H_A - H_{m_1}) \qquad \text{for} \qquad [t_{m_1} \leq t \leq t_s] \qquad (3.17)$$

$$H(t) = H_{m_2} \qquad \text{for} \qquad [t_s \leq t \leq t_{m_2}] \qquad\qquad (3.18)$$

where

H_{m_1} is the mixing height for the first morning

H_{m_2} is the mixing height for the second morning

H_A is the afternoon mixing height of the first day

T_{min_1} is the minimum temperature for the first day

T_{max} is the maximum temperature for the first day

t_{m_1} is the time corresponding to the morning mixing height of the first day

t_{m_2} is the time corresponding to the morning mixing height of the second day

t_s is the time corresponding to the sunset of the first day.

Since the surface temperature is recorded hourly, the mixing height levels can be calculated on an hourly basis using equation (3.17). This linear interpolation approach is similar to that used by Johnson, Ludwig, and Moon (1970) in AP-86 to calculate mixing height variations. Due to the fact that the Tucson International Airport is the only location within Tucson to obtain the meteorological parameters on a regular basis, the data obtained there are applied uniformly throughout the grid. Therefore there are no spatial variations in the meteorological parameters; however, the time variation of the data is accounted for by changing the inputs on an hourly basis in accord with the time interval of record.

Source Field

To analyze the carbon monoxide problem, an evaluation of the sources which emit the air pollutant is required. Since the model used in the analysis of the problem divides the airshed grid into boxes, the emission rate of CO must be determined for each box. The automobile is the main source of carbon monoxide so extensive data are needed to obtain a realistic estimate of emission rate. The rate of emission is calculated in grams per day using a weighted emission factor in grams per mile times the miles traveled per day in each box. The weighted emission factor is based on the yearly emission factors appearing in "Compilation of Air Pollution Emission Factors" (1973), hereafter noted as AP-42, and the automobile age distribution for Pima County. The mileage for each box was obtained using a traffic volume map prepared by the Pima County Association of Governments Transportation Planning Agency. A traffic volume distribution for a 24 hour day is used so that the emission source for each box can be used as an input on an hourly basis. The emission inventory for carbon monoxide used to input the source field for the predictive model is presented in the next chapter.

Diffusivities

The final input quantities needed are the turbulent eddy diffusivity coefficients. An understanding of turbulent diffusion is required so that this mechanism of motion can be included in the predictive model. In the atmosphere the molecular diffusion is neglected compared to the turbulent diffusion. The simple diffusion law is the linear law which says that the diffusion flux is proportional to the

gradient of the concentration. This is called Fick's law for diffusion and is given by the equation

$$\dot{m} = - K \frac{\partial C}{\partial x}$$

This relation expresses the diffusion in one direction only, that is, the x direction. The diffusion occurs in all three spatial directions and is nonisotropic. Here K is the turbulent eddy diffusivity and is given the symbol K_z in the vertical direction. K_H is the value for the horizontal eddy diffusivity and the assumption is made that $K_H = K_x = K_y$. The magnitudes of K_H and K_z are obtained from experimental diffusion data.

The data available for the horizontal eddy diffusivity are relatively sparse and generally for diffusion only in the upper atmosphere. The information needed for this model is for the lower atmosphere within the mixing layer. Angell, Allen, and Jessup (1971) obtained data for diffusion in the lower troposphere in mountainous areas. Tetroons were tracked from a release point to obtain a distribution of their positions after a certain time interval. The wind speed was relatively constant for the experiment and for travel times of slightly less than 1 hour the lateral and longitudinal eddy diffusivities were about $500m^2$/sec at an altitude of about 2500 meters.

A summary of continous-source lateral-diffusion measurements is presented in a paper by Heffter (1965) and later appeared in a publication entitled <u>Meteorology and Atomic Energy</u> which was edited by David H. Slade (1968). The results were obtained using a wide variety of sources including continuous smoke plumes, multiple balloon releases, and clouds from nuclear detonation. For travel times of 1 to 4 hours, the

horizontal eddy diffusion coefficients varied from $100m^2$/sec up to

$4000m^2$/sec for measurements from the surface up to 1000 meters or so.

In another study, Randerson (1972) assumes that the horizontal

diffusion follows the Fickian diffusion law with K_H given by

$$K_H = \frac{\sigma_y^2}{2t} \qquad (3.19)$$

where σ_y is the standard deviation in the crosswind direction for the

distribution of the continuous source for travel time t. The travel time

t can also be represented by x/U where x is the downwind position for a

wind velocity U. Using this relation for the horizontal diffusion coef-

ficient, Randerson followed nuclear debris clouds and found that K_H was

about $1000m^2$/sec for travel times less than 1 hour for altitude of 2 to 3

kilometers.

In determining the horizontal eddy diffusivity needed for the

multi-box model, equation (3.19) could be used if a value for σ_y were

obtainable. For this model, σ_y represents, for example, the distribu-

tion of balloon positions at the time t = L/U, i.e., time to travel a

box of width L with a wind speed U. If all the balloons are released

at t = 0 and x = 0 under conditions of a fairly constant wind speed,

then at t = L/U each balloon will have a different position, (in both

x and y) relative to the starting point, about the location x = L. This

experiment is similar to that done by Angell et al. (1971). The reason

for the distribution of the balloons about x = L instead of every bal-

loon converging on that point is due to turbulent eddy motion. For the

box model, a value of σ_y would be required for a travel time on the order

of one hour or less for diffusion from the surface up to the mixing

height. For these conditions the data available for σ_y or K_H vary by an order of magnitude depending on what reference is used.

To overcome this problem, a parametric study for K_H was performed using the predictive model to see what is the effect of this variable on the concentration field. Two values of K_H which varied by an order of magnitude were employed in the parametric study. For values of K_H equal to $100m^2/sec$ and $1000m^2/sec$, the model predictions showed only a very small difference for the concentration field for wind speeds between 2 and 3 meters/sec. This behavior is substantiated in a paper by Shir and Shieh (1974). They developed an urban air pollution model of SO_2 for St. Louis. In their study they found K_H to have no significant effects on their results and a value of $500m^2/sec$ was assumed for the horizontal eddy diffusivity. Since it appears that the concentration field is relatively insensitive to K_H a value of $500m^2/sec$ is used for this study also.

The vertical eddy diffusion coefficient is easier to ascertain since there is an abundance of data available. In a neutral atmosphere the vertical diffusivity can be obtained using the classical von Karman mixing length theory for the surface layer as pointed out by Pasquill (1962). This approach gives a linear profile for K in the region where the shear forces dominate. In this region K increases to some maximum level; after this point the shear forces no longer dominate and the turbulence effects decay to some low level in the free (upper) atmosphere. There is much disagreement about the profile of K with z above this maximum value of the diffusivity. A summary of the different profiles for

K as a function of height is given in a report by Bergstrom and Viskanta (1972).

The most widely used distribution for K_z is referred to as the trapezoidal distribution. This profile was employed by Roth et al. (1971) in a simulation model for estimating ground level concentrations of photochemical pollutants. The magnitudes for this distribution with height z are presented in a paper by Mahoney and Egan (1971). The vertical diffusion coefficient is

$$K(z) = 0.16z \qquad \text{for} \qquad 0 < z < 100m$$
$$= 16 \qquad \text{for} \qquad 100m < z < 150m$$
$$= 16 - 0.32(z-150) \quad \text{for} \qquad 150m < z < 200m$$

The results presented are for neutral stability of a plane, homogeneous terrain. This profile when plotted has a trapezoidal shape and has a maximum value of $16m^2/sec$. In order to determine a ground level value for the carbon monoxide concentration, the magnitude of K_z is needed at some reference height; this height being where the ground level concentration is predicted. The reference height z_o is 1 meter and at that height $K_z = 0.16m^2/sec$. The reference height was arbitrarily chosen as one meter, although this reference height was used by MacCracken et al. (1972). This value of K_z along with the magnitude of K_H are used as input data for the model.

To substantiate that the values used for K_H and K_z are reasonable, a quote from a paper by Chaudhry and Cermak (1971, p. 128) on simulating flow and diffusion over an urban complex is included.

"In the wind tunnel K_x and K_z are expected to be of the same order whereas in the field K_x is at least one order of magnitude larger than K_z." The value used in the model for K_H is at least one order of magnitude greater than K_z depending on the height at which K_z is evaluated.

The turbulent eddy motion can be attributed to that motion due to both mechanical and thermal turbulence. When the forced advection mechanism is small, the eddy motion due to mechanical turbulence is also small. For the case of zero convection (calm wind), the value for K_H is no longer applicable. The magnitude of K_H is now less since U is small. There is still motion in the vertical direction since only the mean horizontal wind is set equal to zero. Thus the relations above for K_z can still be used. It can be shown that K_z varies only slightly from the neutral case for the case of an unstable atmosphere using the appropriate relations given by Bergstrom and Viskanta (1972). For this unstable case, the turbulent eddy motion is now predominantly due to free or natural convection. The driving force for motion is now caused by buoyancy. For this case the horizontal turbulent eddy diffusion coefficient can be equated to the thermal eddy diffusivity for the atmosphere. Under these conditions the value of K_H can be approximated as $80m^2/sec$ as discussed in a paper by Krishnamurti (1972). The paper is a survey of laboratory and theoretical studies of convection. There is now sufficient input data for K_z and K_H to calculate the concentration field whether or not the forced advection is important.

Vertical Concentration Distribution

In using the multi-box approach, the concentrations obtained from the numerical solution of equation (3.3) are average values for each box of volume L^2H. The air pollutant is assumed to be homogeneously mixed in each box, but in reality, there should be some distribution for the concentration with the vertical height z. In order to predict a ground level concentration for each box, a z-distribution for the concentration is assumed. Physically, the pollutant concentration decreases with z from the ground at z = 0 up to the top of the box z = H, the mixing layer. The technique for handling the concentration distribution in the z direction gives the multi-box model in this study a pseudo-three dimensional dependence.

A profile for the concentration distribution in the vertical direction is chosen so that ground level concentrations can be calculated for comparison with measured experimental data taken within the airshed. A vertical profile is assumed such that the concentration has a logarithmic dependence given by

$$C(z) = a + b \ln \frac{z}{z_o} \qquad z_o \leq z \leq H$$
$$C(z) = a \qquad 0 \leq z \leq z_o \qquad (3.20)$$

where z_o is the reference height, taken to be one meter. In the atmosphere the velocity follows a logarithmic profile so by relating the eddy diffusivity for momentum to the eddy diffusivity for diffusion it appears reasonable to assume that the concentration distribution is also logarithmic. The logarithmic dependence for the concentration in the vertical

direction was used by MacCracken et al. (1972) for an air pollution model of the San Francisco Bay area. The coefficients $\underline{a}$ and $\underline{b}$ are determined by imposing boundary conditions in the z direction. The first condition requires that the integral of the concentration from the surface to mixing height be consistent with the vertical average concentration determined by integrating equation (3.3), that is

$$\overline{C}(x,y,t) = \frac{1}{H(t)} \int_{0}^{H(t)} C(x,y,z,t) \; dz \qquad (3.21)$$

The second requirement is that the divergence of the vertical flux at $z = z_o$ be zero, which means that the source strength must balance the vertical diffusion. The relation for this condition is given by

$$Q(x,y,t) = - K_z(x,y,z_o,t) \frac{\partial}{\partial z} [C(x,y,z,t)]_{z=z_o} \qquad (3.22)$$

where Q is the time dependent pollutant surface source with $Q = S/L^2$ for each box. $K_z(x,y,z_o,t)$ is the vertical eddy diffusivity at the reference height z_o. Equation (3.22) is a relation for Fick's law of diffusion. Another condition that the distribution for the concentration in the z direction satisfies is

$$- K_z(x,y,H,t) \frac{\partial}{\partial z} [C(x,y,z,t)]_{z=H} = 0 \qquad (3.23)$$

Equation (3.23) requires that the diffusion out of the box at $z = H$ be zero. This is the constraint on z at the other spatial boundary. The two real boundary conditions in the z direction are given by equations (3.22) and (3.23).

To calculate the ground level concentration the coefficient a must be obtained since a is the value for the concentration at the

reference height. This can be accomplished by solving for a in equation (3.20) using the conditions in equations (3.21) and (3.22). The algebra involved is contained in Appendix A and results are presented here as

$$C_{GL}(x,y,t) = \overline{C}(x,y,t) + \frac{S}{L^2 K_z} [\ell n \ H-1]$$ (3.24)

where C_{GL} is the ground level concentration and has a constant value from $z = 0$ to $z = 1$ meter. The concentration from that point up to the top of the box $z = H$ has the following form

$$C(x,y,z,t) = C_{GL}(x,y,t) - \frac{S}{L^2 K_z} \ell n \ z \quad \text{for} \quad 1m \leq z \leq H$$ (3.25)

With these results the model now accounts for the fact that the pollutant is not homogeneously mixed in each box. Equation (3.24) can be used to predict the ground level concentrations for the airshed using the average concentration $\overline{C}$ for each box obtained in the numerical solution of equation (3.3). The next chapter presents the source data needed as input for the numerical solution of the mass continuity equation.

CHAPTER 4

EMISSION INVENTORY

Perhaps the most tedious aspect in the development and validation of an air pollution simulation model is the compilation of a complete emissions inventory for the pollutants of interest. Such an inventory must be made before a model can be validated since the temporal and spatial distributions of the pollutant emissions comprise a direct input to the overall simulation model. The ground level sources enter into the boundary conditions of the conservation equation through the function $Q(x,y,t)$ introduced in equation (3.22); and the sources enter directly as $S(x,y,t)$ in the conservation equations (3.3) for each box.

The major sources of the pollutant of interest, i.e., carbon monoxide, may be classified as moving sources. The predominant moving source in the urban airshed is vehicular traffic, primarily automobiles, trucks, and buses. The airplane is another mobile source which emits carbon monoxide, but this source is localized since it is restricted to the region near an airport. The aircraft source is accounted for in the simulation model. All other moving sources, not mentioned above, are neglected when computing the carbon monoxide inventory for the Tucson urban airshed.

Motor Vehicles

The magnitude of emissions from a motor vehicle is a variable in time and is a function of the percentage of time the vehicle is operated in each driving mode -- accelerate, cruise, decelerate, idle. The presence or absence of smog control devices, the car's condition, its size, and many other factors also affect the emissions from a vehicle. To simplify the problem, the emissions from motor vehicles are determined based on a generalized test cycle that involves operation typical of everyday patterns. This test cycle is used by the Environmental Protection Agency in computing emission factor data for light-duty vehicles (AP-42).

The emission factor for motor vehicles relates the quantity of pollutant emitted to the vehicle miles traveled. In AP-42 report on emission factor data the 1975 Constant Volume Sampling (CVS) Federal Test Procedure is utilized for light-duty vehicles. Without going into detail, the procedure involves a predetermined driving schedule comprised of three portions: a "cold start," cold-transient and cold-stabilized portions, and a "hot start" - hot-transient portion. A "cold start" is defined as a start preceded by a 12-hour, no use soak period ("Automobile Exhaust Emission Surveillance," 1973). Each portion of the test is comprised of a sequence of 32 acceleration/deceleration modes with transitions consisting of short steady-state idles or cruises. The duration of the complete driving schedule is 23 minutes. All modes consist of paired combinations of the following speeds:

0 mph, 15 mph, 30 mph, 45 mph, 60 mph. Steady-state operations and cruises are also at these speeds. Using the test procedure an average emission factor in grams/mile is obtained for each light-duty motor vehicle year.

Light-duty Vehicles, Gasoline Powered

In computing the emissions of carbon monoxide from light-duty vehicles, i.e., any vehicle having a gross weight less than 6000 pounds, a weighted emission factor using a Tucson vehicle age distribution is required. The weighted emission factor is obtained using the following relationship:

$$e_{np} = \sum_{i}^{n+1} c_i \, d_i \, a_i \, s_i \qquad (4.1)$$

where

> e_{np} is the weighted emission factor in grams per vehicle mile for the calendar year (n), and pollutant (p),
>
> c_i is the 1975 Federal Test procedure emission rate for pollutant (p) in gm/mi for the ith model year,
>
> d_i is the controlled vehicle pollutant (p) emission deterioration factor for the ith model year at calendar year (n),
>
> a_i is the fraction of the ith model year vehicles registered in the calendar year (n),
>
> s_i is the weighted speed adjustment factor for the ith model year vehicles.

A weighted emission factor is determined using equation (4.1) for the calendar year 1973 for carbon monoxide. The year 1973 is picked since

the vehicle miles traveled (VMT) in the Tucson area is obtainable for that year.

Most of the input needed for equation (4.1) can be found in the EPA publication No. AP-42. The emission factors for carbon monoxide for Tucson, which is about 2500 ft. above sea level, are calculated by taking an average between the values in Table 3.1.2-1 of AP-42 for low altitude (sea level) and high altitude (Denver). These values are then assumed to be the emission factors for Tucson using the 1975 Federal Test Procedure. The deterioration factors for each model year are taken from Table 3.1.2-5 of AP-42. The vehicle age distribution is the same as that used in "State of Arizona Air Pollution Control Implementation Plan — Transportation Control Strategies," (1973) prepared by the state for EPA. The average test speed in the 1975 Federal Test Procedure is 19.6 mph. For the Tucson urban area an average speed of 25 mph is used in accord with Wolsko, Matthies, and Wendell (1972). A speed correction factor is needed for the emission rates, and Figure 3.1.1-1 of AP-42 gives the appropriate correction factor for carbon monoxide. The computation of the weighted emission factor for carbon monoxide for the calendar year 1973 appears in Table 4.1.

The weighted emission factor for carbon monoxide for Tucson for the year 1973 is approximately 60 gm/mile. Note that in computing the weighted emission factor for the calendar year 1973, some 1974 model vehicles are included. The reason for this inclusion is that the 1974 model car comes into production around September, 1973. Using the weighted emission factor just calculated, an emission rate of carbon monoxide on a gm/year basis can be calculated knowing the vehicle miles

Table 4.1 Carbon Monoxide Weighted Emission Factor for Tucson for
Light-duty Vehicles (1973)

Model Year	Vehicle Age Distribution	Emission Factors gm/mi	Speed Correction Factors	Age Deterioration Factors	Corrected Fractional Emission Factors
1974	.0591	30.5	.77	1.00	1.39
1973	.0975	30.5	.77	1.18	2.70
1972	.1046	30.5	.77	1.32	3.24
1971	.1046	54.5	.77	1.38	6.06
1970	.1011	54.0	.77	1.40	5.88
1969	.0955	43.5	.77	1.68	5.37
1968	.0877	60.0	.77	1.58	6.40
1967	.0780	108.5	.77	1.00	6.52
1966	.0670	108.5	.77	1.00	5.60
1965	.0540	108.5	.77	1.00	4.51
1964	.0415	108.5	.77	1.00	3.47
1963 & older	.1004	108.5	.77	1.00	8.39
					$59.53 \frac{gm}{mi}$

traveled (VMT) for light-duty vehicles in 1973. In calculating the

weighted emission factor, it is assumed that each model year vehicle

travels the same number of miles per year. A correction for the number

of miles actually driven as a function of model year can be made but was

not. Since there are so many variables, each with some uncertainty,

there was no reason to make any further additions or changes.

Heavy-duty Vehicles, Gasoline Powered

Another class of motor vehicles is the heavy-duty gasoline powered

vehicle. A weighted emission factor for this vehicle class can be calcu-

lated in a similar manner using equation (4.1). The emission factors

used for Tucson are an average between the low altitude and high altitude

values presented in Table 3.1.4-1 of AP-42. The emission rates for heavy-

duty gasoline powered vehicles are based on dynamometer test results,

on-the-road emission sampling, and emission standards. Because of the

lack of actual heavy-duty deterioration information, the deterioration

factors are taken as 1.0 for vehicles older than 1975 (AP-42). No emis-

sion controls are included on heavy-duty gasoline powered vehicles before

1975. Again due to lack of data, Fig. 3.1.1-1 of AP-42 is used to deter-

mine the speed correction factors. The vehicle age distribution for

heavy-duty gasoline powered vehicles is obtained from "State of Arizona

Air Pollution Control Implementation Plan -- Transportation Control

Strategies," (1973). Using this information, the weighted emission fac-

tor for carbon monoxide for heavy duty vehicles is calculated in Table 4.2.

The weighted emission factor for carbon monoxide for a heavy-

duty gasoline powered vehicle for 1973 is approximately 130gm/mile. The

Table 4.2 Carbon Monoxide Weighted Emission Factor for Tucson for
Heavy-duty Gasoline Powered Vehicles (1973)

Model Year	Vehicle Age Distribu- tion	Emission Factors gm/mi	Speed Correc- tion Factors	Age Deteriora- tion Factors	Corrected Fractional Emission Factors
1974	.011	160	.77	1.0	1.35
1973	.090	160	.77	1.0	11.10
1972	.105	160	.77	1.0	12.91
1971	.085	160	.77	1.0	10.48
1970	.080	160	.77	1.0	9.85
1969	.083	175	.77	1.0	11.18
1968	.075	175	.77	1.0	10.10
1967	.064	175	.77	1.0	8.62
1966	.054	175	.77	1.0	7.27
1965	.045	175	.77	1.0	6.06
1964	.034	175	.77	1.0	4.58
1963 & older	.274	175	.77	1.0	36.90

$$130.4 \frac{gm}{mi}$$

same assumptions apply that were stated when the weighted emission factor for light-duty gasoline powered vehicles was obtained. The emission rate in grams/year can be calculated using VMT for Tucson for heavy-duty gasoline powered vehicles.

Heavy-duty Diesel Powered Vehicles

The heavy-duty diesel powered vehicles comprise another class of motor vehicles largely consisting of trucks and buses. Because diesel engines allow more complete combustion and use less volatile fuels than spark-ignited engines, their carbon monoxide emissions are relatively low. The emission factors for heavy-duty diesel powered vehicles are not a function of vehicle year and a value for the emission factor can be obtained directly from Table 3.1.5-1 of AP-42 as 20.4gm/mile. The data used in obtaining the emission factor are based on weighting factors applied to actual tests conducted at various load and idle conditions with an average gross vehicle weight of 30 tons and a fuel consumption of 5.0 miles/gallon. Using this emission factor along with the VMT for Tucson for heavy-duty trucks and buses, an emission rate due to this vehicle class can be computed.

Motorcycles

The final motor vehicle class of interest is motorcycles. Because of their recent increase in sales the motorcycle can be considered as a significant source of carbon monoxide. Since Tucson has a warm weather climate the number of motorcycles on a per capita basis probably exceeds any midwest or eastern city. The majority of motorcycles are powered by

either 2- or 4-stroke air cooled engines. Currently the nationwide population of motorcycles is approximately 38 per cent 2-stroke and 62 per cent 4-stroke (AP-42). The quantity of motorcycle emission data is rather limited. For instance, data on motorcycle average speed versus emission levels are not available. Average emission factors for motorcycles used on highways are reported in Table 3.1.7-1 of AP-42. These data, from several test vehicles, are based on the Federal light-duty vehicle test procedure. A weighted emission factor for carbon monoxide can be calculated for motorcycles using Table 3.1.7-1 with the nationwide breakdown between 2-stroke and 4-stroke models. The weighted emission factor for motorcycles in Tucson is 30.7 gm/mile for carbon monoxide. The emission rate of carbon monoxide due to motorcycle can be obtained using VMT for motorcycles for 1973.

Vehicle Miles Traveled (VMT)

The number of vehicle miles traveled in the Tucson urban area is needed so that the total emission of carbon monoxide can be calculated due to all classes of motor vehicles. The vehicle miles traveled in the urban area has consistently risen year by year due to the large increase in vehicle registration. Table 4.3 on the following page shows the increase in VMT over the last three years on a daily and annual basis.

Table 4.3 can be used in approximating the VMT for each motor vehicle class. The data in this table are obtainable from the Pima Association of Governments-Transportation Planning Agency. The registration breakdown of motor vehicle classes is available from the Arizona Motor Vehicle Division. Using this information along with Table 4.3,

Table 4.3   Vehicle Miles Traveled in Tucson Area

Year	Miles/Day (10^6)	Miles/Year (10^9)
1971	4.27	1.56
1972	4.65	1.69
1973	4.98	1.82

the approximate mileage is determined for each motor vehicle class of

interest and is presented in Table 4.4.   These data are needed so that

the emission for carbon monoxide can be calculated for each motor

vehicle class.   The calculations are carried out by multiplying the

appropriate weighted emission factor by the VMT for that motor vehicle

Table 4.4   Vehicle Miles Traveled in Tucson Area Divided into Motor
Vehicle Classes for 1973

Motor Vehicle Class	VMT Miles/Day	VMT Miles/Year
Light-duty Vehicles	3.93×10^6	1437.0×10^6
Heavy-duty Gasoline Powered Vehicles	0.74×10^6	270.5×10^6
Heavy-duty Diesel Powered Vehicles	0.19×10^6	69.2×10^6
Motorcycles	0.12×10^6	43.3×10^6
	4.98×10^6	1820.0×10^6

class. The final results are summarized at the end of the chapter in Table 4.6 along with the emission rate from all other sources of carbon monoxide.

Aircraft

The airplane is another emission source of carbon monoxide. However, the source is localized within the urban airshed. Within the Tucson urban area, there are two major locations where air traffic occurs. Tucson International Airport is the metropolitan public airport facility for the area. The other significant emission source is the airfield at Davis-Monthan Air Force Base.

In order to determine approximate emissions from aircraft many variables are again involved. Since the urban simulation model uses the mixing layer as the top of the airshed, it would seem reasonable to be concerned with an airplane's movement only up to this altitude. Therefore, the aircraft emissions are determined only during its modes of operation while on the ground and in the air up to the atmospheric mixing height. A standardized height of 3500 ft. is used as the height of the mixing layer since this is the height used in AP-42 to obtain the emission factor data. There are many classifications of aircraft with both reciprocating (piston) and gas turbine engines. Emission factors are obtainable from AP-42 in Table 3.2.1-3. The table gives the emission factors per engine for a single aircraft landing-takeoff cycle. The emission factors can be obtained for carbon monoxide for different aircraft classifications as explained in Table 3.2.1-1 of the same EPA report.

The landing-takeoff cycle, used in determining the emission factors appearing in Table 3.2.1-3 of AP-42, includes all normal operation modes performed by an aircraft between the time it descends through an altitude of 3500 ft. (1100 m) on its approach and the time it subsequently reaches the 3500 ft (1100 m) altitude after takeoff. In determining emissions, the landing-takeoff cycle is separated into five distinct modes: taxi-idle, takeoff, climbout, approach and landing, and taxi-idle. Typical operating times for each mode were used in determining the emission factors for each class of aircraft.

The emission rate of carbon monoxide can be determined at each of the two major sources of air traffic once the number of movements at each location is obtained. This information is presented in Table 4.5 where a movement is defined as one landing-takeoff cycle. The movements data are divided into different aircraft categories similar to the classes appearing in Table 3.2.1-1 of AP-42. The information for Tucson International Airport was obtained from the Tucson Airport Authority and the data are assumed reliable. The data, obtained from Davis-Monthan Air Force Base, are only approximate values given with some reluctance. The movement data presented in Table 4.5 are average daily values for 1974. Using these data along with the emission factors for each aircraft class, an approximate emission rate of carbon monoxide can be calculated for each air traffic center in the Tucson area. These results are summarized in Table 4.6 along with the emission rates of carbon monoxide for motor vehicles. Neglecting some small mobile sources, the total emission rate of carbon monoxide during the calendar year 1973 is approximately

Table 4.5 Aircraft Movements at Major Air Traffic Centers in Tucson
          Area

Tucson International Airport

Aircraft Category		Movements/Day
1) Commercial Jets	Jumbo Jet	5
	Long-range Jet	25
	Medium-range Jet	25
2) Air Carrier (TurboProp)		50
3) Commercial (TurboProp)		5
4) General Aviation	Piston	205
	Business Jet	6
5) Military Jets		
(Air National Guard)		44
		365

Davis-Monthan Air Force Base

---

1) Military Jets		205
2) Military	Transport	10
	Piston	10
		225

Table 4.6 <u>1973</u> Summary of Emission of CO

Motor Vehicles	Tons/Day
Light-duty Vehicles	260.0
Heavy-duty Gasoline Powered Vehicles	106.0
Heavy-duty Diesel Powered Vehicles	4.3
Motorcycles	4.1
	374.4

Aircraft	
Tucson International Airport (all classes of aircraft)	5.5
Davis-Monthan Air Force Base	3.2
	8.7

Total all sources: <u>383.1 tons/day</u>

383 tons/day for the Tucson urban area. This carbon monoxide rate is an average daily level which smooths out the fluctuations that can occur in value through the weekdays and weekend.

The total emission of carbon monoxide for the Tucson urban area is of interest by itself for air pollution work. However, for calculations leading to predicting carbon monoxide concentrations using a box model, local emission rates are needed for each box. This total emission rate can be used for comparison since the sum of the emission rates for each box should add up to the global emission rate for the urban area. Using the emission factors determined in this chapter it is now possible to calculate the contribution of the total emission rate of carbon monoxide which applies to each box in the airshed grid. Using a traffic volume map of the Tucson area, it is possible to calculate the miles traveled in each box of the grid. These data, in conjunction with the motor vehicle emission factors, allow calculation of the source emission rate of carbon monoxide in each box. A presentation of this information along with an explanation of the box model as applied to Tucson is contained in the next chapter. The numerical procedure used in predicting the carbon monoxide levels in the urban grid as a function of time is also discussed in Chapter 5.

CHAPTER 5

PRESENTATION OF MODEL AND

NUMERICAL PROCEDURES

In applying the multi-box model to an urban airshed, there are
certain requirements which must be satisfied. For accuracy in a multi-
box approach, the choice of the size of the boxes must be made so that
the restriction that the pollutant is mixed uniformly, in one Eulerian
box before moving into the next box, is realistic. Typical horizontal
spatial resolution suitable for modeling an urban airshed is one square
block to several square miles as pointed out by Seinfeld et al. (1972).
The vertical spatial resolution of the model is determined by the height
to which pollutants are expected to mix. Often vertical resolution is
much finer than horizontal resolution because the vertical mixing depth
in the airshed is considerably smaller than the horizontal distances for
the urban area. The temporal resolution of the model can be of the
order of several minutes to several hours since the model should be able
to be used to compute concentrations over the course of one or more days.

Tucson Urban Airshed

The multi-box model as described and developed in this report is
sufficiently general to be applicable to any urban area, and was chosen
as the model for the Tucson urban area. The urbanized Tucson area is
approximately 200 miles square, but to include the surrounding area the

actual airshed is over 600 square miles. The airshed encompasses the Tucson basin from the Santa Catalina Mountains on the north, to 5 miles south of the International Airport on the south, to the Tucson Mountains on the west, and to the Rincon Mountains on the east. The horizontal resolution initially chosen using the multi-box approach is 4 square miles. The airshed is divided into 13 by 12 cells, each having a base which is 2 miles (3218m) by 2 miles (3218m). The vertical dimension or lid of each box is the mixing depth of the atmosphere. The vertical height of each box changes throughout the day due to the variation in the mixing layer. The temporal resolution employed is one hour since this is the time interval for which meteorological data are available. The model predicts the concentration in each box (cell) on an hourly basis and allows for variations in the meteorological parameters so that a 24 hour day is simulated.

The sides of the 156 boxes are oriented parallel to the compass directions. This was a convenient arrangement since most of the city streets run either north-south or east-west. A layout of the Tucson airshed with the box structure is shown on Fig. 5.1. Some of the main streets and highways are shown along with four possible large area sources of carbon monoxide. UA stands for University of Arizona and CBD stands for Central Business District.

It is necessary to have emission source data for each box in the Tucson airshed pictured in Fig. 5.1. This information can be obtained knowing the vehicle miles traveled, VMT, in each box on a daily basis. The VMT along with an average weighted emission factor for all vehicles can be used to calculate an emission rate for each cell in the grid. A
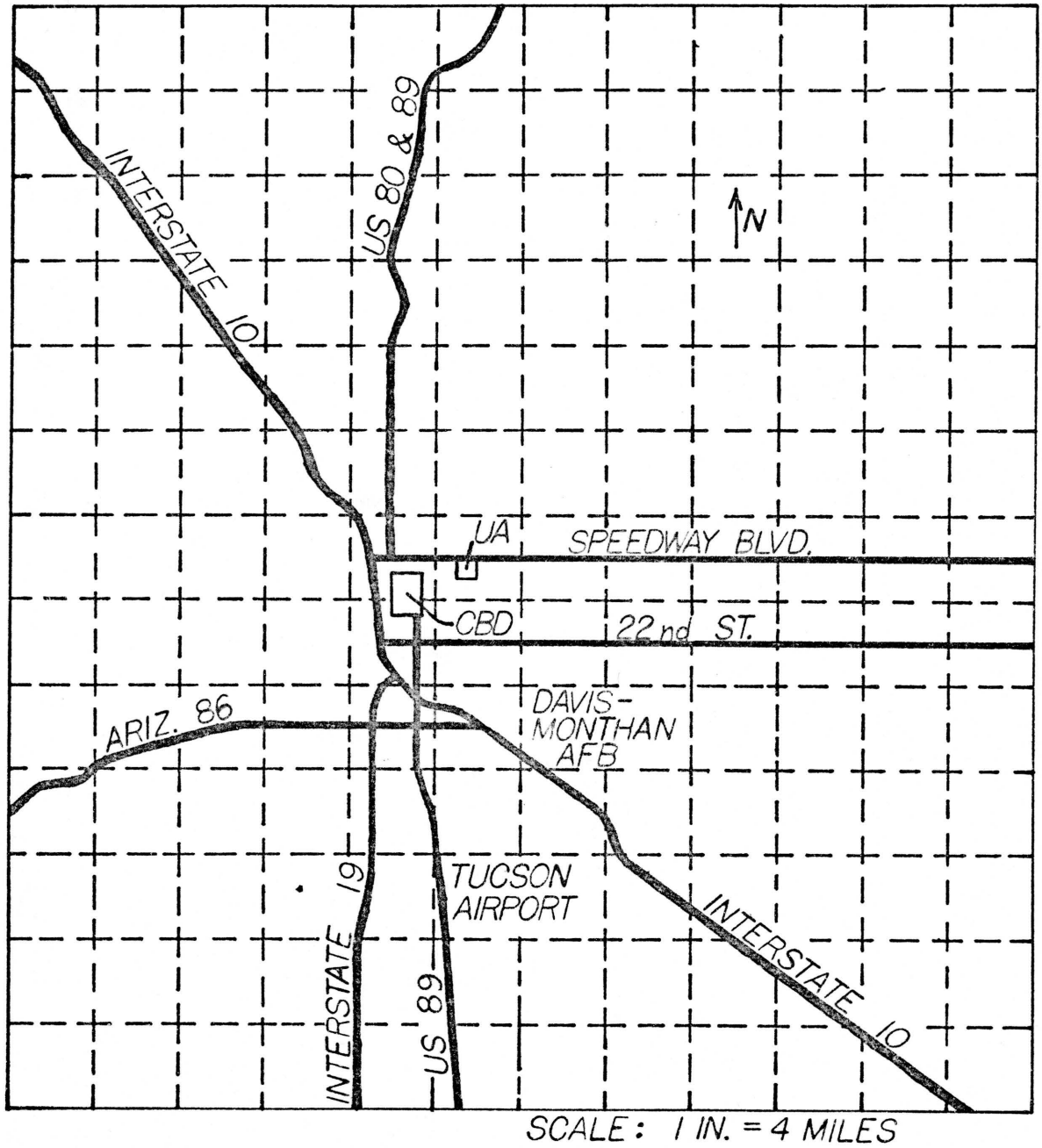
Fig. 5.1 156 Box Model of the Tucson Airshed

traffic volume map for the Tucson Area for 1973 was obtained from the Pima
Association of Governments Transportation Planning Agency. A reproduc-
tion of this map is contained in Fig. 5.2. The average daily VMT for each
box in the airshed is calculated using this traffic volume map. These
data are appropriate for predicting VMT on a weekday basis. With these
data and the weighted emission factor information obtained in Chapter 4,
the emission rate of carbon monoxide is computed for each box on a grams
per day basis. The results of these tedious computations are presented
in Fig. 5.3. It is still necessary to break the data in Fig. 5.3 down to
an emission rate as grams per hour so that the numerical model can pre-
dict concentrations of carbon monoxide for each box on an hourly basis.
This problem can be solved if one knows the daily emission cycle of car-
bon monoxide for the mobile sources. The daily emission cycle is similar
to the daily traffic volume variation. This information is presented in
Fig. 5.4 of this report. The data were obtained from a report entitled
"Tucson Area Transportation Study," (1960), prepared by government agencies
of the city, county, and state. The figure presents an average weekday
traffic volume cycle for all central business district (CBD) streets.

From the emission cycle for a day and the emission rates from
Fig. 5.3, the emission source data for each box can be calculated and
put into the numerical program on an hourly basis. All the required data
are now available to start the numerical predictions for the concentra-
tions of carbon monoxide. The concentration field for the Tucson area is
presented as a function of time for various meteorological conditions in
the next chapter.
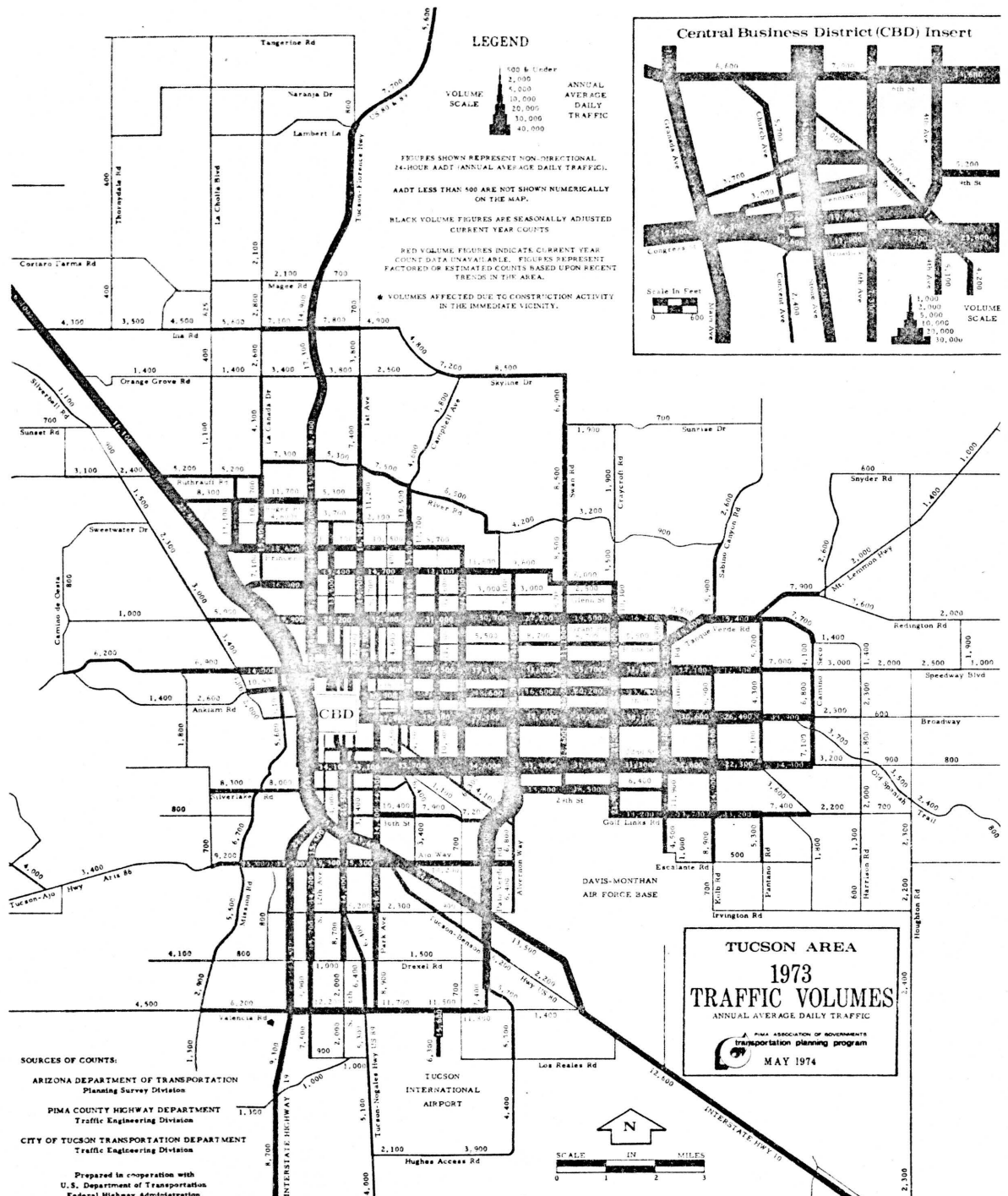
Fig. 5.2 Traffic Volume Map for the Tucson Area

			2.28								
	2.61	0.45	0.64	3.21							
	1.09	2.54	0.99	4.28	1.79	1.63					
		2.22	4.32	6.11	2.77	0.96	1.24	0.49			
		0.32	9.28	12.43	11.47	7.33	3.46	1.58	1.44	0.49	
		1.08	2.56	22.04	21.82	19.84	17.04	8.37	2.89	0.71	
			0.96	13.02	11.10	14.36	13.75	10.26	3.66	0.91	
	0.79	0.61	2.09	9.57	9.58	7.70	4.01	2.35	0.95	0.44	
			1.34	5.83	3.36	5.61	2.42				
			0.68	2.87	7.28	0.93	1.71	1.07			
				1.18	0.99	0.56		0.99	2.01		

Fig. 5.3 Emission Rate of CO for Each Box in Units of 10^6 grams/day
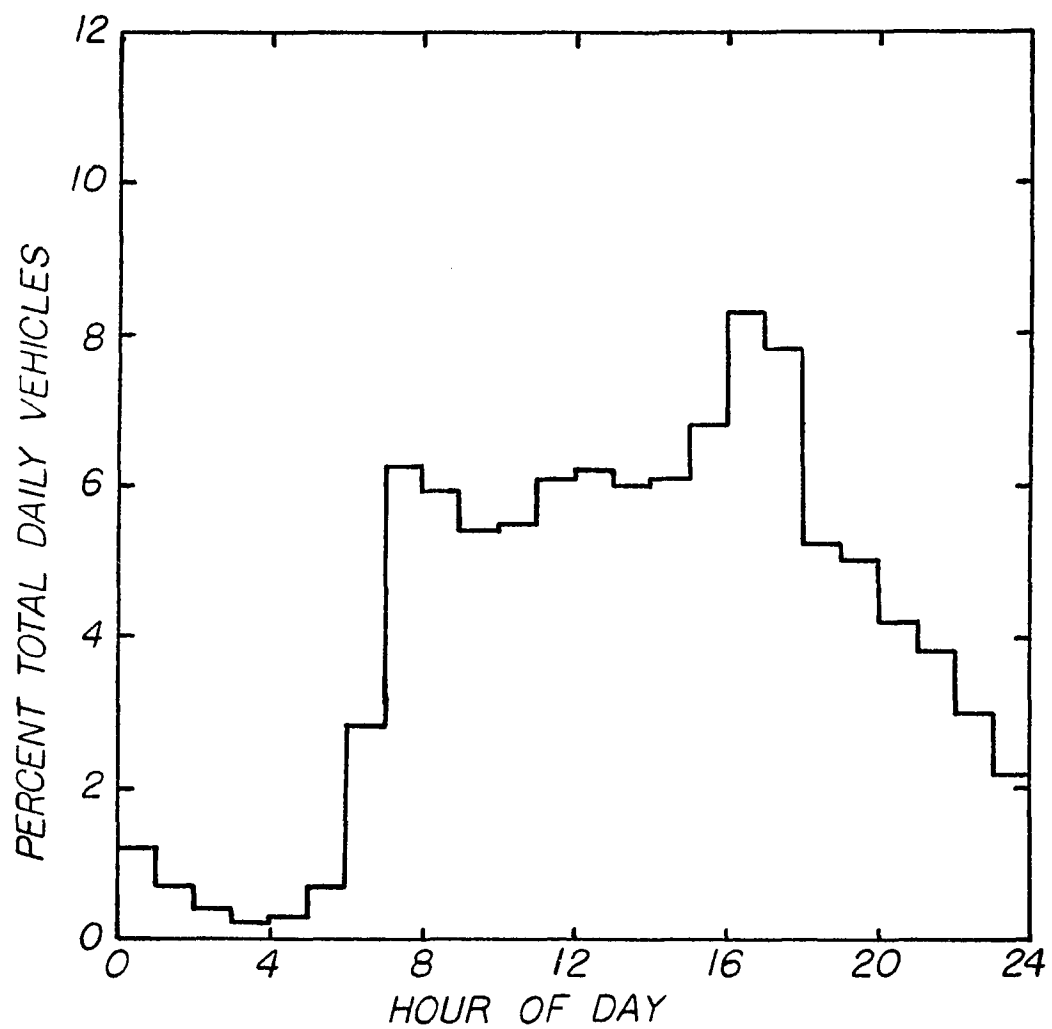
Fig. 5.4   Daily Traffic Volume Cycle for Motor Vehicles
in the Tucson area

Micro-model

The concentrations obtained for the 156 boxes represent carbon monoxide densities averaged over each 4 square mile cell. Since the 156 box model represents the entire Tucson urban airshed, the model can be considered as a macro-model. The predicted levels from the macro-model greatly underestimate the actual carbon monoxide concentrations measured near busy intersections. However, the predicted levels do represent concentrations measured in areas of low traffic density within the boxes.

A sub-model or micro-model is needed to predict within each box the carbon monoxide levels in residential areas close to centers of high traffic density. Therefore, a micro-model is developed using the same mathematical approach as employed in the macro-model. A single box from the macro-model is subdivided into smaller boxes. The horizontal resolution for each small box is limited mainly by the availability of accurate emission data for each box in the micro-model and also by computer capability. The horizontal resolution used in the micro-model is about two square blocks.

The same numerical approach is used as in the macro-model with the exception that the boundary conditions are treated in a different manner. Information is now available from the macro-model for the concentration time history of the four boxes surrounding the box of interest which is subdivided for the micro-model. These results can be used to handle the downwind boundary conditions. In the macro-model these data were not known. There the actual grid was surrounded with extra rows of boxes having a zero source and the diffusion was turned off at

the last row of boxes. Thus no boundary conditions were needed at the outflow edge of the airshed. This approach was discussed in Chapter 3. The downwind boundary conditions in the micro-model are just the concentrations at the adjacent downwind boxes as calculated in the macro-model. These values are applied at the boundaries of the single box which is subdivided in the micro-model. Diffusion out can now occur at the downwind boundaries. The inflow boundary conditions are now a function of time since they are also available from the macro-model.

The use of the micro-model in conjunction with the macro-model allows predictions of carbon monoxide concentrations in areas adjacent to high traffic density as well as areas of lower traffic density. For a set of meteorological conditions representing a day, the macro-model computes the carbon monoxide concentration field for the 156 box model as a function of time for 24 hours. The micro-model then computes the concentration distribution within any of the boxes from the macro-model using the same meteorological data but now boundary conditions obtained from the macro-model results. In the micro-model the horizontal resolution limitation will still affect direct comparison between the predicted level for a box and the measured data at a single point in the same box. This is because the box has some finite size and the predicted level is still an average value for the total micro-box. The results from the macro- and micro-models for different meteorological conditions are presented in the next chapter.

Solution Procedure

The solution for the concentration field is obtained by first applying an upwind finite differencing approximation to each derivative term in equation (3.3). The resulting equation is either (3.7) or (3.13) depending on whether the convection terms are included. This method is the same as applying the conservation of mass equation to the control volume in Fig. 3.2. Equation (3.7) or (3.13) can be written for each of the 156 boxes in the Tucson airshed pictured in Fig. 5.1. A set of 156 simultaneous algebraic equations is then obtained. The solution is determined using a Crank-Nicholson implicit technique. The concentrations at the new-time t+Δt all appear on the left-hand side of the equation while the concentrations at the previous time t are on the right-hand side. The solution of the set of simultaneous equations requires matrix inversion or an equivalent type method.

The set of 156 algebraic equations can be put in matrix form as shown

$$[X] \ [C] = [Z] \tag{5.1}$$

X = the coefficients of the unknown concentrations.

C = the unknown concentrations (for this model there are 156 unknowns).

Z = the constants which include the emission source term along with the known concentrations at the previous time step.

To obtain the unknown concentrations the matrix [X] is inverted. Since there are at most 5 unknowns in each algebraic equation, the matrix [X]

has 5 non-zero coefficients in each row and is called pentadiagonal

matrix. Upon inverting [X] and multiplying both sides of (5.1) by the

inverse the following result is obtained

$$[X^{-1}] \ [X] \ [C] = [X^{-1}] \ [Z]$$

where X^{-1} = inverse of X. But by definition $X^{-1} \ X = I$, where I is the

identity matrix, so

$$[C] = [X^{-1}] \ [Z] \qquad\qquad (5.2)$$

Equation (5.2) is the solution for the unknown concentration field.

Numerical Technique

The solution of (5.2) is carried out by using a MATRIX sub-

routine which is a library program on the CDC 6400 computer at The

University of Arizona. The MATRIX program has been carefully coded in

FORTRAN to take full advantage of the hardware features of the CDC 6600

central processor.

The method used in the MATRIX subroutine is basically the classi-

cal Gaussian elimination method. The Gaussian elimination method is a

direct method for solving a set of simultaneous linear equations

(Scarborough, 1962, and Ralston, 1965). The unknowns are eliminated suc-

cessively by solving an equation for one unknown in terms of all others;

this result is then substituted for the same unknown in all the remain-

ing equations, thereby eliminating the unknown from the set. This pro-

cess is repeated on the new set of equations, thus eliminating another

unknown and so on until the system is reduced to a single equation in one

unknown. The equations which express one unknown explicitly in terms of

all the others are called pivotal equations. After one unknown has been found, the remaining unknowns are found by back substitution into the pivotal equations.

The solution of (5.2) is repeated for each time step Δt by changing the matrix [Z]. The process is continued until the concentration field has been simulated for a 24 hour day. Some initial concentration distribution is needed at zero time to start the program. The coefficient matrix X is changed on an hourly basis in the calculations since the meteorological parameters are inputs for this matrix. The computer programs for macro- and micro-models appear in Appendix B.

Stability and Convergence

To analyze the stability and convergence of the solution, it is necessary to look back at the conservation of mass equation (3.3) used in the problem. By non-dimensionalizing equation (3.3) the following is obtained

$$\frac{\partial C^*}{\partial t^*} + u^* \frac{\partial C^*}{\partial x^*} + v^* \frac{\partial C^*}{\partial y^*} = \beta \left(\frac{\partial^2 C^*}{\partial x^{*2}} + \frac{\partial^2 C^*}{\partial y^{*2}} \right) + S^* \qquad (5.3)$$

where,

$$u^* = \frac{u}{U}, \quad v^* = \frac{v}{U}$$

$$t^* = t \frac{U}{L}, \quad x^* = \frac{x}{L}, \quad y^* = \frac{y}{L}$$

$$C^* = \frac{C}{C_o}, \quad S^* = \frac{S}{LUH} \frac{1}{C_o}$$

All the * terms in equation (5.3) are in non-dimensional form. What is of interest is the resulting non-dimensional paramter β which relates

the diffusion to the advection mechanisms. This parameter is of importance when choosing the proper differencing equation to employ so that stability and convergence of the final solution is satisfied. Note that β is defined in equation (3.9).

When analyzing a problem involving transport by simultaneous convection and diffusion, a choice can be made between a central-difference scheme (CDS) and an upwind-difference scheme (UDS). The criterion for choosing the proper scheme is that if

$$P = \frac{1}{\beta} = \frac{UL}{K_H} > 2 \quad \text{use UDS} \quad \text{and if } P = \frac{1}{\beta} = \frac{UL}{K_H} < 2 \quad \text{use CDS}$$

The upwind difference scheme, though it shows mild departure from exact analysis over part of the P region, is never grossly in error. An UDS is used throughout this work in the solution of equation (3.3). The criterion for $P > 2$ is always satisfied; therefore the solution should be both accurate and convergent. The criterion for "accuracy and convergence" discussed above appears in papers by Spalding, 1972, and Patankar, 1972.

When using an implicit technique treating both advection and diffusion, the solution is not unconditionally stable, as it is for the case of transient diffusion only. The criterion from above must be satisfied to insure the stability requirement. There is, however, no requirement on the time step size taken since this is an implicit technique. However, from a physical standpoint, the time step should be less than or at most the same as the actual time it would take for the pollutant to traverse the box. Using this type of reasoning Δt should be less than or equal to L/U so θ in equation (3.8) is less than or equal to 1/4. This criterion

for the time step allows the pollutant advected through a box to be accounted for in that box.

Verification of Model

Using the upwind differencing scheme the numerical solution should be stable and convergent, but do the results converge to the correct solution? In order to verify that the model predicts the correct solution, some simple cases can be analyzed so as to increase the confidence level for the final results obtained for the more general case.

Three separate cases are chosen such that the concentration distribution for each case can be qualitatively determined on a physical basis. This qualitative comparison can be used to show that the solution from the numerical model probably converges to the correct solution. The three cases use the geometry shown in Fig. 5.5. The large grid of area L^2 is divided into 64 boxes. The initial condition to start each case is that at t=0, C=0. The boundary conditions on all four sides are that the concentration is 1 ppm for all time.

Case A: The easiest case to visualize is the transient diffusion problem with a zero source. The partial differential equation representing this case is given as

$$\frac{\partial C}{\partial t} = K_H(\frac{\partial^2 C}{\partial x^2} + \frac{\partial^2 C}{\partial y^2}) \qquad (5.4)$$

Equation (5.4) can be put in finite difference form and written at each of the 64 nodes in Fig. 5.5. From a physical standpoint the solution should lead to parabolic-like curves in x and y. As time progresses the concentration at any (x,y) approaches 1 ppm, which is the boundary
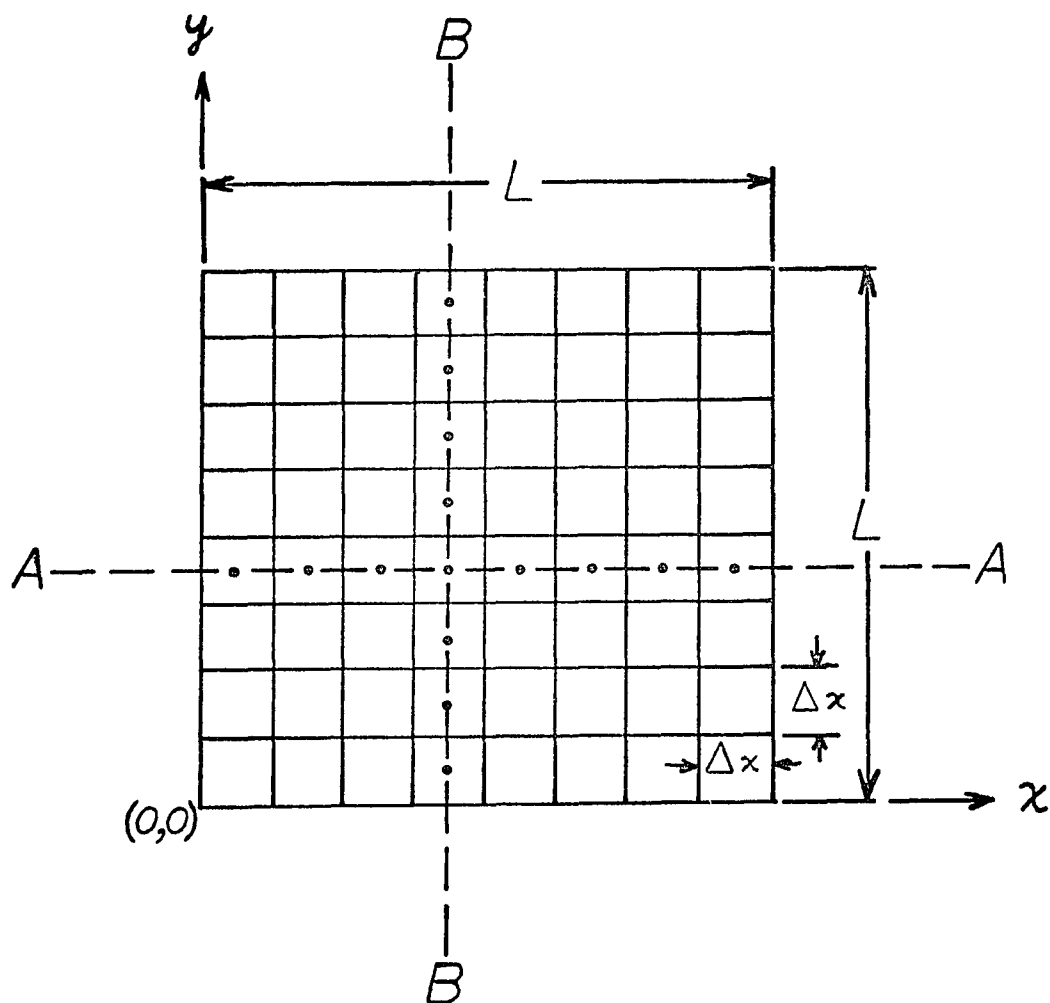
INITIAL CONDITION : $\quad C(x,y,0) = 0$

BOUNDARY CONDITIONS : $\quad C(x,0,t) = C(x,L,t) = 1\,PPM$

$$C(0,y,t) = C(L,y,t) = 1\,PPM$$

Fig. 5.5 64 Box Geometry and Conditions Used for Model Verification

condition, since diffusion occurs from the boundary in towards the center of the grid. The concentration distribution is symmetric in both x and y. This physical solution is verified by Fig. 5.6 which contains the pollutant distributions for different times obtained from a numerical solution of Case A for the 64 box model. Figure 5.6 plots the concentrations at each node for the cross-section A-A shown in Fig. 5.5. The steady state solution is reached after approximately 16 hours for a box having a length L of 3218m and a horizontal diffusion coefficient of $80m^2/sec$. The steady state time is defined as the time when the concentration reaches 99 percent of the actual steady state solution.

Case B: The next case analyzed treats the transient diffusion problem but now with a constant source instead of a zero source. The partial differential equation representing this case is given as

$$\frac{\partial C}{\partial t} = K_H(\frac{\partial^2 C}{\partial x^2} + \frac{\partial^2 C}{\partial y^2}) + \frac{S}{V} \tag{5.5}$$

As in Case A, Equation (5.5) is finite differenced and written at each of the 64 nodes of Fig. 5.5. Physically, the concentration distribution fills in as in Case A, but due to the source it continues to grow and reaches some final steady state parabolic-like shape. Initially, diffusion occurs from the boundaries towards the center but after some time the diffusion flow is towards the boundaries. Figure 5.7 shows this distribution growth just discussed. The figure was developed using the numerical solution of Case B for the 64 box model. The node concentration values used in the plots are again for the cross-section A-A on
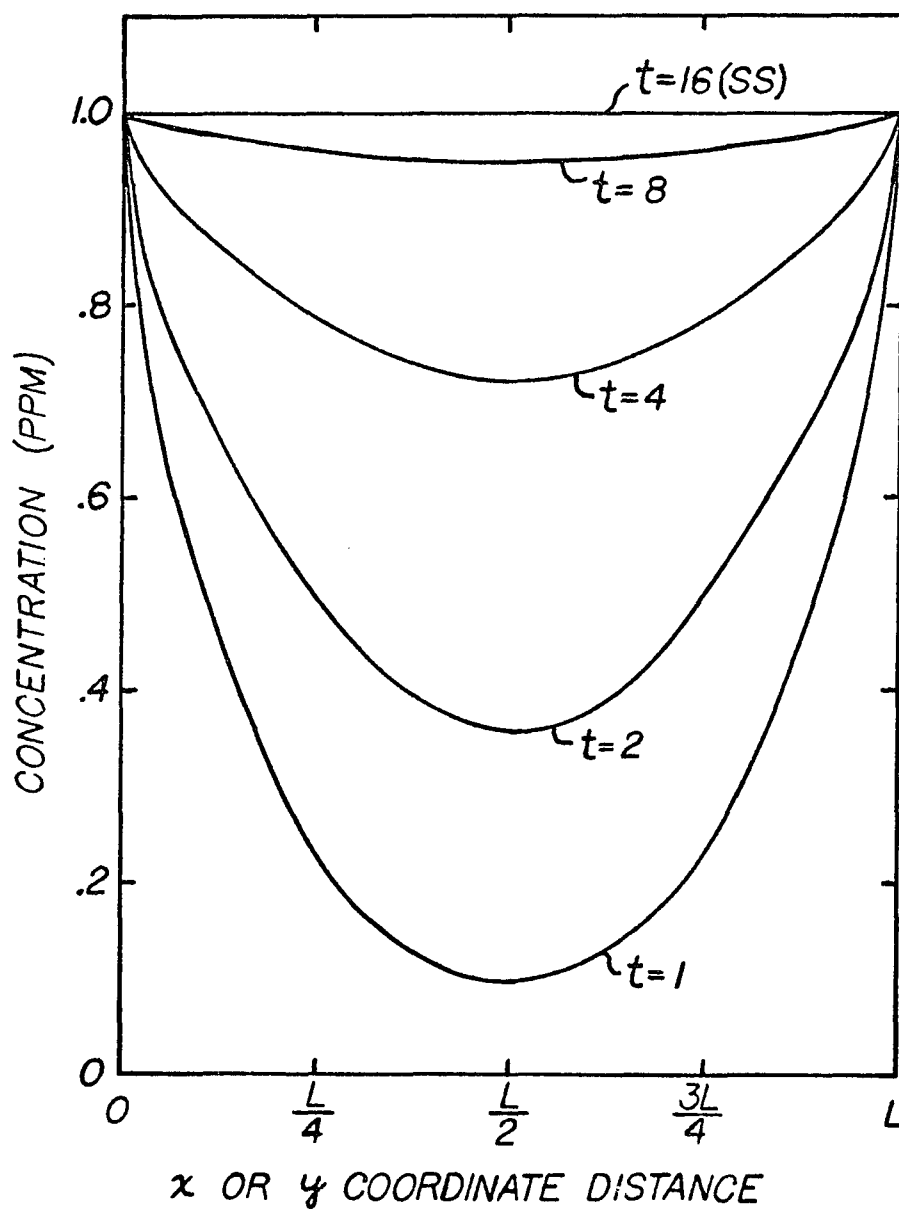
Fig. 5.6 Concentration Distribution as a
Function of Time for Case A
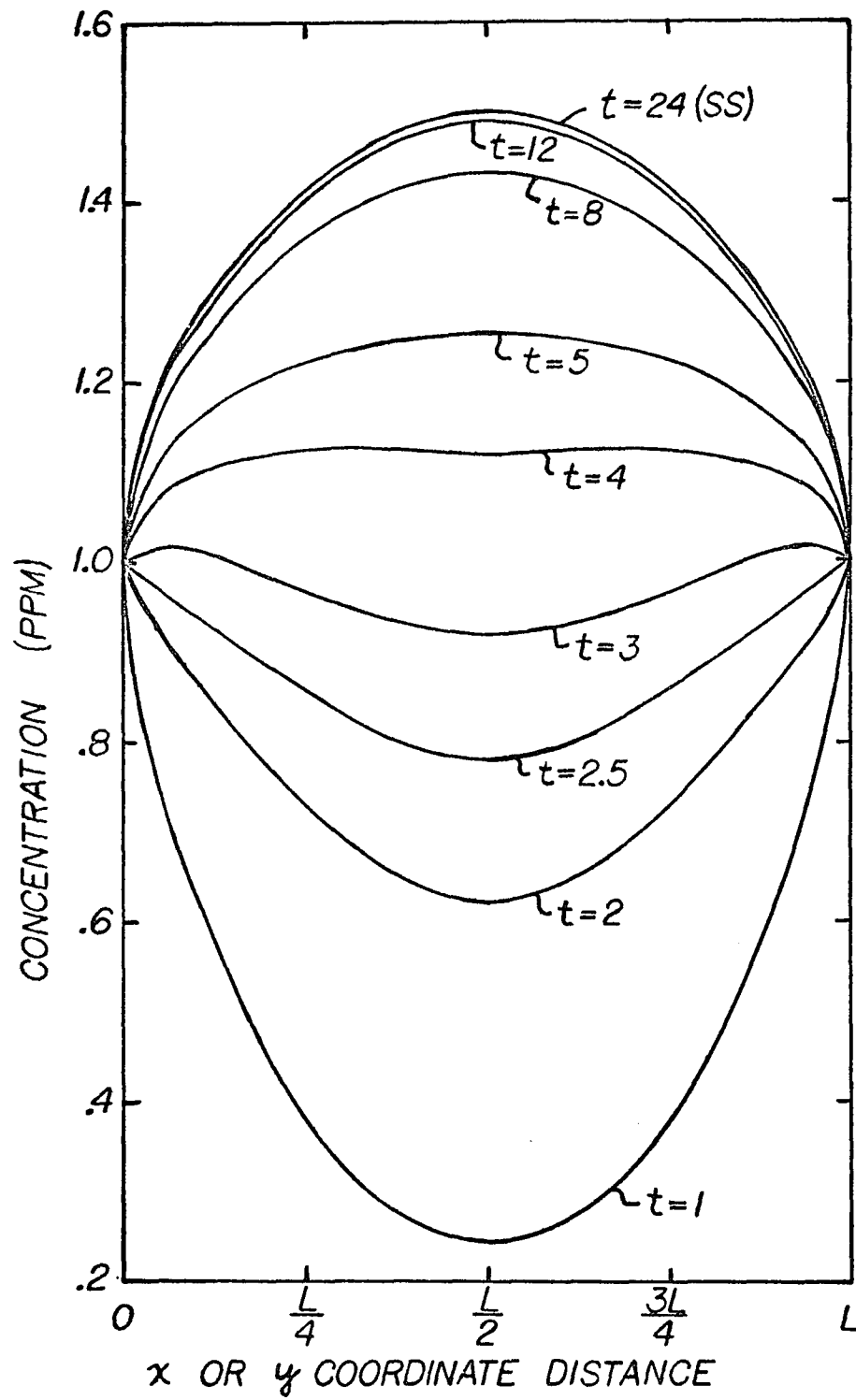
Fig. 5.7 Concentration Distribution as a
Function of Time for Case B

Fig. 5.5. The steady state solution is reached after 24 hours for the box of 3218m length with an eddy diffusion coefficient of $80m^2/sec$.

Case B represents the circumstances under which a calm or stagnation meteorological condition occurs with a constant emission source; note, however, that the concentrations of the pollutant do not continue to build up but reach some steady state distribution after about one day. The input parameters for this case are a mixing height of 500m, a source strength of 2.2×10^7 g/day and the same box length and diffusion coefficient mentioned earlier.

Case C: The third case includes transient diffusion with a constant source as in Case B, but now includes convection in the y direction with a mean wind speed U. This case is mathematically represented by the following partial differential equation:

$$\frac{\partial C}{\partial t} + U \frac{\partial C}{\partial y} = K_H (\frac{\partial^2 C}{\partial x^2} + \frac{\partial^2 C}{\partial y^2}) + \frac{S}{V} \tag{5.6}$$

The solution of equation (5.6) physically represents the same concentration distribution in the x direction as for Case B except the final steady state distribution is less in magnitude since the pollutant is allowed to be convected out in the y direction and therefore the pollutant build up is not so great.

Figure 5.8 presents the solution in the x direction using the concentrations at the nodes along the cross-section A-A of Fig. 5.5. The time to reach steady state is much less than in Cases A and B since the advection mechanism of motion is now included. The final parabolic-like steady state distribution in the x direction is reached after 1 hour.
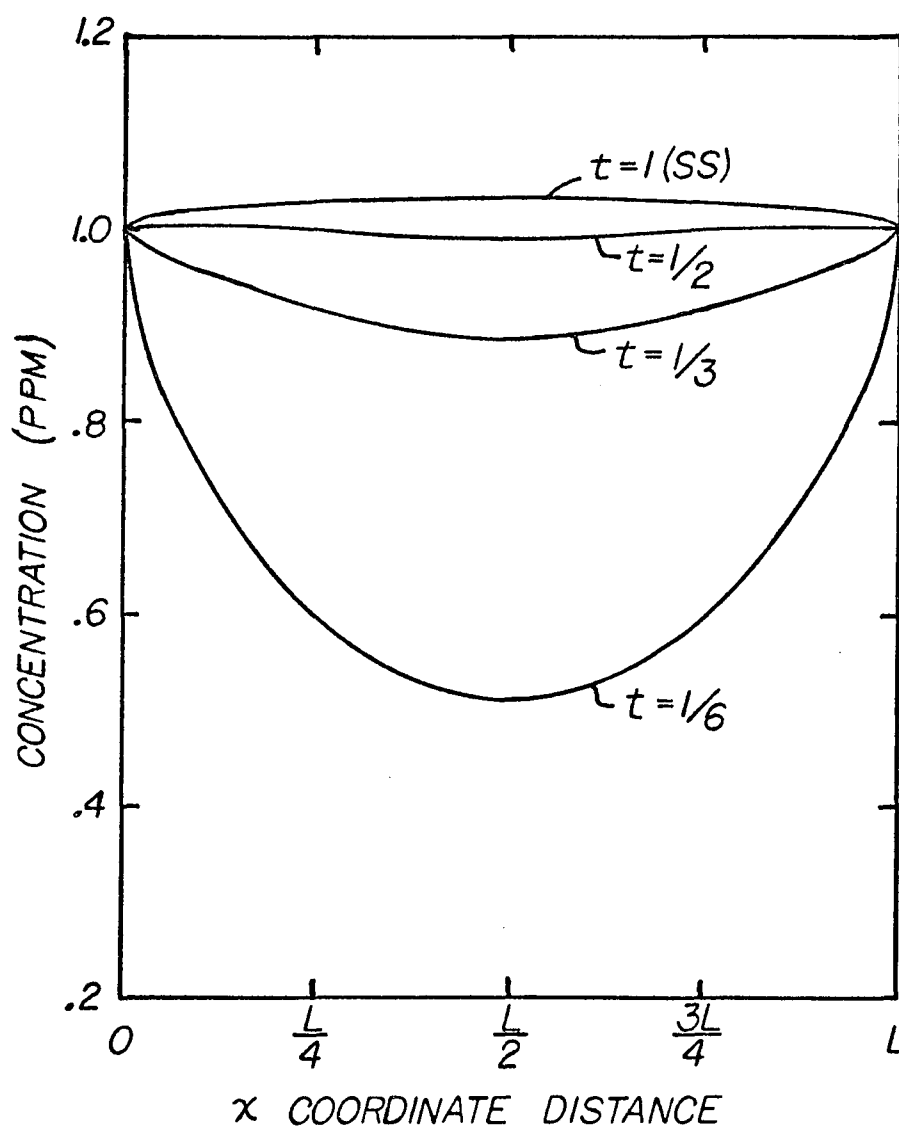
Fig. 5.8 Concentration Distribution in x
Direction as a Function of Time
for Case C

Due to the y-advection, the concentration distribution in that direction is no longer the same as in the x direction. Physically due to the non-zero wind speed, the concentration distribution is not symmetric but should be skewed in the y direction. Again this physical reasoning is substantiated by the results of Fig. 5.9, the point of zero slope is no longer at $x = \frac{L}{2}$ as in the x direction but now is closer to the downwind boundary. The concentration values used to develop Fig. 5.9 are obtained from the numerical solution of Case C for the 64 box model at the nodes along the cross-section B-B of Fig. 5.5. The input parameters used for Case C were a wind speed U of 2m/sec (4.5 mph), a mixing height H of 500m, a source strength of 2.2×10^7 g/day, a box length of 3218m, and a horizontal diffusion of 500m^2/sec.

Note that each case is progressively approaching the actual partial differential equation used in the general model throughout this report: that is equation (3.3). Using the same initial and boundary conditions with the geometry in Fig. 5.5, a solution of equation (3.3) should physically give a skewed concentration distribution in both the x and y directions, similar to Fig. 5.9, since both the x and y convective mechanisms are now included. The three cases discussed using the results from the numerical model seem to substantiate the fact that each solution does converge to a physically correct distribution, but the question of accuracy is not answered.

Accuracy

To determine the accuracy of the numerical model, it is necessary to compare the numerical results to the exact solution for some
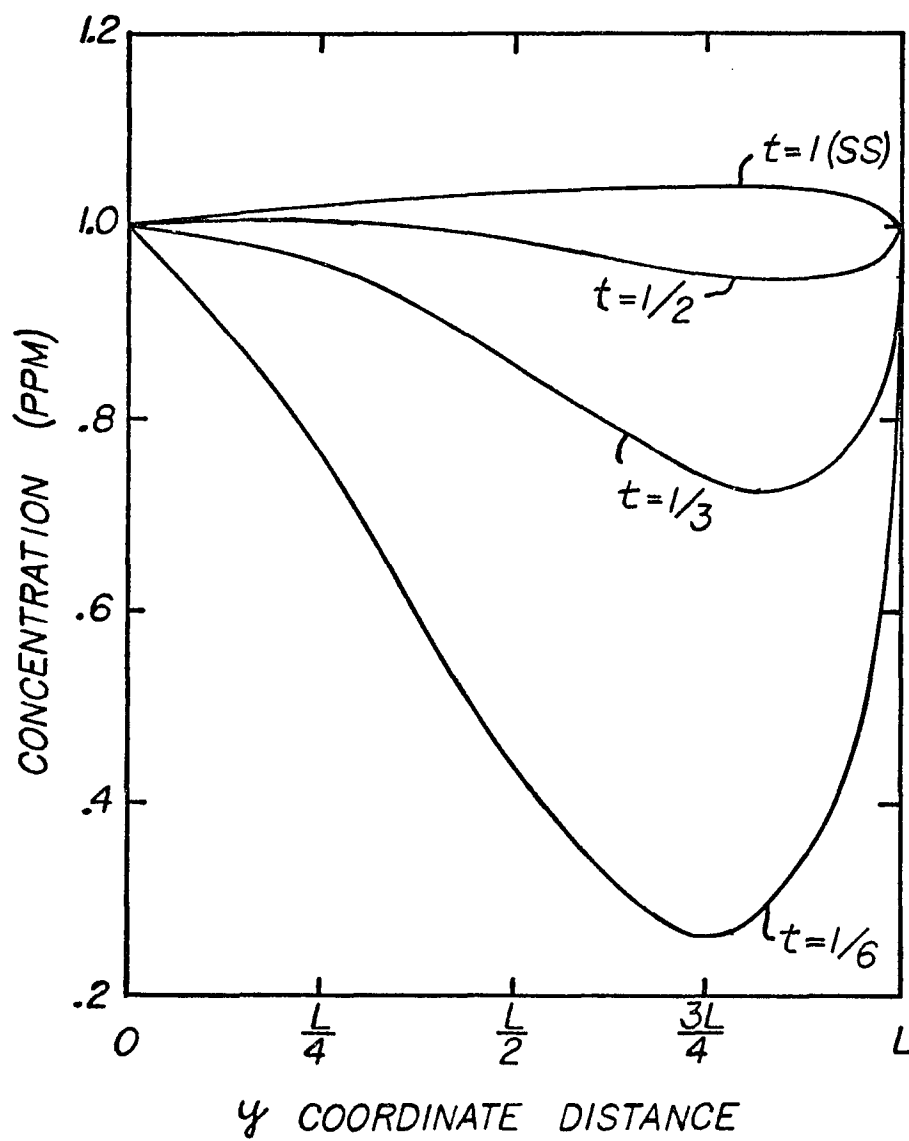
Fig. 5.9 Concentration Distribution in y
Direction as a Function of Time for
Case C

simple case. Case A is the easiest of the three problems for which an exact solution can be found mathematically. Using the initial condition and boundary conditions mentioned earlier with the geometry of Fig. 5.5, the exact solution of equation (5.4) can be found by separation of variables. The solution is given below as

$$C = C_o + (C_o - C_i) \sum_{n=1}^{\infty} \frac{16}{(2n-1)^2 \pi^2} e^{-2K_H [\frac{(2n-1)\pi}{L}]^2 t} \sin \frac{(2n-1)\pi x}{L} \cdot$$

$$\sin \frac{(2n-1)\pi y}{L} \qquad (5.7)$$

In equation (5.7), the concentrations in the x and y directions are each represented by a series of sine functions and the variable t is represented by a decaying exponential function. C_o is the boundary condition which is 1ppm, and C_i is the initial condition set at zero.

Using equation (5.7) the concentration distribution can be calculated for different times t to compare with the numerical results for Case A. A computer program was written so the summation for a large number of terms could be carried out in equation (5.7) for the concentration C. Since the numerical results used to obtain Fig. 5.6 were the values at the nodes along cross-section A-A, the x and y coordinates for the center of each node point were used as inputs x and y to obtain the concentration C from equation (5.7) for each node. The comparisons between the analytical and numerical solution are shown in Fig. 5.10. Unfortunately, the exact solution does not compare very well to the numerical solution. The reason for the divergence between the two results is that the exact solution gives the value for concentration C
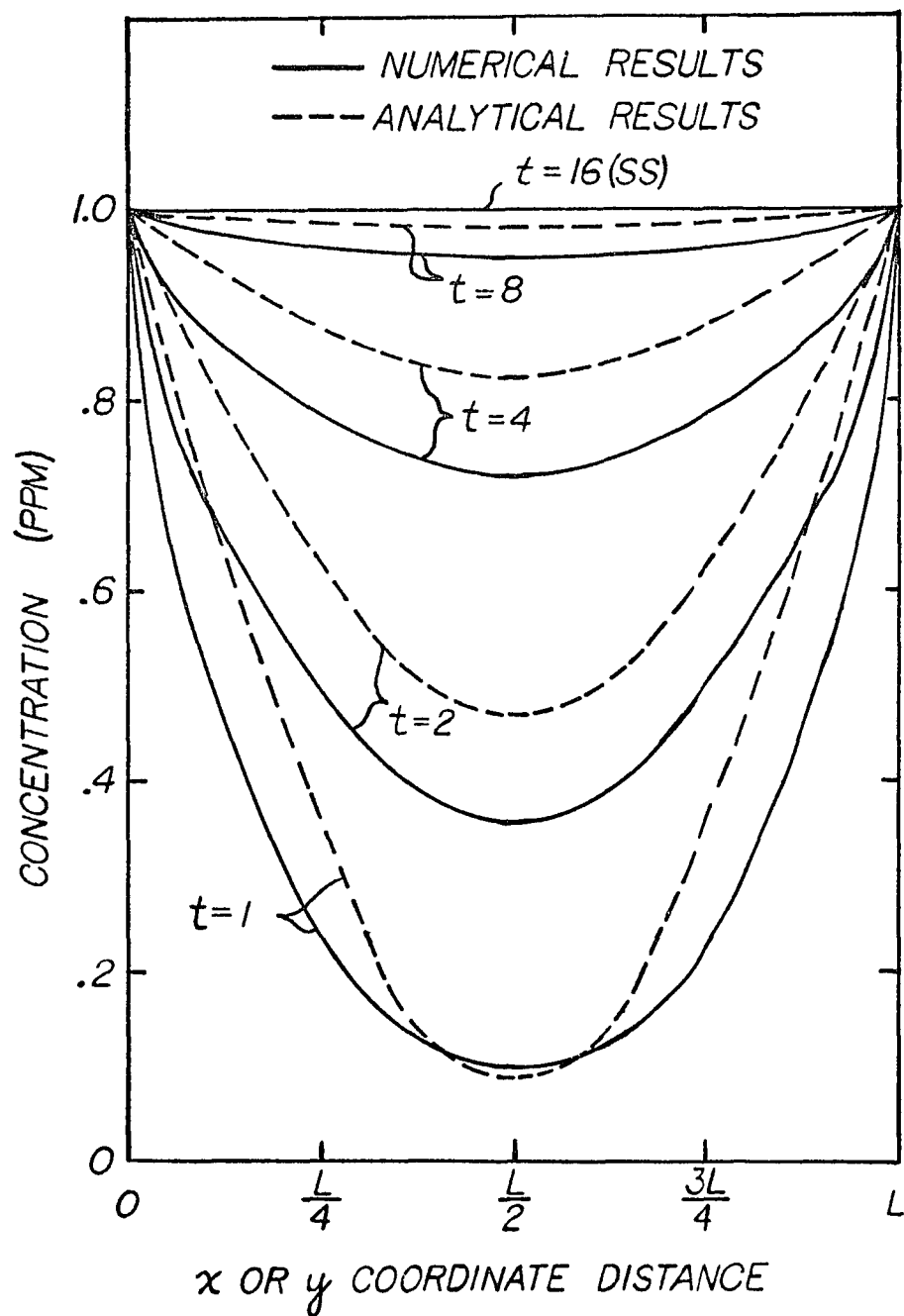
Fig. 5.10 Comparison of Analytical and Numerical Results for the Concentration Distribution for Case A

at any point (x,y) from equation (5.7), whereas the numerical solution
gives an average concentration value for some finite size box of area
$(\Delta x)^2$. Δx is the finite length of one side of a box as shown in Fig. 5.5.
In general, the numerical solution underpredicts the actual concentration
at a point. In the numerical solution, the actual steep concentration
gradients near the boundary are smoothed out so the levels build up
slower and therefore underpredict the exact solution. However, the numer-
ical solution approaches the same steady state distribution as the exact
solution as seen in Fig. 5.10.

It was found that by decreasing Δx the numerical predictions more
closely approach the exact solution. Using a grid of 16 boxes having a
Δx of L/4, the exact concentration value at a point near the center of
the grid is underpredicted by 34%. For the case of 64 boxes, Δx is L/8
and the exact solution is underestimated by 24%. This case appears at
$x = \frac{L}{2}$ in Fig. 5.10 at t = 2 hours. For the same conditions using 144
boxes with Δx equal to L/12 the numerical concentration C underpredicts
the exact concentration by 17%. The point used to compute the percent
underprediction of the exact solution is located near the center of the
grid of total area L^2. The trend for the three different Δx values shows
that as Δx approaches zero the numerical solution approaches the exact
solution. As $\Delta x \rightarrow 0$, the area of the finite box approaches a point
located at the center (x,y), so the numerical solution should become the
solution for the concentration C at a point (x,y) which is the same as
the exact solution of equation (5.7) at the point (x,y).

For Case B, an exact solution can also be found using separation
of variables. The resulting solution again verifies the fact that the

numerical solution underpredicts the exact solution. However, for this case for a finite size Δx, i.e., Δx equal to $L/8$, a different steady state distribution than the exact is obtained after a long time period. This seems reasonable since now Case B includes a constant source term, whereas in Case A there was no source so the distribution approached the constant boundary condition of $C_o = 1$ppm. For the finite box grid, the smoothing of the concentration gradient in the numerical solution effects the final steady state shape of the distribution for Case B. For the steady state case the exact solution of equation (5.5) reduces to

$$C = C_o + \frac{S}{2K_HH} \frac{x}{L} (1 - \frac{x}{L}) + SUM \qquad (5.8)$$

The term SUM in equation (5.8) is an infinite series containing hyperbolic sines and cosines in the variable y and sine functions in the variable x. Using the input parameters for Case B, the concentration at $x = \frac{L}{2}$ and $y = 0.4375\ L$ obtained from this exact solution is about 11 percent greater than the corresponding value for the numerical solution for a finite Δx of $L/8$. Again as $\Delta x \to 0$, the values from the numerical solution should approach the exact solution more closely.

The results for Case C again confirm the information already obtained concerning the comparison between the exact solution and the numerical solution for Cases A and B. It appears that the comparison between measured data and numerical predictions is going to depend on the magnitude of the emission source near the point of measurement, along with the mesh size Δx used in the numerical model. This reasoning establishes the idea for the use of the macro-model to predict levels in areas of low source strength and the use of the micro-model to predict

concentrations under higher source strength conditions. Since the numerical accuracy increases as Δx approaches zero, decreasing Δx may better the comparison between numerical and measured data for both the macro- and micro-models. However, the lower limit for decreasing Δx is dependent on the magnitude of the mixing height H. Since each box or cell is assumed to be uniformly mixed, the box must be long enough in x such that ground sources of carbon monoxide can mix in z up to the mixing depth H.

The conclusion discussed in this section of the chapter may be helpful in explaining the comparison or lack of comparison between the experimental and numerical results presented in the following chapters.

CHAPTER 6

NUMERICAL RESULTS

Applying the multi-box model developed in Chapter 3 to the air-shed, which is visualized in Fig. 6.1, one can predict the concentration field for carbon monoxide for varying meteorological conditions. Results are obtained for both the macro- and micro-model. The concentration distribution is determined as a function of time using actual weather data obtained from the Tucson Weather Service. The numerical results will be compared in Chapter 8 to actual measured carbon monoxide data taken in the Tucson area.

Single Box Model

The simplest model representing the Tucson area is a one box model. This model can be used to calculate a single value for the pollutant concentration which is then assumed to apply everywhere in the one box. As discussed in Chapter 3, the solution for a chemically conservative pollutant in a large single box has two parts. Looking at the steady state solution only, the result is given as

$$C = \frac{S}{LUH} \tag{6.1}$$

which is also equation (3.11). This assumes that the concentration of the pollutant surrounding the box is zero.
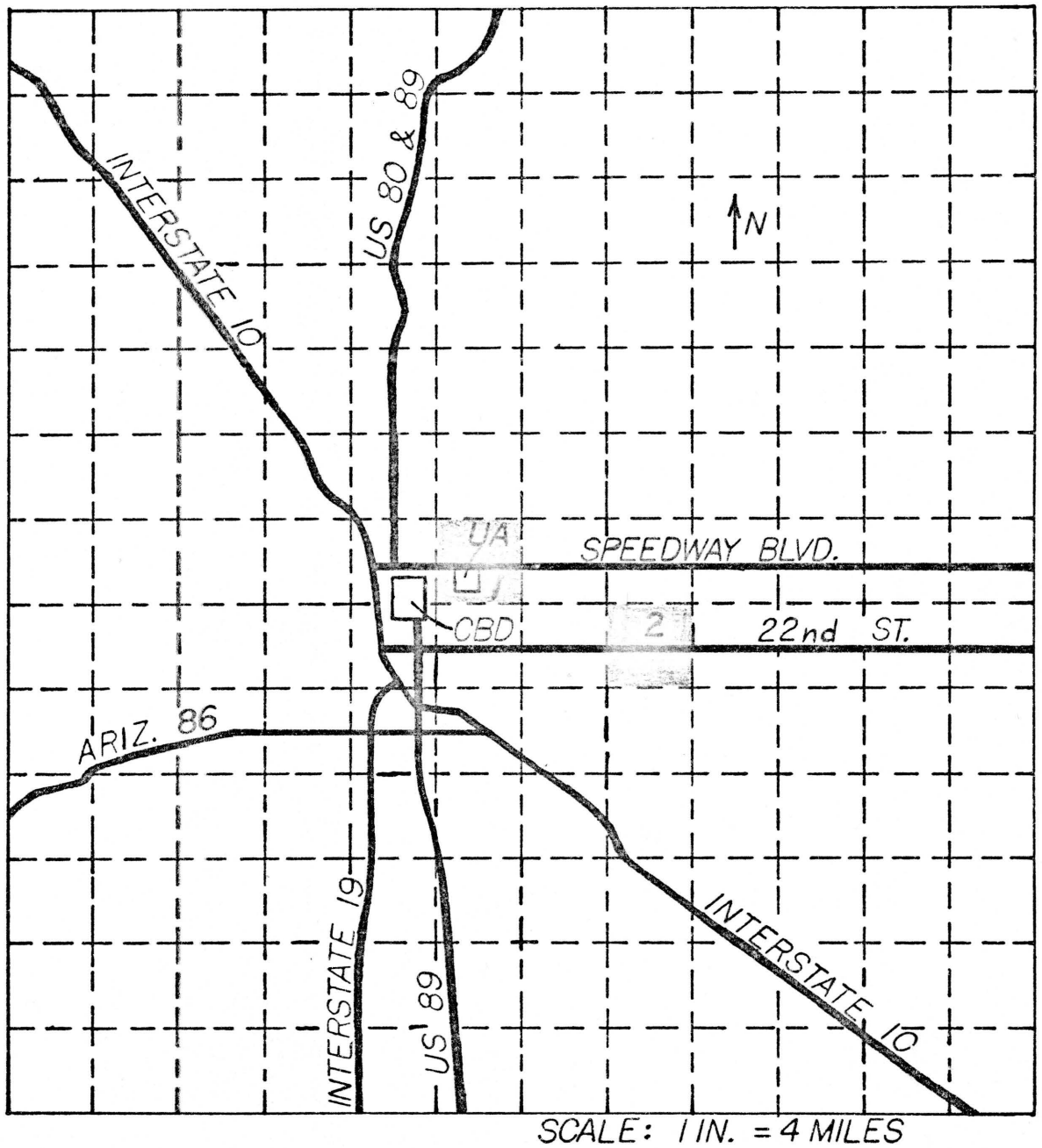
Fig. 6.1 Box Structure for the Tucson Urban Airshed

This solution is used to obtain a worst case background concentration treating the Tucson airshed as a single box. A minimum mixing height of 50 meters is assumed with a wind speed of 1.5 meters/second which is a typical wind speed observed during the 1966 Thanksgiving air pollution episode in the Eastern States (Fensterstock and Fankhauser, 1970). Assuming the wind is east or south the length of the box can be approximated as 20 miles (32.2 km). The emission rate of carbon monoxide for the airshed is 383.1 tons/day. Substituting into equation (6.1), a steady state concentration of 1.45 ppm is calculated.

This concentration of carbon monoxide is the level leaving a box 20 miles (32.2 km) by 20 miles (32.2 km) by 50 meters high on the downwind side. The assumption involved is that the carbon monoxide is uniformly mixed in the air by the time it leaves the box. This is the steady state level obtained at the downwind exit of the box after a long time. This predicted level compares quite well to background levels found in Tucson. These background readings, presented in Chapter 7, have been generally measured as less than 2.0 ppm.

An improvement over the one box model is a grid of boxes, each having a concentration given by equation (6.1). However, this approach is still a steady state technique and does not allow for time varying values of U and H. The mechanism of diffusion is still not included and if $U = 0$ the predicted concentration is infinite. All of these shortcomings are accounted for in the multi-box model developed in this study.

Macro-model

The macro-model employs a multi-box approach for predicting the concentration for each of the 156 boxes shown in Fig. 6.1 as a function of time. The model has been used to predict the concentration field for the Tucson airshed for three different days in 1974. January 3, 1974, is the low wind speed day for the entire year of 1974 and includes 6 hours of calm conditions. February 15, 1974, represents a typical winter day in Tucson, while June 5, 1974, represents a typical summer day for 1974. The meteorological data for these days are contained in Table 6.1 and Table 6.2. The information for wind speed and direction is from the Tucson Weather Service located at the International Airport. The wind speed U is in meters/sec, and the wind direction α is the angle measured counterclockwise with respect to the east, that is, $\alpha = 0^o$ is due East and $\alpha = 90^o$ is due North. α tells the direction in which the wind is blowing. This is opposite from the normal representation for wind direction, but α is treated in this way because of the technique for its input to the computer model. The mixing height data for January 3 and February 15 were obtained from radiosonde data using the technique discussed in Chapter 3. The mixing heights for June 5, 1974, appearing in Table 6.2 were taken directly from AP-101 for Tucson. The boundary conditions on the inflow side of the airshed is 1.0 ppm with an initial condition at t = 0 also of 1.0 ppm. The initial condition has little effect on the concentration distribution after a short time since this condition is put in to start the simulation at midnight when the sources are small. The convection and diffusion mechanisms work quickly to disperse

Table 6.1 Meteorological Data for Computer Model (Hour)

Hr.	January 3, 1974 U	January 3, 1974 α	February 15, 1974 U	February 15, 1974 α	June 5, 1974 U	June 5, 1974 α
1	3.1	350°	3.6	140°	2.1	190°
2	2.6	340°	2.6	110°	4.1	130°
3	2.1	0°	3.6	130°	4.6	150°
4	1.5	10°	3.1	110°	3.1	140°
5	0	--	4.1	130°	4.1	130°
6	2.1	100°	5.7	120°	4.1	110°
7	0	--	6.2	130°	4.6	120°
8	2.6	70°	5.2	120°	4.1	110°
9	1.5	90°	5.2	120°	5.2	110°
10	3.6	90°	4.1	140°	2.1	140°
11	2.6	120°	1.5	140°	2.1	330°
12	0	--	2.6	110°	2.1	320°
13	2.1	60°	2.1	190°	3.6	0°
14	2.6	310°	2.6	300°	6.7	340°
15	1.5	190°	3.6	250°	5.2	350°
16	2.6	20°	3.6	320°	6.7	30°
17	3.1	330°	3.6	300°	7.7	350°
18	3.1	300°	3.6	290°	7.7	330°
19	2.1	350°	3.1	320°	6.7	350°
20	3.6	10°	0	--	4.6	0°
21	0	--	3.6	90°	4.1	0°
22	0	--	3.1	140°	3.6	10°
23	0	--	3.1	130°	3.1	20°
24	1.5	70°	3.1	90°	3.6	180°

Table 6.2 Meteorological Data for Computer Model - Mixing Heights

Mixing Height	January 3, 1974	February 15, 1974	June 5, 1974
Minimum	80 m	80 m	200 m
Maximum	1300 m	1300 m	2000 m

the initial concentration. These conditions are used in all macro-model results; however, other values could have been used if appropriate.

For January 3, 1974, the simulation of hour 23 (10 to 11 pm) predicted the maximum concentrations in the airshed grid for that day. An isopleth map of 1-hour average carbon monoxide concentrations for the Tucson airshed for hour 23 of January 3, 1974 (low wind speed case), is presented in Fig. 6.2. This figure was obtained using the predicted ground-level carbon monoxide concentration for each box from the macro-model. The readings are all in parts per million (ppm). The maximum level of 4.0 ppm occurs along Speedway Boulevard with its center very near to Alvernon Boulevard. The wind direction previous to hour 23 was generally from the west followed by calm conditions. These meteorological conditions explain the higher levels obtained to the east of town. Note these readings each represent an average ground level 1-hour carbon monoxide level for a box of 2 miles by 2 miles.

Figure 6.3 presents the 24 hour distribution for January 3, 1974, for two different boxes in the airshed. These carbon monoxide levels are ground-level values. The concentration distributions are for the two
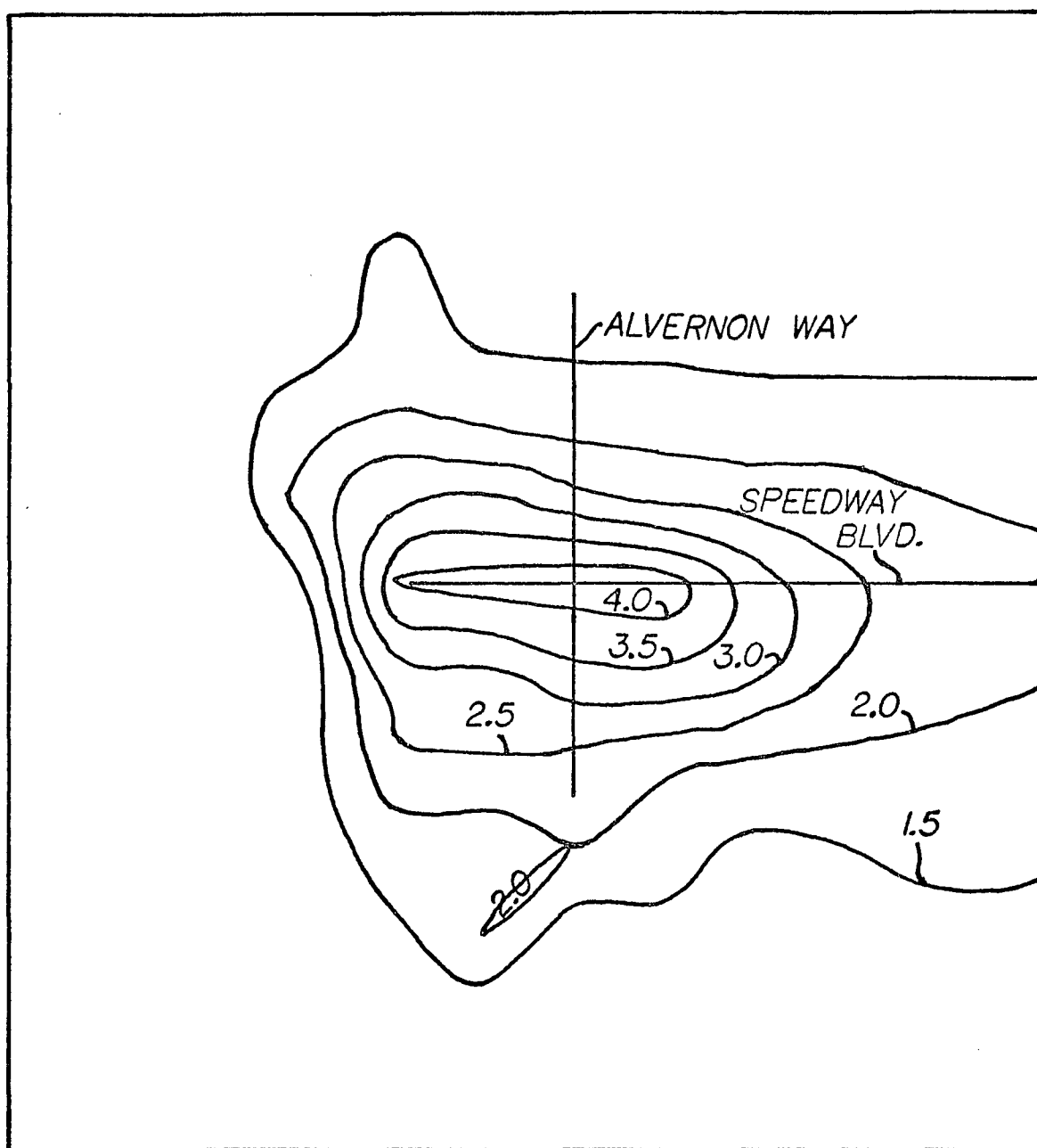
Fig. 6.2 An Isopleth Map of 1-hour Average Carbon Monoxide Concentrations from 10 to 11 pm for January 3, 1974
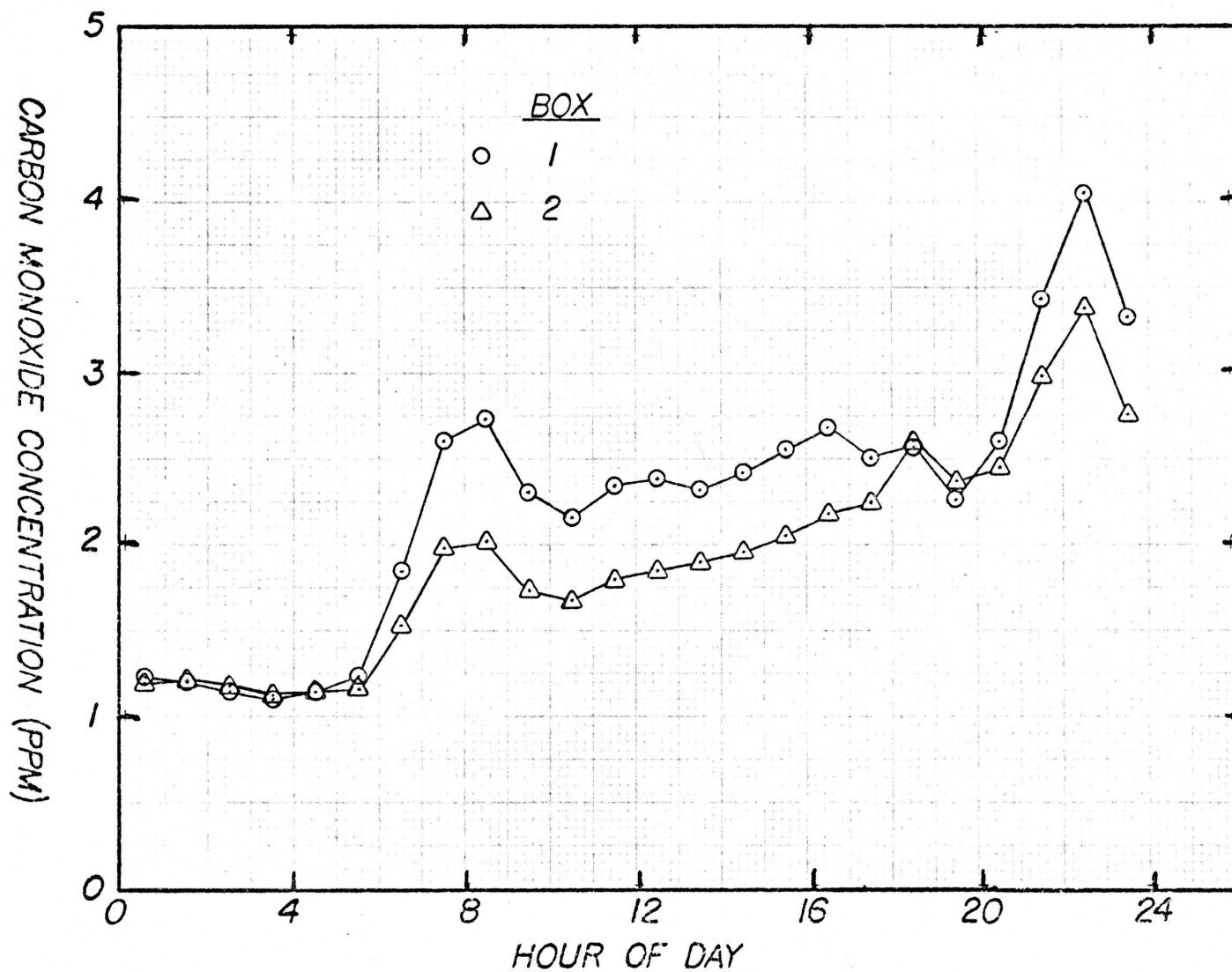
Fig. 6.3 Carbon Monoxide Concentration Distribution for January 3, 1974 for Two Different Boxes in the Airshed

shaded boxes marked 1 and 2 in Fig. 6.1. The box marked 1 represents the cell in which The University of Arizona is located. This box is bounded on the west by First Avenue, on the north by Grant, on the east by Country Club and on the south by Broadway. The box marked 2 is centered about the intersection of 22nd Street and Craycroft. This box is bounded on the west by Swan, on the north by Broadway, on the east by Wilmot and on the south by Golf Links.

The box in which the University is located has the highest levels in the airshed for the simulation of January 3, 1974. Locations such as the Central Business District, Broadway at Alvernon, and Grant at Campbell have slightly lower concentrations than the values for the University area. Concentrations at other locations such as Oracle at Prince, 22nd at Kolb, and the Tucson International Airport are much less when compared to the carbon monoxide levels in the University area. Note that the maximum CO levels for the two boxes in Fig. 6.3 occur at the 23rd hour as mentioned earlier. The results plotted in Fig. 6.3, and all remaining plots, graph the 1-hour average carbon monoxide levels at the half-hour in which the hour average concentration occurs.

Figure 6.4 shows the comparison of 24 hour ground-level carbon monoxide distributions for the box containing The University of Arizona for January 3, 1974, and February 15, 1974. The graph compares the CO distribution for a typical winter day to that of a low wind speed winter day. The results for January 3, 1974, are greater than for February 15, 1974, since the wind speed is an important parameter in atmospheric dispersion. The calm conditions during January 3, 1974, cause the larger morning CO peak and also cause the late evening peak. This is
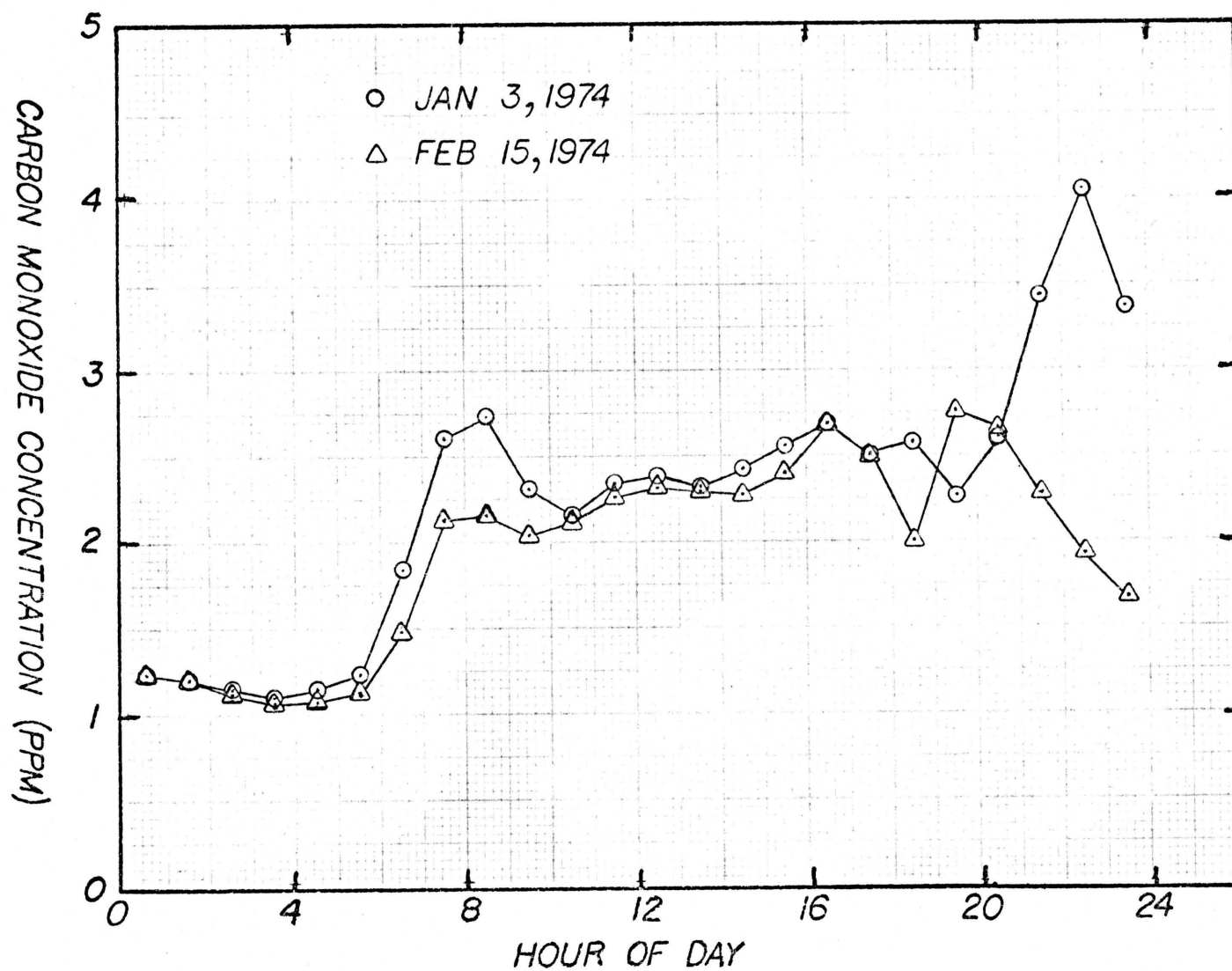
Fig. 6.4 Carbon Monoxide Concentration Distribution for January 3, 1974 and
February 15, 1974 for the University Area Box

because the mixing height is low, in spite of the fact that the vehicle traffic is also low. The CO levels in the evening drop off for February 15, 1974, since there is a wind speed of 3 meters/second to keep the pollutant from accumulating.

A comparison of the carbon monoxide distribution for a typical winter day and summer day is made in Fig. 6.5 using the University area box. The ground-level CO values for both days are similar except that after the evening rush hour peak the CO level drops off for June 5, 1974. This is due to the fact that a strong radiative inversion does not occur in the early evening hours in the summer. Such an inversion helps to trap the pollutant. During the winter after sunset the mixing height is quite low and in the case of February 15, 1974, there is a calm condition at hour 20, which is the cause of the peak between 7 and 9 pm. The high pollutant levels are dependent on a combination of wind speed and mixing height. The product of these two variables is called the ventilation rate. This product is sometimes just called the "Ventilation" and is considered as the flow through a 1 meter wide column of height H (AP-45).

The results presented thus far have been ground-level concentration values obtained by assuming a logarithmic profile for the concentration in the vertical direction. The ground-level concentration is calculated using equation (3.24) where $\bar{C}$ is the average carbon monoxide value for the box of height H. Figure 6.6 plots the ground-level concentration distribution and the average concentration $\bar{C}$ distribution for February 15, 1974, for the University area box. The results show that when the mixing height is large the ground-level concentration is markedly
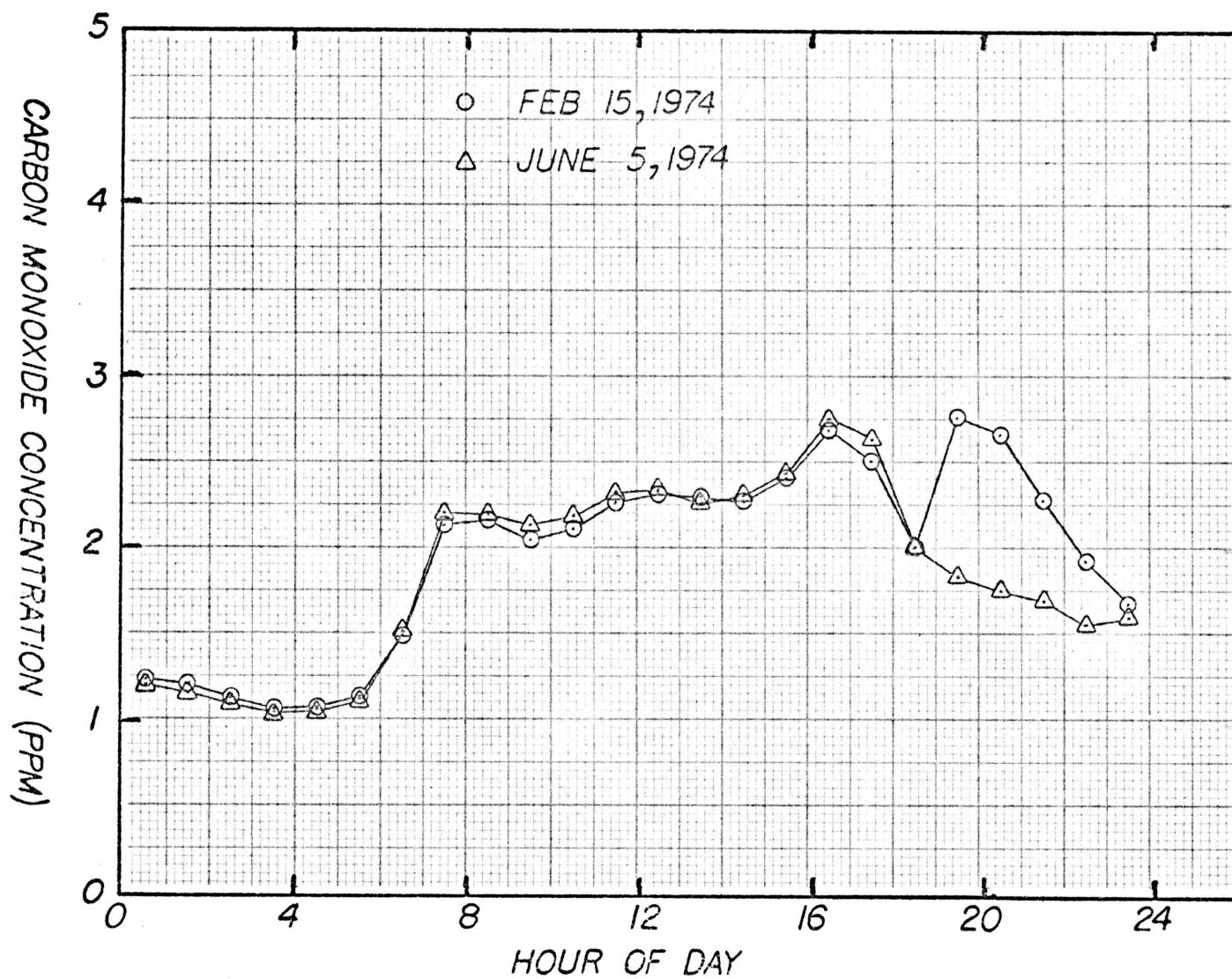
Fig. 6.5   Carbon Monoxide Concentration Distribution for February 15, 1974 and June 5, 1974 for the University Area Box
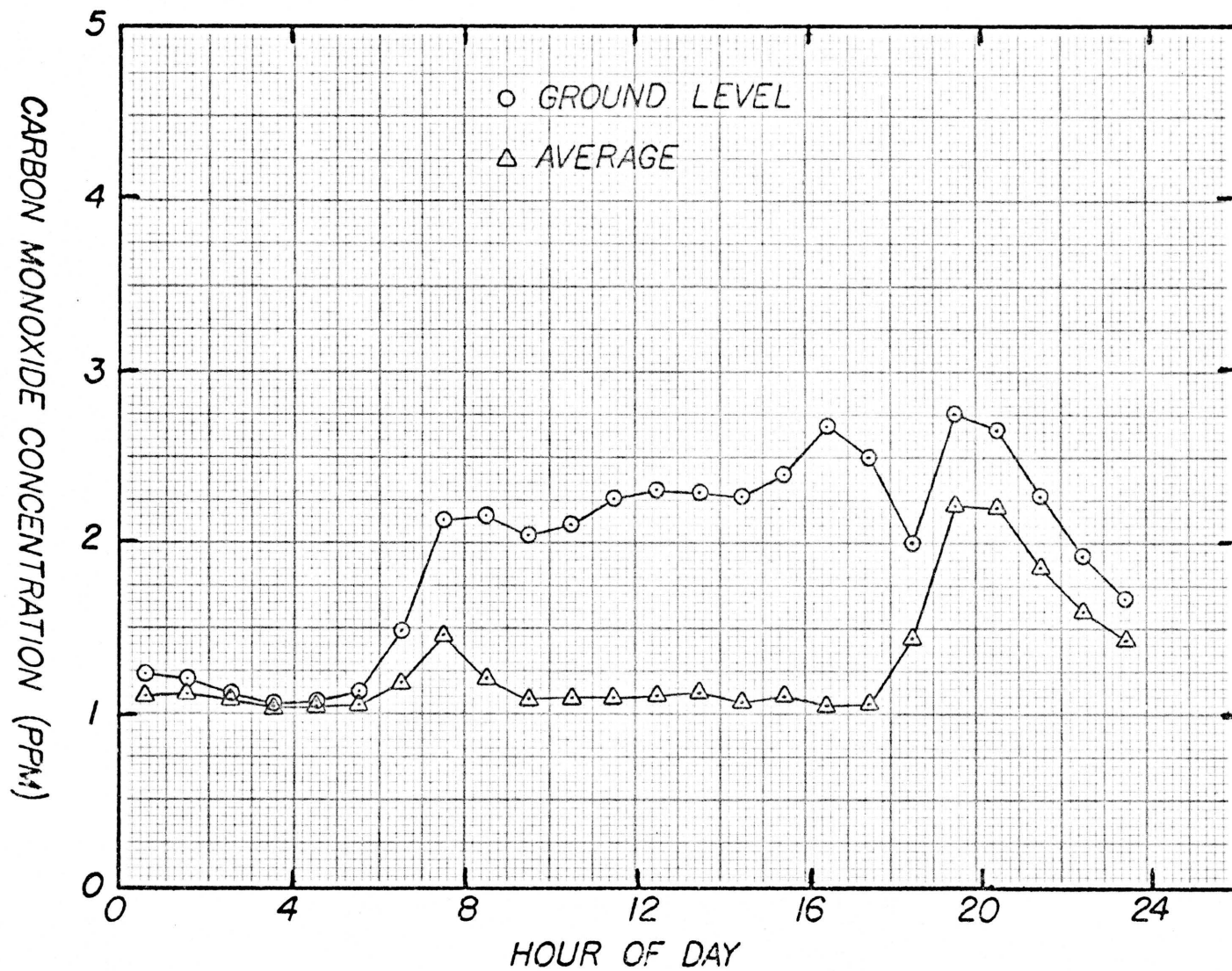
Fig. 6.6   Ground-level and Average Carbon Monoxide Concentration Distributions
for February 15, 1974 for the University Area Box

larger than the average value. In the morning and the evening, the mixing height is small so the two concentrations are similar.

All the previous results presented were obtained using the macromodel representing the entire Tucson airshed. These concentrations represent 1-hour average values for a box having a base of 4 square miles at the ground. These predictions can not be correlated to measured carbon monoxide data taken at or near areas of high traffic density; however, the results can be expected to agree with data from areas of lower traffic density. The results from the macro-model can be used to predict the areas of the airshed in which high levels of carbon monoxide can be expected. This conclusion can be drawn from the isopleth map of Fig. 6.2.

Micro-model

The micro-model is developed so that comparison can be made with carbon monoxide levels in residential areas close to centers of high traffic density. The micro-model takes a single box from the macro-model and subdivides it so that carbon monoxide concentrations can be predicted for each subdivided box in the macro-box. The initial condition used at t = 0 is 1.0 ppm. The boundary conditions are obtained from the macro-model results and are employed as discussed in Chapter 5. The micro-model predicts ground-level carbon monoxide concentrations as a function of time for each subdivided box.

The micro-model is initially applied to the box which encompasses The University of Arizona. This macro-box is subdivided into 64 boxes each having a size of 1/4 mile by 1/4 mile and a base area of 1/16 mile squared. The concentration distribution for the micro-box having the

maximum levels is compared in Fig. 6.7 to the distribution for the macro-box for January 3, 1974. The figure shows that the micro-model solution is always greater than or equal to macro-model results. The difference between the two models is small when the mixing height is low since under these conditions the pollutant is well mixed in the macro-model so the effect of using the micro-model is not so significant. The difference in magnitude between the two models is never very large due to the fact that both models predict ground-level carbon monoxide concentrations for some relatively large finite area. The results of either model cannot be compared directly to measured data at a single point in high traffic density areas.

Stadium Event

The macro- and micro-models can be useful in predicting area-wide increases in carbon monoxide levels due to a large increase in traffic such as would occur during a stadium event on the University of Arizona campus. During the evening of November 30, 1974, the football stadium was in use for the game between University of Arizona and Arizona State University. Since this is a big event, the stadium was filled to capacity with over forty thousand people. With this large crowd and the corresponding increase in traffic, the possibility existed for high levels of carbon monoxide being present. The macro-model was used to simulate the increased levels of carbon monoxide that the population living adjacent to the area would be exposed to due to the large influx of traffic arriving and then leaving the stadium area.
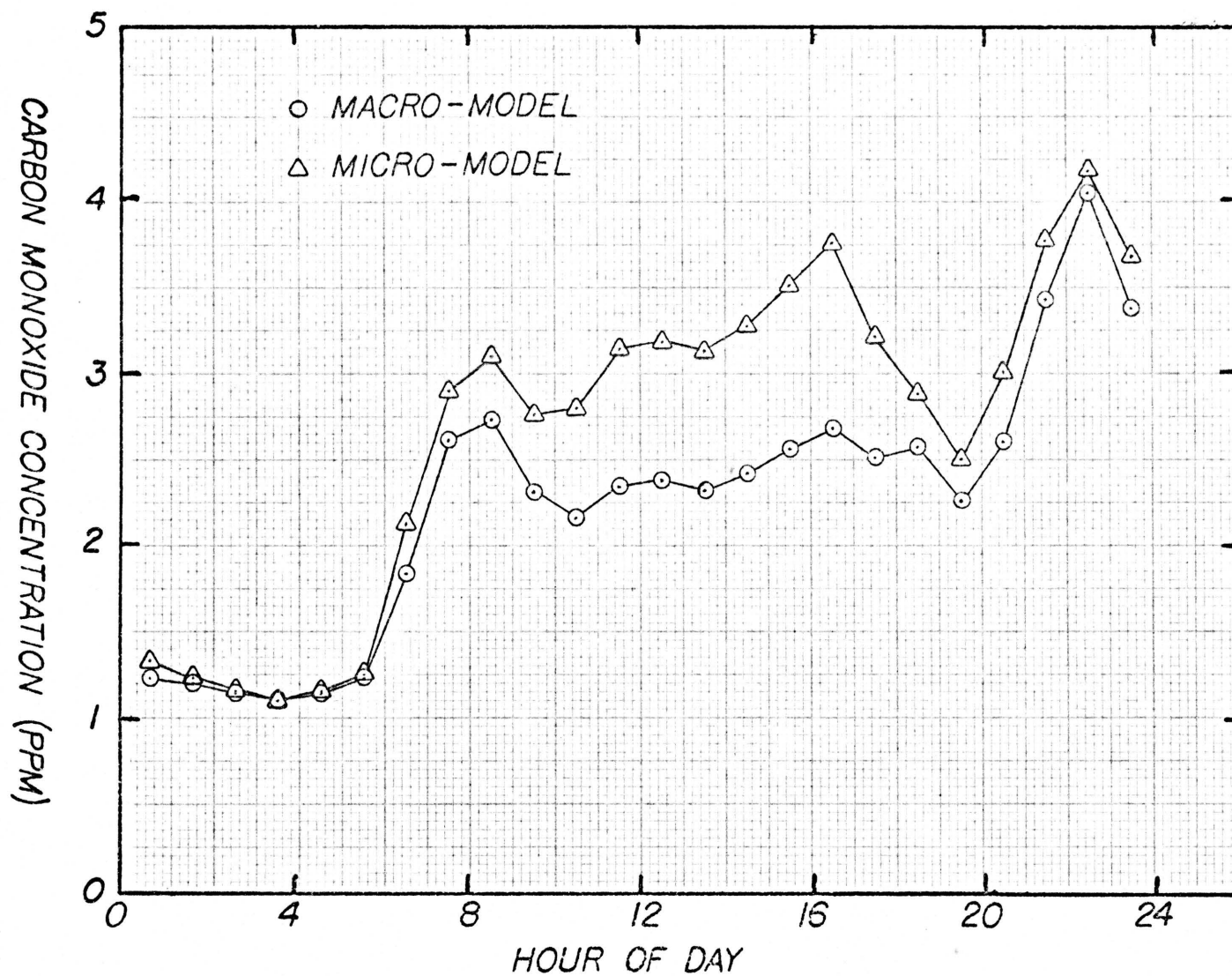
Fig. 6.7 Carbon Monoxide Concentration Distribution for January 3, 1974 for the
University Area Box Using Both the Macro- and Micro-model

The meteorological data from the Tucson International Airport was used as an input to the macro-model to simulate the carbon monoxide distribution for that day. These data of wind speed, direction, and mixing height appear in Table 6.3. The carbon monoxide levels are first simulated by assuming that the event did not occur. The normal traffic distribution for the area is used for these predictions. The increased levels due to the event are calculated by now accounting for the stadium traffic which directly affects the source strength of carbon monoxide used as an input parameter for the macro-model.

Since the crowd at the football game was in the vicinity of forty thousand it was assumed that there were 20,000 vehicles in the University area for the event. The game started at 7:30 p.m. so the increased arriving traffic was accounted for between 6:00 p.m. and 7:45 p.m. The game ended at approximately 10 p.m. so the traffic leaving the area occurred between 10 and 11 p.m. This criterion was used in determining the time of increased source strengths for the model. The traffic leaving and arriving the stadium was assumed to be traveling mainly on Speedway, Broadway, 5th Street, and Campbell Avenue with other access streets used when nearing the stadium parking areas. Along with the University area box, the increased traffic was also accounted for in the surrounding macro-boxes.

Using the assumptions mentioned above, the carbon monoxide distribution for November 30, 1974, is calculated using the macro-model for these two situations. The predictions are made using meteorological data in Table 6.3 for the hypothetical case of no football game and for the actual conditions which did occur. The comparison between the two cases is shown in Fig. 6.8. Note the large increase in carbon monoxide levels

Table 6.3 Meteorological Data for November 30, 1974

HR	U	α	HR	U	α
1	1.5	110°	13	5.2	150°
2	4.1	120°	14	5.7	190°
3	3.6	140°	15	4.1	190°
4	3.1	150°	16	2.1	220°
5	3.6	150°	17	1.5	250°
6	3.1	150°	18	1.5	250°
7	2.6	170°	19	2.6	330°
8	2.6	100°	20	1.5	150°
9	2.1	130°	21	1.5	160°
10	4.1	110°	22	1.5	330°
11	3.1	90°	23	2.1	210°
12	7.2	150°	24	2.6	90°

	Minimum	Maximum
Mixing Height	100m	1000m
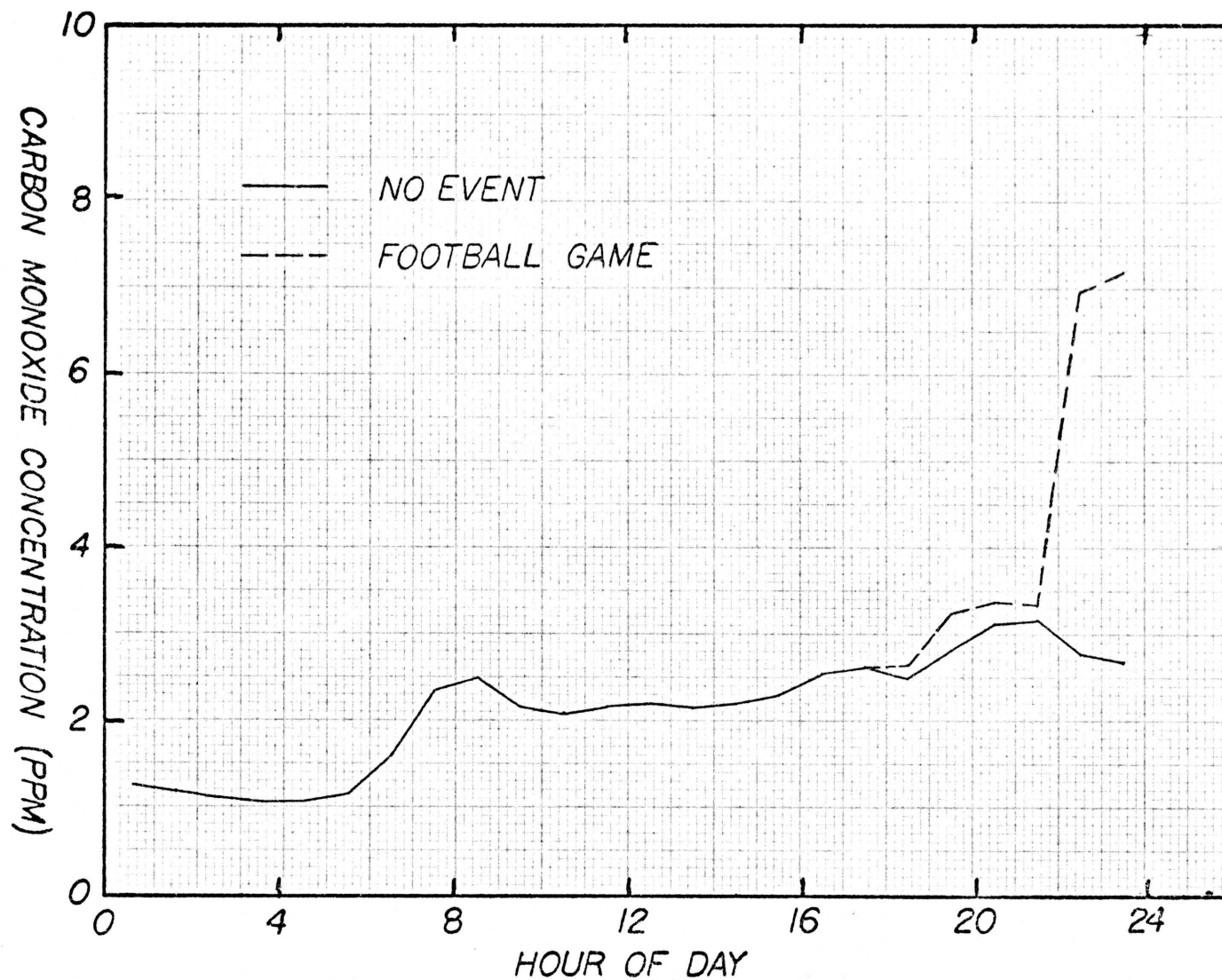
Fig. 6.8 Carbon Monoxide Concentration Distribution for November 30, 1974 with and without the Stadium Traffic Due to the Football Game

which occurs between 10 and 12 p.m. and which corresponds to the traffic leaving the stadium area. The same increase is not apparent before the game due to the arriving traffic. The reason for the small effect of the arriving traffic is two-fold. First of all, the wind speed was slightly greater during hour 19, the first hour of arriving traffic, than hour 23. The second reason is the fact that the source of carbon monoxide due to the large traffic was handled over approximately a two-hour period before the game, whereas after the game the increase traffic source occurred during the hour immediately following the game. Also worthy of note is that the additional source due to the stadium traffic was only about 80% of the normal carbon monoxide source for the macro-box for hours 19 and 20. However, for hour 23 the source of carbon monoxide due to the stadium traffic was about 2.5 times the normal source for the macro-box encompassing the University area. Therefore, this large additional source is quite significant in explaining the large peak in carbon monoxide due to the traffic leaving the stadium area.

Figure 6.8 shows that an area wide increase of about 4.5 ppm occurs due to the traffic leaving the football game over the normal level which would have existed. The predicted results in Fig. 6.8 plot the average concentrations for one hour which are determined by averaging six 10 minute concentrations calculated during each hour in the macro-model. This time step of 10 minutes is used for all the macro-model results. The one hour average levels are of interest since EPA has set a one hour average carbon monoxide level of 35 ppm. However, the results of the last two hours, 23 and 24 in Fig. 6.8, do not show the true picture of the concentration distribution which corresponds to the traffic leaving

the area. Figure 6.9 shows this variation in the carbon monoxide levels by plotting the ten minute average values for the two cases simulated for November 30, 1974, from 10 to 12 p.m. The source of carbon monoxide due to the statium traffic was put into macro-model between 10 and 11 p.m., so therefore the total source effect is accounted for by 11 p.m. which corresponds to the peak seen in Fig. 6.9. The carbon monoxide continues to build between 10 and 11 p.m. due to the low wind speed and mixing height. After 11 p.m., the CO levels then decrease since the source is now low. Figure 6.8 is unable to show the significant decrease in CO level since it plots the average value for 1 hour. However, if the simulation were continued for another hour, the 1-hour average level would decrease from the previous hour.

A one hour level of 7.0 ppm is approximately the maximum concentration of carbon monoxide that people living in the vicinity of the stadium were exposed to on the evening of the football game, November 30, 1974. This is not, however, the carbon monoxide level that the people attending the game were exposed to while walking to or from the stadium. These levels would be significantly higher since people walking adjacent to traffic in the stadium area would be directly exposed to the auto exhaust.

1980 Projection

The previous results were computed with an emission rate of carbon monoxide obtained using an emission inventory for the year 1973. In order to project what the carbon monoxide levels might be in 1980, it is necessary to develop an emission inventory for that year. Since the EPA
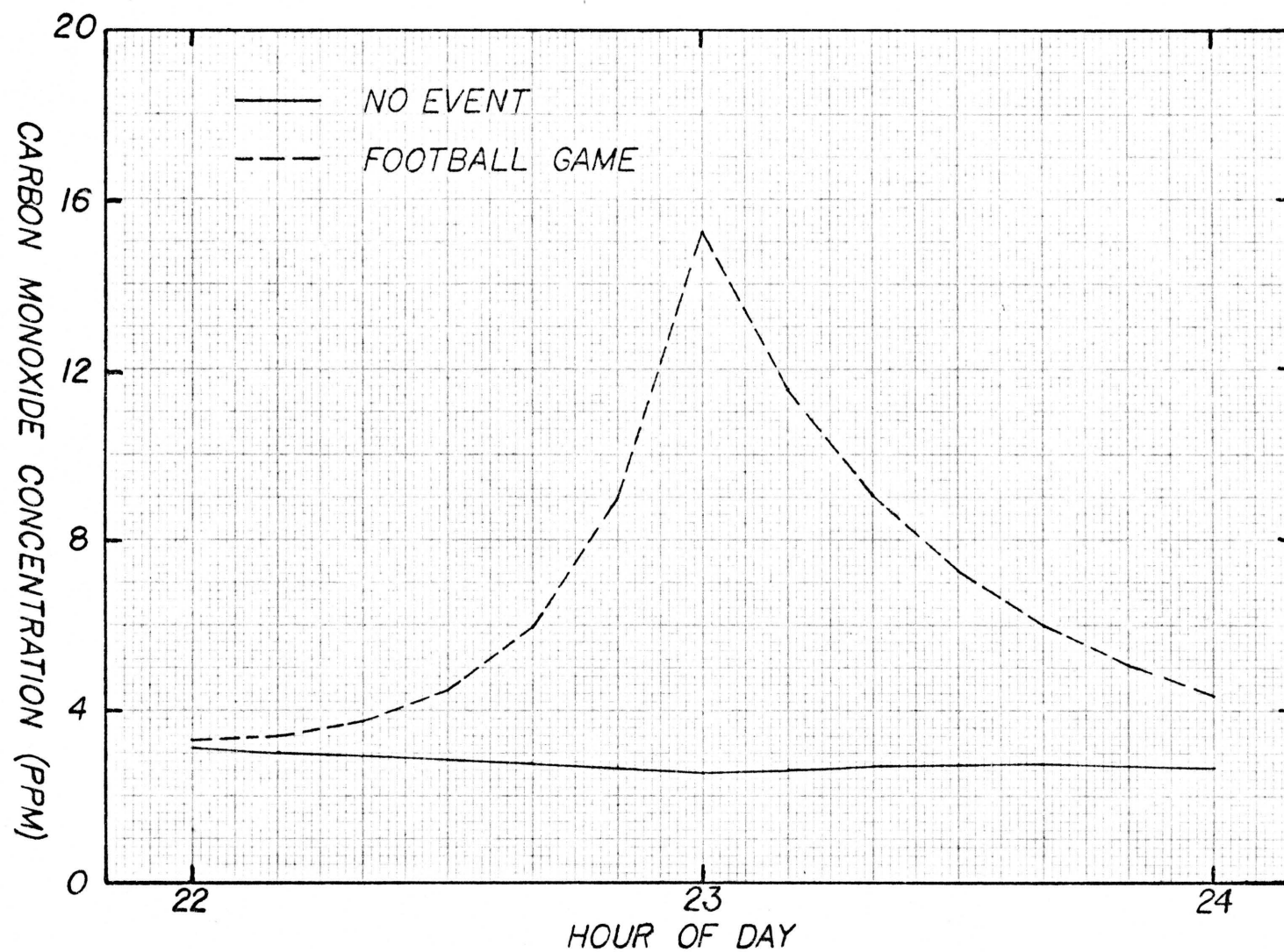
Fig. 6.9 Carbon Monoxide Variation for Ten Minute Average Values from 10 to 12 pm
for November 30, 1974 with and without the Stadium Traffic

has required the automobile companies to meet stringent requirements for carbon monoxide by 1976, the weighted emission factor for the motor vehicle population for 1980 is less than for 1973. However, in 1980, there will be more motor vehicles on the road and therefore more vehicle miles traveled than in 1973. The product of the two pieces of information is necessary to calculate the emissions rate of carbon monoxide for 1980.

Using the EPA report AP-42, it is possible to calculate a weighted emission factor for carbon monoxide for light-duty gasoline powered vehicles for 1980. In a similar fashion as before using equation (4.1) a result of 24.6 grams/mile is obtained. This value is obtained by using the same vehicle age distribution as employed in Table 4.1. The emission factor and age deterioration factor for each vehicle year is taken from AP-42. The weighted emission factor for heavy-duty gasoline powered vehicles for carbon monoxide for 1980 is 126.4 grams/mile. This value is obtained using the same type calculations performed in Table 4.2. The emission factor for heavy-duty diesel powered vehicles for carbon monoxide is 20.4 gm/mile unchanged from the value for 1973. Using the same motor-cycle distribution for 2-stroke and 4-stroke engines as before, the weighted emission factor of carbon monoxide for motorcycles is 30.7 gm/ mile. The emission factors for 1980 have changed only for gasoline pow-ered heavy- and light-duty vehicles.

The vehicle miles traveled for 1980 are also needed in order to calculate the emission rate of carbon monoxide. Using Table 4.3, the rate of growth of VMT is seen to have been approximately 8 per cent a year. Assuming this rate of growth continues, the VMT for 1980 will be approximately 8.55×10^6 miles/day and 3.12×10^9 miles/year. This

compares with 4.98 x 10^6 miles/day and 1.82 x 10^9 miles/year for 1973. A breakdown of VMT for 1980 for motor vehicle classes is presented in Table 6.4. The same fraction of VMT for each motor vehicle class is used as for 1973. This table is similar to Table 4.4.

Using the data in Table 6.4 along with the weighted emission factor for each vehicle class it is possible to calculate the total rate of emission of carbon monoxide for 1980. The results of these calculations are presented in Table 6.5. The total emission rate of carbon monoxide projected for 1980 is 373.9 tons/day for all motor vehicles compared to 374.4 tons/day in 1973. It appears that the emission rate of carbon monoxide for 1980 will be approximately the same as for 1973. This analysis neglects the carbon monoxide emissions from aircraft, but this emission rate is insignificant when compared to the contribution due to all the motor vehicle sources.

The projection for 1980 shows that the stringent requirements by EPA for controlling carbon monoxide emissions will allow Tucson to remain unchanged from the levels of carbon monoxide now existing in the atmosphere. Therefore, the numerical results predicted for 1980 are essentially the same as those for 1973 under the same meteorological conditions. The reason for little change in the carbon monoxide emission rate is the fact that the increase in VMT is balanced by the decrease in the weighted emission factor. Since the emission rate for 1980 is the same as for 1973, the measured carbon monoxide concentrations presented in Chapter 7 should be similar to those that one might expect to measure in 1980 assuming the conditions used to calculate the 1980 emission rate are correct.

Table 6.4 Projected Vehicle Miles Traveled in the Tucson Area Divided
into Motor Vehicle Classes for 1980

Motor Vehicle Class	VMT Miles/Day	VMT Miles/Yr
Light-duty vehicles	6.75×10^6	2463.4×10^6
Heavy-duty gasoline powered vehicles	1.27×10^6	463.7×10^6
Heavy-duty diesel powered vehicles	0.33×10^6	118.6×10^6
Motorcycles	0.20×10^6	74.3×10^6
	8.55×10^6	3120.0×10^6

Table 6.5 Summary of Emissions of Carbon Monoxide
from Motor Vehicles in 1980

Motor Vehicle Class	Tons/Day
Light-duty	182.9
Heavy-duty gasoline powered	176.8
Heavy-duty diesel powered	7.4
Motorcycles	6.8
	373.9

If the vehicle growth rate decreases in the future then the projected date for which concentrations again reach 1973 values will be merely extended beyond 1980. Naturally concentrations in regions of new residential and commercial development will be increased from present-day levels. However, the calculations just presented indicate that on the average 1980 carbon monoxide concentrations will be close to those presently existing. Some actual measured carbon monoxide concentrations which presently exist in the Tucson area are given in the next chapter.

CHAPTER 7

EXPERIMENTAL DATA

The results presented in Chapter 6 show that the multi-box
model developed in this study can only predict carbon monoxide concen-
trations in areas of moderate to low traffic density since the sources
due to the motor vehicles are averaged over each box. However, in
order to analyze the entire carbon monoxide problem for Tucson meas-
ured levels existing in areas of high traffic density are required. The
combination of data and model results gives the levels that the average
population are exposed to and also determine the extent to which the
ambient standards are being exceeded at locations of heavy traffic
within the Tucson airshed.

Carbon Monoxide Measurement Technique

The most widely used technique for measuring carbon monoxide is
the nondispersive infrared (NDIR) system (Robbins, Borg, and Robinson,
1968). The NDIR method is accepted by EPA as the standard technique for
measurement of carbon monoxide in the ambient air (Federal Register,
April 1971b). In studies of CO concentrations in urban areas an instru-
ment using this method is normally designed for operation over a range
of 1-50 to 1-100ppm. The accuracy with the infrared system is about
plus or minus 0.5ppm. This technique is not the best method for use
in nonurban areas where the CO levels may be a few ppm or less. The gas

chromatography (GC) system is better suited for ambient CO measurements in a relatively clean atmosphere. The accuracy using the GC method is much better than the NDIR system; however, an instrument using the GC system is much more expensive. Due to economic considerations a Beckman model 865 instrument employing the NDIR method is used for the present ambient carbon monoxide measurements.

A schematic showing the detection system using the NDIR technique appears in Fig. 7.1. The model 865 produces infrared radiation from two separate energy sources. Once produced, this radiation is beamed separately through a chopper which interrupts it at 10 hertz. The infrared beams then pass through the two cells. The gas to be analyzed flows through the sample cell at about 1.5 scfh. The reference cell is filled with nitrogen, which does not absorb any infrared energy. During operation, a portion of the infrared radiation is absorbed by carbon monoxide in the sample gas, with the percentage of the infrared radiation absorbed being proportional to the CO concentration. A detector is used to convert the difference in energy between the sample and reference cells to a capacitance change. This capacitance change, equivalent to CO concentration, is amplified and indicated on the instrument meter.

Sampling Technique

The air samples are collected in air bags 12" x 18" having a volume of about 6 liters. The bags are made of an aluminized-mylar material called scotch-pak 20 and obtainable from Environmental Measurements, Inc. of San Francisco, California. The grab samples are obtained by
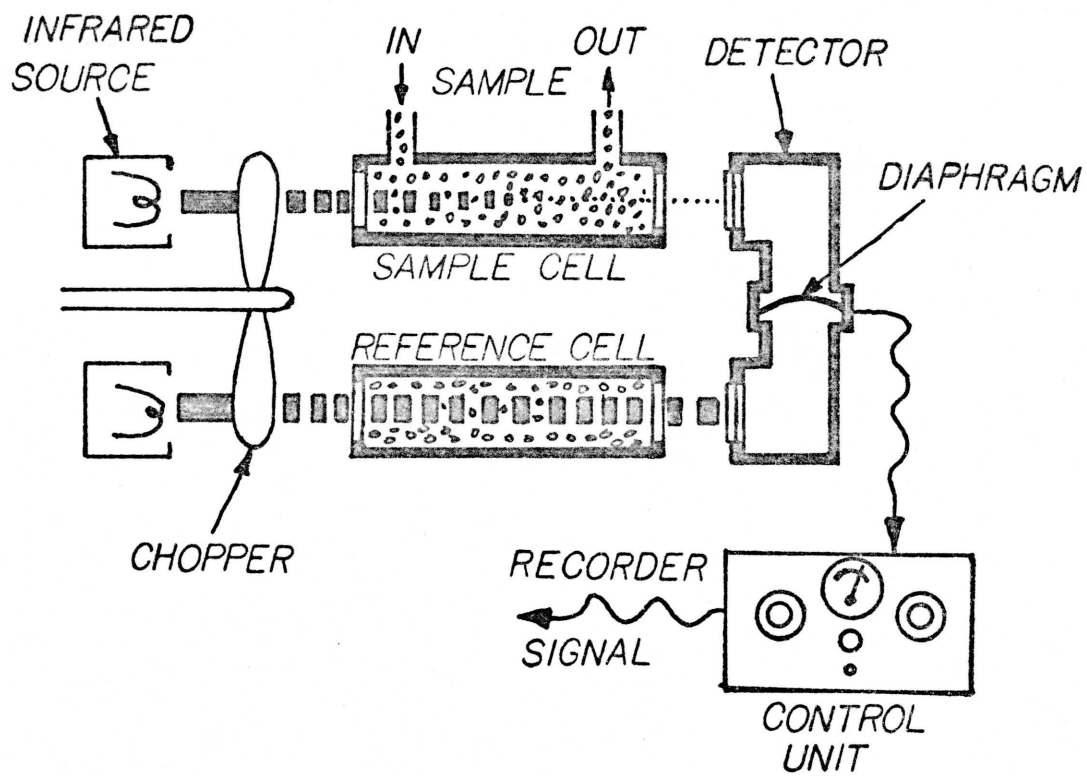
Fig. 7.1 Functional Diagram of Detection System

filling the air bags with a bicycle or air pump and are taken over a few minute period. The 1-hour average samples are taken using an impulse pump which fills a 5 liter bag in one hour. The impulse pump operates such that it pumps air for 2 seconds with a 20 second interval between cycles. The impulse pump used was also obtained from Environmental Measurements. The air from each bag is pumped out into the Beckman analyzer for measurement of the carbon monoxide concentration. This bag sampling technique is accurate, reliable, and inexpensive. The method has been used by the Alaska Department of Environmental Conservation in monitoring carbon monoxide in Fairbanks (Gilmore and Hanna, 1974).

Sampling Locations

The locations for collecting carbon monoxide samples are distributed through the urban area. However, most of sampling site are in areas of high traffic density such as major intersections. A map of the Tucson area with all the sampling locations is shown in Fig. 7.2. DM is Davis-Monthan Air Force Base and TIA is the Tucson International Airport. There are 28 collection points with numbers 27 and 28 belonging to the Air Pollution Control District of Pima County. At these two locations, the carbon monoxide levels are monitored on a continuous basis. The location of each sampling site and the time when samples are taken is given in Table 7.1.
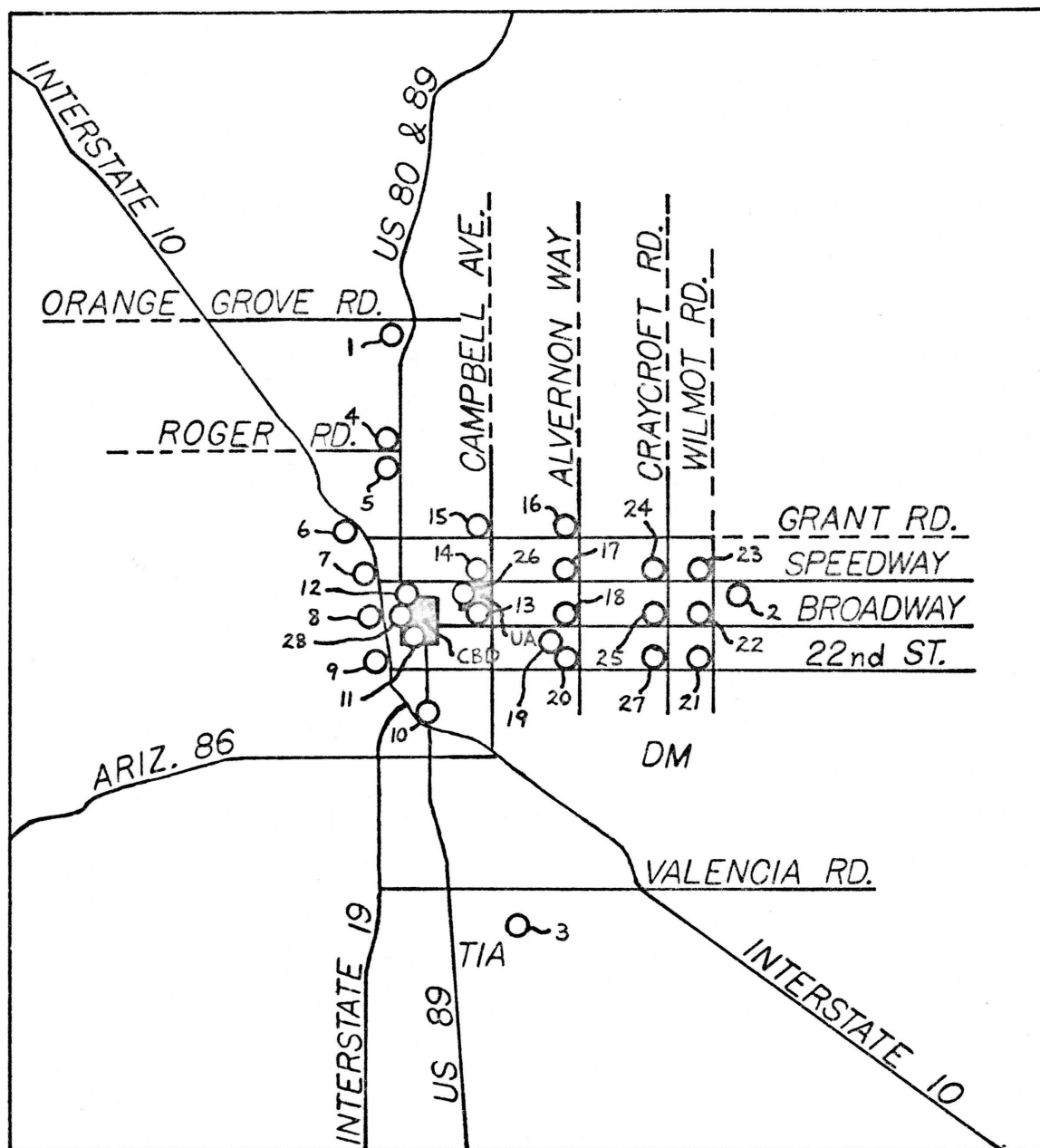
Fig. 7.2 A Map of the Tucson Area Showing the Carbon Monoxide
Sampling Locations

Table 7.1 Location of Sampling Sites

No.	Location	Corner	Distance from Street (ft.)	Height Above Ground (ft.)	When	Nominal Time
1	6311 N. Barcelona Ct.	–	250	10	Weekdays	8 am and 6 pm
2	6758 E. Rosewood Cir.	–	15	3	Weekdays	7 am and 6 pm
3	Environmental Research Lab	–	–	0	Weekdays	8:30 am and 4:30 pm
4	Oracle at Roger Rd.	NW	15	0	Tuesday	9 am
5	Oracle at Prince Rd.	NW	20	0	Tuesday	9:15 am
6	I-10 at Grant Rd.	NW	10	12	Tuesday	9:30 am
7	I-10 at Speedway	NW	15	0	Tuesday	9:45 am
8	I-10 at Congress	NW	10	0	Tuesday	10 am
9	I-10 at 22nd St.	NW	10	0	Tuesday	10:15 am
10	I-10 at 6th Ave.	NW	15	0	Tuesday	10:30 am
11	Stone at Congress	SW	5	0	Tuesday	10:45 am
12	Speedway at Stone	SW	10	0	Tuesday	11 am
13	Broadway at Campbell	NW	15	0	Friday	11 am
14	Speedway at Campbell	NW	12	0	Friday	11:15 am
15	Grant at Campbell	NW	10	0	Friday	11:30 am
16	Grant at Alvernon	NW	10	0	Friday	11:45 am
17	Speedway at Alvernon	NW	15	0	Friday	12 am
18	Broadway at Alvernon	NW	10	0	Friday	12:15 pm
19	Randolph Park – Hi Corbett Field	–	15	0	Friday	12:30 pm
20	22nd St. at Alvernon	NW	12	0	Friday	12:45 pm
21	22nd St. at Wilmot	NW	15	0	Friday	1 pm
22	Broadway at Wilmot	NW	15	0	Friday	1:15 pm
23	Speedway at Wilmot	NW	10	0	Friday	1:30 pm
24	Speedway at Craycroft	NW	10	0	Friday	1:45 pm
25	Broadway at Craycroft	NW	15	0	Friday	2 pm
26	University of Arizona Campus	–	45	4	Monthly	7 am to 7 pm
27	22nd St. at Craycroft	SW	330	13	Daily	Continuous
28	Congress – West of Church	–	–	12	Daily	Continuous

Weekday Sampling

The locations at which weekday samples are taken are numbers 1, 2, and 3. Location 1 is the residence of the author of this study, while location 2 is the home of Professor H. C. Perkins. Location 3 is the Environmental Research Lab of The University of Arizona located at the Tucson International Airport some seven miles from the downtown area. Locations 1 and 2 are also about 7 miles from downtown. Grab samples were taken twice daily on weekdays at the specified time noted in Table 7.1, from September 1974, through February, 1975. Table 7.2 summarizes the high, low, mean and median carbon monoxide concentrations for each of these three locations. The number of samples taken at locations 1, 2, 3 are also noted in Table 7.2. The average or mean value for the carbon monoxide concentration is greatest at location 2. This concentration ranking corresponds to the traffic density in each of these areas with location 2 having the highest traffic density of these sampling sites. A cumulative probability plot for all the data at each location appears

Table 7.2 Summary of Carbon Monoxide Concentrations from Weekday Samples

Location No.	No. of Samples	High Level (ppm)	Low Level (ppm)	Mean Level (ppm)	Median Level (ppm)
1	210	6.5	0.2	1.9	1.5
2	220	9.5	0.2	2.3	2.0
3	180	9.7	0.2	1.7	1.1

in Fig. 7.3. The figure shows that over a large portion of the concentration range, the measured data for each location are lognormal. Note the 50 percentile reading for each location corresponds to the median level appearing in Table 7.2. A listing of all the data for the three locations is found in Appendix C.

Tuesday Sampling

The locations sampled on Tuesday morning are numbered 4 through 12. These locations are all at intersections in areas of high traffic density. These sites were sampled for 22 continuous weeks from October, 1974, through February, 1975. The time of sampling appearing in Table 7.1 is approximately the same each week. The same corner is sampled each week to account for the effect of variation in wind direction. The samples are all grab samples taken over a four minute period to average out the effect of the traffic light cycle. Figures 7.4 through 7.7 contain the variations in the carbon monoxide levels from week to week at each location. A summary of the data for locations 4 through 12 appears in Table 7.3 containing the high, low and mean values for each location. The highest reading of all the Tuesday samples is 25ppm and was measured at the intersection of Oracle and Roger; however, the highest mean reading, 12.7ppm, occurs at Oracle and Prince.

Friday Sampling

The Friday sampling occurs between 11 am and 2 pm at locations 13 through 25. As with the Tuesday samples, these locations are mainly in areas of high traffic density. The Friday locations are on the east side
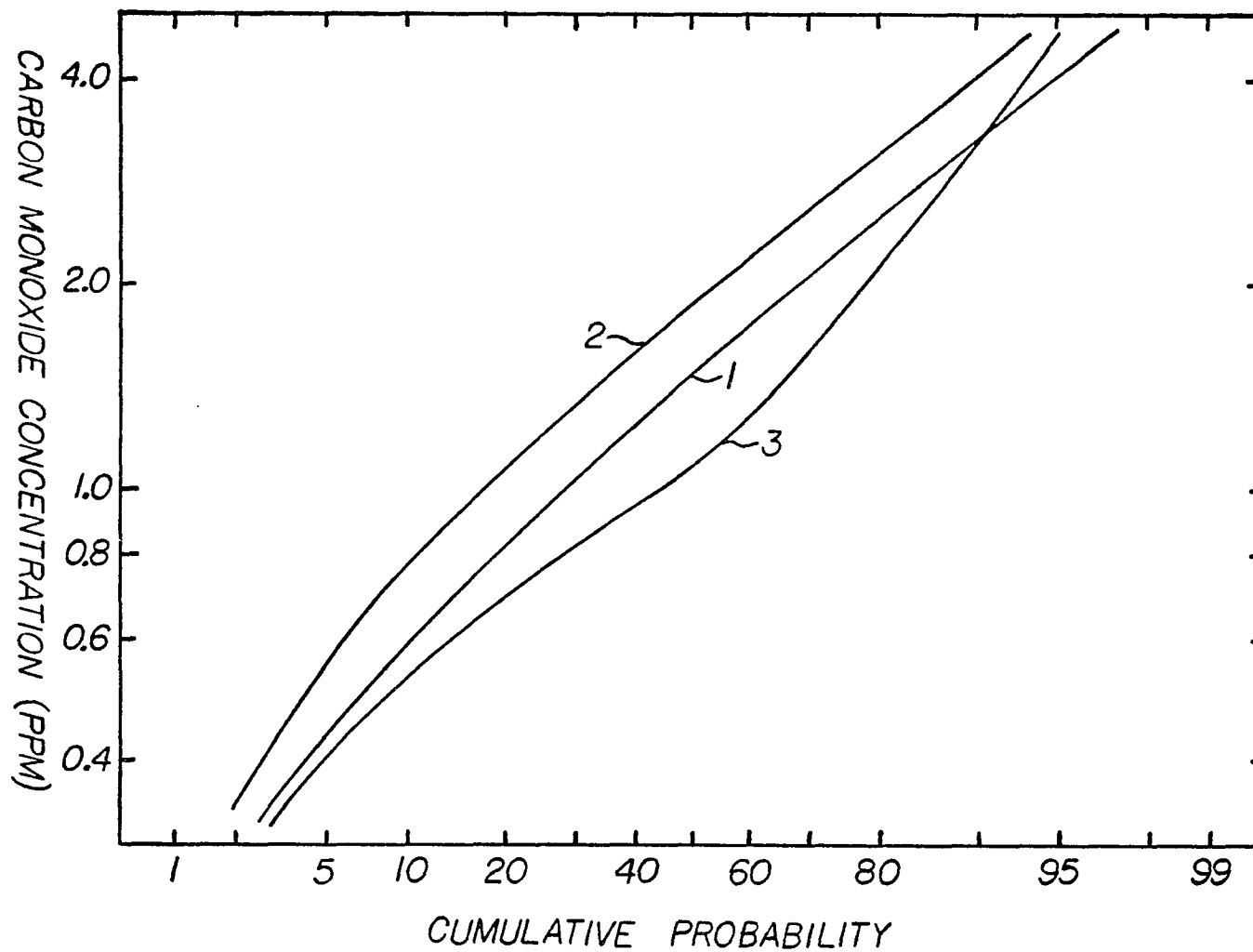
Fig. 7.3   A Cumulative Probability Plot of Measured Carbon Monoxide Concentrations
at Locations 1, 2, and 3
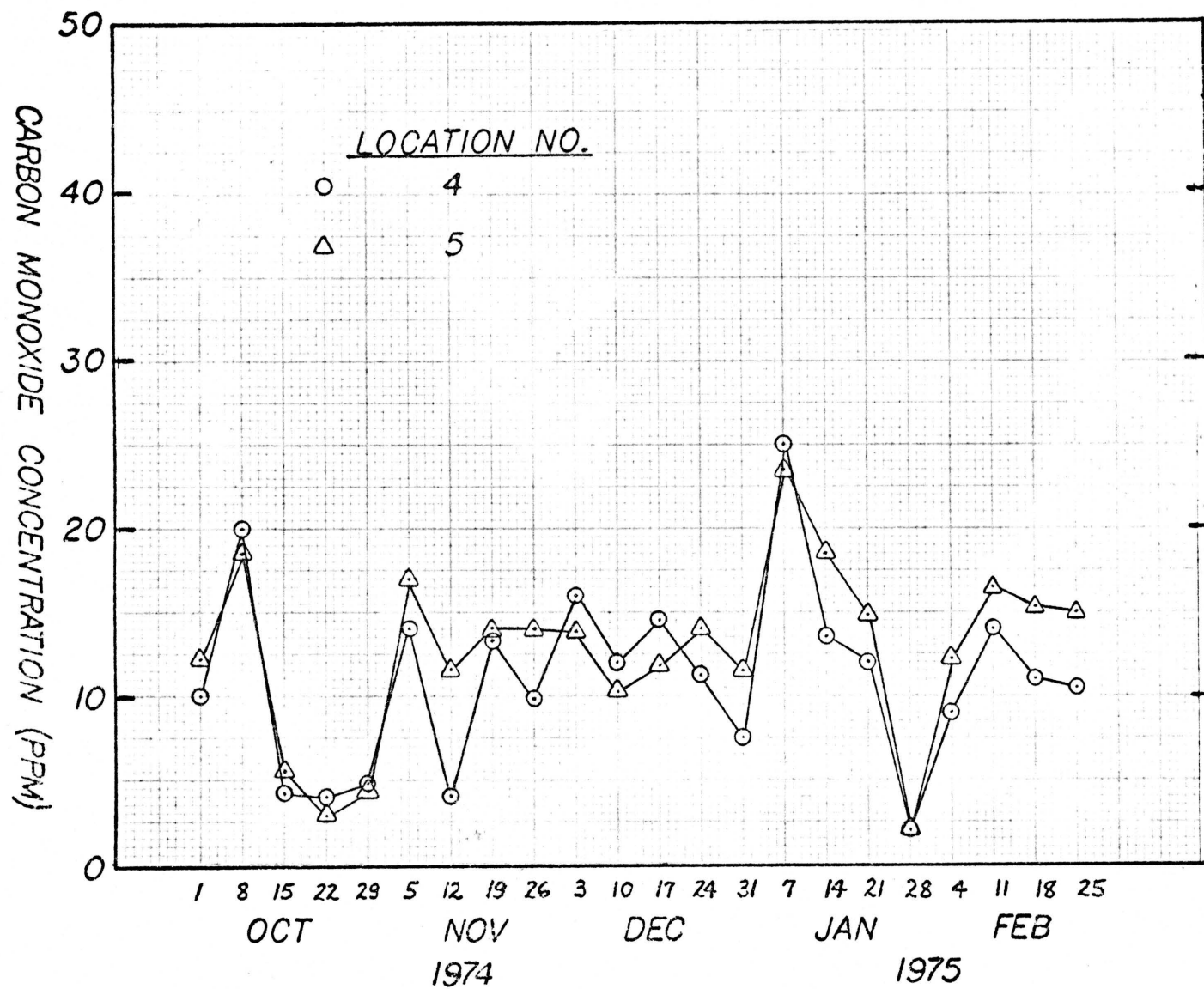
Fig. 7.4   Carbon Monoxide Concentration Variation for Locations 4 and 5
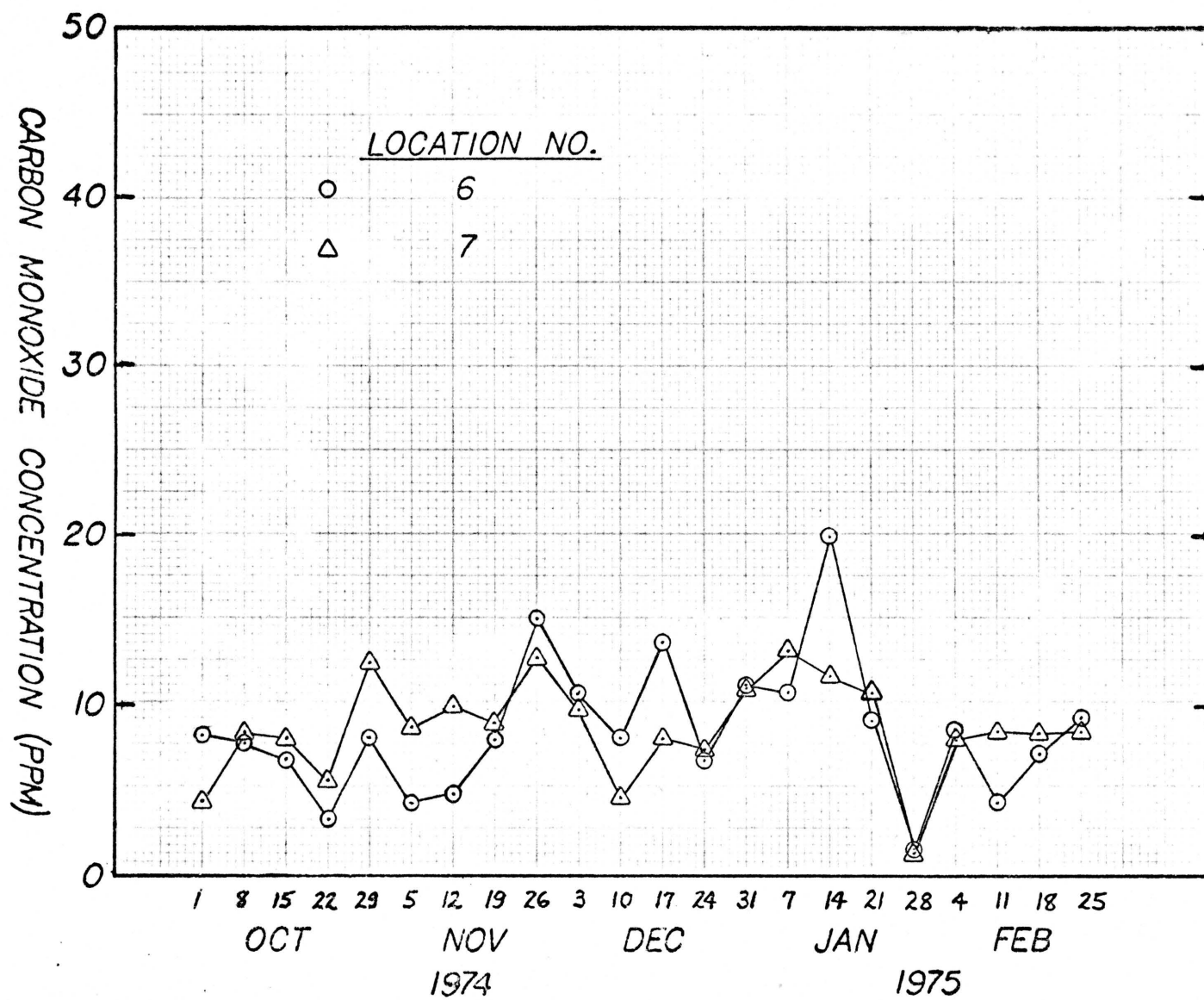
Fig. 7.5 Carbon Monoxide Concentration Variation for Locations 6 and 7
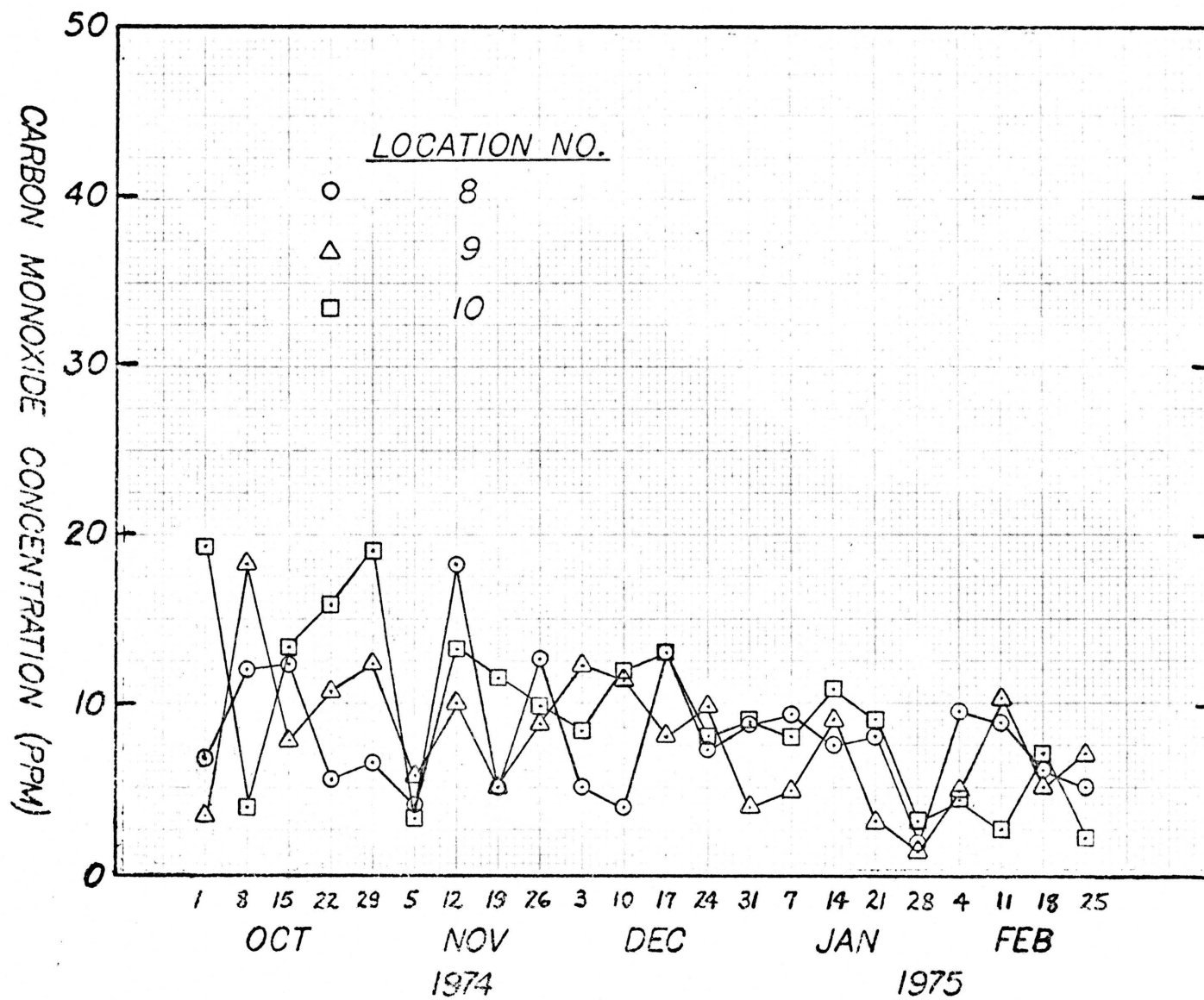
Fig. 7.6 Carbon Monoxide Concentration Variation for Locations 8, 9, and 10
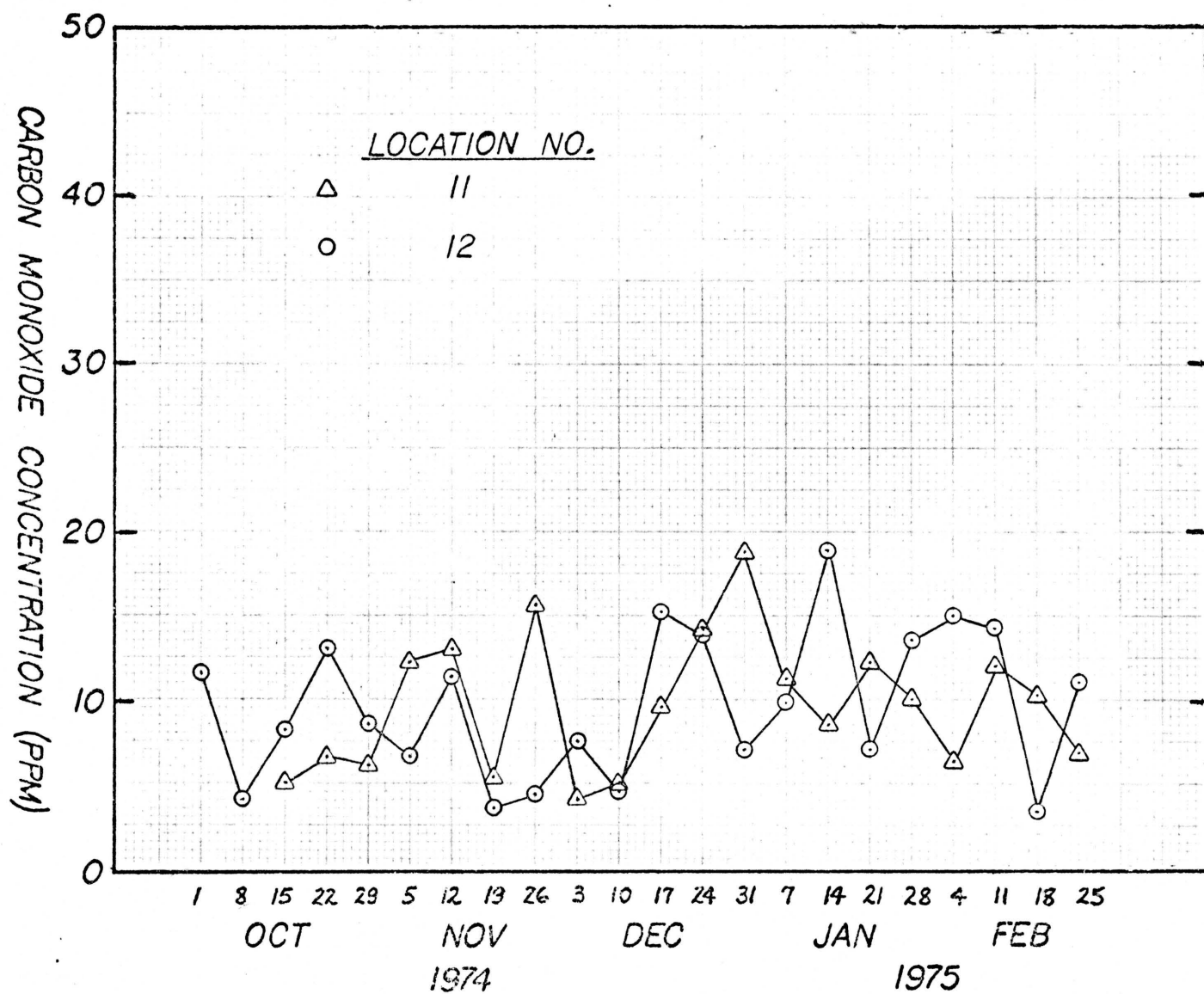
Fig. 7.7   Carbon Monoxide Concentration Variation for Locations 11 and 12

Table 7.3   Summary of Carbon Monoxide Concentrations from Tuesday Samples

Location No.	High Level (ppm)	Low Level (ppm)	Mean Level (ppm)
4	25.0	2.0	11.0
5	23.5	2.0	12.7
6	19.8	1.2	8.3
7	13.0	1.0	8.4
8	18.2	1.7	8.0
9	18.2	1.2	7.8
10	19.3	2.0	9.3
11	18.8	4.0	9.6
12	18.8	3.3	9.6

of town, whereas the Tuesday sampling sites are located on the west side of the city. These grab samples are also taken over a four minute period at the appropriate time as given in Table 7.1 and were obtained during the period from October, 1974, through February, 1975. The variation in the carbon monoxide concentration from week to week for each location is shown in Figs. 7.8 through 7.12. A summary of the high, low, and mean carbon monoxide concentrations for each Friday location appears in Table 7.4. The highest measurement and highest mean carbon monoxide concentration both occur at the intersection of Speedway and Campbell. The second highest mean level occurs at Speedway and Alvernon. This confirms the numerical predictions that Speedway is the center of the high carbon monoxide levels existing in the Tucson airshed. The reason for the low carbon monoxide readings at location 19 is that this sampling site is not in an area of high traffic density but located in the Randolph Park area near Hi Corbett Field.

The samples taken at locations 4 through 25 are all in areas of high traffic density with the exception of location 19. Therefore, the total number of grab samples taken at traffic intersections in the Tucson area are over 450. These samples represent levels measured during the weekday hours between 9 am and 2 pm. During the peak morning and evening rush hours the carbon monoxide levels existing are somewhat higher. A cumulative probability plot for all the intersection data appears in Fig. 7.13. The measured data are lognormal over most of the concentration range with some discrepancy in the data for the low concentration values. The figure gives the percent of time that the concentration of carbon monoxide at an intersection in Tucson is less than a certain value.
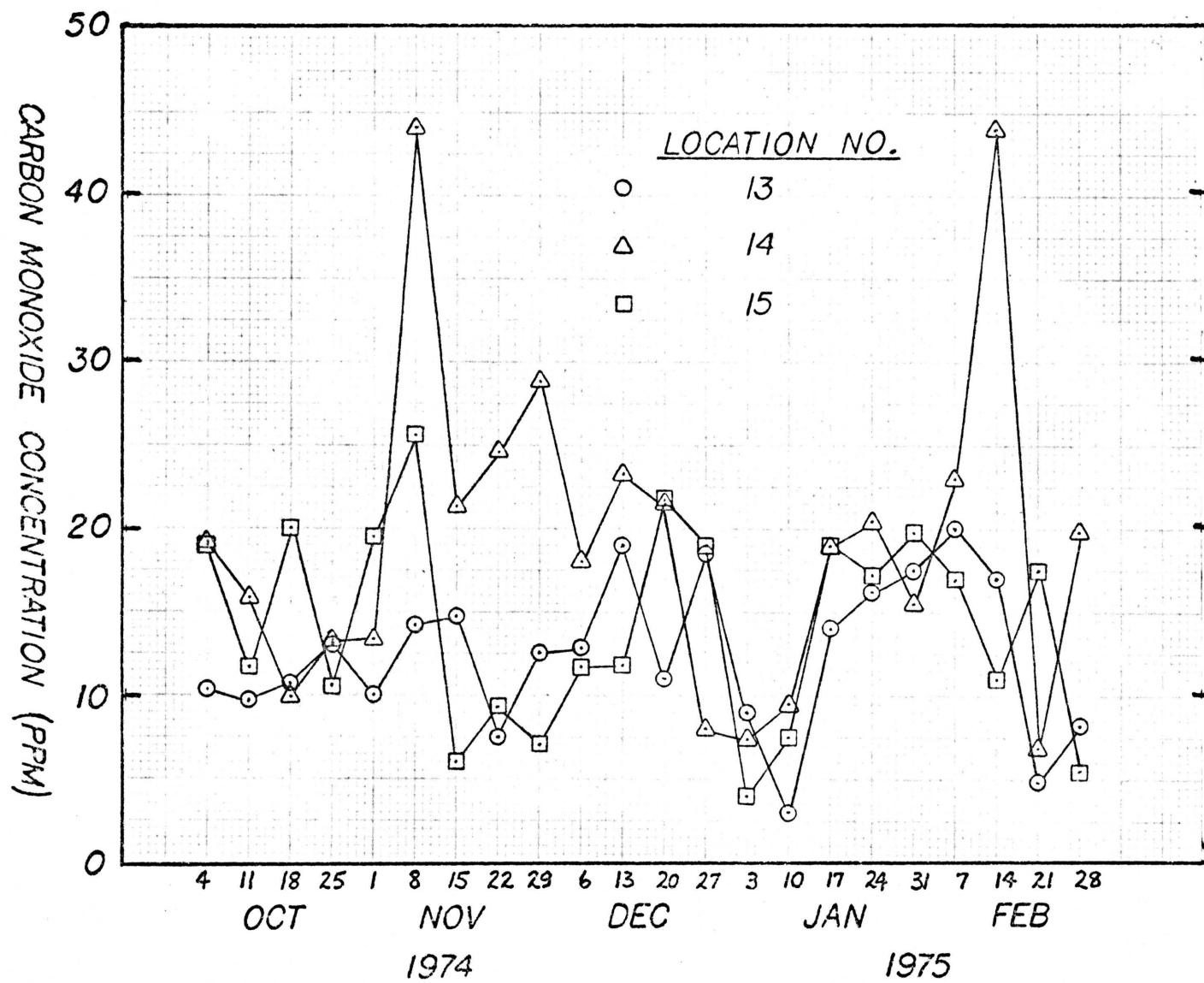
Fig. 7.8   Carbon Monoxide Concentration Variation for Locations 13, 14 and 15
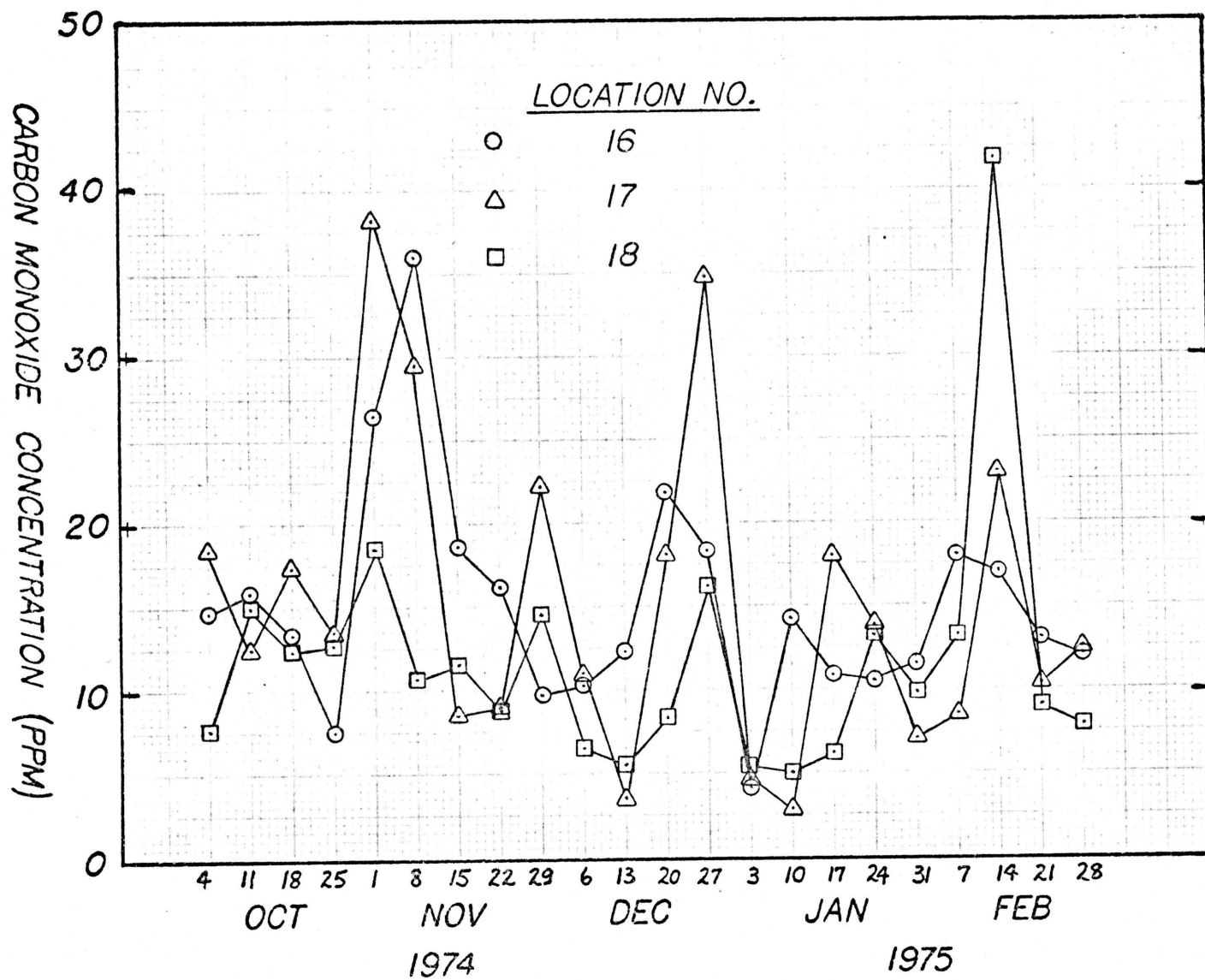
Fig. 7.9 Carbon Monoxide Concentration Variation for Locations 16, 17, and 18
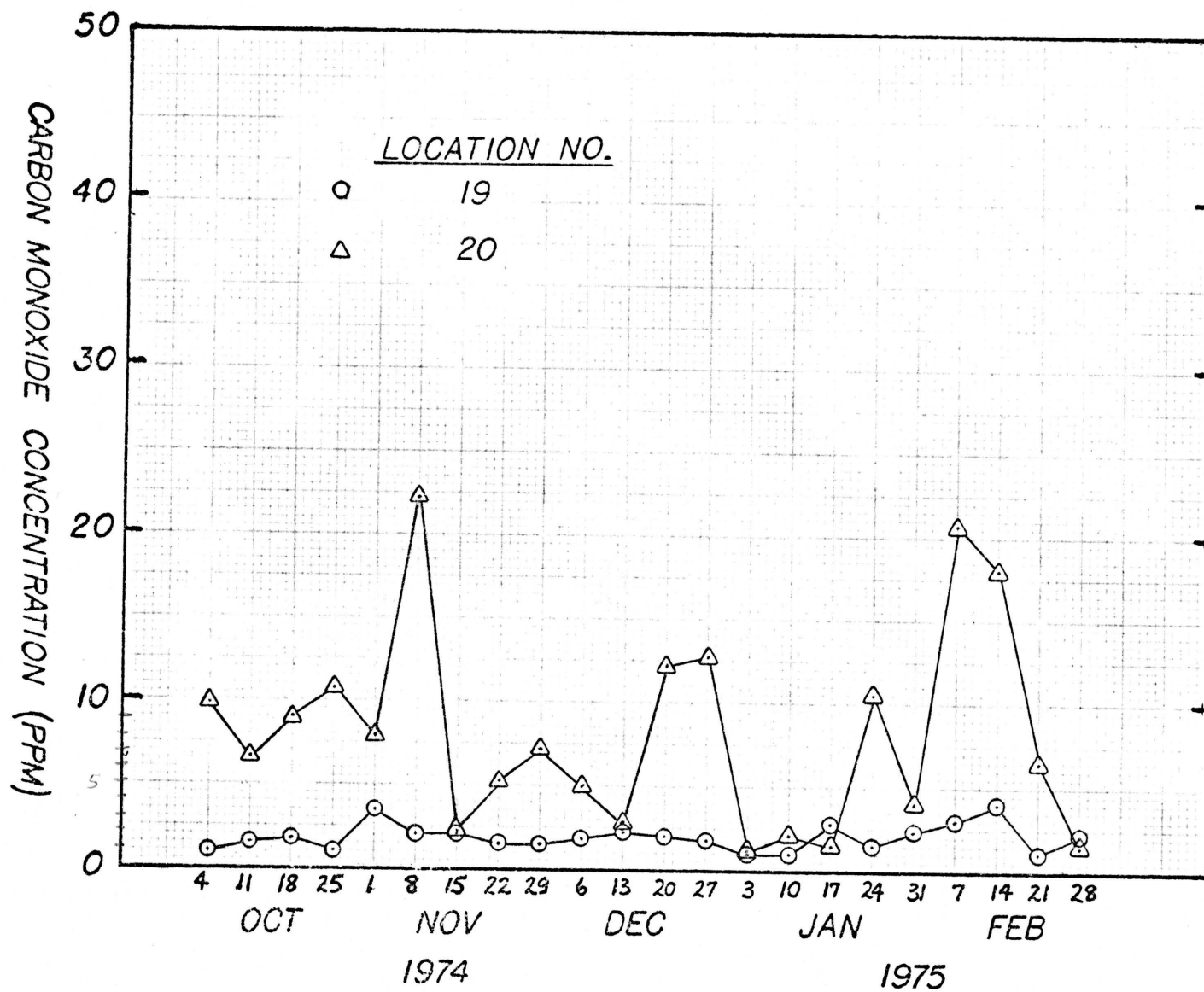
Fig. 7.10   Carbon Monoxide Concentration Variation for Locations 19 and 20
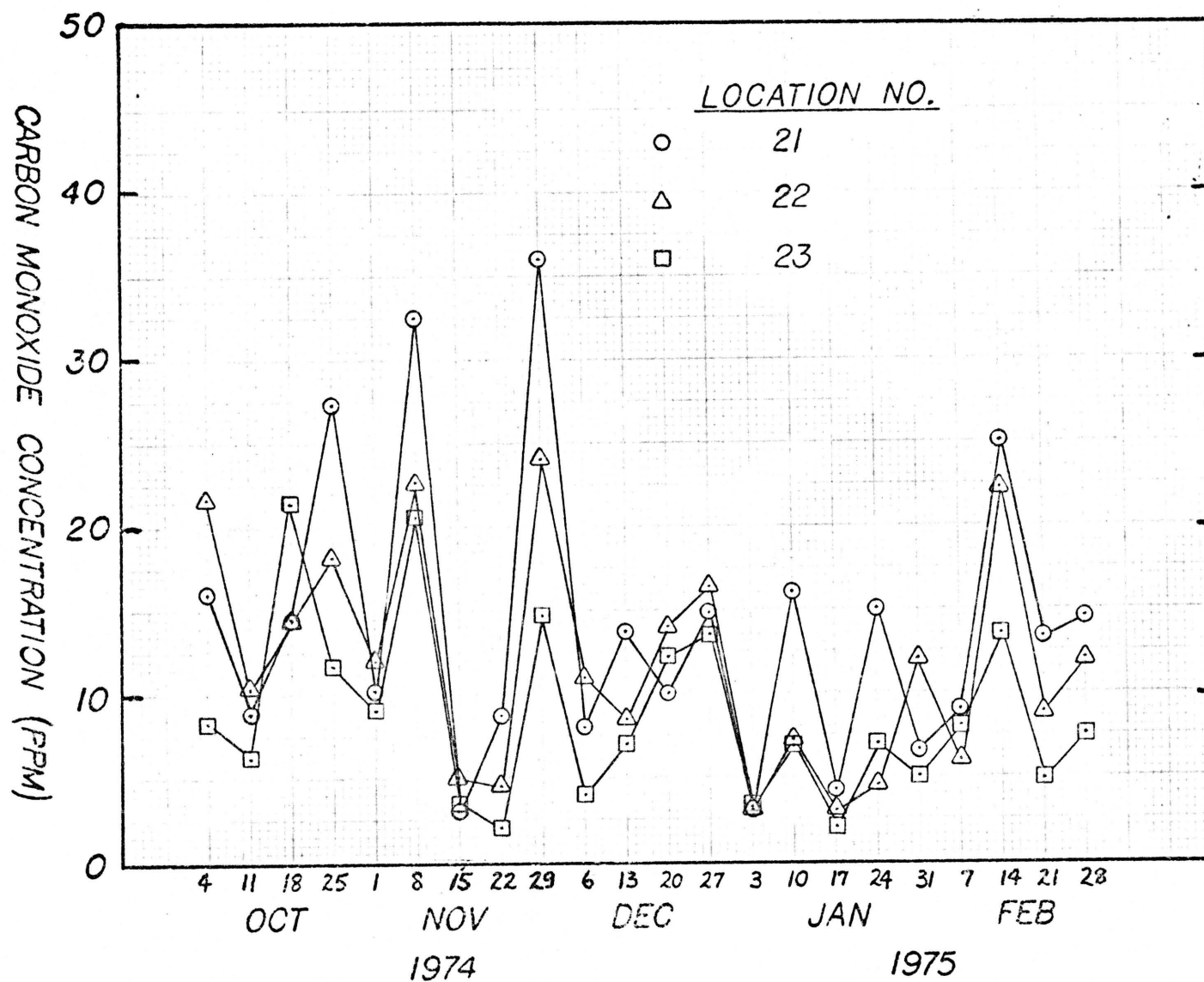
Fig. 7.11 Carbon Monoxide Concentration Variation for Locations 21, 22, and 23
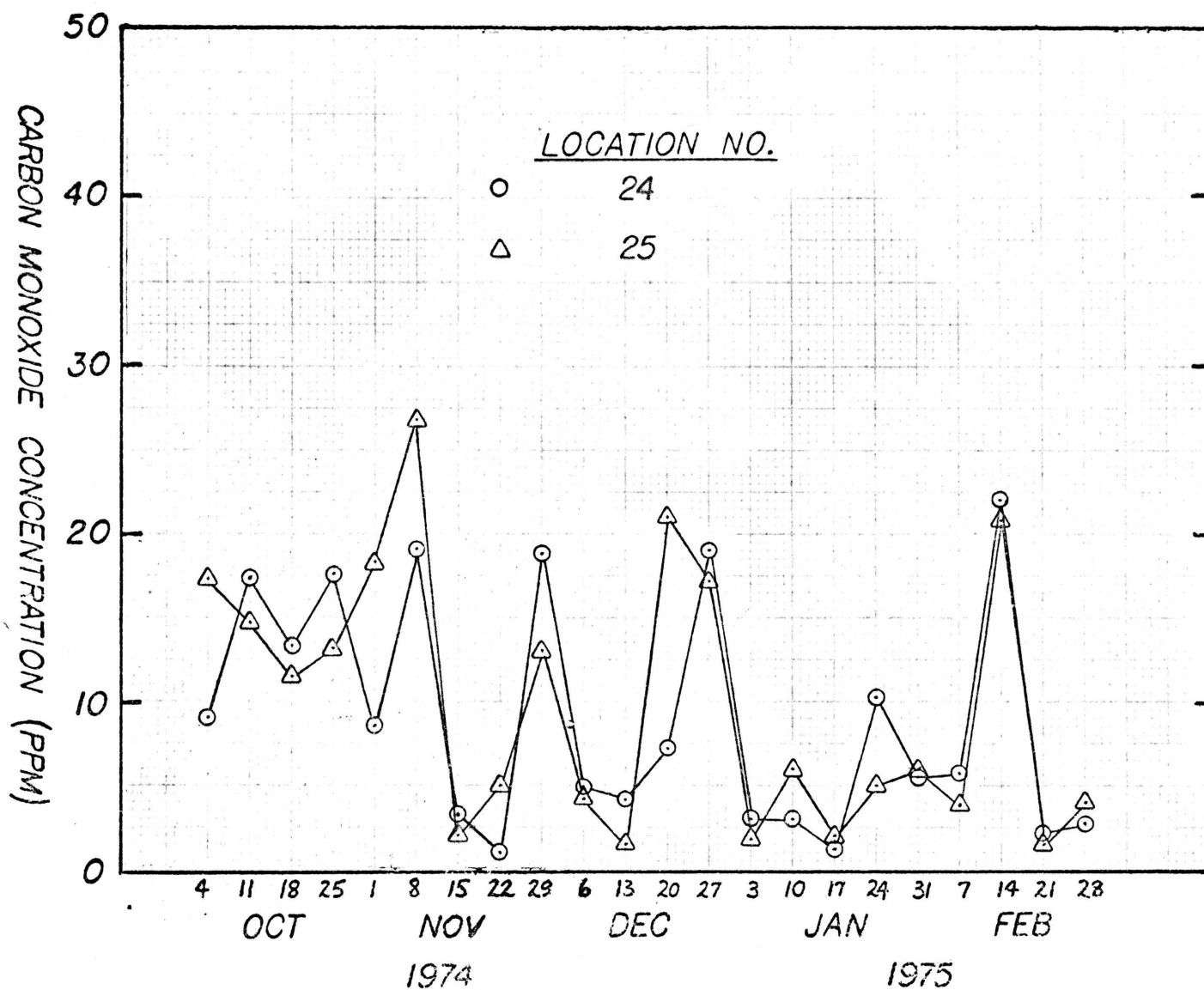
Fig. 7.12   Carbon Monoxide Concentration Variation for Locations 24 and 25

Table 7.4 Summary of Carbon Monoxide Concentrations from Friday Samples

Location No.	High Level (ppm)	Low Level (ppm)	Mean Level (ppm)
13	20.0	3.0	12.4
14	44.1	6.8	19.4
15	25.6	4.0	14.1
16	36.0	4.1	15.1
17	38.2	2.8	15.3
18	41.8	5.0	11.8
19	4.0	1.0	2.0
20	22.2	1.5	8.2
21	36.0	3.0	14.1
22	24.0	3.0	11.9
23	21.4	2.0	8.7
24	22.0	1.0	9.0
25	26.8	1.5	9.8
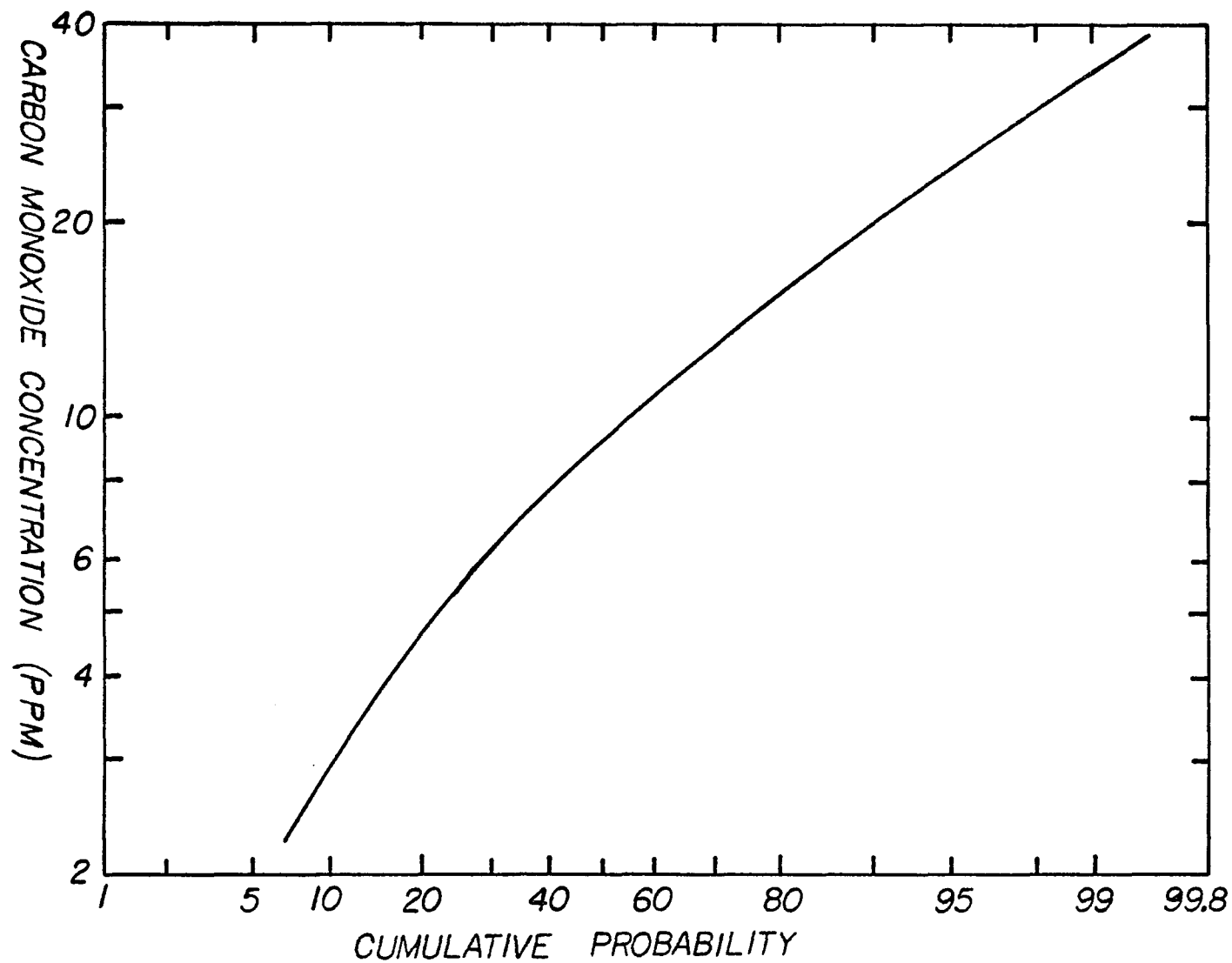
- Fig. 7.13 A Cumulative Probability Plot of Measured Carbon Monoxide Concentrations
at Major Intersections in the Tucson Area

For instance, 50 percent of the time the level is less than about 9.5ppm. This corresponds to the median values for all the samples taken; however, the average or mean of all the samples is 11.7ppm. Since the same corner at each location was used throughout the 22 weeks of the sampling, these measured levels do not always represent the maximum levels existing at any intersection. This is the case since the sampling site is not always on the downwind corner of the intersection. Most of the sampling sites are on the northwest corner. Prevailing wind direction in the Tucson area is southeast in the am hours and northwest during the pm hours.

Monthly Sampling

Samples were taken at location 26 which is on the University of Arizona campus adjacent to Speedway about one block west of Mountain and across the street from the Arid Lands Center. The samples at this location were taken on Wednesdays from approximately 7 am to 7 pm on a monthly basis. During the months of September and October, 1974, only grab samples were taken. The samples were taken on the hour with half hour measurements during the morning and evening traffic peaks. The samples were again taken over a four minute period to average out the effect of the traffic lights to the East and West on Speedway. Figure 7.14 shows the comparison in the carbon monoxide distributions for September 25 and October 30, 1974. The carbon monoxide variation for these two days is obviously quite different.

Grab samples and 1-hour average samples were collected at location 26 on November 20, 1974. These samples were taken during the hours from 4 am to 12 midnight. A comparison of the grab and 1-hr average
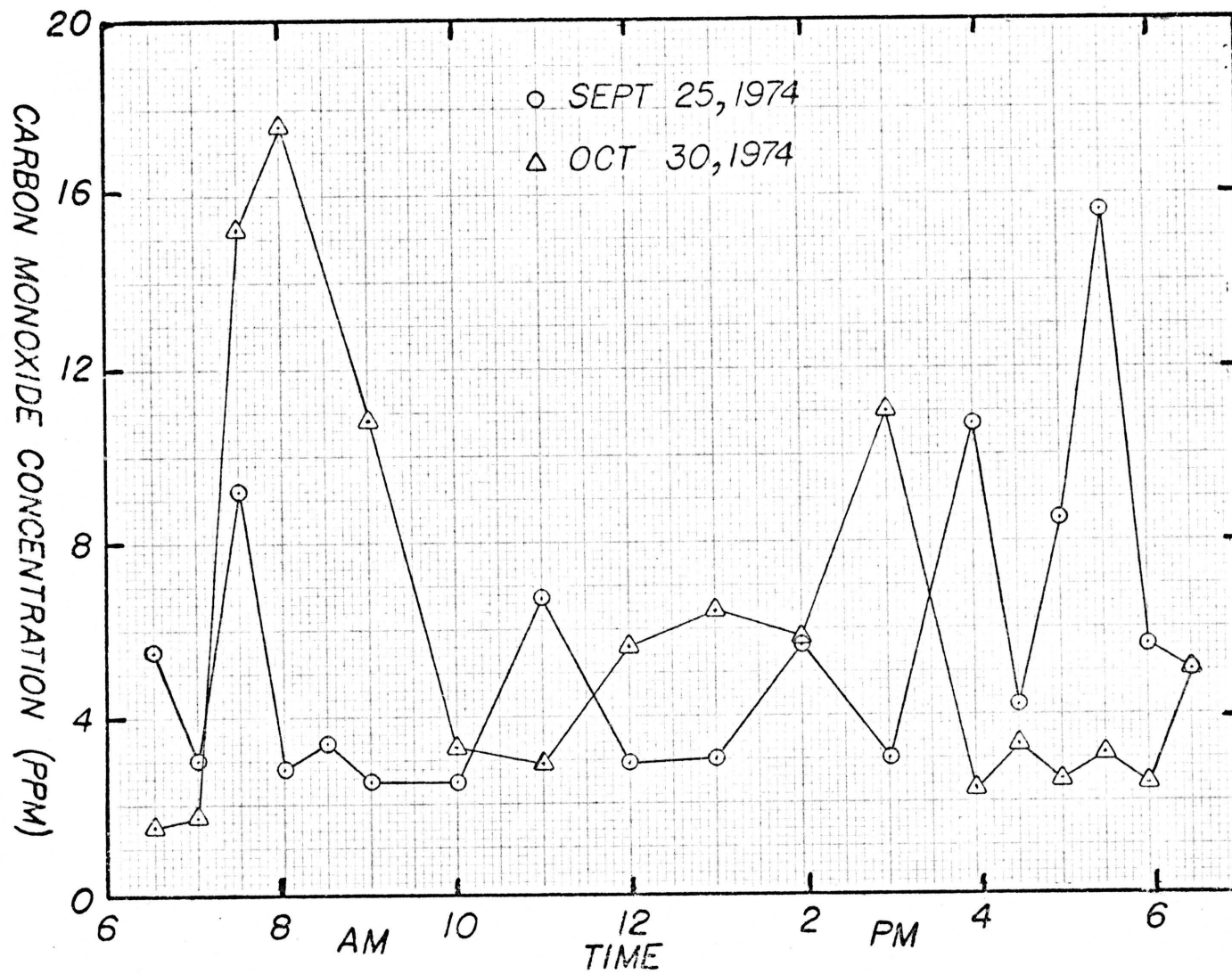
Fig. 7.14 Carbon Monoxide Concentration Distribution for September 25, 1974 and October 30, 1974 for Location 26

samples is shown in Fig. 7.15. The 1-hr average readings are plotted at the half-hour falling between the hours for which they were taken. The correlation between the grab samples and 1-hr average samples is quite good. The 1-hour average readings for location 26 are also compared to 1-hour average levels for location 27 for the same day. The readings for location 27 were obtained from the Air Pollution Control District of the Pima County Health Department. The comparison appears in Fig. 7.16 and in general the levels at location 26 are higher than those measured at location 27. This seems reasonable since location 26 is much closer to a traffic intersection than location 27. Location 26 is affected both by traffic on Speedway and also by the large University parking lot at the site. The parking lot traffic is heavy from 7:30 to 8 am and then on the hour until the evening classes are concluded. The meteorological data corresponding to November 20, 1974, at location 26 are presented in Table 8.3 for the micro-model.

One hour average samples were again collected at location 26, but this time on December 18, 1974. The readings were made during the hours of 7 am to 7 pm. A comparison between the one hour average carbon monoxide readings for November 20 and December 18, 1974, is made in Fig. 7.17. The magnitudes of the readings for the two days are quite similar; however, the shape of the distributions is different.

Miscellaneous Sampling Data

Along with the routine sampling programs at locations 1 through 26, some 1-hour average samples were collected during the peak morning and evening rush hours at major intersections in the Tucson area. Grab
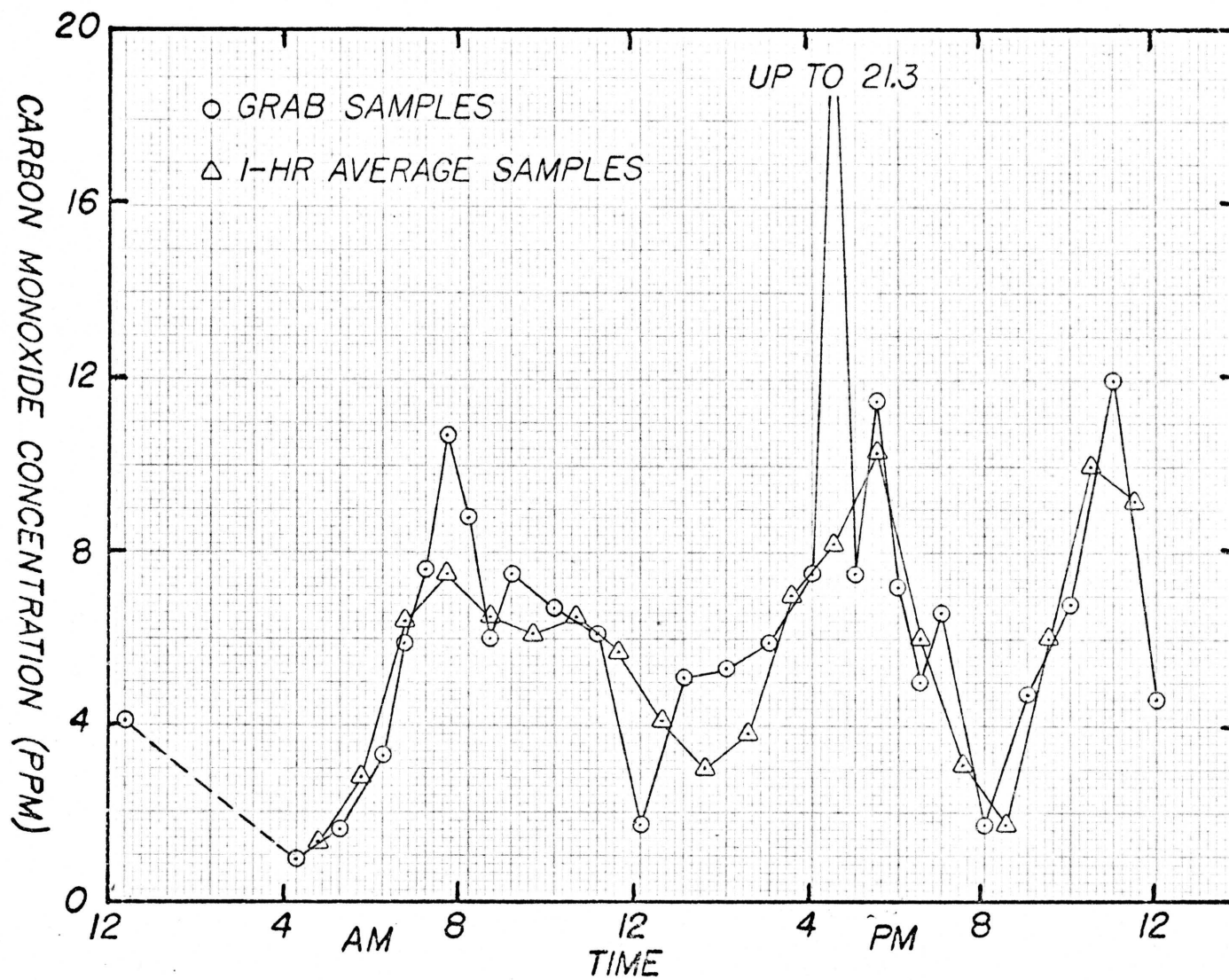
Fig. 7.15 Grab and 1-hour Average Carbon Monoxide Samples for November 20, 1974 for Location 26
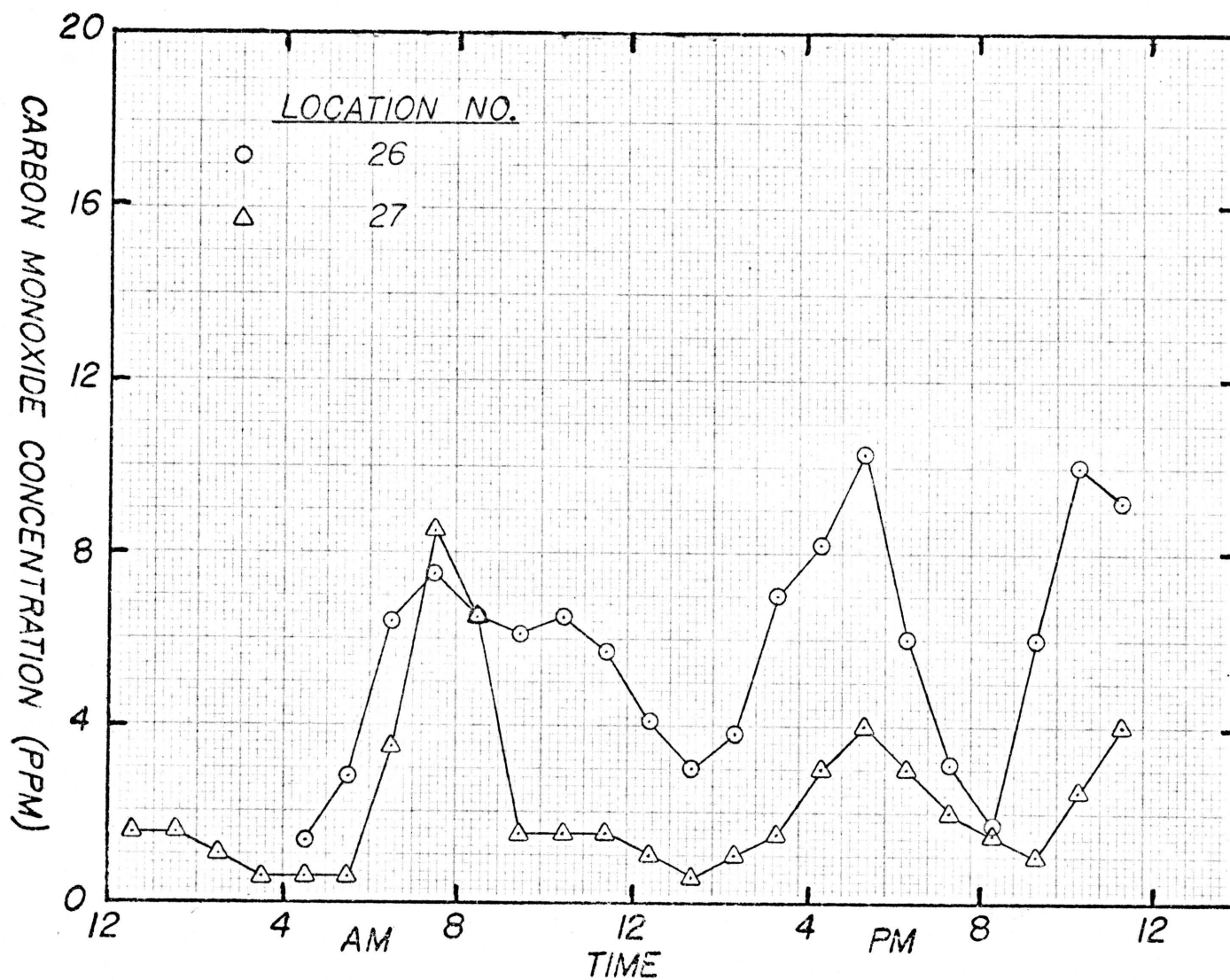
Fig. 7.16   Carbon Monoxide Concentration Distribution for November 20, 1974
at Locations 26 and 27
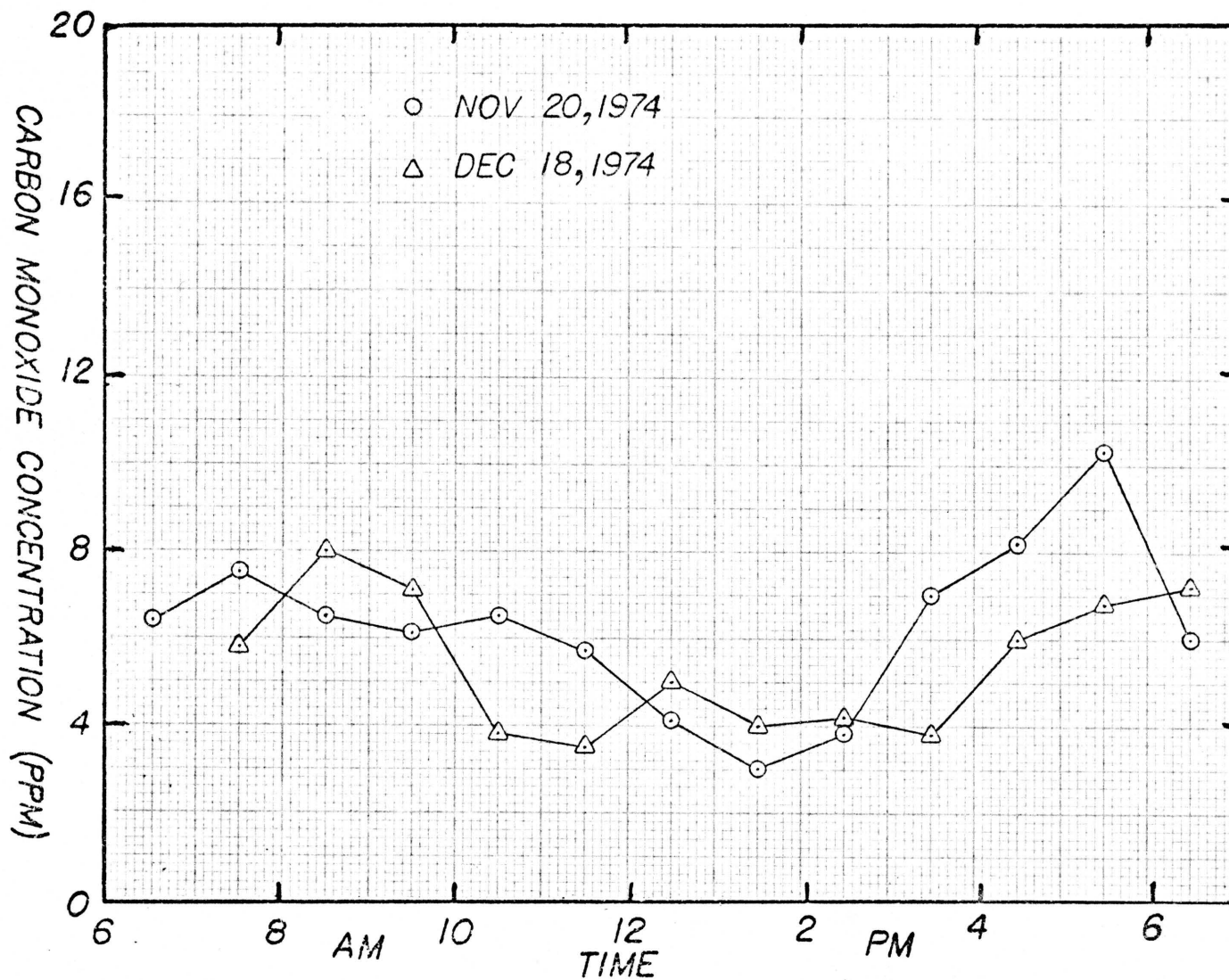
Fig. 7.17   Carbon Monoxide Concentration Distribution for November 20, 1974 and
December 18, 1974 for Location 26

samples were also taken at 15 minute intervals between each 1-hour sample. These grab samples were taken over a four minute time span to average out the effect of the traffic light cycle. This sampling was done on five separate occasions with four of them during the morning rush hour while the fifth occurred during the evening rush hour. The morning samples were taken from 7 to 9 am while the evening samples were taken between 4 and 6 pm. The 1-hr average and grab sample results for these five separate cases are presented in Table 7.5. All the locations were sampled on the northwest corner. During the evening sampling there was a light NW breeze while there was a light SE breeze for the morning sampling. Note the large difference in the readings at location 15 for the morning and evening sampling. This occurs since for the morning rush hour the NW corner is downwind while for the evening traffic peak the NW corner is upwind of the intersection. Concentrations at locations 14 and 17 are over the 1-hour ambient standard of 35ppm for the hour 8-9 am. These locations are at Speedway-Alvernon and Speedway-Campbell. Concentrations at the other two locations are under the standard for the morning rush hour traffic. The comparison in magnitude between the grab samples and 1-hr average samples of Table 7.5 is good.

Since the results from Table 7.5 show that the wind direction has a large effect on the CO level depending on which corner is sampled, some data were collected simultaneously to determine the difference in the CO levels at the four corners of an intersection. Since the intersection of Speedway-Campbell has large CO levels, it was used for the four corners sampling. Grab samples were taken simultaneously at the four corners, again over about a four minute period. The four corners program was

Table 7.5 One-hour Average and Grab Sample Readings at Some Major Inter-sections During Peak Rush Hours

	Loc. 15 11/13/74		Loc. 15 11/14/74	Loc. 17 11/27/74	Loc. 14 12/4/74	Loc. 22 12/11/74
Time	CO(ppm)	Time	CO(ppm)	CO(ppm)	CO(ppm)	CO(ppm)
4 pm	8.6	7 am	21.7	19.8	14.8	16.8
4:15 pm	7.8	7:15 am	25.0	29.6	16.0	25.0
4:30 pm	11.0	7:30 am	27.3	55.3	29.7	29.0
4:45 pm	6.5	7:45 am	31.5	47.2	34.6	36.0
5 pm	8.2	8 am	25.8	32.2	51.0	31.0
5:15 pm	15.2	8:15 am	26.6	32.6	31.8	22.7
5:30 pm	9.0	8:30 am	27.3	57.2	42.3	27.0
5:45 pm	14.8	8:45 am	22.7	39.0	35.7	23.0
6 pm	5.6	9 am	19.8	44.3	22.0	30.3
4-5 pm	6.7	7-8 am	30.5	34.3	30.5	28.7
5-6 pm	12.7	8-9 am	27.0	42.5	37.8	26.2

performed on three separate days and twice each day at about a 15 minute

interval between the two sampling times. The results for these six cases

are presented in Table 7.6. Note the large difference in readings

obtained for the four corners. In general, the highest reading occurs at

the downwind corner of the intersection. From the results the readings at

the four corners can vary from a factor of 5 to as much as a factor of 20

between the highest and the lowest CO level.

Along with measuring the CO variation at the four corners of an

intersection, some measurements were made to determine the CO variation

with height. This study was performed using the Plaza International Hotel

located at Speedway and Campbell. The west side of the building has an

open fire escape on each floor. Grab samples were taken simultaneously

Table 7.6 Grab Sample CO Levels Taken at the Four Corners of Speedway
and Campbell

Time	3:40 pm	3:55 pm	2:20 pm	2:35 pm	1:20 pm	1:35 pm
Date	12/19/74	12/19/74	2/4/75	2/4/75	2/5/75	2/5/75
Wind Speed (m/sec)	1.5	1.0	1.0	2.0	1.5	1.5
Wind Direction	W	NW	SE	SW	W	SW
Corner	CO(ppm)	CO(ppm)	CO(ppm)	CO(ppm)	CO(ppm)	CO(ppm)
SE	20.8	36.5	9.7	4.0	14.0	11.8
SW	16.7	15.8	6.5	3.8	3.0	1.5
NW	6.0	2.8	27.5	15.0	11.0	22.0
NE	29.3	22.2	6.0	25.8	16.5	33.0

on the west side of the building at the ground and at the 3rd, 5th, and

7th floor fire escape landings. In order to obtain the CO levels due to

the Speedway-Campbell intersection the study was performed only when the

wind was generally from the northwest. Along with taking the CO samples,

the wind speed and direction were measured at the ground and on the 7th

floor. The carbon monoxide levels as a function of height and the

meteorological data are presented in Table 7.7 for the two sampling times

of December 19, 1974.

For the sampling at 3:30 pm the CO level at the ground is not

much different than the level at 19.5 meters above the ground since the

horizontal motion is very small. The initial ground level value at this

time is low since the wind is from the north. At 3:45 pm, the horizontal

Table 7.7 Carbon Monoxide Variation as a Function of Height for December 19, 1974. Case 1 Occurs at 3:30 pm; Case 2 Occurs at 3:45 pm

Height	(m)	(ft)	Wind Speed (m/sec)	Wind Direction	CO (ppm)	Wind Speed (m/sec)	Wind Direction	CO (ppm)
Ground	0	0	0.5	N	5.8	1.5	NW	12.5
3rd Floor	8.3	27.3	-	-	3.7	-	-	7.0
5th Floor	13.9	45.6	-	-	2.9	-	-	4.7
7th Floor	19.5	64.0	0	-	2.9	2.5	NW	2.1

motion is greater and the vertical CO gradient is larger. The CO does not have time to mix vertically due to the stronger horizontal motion. The ground level value is larger now since the wind speed has increased and is from the northwest.

Summary of Measured Data

Several conclusions can be drawn based on the carbon monoxide samples taken at the intersections in the Tucson area. In general, CO levels are higher on the east side of town than the west side. Intersections along Speedway Boulevard appear to be those having the largest concentration of carbon monoxide in the urban area. Figure 7.15 and Table 7.5 show that the agreement between 1-hour average samples and grab samples taken over a few minutes period are good. This result should be quite useful when a large number of samples are required, as far as saving sampling time is concerned. Assuming the samples taken at locations 4 through 25 are similar to 1-hour levels, then from Fig. 7.15, there is about a one percent probability that the CO level at an intersection in the Tucson area is greater than 35ppm between the hours of 9 am and 2 pm. Note, this says nothing about the CO levels existing during the peak morning and evening rush hours. From the small number of 1-hr average samples taken during rush hours, two locations have been found which are over the 1-hour average of 35ppm. They are at Speedway-Campbell and Speedway-Alvernon. However, no one lives at a street intersection so no one is directly affected by these high levels. The CO levels which the population of Tucson is usually exposed to are

predicted by the multi-box model developed in this study. These numeri-
cal predictions are compared in Chapter 8 to some of the measured data
that are presented in this chapter.

CHAPTER 8

COMPARISON OF NUMERICAL AND

MEASURED RESULTS

The multi-box model developed for the Tucson airshed should be quite useful for predicting carbon monoxide levels for a variety of problems. For example, under episode conditions one can determine whether concentrations are above levels affecting health. The model can also be used to project the effects of growth as related to land-use planning. However, the verification of this model is necessary before it can be used. The conditions under which the model is applicable are explained in this chapter when the comparison is made to measured data for different locations in the Tucson area. Since the multi-box model is an area source model, it is not expected that the numerical results should compare to data taken at locations of major carbon monoxide sources, e.g., parking lots and traffic intersections. Since the numerical model predicts an average carbon monoxide level for each Eulerian box of some finite size, there will always be measured values within each box, which are higher, and lower than that predicted. It is the representative value that should be compared to the predicted results.

Model Verification

During the three-day period from Friday, November 9 to Sunday,
November 11 of 1973, a high pressure system existed over the Tucson basin
causing stagnation conditions to occur. The ventilation was quite low
during this period allowing for accumulation of pollutants in the airshed.
These three days were simulated using the meteorological data obtained
from the Tucson Weather Service. The wind speed and direction for these
days are tabulated in Table 8.1 in the same way that the meteorological
data were given in Chapter 6. The minimum and maximum mixing heights are
presented in Table 8.2, and they are determined using the EPA procedure
contained in AP-101. The numerical predictions are simulated using an
initial condition of 0.1 ppm with incoming boundary conditions for
November 9, 1973, having this same value. The initial conditions for
November 10 and 11, 1973, use the predicted concentrations for each box
obtained from the last time step of the previous day. The incoming boun-
dary conditions are still 0.1 ppm as they were for November 9.

The numerical results are compared to data taken at location 27
of Fig. 7.2. The data were obtained by the Pima County Health Department
on a continuous basis. This is the only location at which carbon monoxide
measurements were taken in the Tucson area between November 9-11, 1973.
This sampling location is near the intersection of 22nd and Craycroft on
the east side of Tucson. The comparison of the numerical results for
this box with 1-hour average measured levels are presented for November 9,
10, 11, 1973, in Figs. 8.1, 8.2, and 8.3, respectively. These predicted
results were all obtained using the macro-model. The measured data show
the expected peaks due to the diurnal traffic variation on Friday and

Table 8.1 Meteorological Data for Computer Model, Nov. 9-11, 1973

Hr.	November 9, 1973 U	α	November 10, 1973 U	α	November 11, 1973 U	α
1	2.6	120°	2.6	130°	3.6	120°
2	3.6	120°	3.6	140°	2.1	110°
3	4.6	140°	3.6	120°	3.6	120°
4	4.1	140°	4.1	120°	4.1	130°
5	4.6	140°	3.6	130°	4.6	130°
6	6.2	140°	3.6	140°	4.6	110°
7	5.2	130°	4.1	130°	2.1	140°
8	6.2	130°	4.6	130°	5.2	110°
9	3.6	130°	2.6	100°	5.2	110°
10	3.6	110°	1.5	40°	2.6	90°
11	1.5	90°	1.5	110°	1.5	60°
12	0.0	--	0.0	--	1.5	330°
13	1.5	190°	1.5	340°	2.6	290°
14	1.5	330°	2.1	290°	1.5	300°
15	2.1	330°	3.1	290°	2.1	280°
16	2.1	280°	3.6	270°	3.6	280°
17	3.1	280°	4.1	290°	3.1	300°
18	3.1	310°	3.6	310°	2.6	310°
19	3.6	350°	2.1	30°	1.5	110°
20	0.0	--	4.1	140°	3.6	100°
21	3.6	90°	2.6	130°	2.1	130°
22	3.6	100°	3.1	110°	3.1	140°
23	3.1	120°	2.6	110°	2.6	120°
24	4.1	130°	2.6	140°	3.1	140°
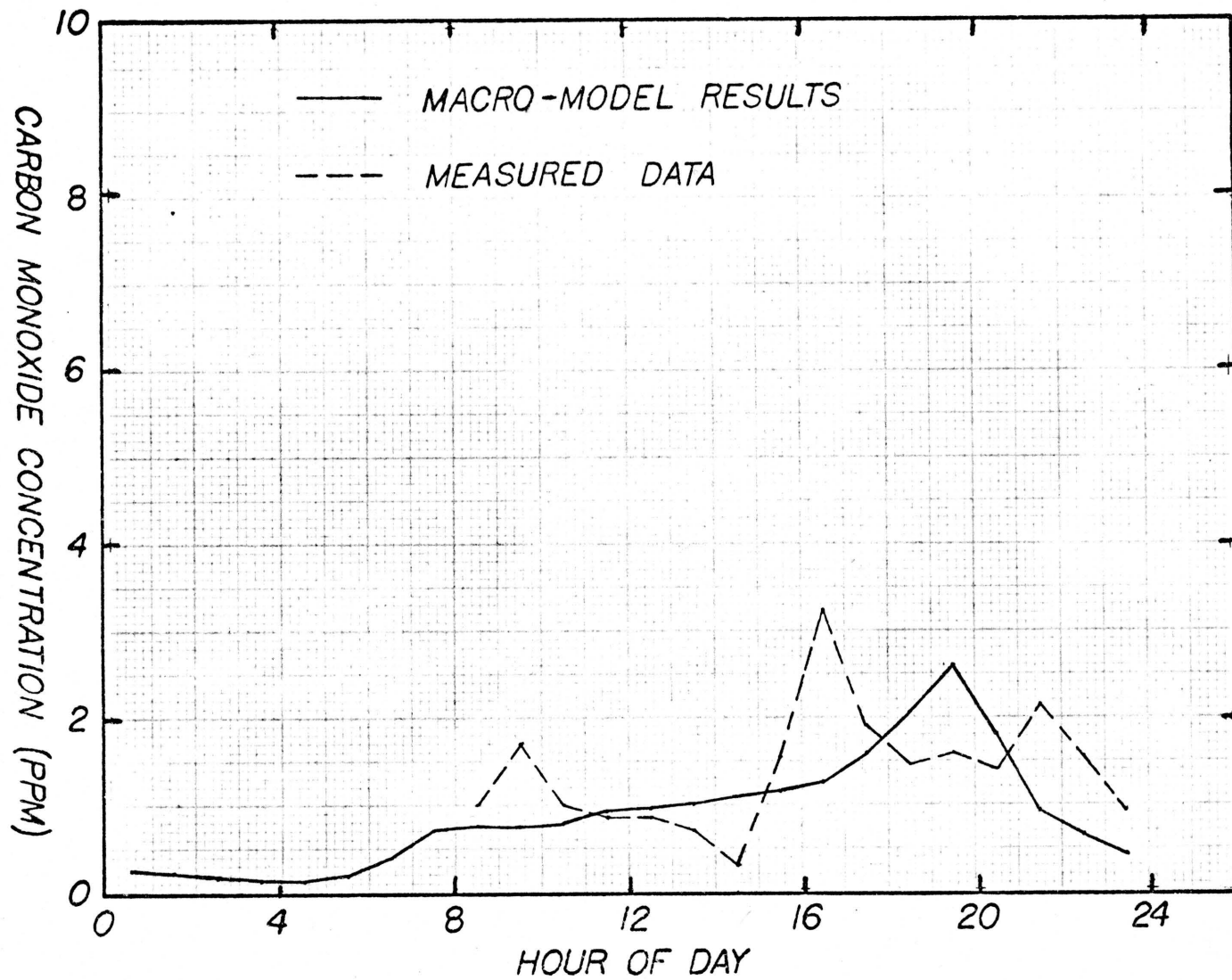
Fig. 8.1 Comparison of Macro-model Results and Measured Data for Carbon
Monoxide for November 9, 1973 for Location 27
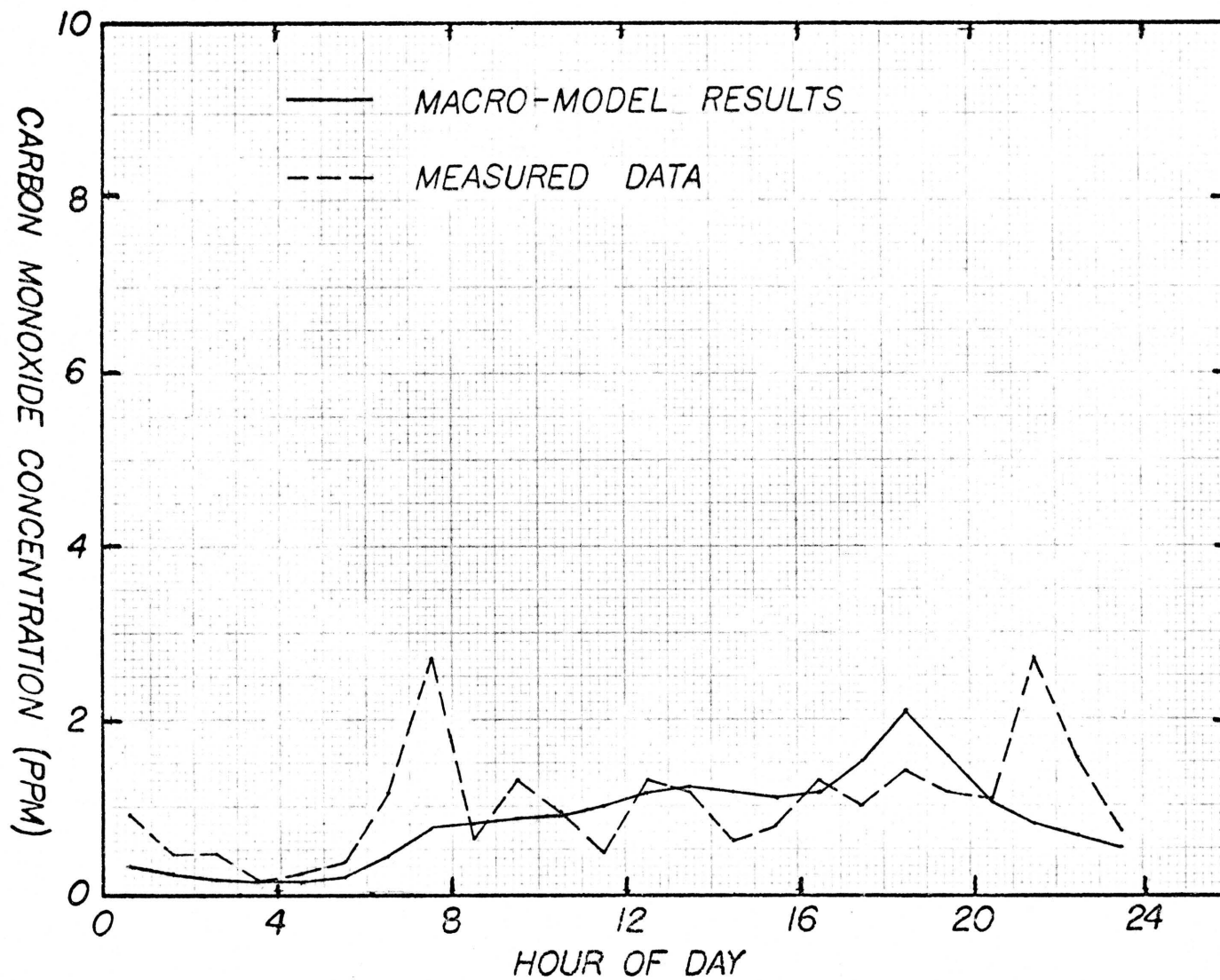
Fig. 8.2 Comparison of Macro-model Results and Measured Data for Carbon
Monoxide for November 10, 1973 for Location 27
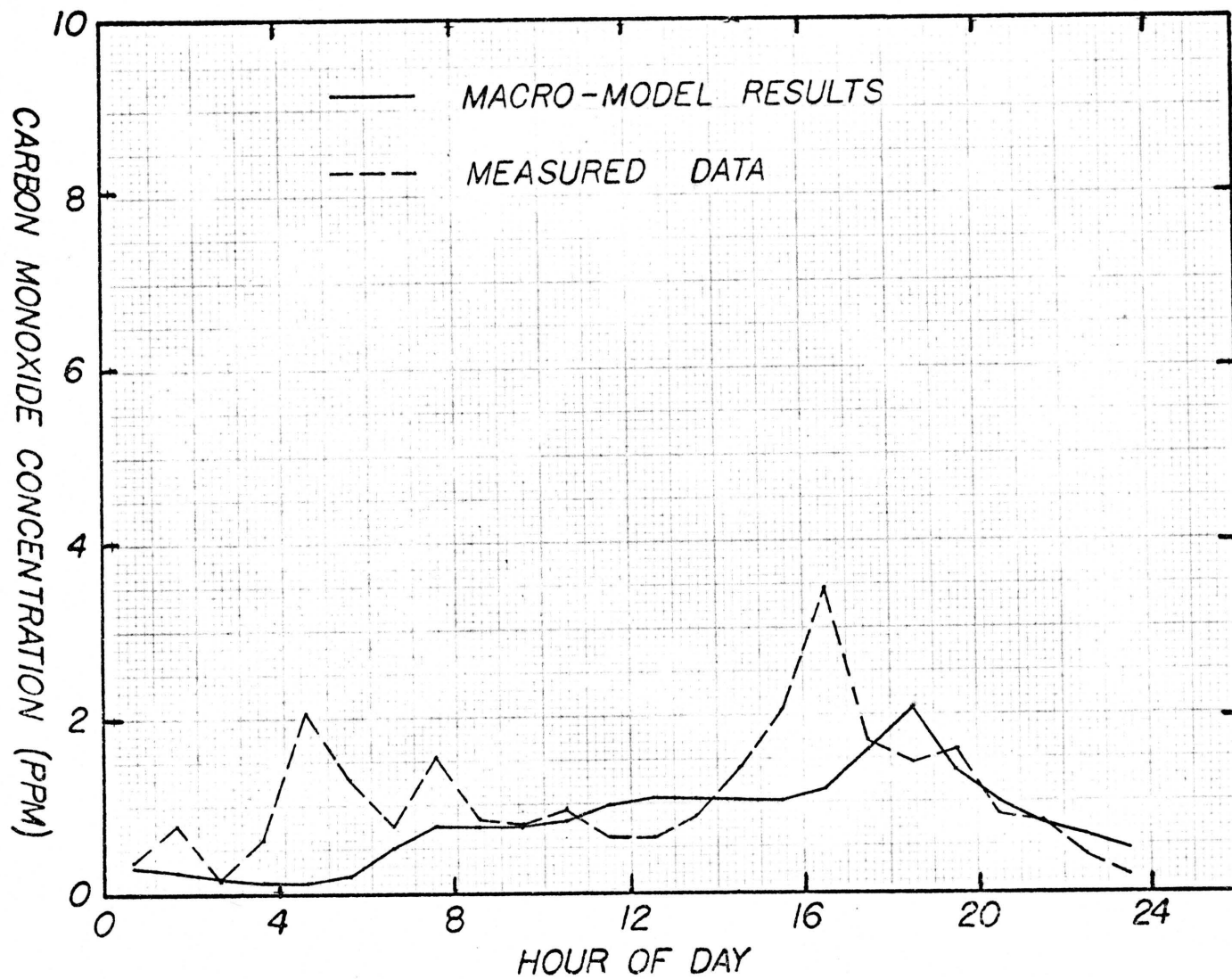
Fig. 8.3 Comparison of Macro-model Results and Measured Data for Carbon
Monoxide for November 11, 1973 for Location 27

Table 8.2 Meteorological Data for Computer Model

Date	Mixing Height	
	Min. H	Max. H
November 9, 1973	50 m	980 m
November 10, 1973	50 m	870 m
November 11, 1973	50 m	920 m
November 20, 1974	100 m	1300 m
January 8, 1974	80 m	1200 m

Saturday morning, whereas the numerical model since it is an area source model can not accurately predict these local effects. The numerical model predicts an increase in the concentration of carbon monoxide throughout the day due to the continuous vehicle traffic sources. The concentration reaches a maximum as the mixing height decreases in the evening. The carbon monoxide level then decreases since the sources of carbon monoxide are now low. All three graphs show the same numerical characteristics just stated. The comparison of magnitudes between the measured data and the macro-model results is good.

On November 20, 1974, extensive sampling for carbon monoxide took place at location 26 on Fig. 7.2. This location is on the south side of Speedway about one block west of the intersection with Mountain and is at the north end of a faculty-student parking lot. Parking lot traffic peaks occur on the hour as classes change and are particularly high from

7 to 7:30 a.m. and near noon. Grab samples and 1-hour average samples were taken for the 24 hour period. At the same time a traffic counter was used to determine the number of vehicles traveling on Speedway on an hourly basis. The wind speed, direction, temperature and relative humidity were taken hourly throughout the day. These data were obtained so that the carbon monoxide measurements could be compared to the concentration distribution calculated using the multi-box model. Winds from the north would bring pollution from Speedway to the sampler, whereas those from the south would bring air from the parking lot.

The macro-model simulation for November 20, 1974, was computed using the meteorological data from the Tucson Weather Service. The wind speed and direction are noted in Table 8.3 with the mixing heights given in Table 8.2. The meteorological conditions were applied uniformly throughout the airshed grid along with the traffic volume distribution plotted in Fig. 5.4. The initial condition to start the simulation is 1.0ppm, and the boundary conditions are also 1.0ppm. The initial and boundary conditions used for all the numerical predictions were chosen such that their magnitudes corresponded to the measured data for which the numerical model was simulating. The concentration distribution as a function of time is calculated for each of the 156 boxes in the airshed grid.

Since the monitoring location for the carbon monoxide is near an area of high traffic density, the macro-model is not expected to agree closely with the measured results. The micro-model is then used to simulate the carbon monoxide distribution within the single macro-box in which the data were taken. For the micro-model the meteorological

Table 8.3 Meteorological Data for Computer Model,
          November 20, 1974

Hr	Macro-model U	Macro-model α	Micro-model U	Micro-model α
1	2.6	110°	1.0	130°
2	2.1	100°	0.8	100°
3	2.6	100°	1.0	100°
4	4.1	100°	1.6	100°
5	3.1	140°	0.0	--
6	4.6	100°	0.0	--
7	4.1	110°	0.0	--
8	4.6	100°	0.0	--
9	4.6	110°	1.0	130°
10	8.2	140°	0.5	110°
11	7.7	140°	0.5	120°
12	5.2	170°	0.5	180°
13	6.7	160°	2.0	140°
14	7.2	170°	2.0	180°
15	3.6	150°	2.5	140°
16	5.2	170°	2.0	160°
17	4.6	220°	1.3	180°
18	3.1	210°	1.0	210°
19	2.6	150°	1.8	210°
20	2.6	140°	1.0	190°
21	3.1	150°	1.5	200°
22	1.5	70°	0.5	320°
23	1.5	120°	0.5	90°
24	1.5	90°	0.0	--

conditions obtained locally for this box are used instead of the data
from the Tucson Weather Service. The meteorological conditions for
this single macro-box for November 20, 1974, are tabulated in Table 8.3.
Note the larger differences in wind speeds between the data taken at loca-
tion 26 and that from the Tucson International Airport (TIA). The mixing
height data are the same as that used for the macro-model. The traffic
volume distribution obtained from the traffic counter is used for the
micro-model instead of the data in Fig. 5.4. The concentration distribu-
tions for the four boxes surrounding the macro-box are used as time
dependent boundary conditions for the micro-model. These boundary condi-
tions are obtained from the macro-model results for November 20, 1974.
The initial condition for the micro-model is 4.0ppm. This concentration
was measured at location 26 at 12 midnight on November 20, 1974. Note
this initial condition has little effect on concentration distribution
after an hour or so.

The 1-hour average carbon monoxide data taken at location 26 are
compared in Fig. 8.4 to the concentration distribution for the cor-
responding box obtained from the macro-model and micro-model. Both models
underpredict the measured data since the monitoring site is in an area of
high traffic density. The traffic volume on Speedway is approximately
37,000 cars per day. The micro-model prediction is better than the macro-
model but still not able to approximate the measured data. The measure-
ments at location 26 are not representative levels of carbon monoxide for
the box analyzed. The measured peak near 10 p.m. is due to traffic gener-
ated when a University Artist Series event was completed. Traffic on
both Speedway and the parking lot was high.
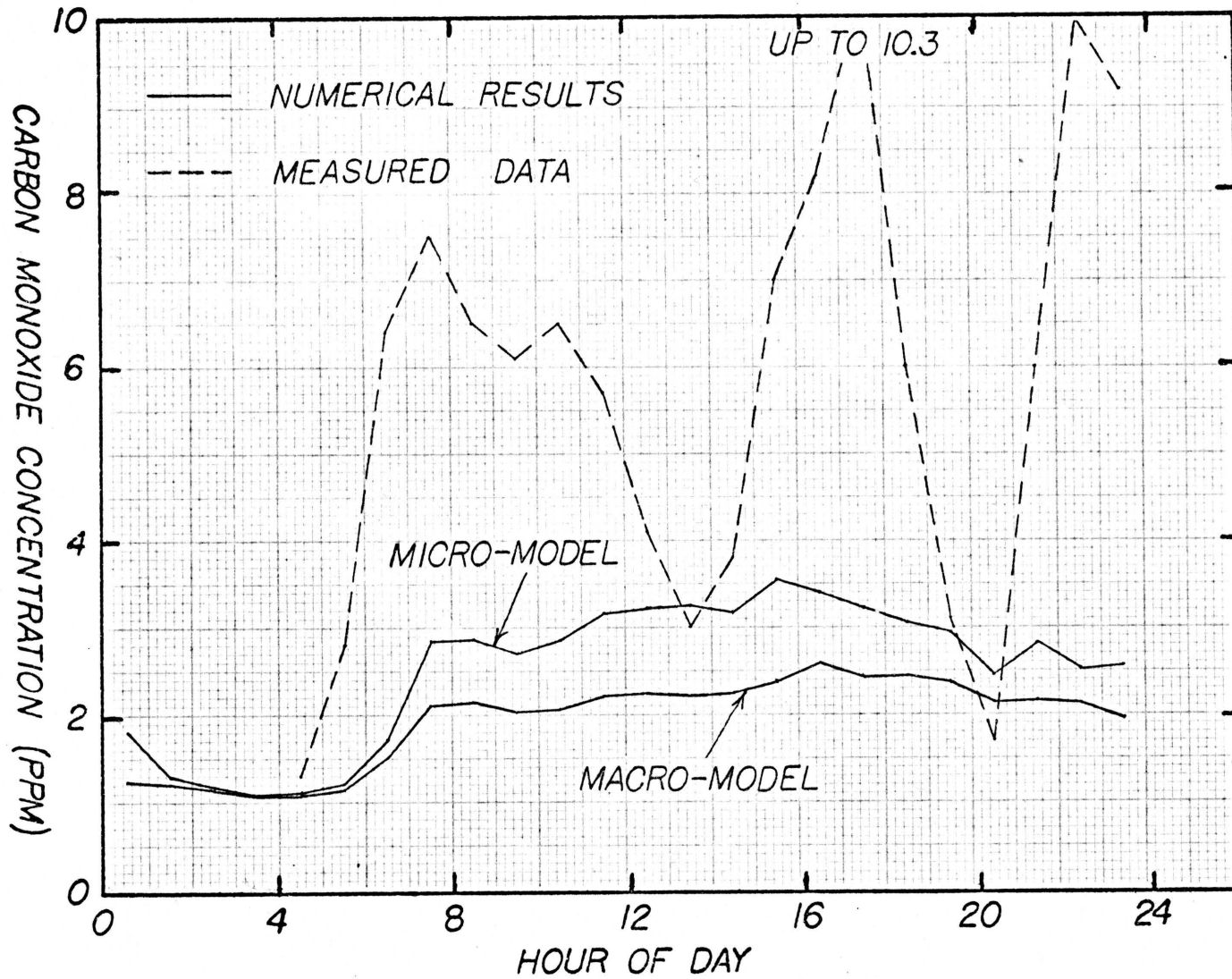
Fig. 8.4 Comparison of Macro- and Micro-model Results and Measured Data
for Carbon Monoxide for November 20, 1974 for Location 26

The results for November 20, 1974, for the micro-model are compared to the traffic volume distribution for Speedway at the same location. The comparison is shown in Fig. 8.5. The shape of the curves is quite similar since the traffic volume distribution is the same as the variations in source magnitude used to compute the carbon monoxide levels.

Carbon monoxide data were also available at two other locations within the Tucson airshed for November 20, 1974. These locations were 27 and 28 of Fig. 7.2, and the data were obtained from the Pima County Health Department. The carbon monoxide monitoring is continuous at both these locations. As mentioned earlier location 27 is near the intersection of 22nd and Craycroft. The concentration distribution for the box corresponding to this location for November 20, 1974, is obtained from the macro-model. The concentration distribution for this location is also simulated using the micro-model. However, this macro-box does not have local meteorological measurements and local traffic volume data that correspond to the area in which the macro-box is located. The meteorological data obtained at the airport along with the traffic volume distribution from Fig. 5.4 are used for the micro-model of location 27 for November 20, 1974. The time dependent boundary conditions for the micro-model are obtained from the macro-model for the four boxes surrounding the macro-box. The initial condition is 1.0ppm. The comparison of the 1-hour average carbon monoxide levels at location 27 with the macro- and micro-model data for November 20, 1974, is presented in Fig. 8.6. The comparison is better than that of Fig. 8.4 but still not adequate, showing that the sampling location is not representative for measuring an average carbon monoxide level for the entire box analyzed.
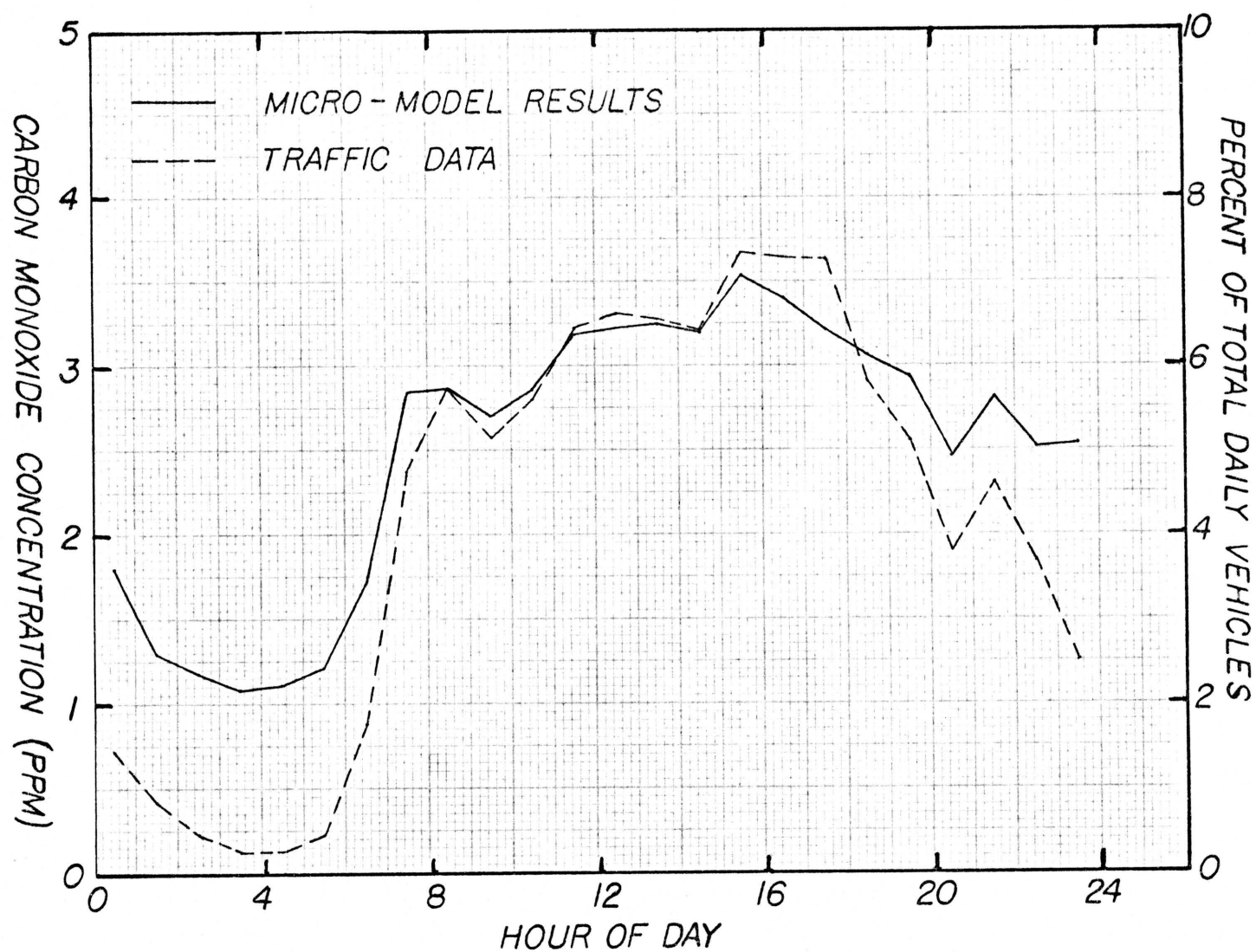
Fig. 8.5 Comparison of Micro-model Results and the Traffic Volume Distribution for Speedway at Location 26 for November 20, 1974
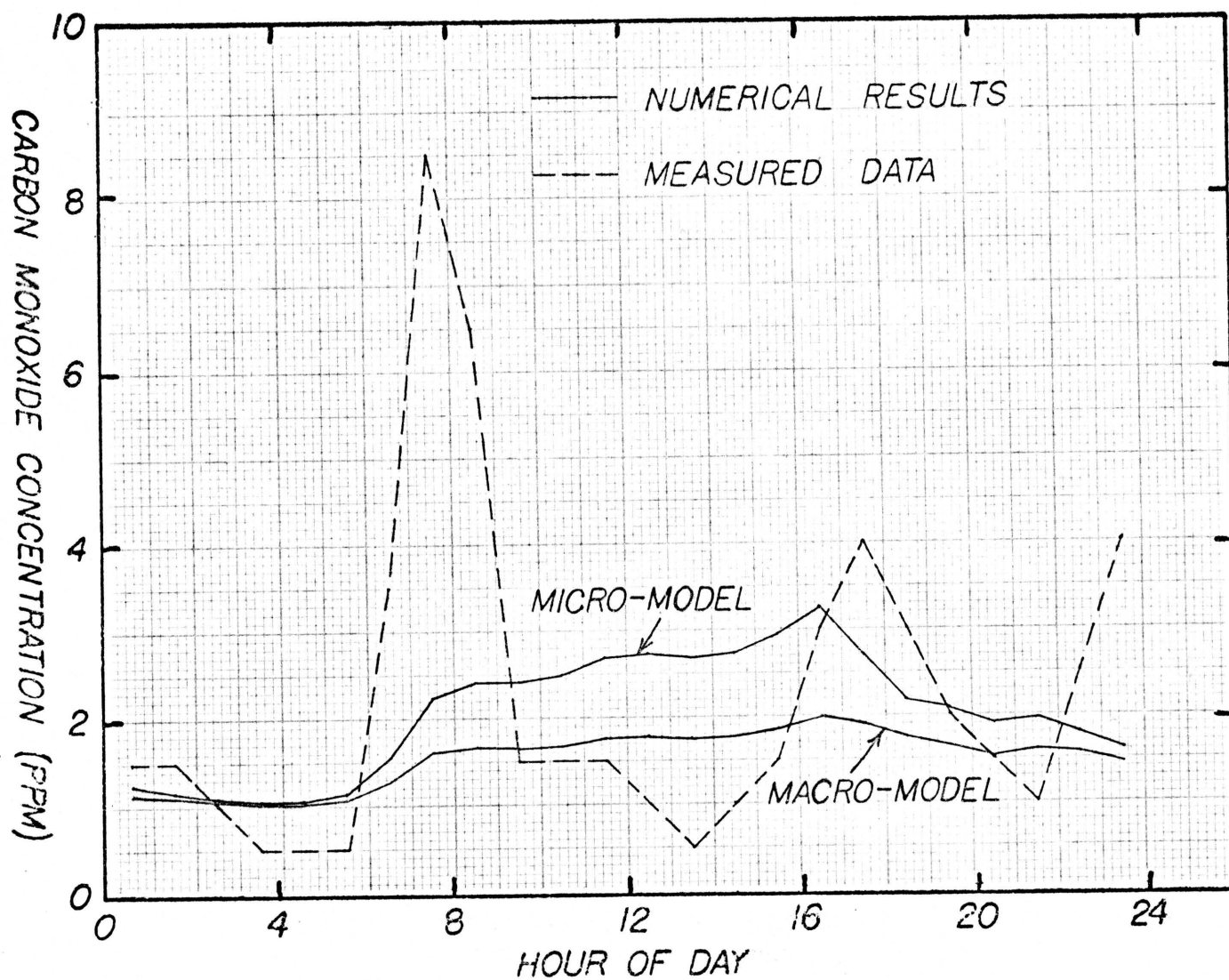
Fig. 8.6 Comparison of Macro- and Micro-model Results and Measured Data for Carbon Monoxide for November 20, 1974 for Location 27

The other Pima County sampling site, 28, is located in the central business district on Congress about one block west of Church. The 1-hour average measured carbon monoxide levels for this location are compared to the concentration distribution for the corresponding box obtained from the macro-model for November 20, 1974. The results are plotted in Fig. 8.7. The shape of the distributions is not similar; however, the magnitude differences between the measured data and simulated results are small. This sampling site seems to be more representative for measuring average carbon monoxide levels for the box in which it is located than the sites at locations 26 and 27.

In order to show better comparison between the measured data and macro- and or micro-model results the sampling site should be more representative for the box in which it is located. A sampling location well within the University of Arizona area was also used since the traffic at the site is low but the location is still only a few blocks from areas of high traffic density. The location on campus is University Boulevard about one block east of Park Avenue and is just west of Old Main. One-hour average carbon monoxide samples were taken on January 8, 1975, at this location between the hours of 0700 and 2000. The carbon monoxide concentration distribution for this day was calculated using the macro-model. The meteorological data were obtained from the Tucson Weather Service. The wind speeds and directions are given in Table 8.4 while the minimum and maximum mixing heights for January 8, 1975, appear in Table 8.2. Table 8.4 also contains the wind speed and direction measurements taken between 0700 and 2000 at the monitoring site. Note the difference in magnitude of the wind speeds for the two locations in the
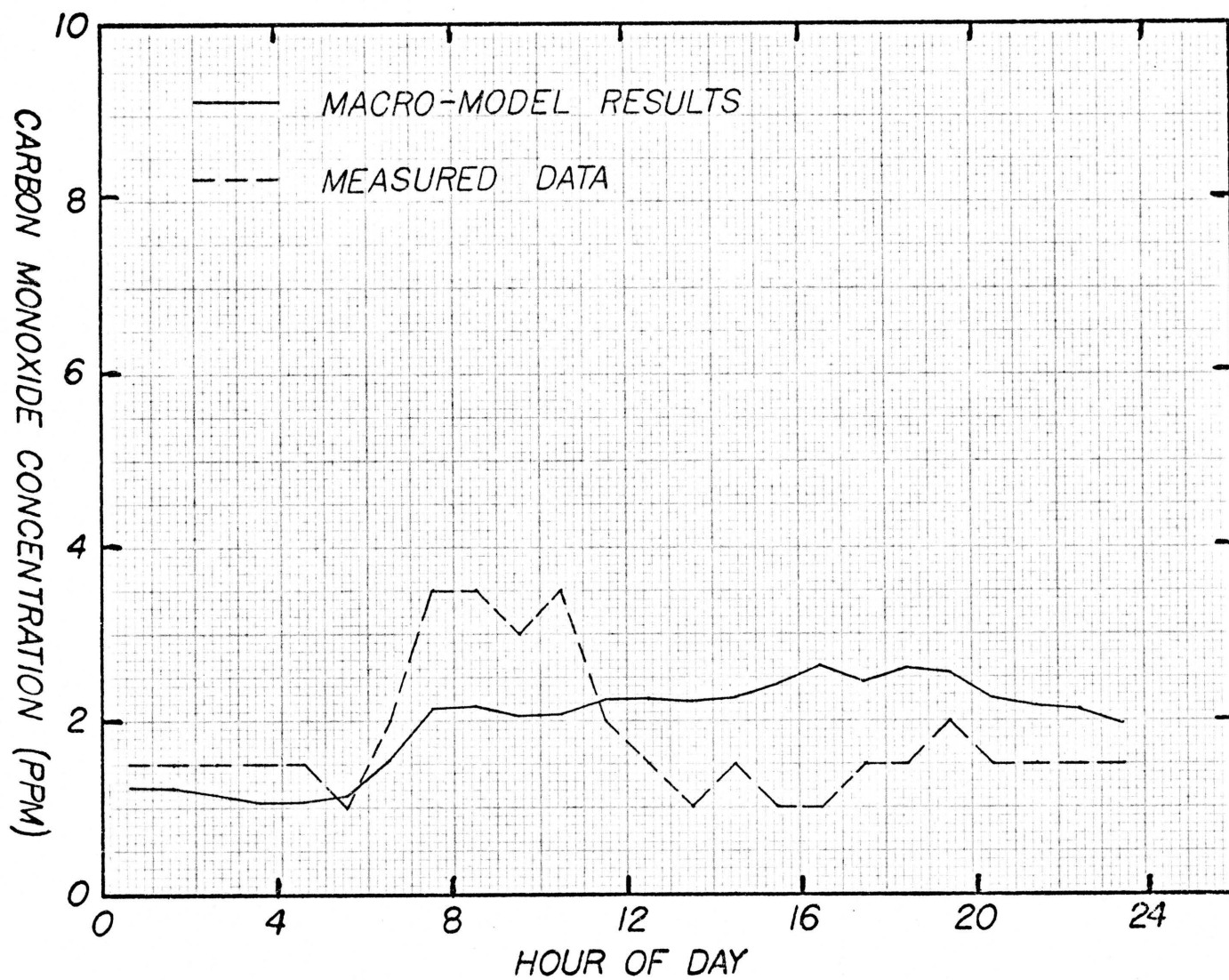
Fig. 8.7 Comparison of Macro-model Results and Measured Data for Carbon
Monoxide for November 20, 1974 for Location 28

Table 8.4   Meteorological Data for January 8, 1975

Hr	TIA U	TIA α	Sampling Location U	Sampling Location α
1	4.1	140°	--	--
2	3.1	130°	--	--
3	3.6	140°	--	--
4	3.1	160°	--	--
5	4.6	150°	--	--
6	5.2	120°	--	--
7	5.2	130°	1.0	140°
8	4.1	140°	0.5	90°
9	4.1	160°	1.3	160°
10	3.6	110°	1.8	180°
11	4.6	90°	1.5	150°
12	6.7	80°	0.0	—
13	7.7	50°	0.8	150°
14	7.2	50°	2.3	0°
15	7.2	50°	2.6	20°
16	8.2	40°	2.6	10°
17	3.6	10°	1.5	0°
18	9.3	30°	2.3	0°
19	5.2	30°	1.0	70°
20	4.6	40°	1.0	70°
21	4.6	60°	--	--
22	4.1	60°	--	--
23	8.2	50°	--	--
24	12.9	70°	--	--

airshed. The inflow boundary conditions and initial condition are all taken to be 1.0ppm. Figure 8.8 shows the comparison of the concentration distribution obtained from the macro-model with the measured data for the thirteen sampling hours of January 8, 1975. The figure shows that this sampling location within the University of Arizona area is fairly representative of the carbon monoxide levels predicted for the macro-box. The first two hours of measurement disagree with the predicted levels since there was moderate traffic traveling within the University area. The University is normally closed to vehicular traffic during the day, but because of semester break the area was open. This moderate traffic along with the effect of near calm conditions at the measurement site resulted in larger measured values of carbon monoxide than the macro-model predicted. The University of Arizona area seems to be a representative location for which comparison between predicted carbon monoxide levels and measured data is good. The conclusions to be drawn from this study and the recommendations for future work are presented in Chapter 9.
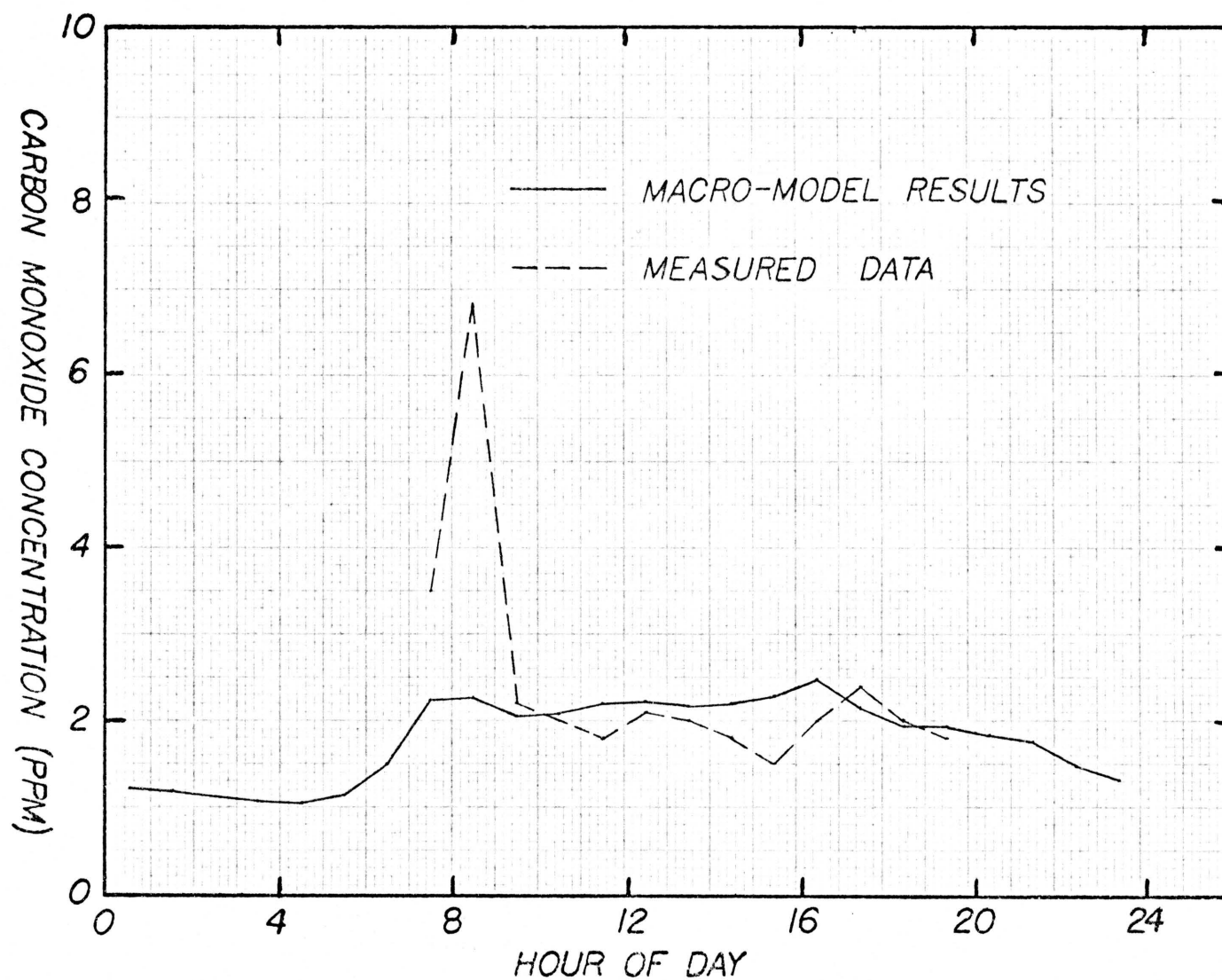
Fig. 8.8 Comparison of Macro-model Results and Measured Data for Carbon Monoxide for January 8, 1975 for a Location on the University Campus

CHAPTER 9

DISCUSSION AND RECOMMENDATIONS

Discussion

The comparisons between measured data and macro- and micro-model predictions presented in Chapter 8 show that the model is unable to simulate actual carbon monoxide levels at or near areas of high traffic density. Since the model is an area source model it predicts an average ground-level concentration for some finite size box. These predicted levels are similar to concentrations measured in residential areas and areas of low traffic density. In order to predict levels at intersections which are areas of high traffic density a Gaussian line source model can be employed as described by Turner (1969). This model was applied in Tucson at location 27 of Fig. 7.2 by Sellars (1974) for predicting carbon monoxide levels for comparison to those measured by the Pima County Health Department. The agreement between data and prediction for that study was fairly good.

These two different models predict the carbon monoxide levels at opposite ends of the source spectrum. There is no single model which can handle the total prediction of carbon monoxide at any location within the Tucson airshed. A more sophisticated three dimensional model could possibly simulate the concentrations of carbon monoxide in areas of high traffic density as well as areas of low traffic sources. Computer

storage capability is, however, a restriction on the airshed grid refinement required for a three dimensional time dependent model.

Use of the multi-box model developed in this report was handicapped due to the fact that continuous meteorological data were available only at one location, that being the Tucson International Airport. On November 20, 1974, local meteorological data were taken at location 26 of Fig. 7.2. There was much disagreement between that data and the information obtained from TIA. The meteorological data for both locations is tabulated in Table 8.3. The assumption that the same meteorological conditions apply throughout the airshed for the macro-model is a bad one. The meteorological data from the airport are not realistic for use in the entire airshed; however, there was no other choice but to apply that data uniformly.

Other variables which affected the macro-model results were the mixing height data, the traffic volume distribution, and the vertical profile chosen for the concentration distribution. The minimum mixing height levels used are possibly not accurate since in Tucson after sunset the radiative inversion begins from the ground and builds to some level. The mixing height may never reach the so-called minimum value obtained using the procedure from AP-101. However, due to a lack of actual data this EPA procedure was used to determine the minimum mixing height. This parameter is quite important since the mixing height times the wind speed is the ventilation rate.

The traffic volume distribution was applied uniformly throughout the airshed in the macro-model. This assumption is probably valid since the traffic distribution obtained at Speedway for November 20, 1974,

appearing in Fig. 8.5 is not too different from the traffic volume varia-
tion of Fig. 5.4. On the average for the macro-model the distribution of
Fig. 5.4 is satisfactory; however, for the micro-model a distribution
for each macro-box such as Fig. 8.5 for location 26 is more appropriate.
A more accurate knowledge of this variable is not as important as know-
ing more about meteorological conditions.

The vertical profile for the concentration distribution affects
the calculated ground-level value. A logarithmic profile is used in both
the macro- and micro-models. This vertical profile was chosen since it
was used by MacCracken et al. (1972) for a multi-box air pollution model
for the San Francisco Bay Area. However, this profile is not generally
applicable under all atmospheric stability conditions. The logarithmic
profile is best suited for a near neutral atmosphere, whereas a linear
profile seems more appropriate for the stable case. When the atmosphere
is quite unstable the concentration is probably near-uniform and equal to
the average concentration for the box.

In the micro-model, the size of each box is smaller in base area
but the height of each box is not changed from that of the macro-model.
The assumption involved in the box model that the pollutant is uniformly
mixed in the vertical direction may no longer be valid. Since the box
height is the same or greater than the width of the box the sources of
carbon monoxide at the ground will not have a chance to mix to the top of
the box by the time the pollutant is transported to the next cell. The
assumption is definitely violated during the day when the mixing height
is large; however, when H is small the assumption is still valid. There-
fore, the results of the micro-model underpredict the actual average

ground-level value for each box during the day since the pollutant is mixed in a smaller volume than that used in the model. The mass in each box is the same, but now the actual volume for dilution is smaller so the density or concentration of the pollutant is actually larger than the level predicted by the micro-model. This problem can be solved by going to a three dimensional model to represent the airshed.

The uncertainty in all the variables involved along with the fact that the area source method of the multi-box model can not simulate measured data at a single point accounts for the inability to predict accurately the measured data in areas of high traffic. However, the model can be used to predict the carbon monoxide levels that the average population in Tucson might be exposed to, for example, locations such as 1, 2, and 3 in Fig. 7.2. The model can also be used to predict area-wide increased levels due to new land development such as a satellite city or a shopping center.

Recommendations for Future Work

As just discussed there is a need for meteorological data on a regular basis at locations other than the TIA so that air flow patterns for the Tucson airshed can be determined. This would allow for spatial input of the wind speed and possibly wind direction. It would be very helpful to have experimental measurements available for the minimum mixing height so that this parameter can be known with more certainty. A stability criterion could be built into the numerical program to allow for changing the vertical profile used to calculate the ground level concentration for each box.

Instead of the pseudo three dimensional method used in this study another approach might be considered. First of all, since Tucson's wind is generally either southeast or northwest, the (x,y) airshed grid could be aligned such that the wind directions are parallel to the x axis. There is now advection in the x direction only. If the crosswind y diffusion is neglected, the airshed grid could be divided into boxes in the vertical z direction from the ground up to the mixing height H such that the modeling problem reduces to solving an equation similar to (3.2) except now in the (x,z) plane. The equation to be solved is

$$\frac{\partial C}{\partial t} + u \frac{\partial C}{\partial x} + w \frac{\partial C}{\partial z} = K_H \frac{\partial^2 C}{\partial x^2} + K_z \frac{\partial^2 C}{\partial z^2} + \frac{S}{V} \qquad (9.1)$$

This solution would give the concentration distribution in the (x,z) plane at each y location. Instead of y advection, there is z advection due to the vertical wind speed w. There is also z diffusion with a vertical eddy diffusivity K_z. The advantage of this method is that only a two dimensional time dependent partial differential equation is needed to solve a three dimensional problem. This solution for the concentration distribution in the (x,z) plane is similar to that applied by Mahoney and Egan (1971). The assumption in this approach of neglecting crosswind diffusion is probably not bad if the method is applied to the macro-model in this study where the size of the boxes is large. However, for the micro-model, the macro-box of interest contains a number of large sources of carbon monoxide so when subdivision occurs the crosswind diffusion between these micro-boxes is no longer insignificant. Therefore, this method is not suitable for the micro-model grid.

In general the wind direction is not always southeast or northwest nor even uniform in direction. Then the crosswind y diffusion becomes important for the approach just discussed, so a more sophisticated three dimensional time dependent model is needed. However, reliable input data for a model of this caliber is not readily available. Further the computer storage requirement would be quite large in order to handle the four variables involved in the problem. This approach is feasible, but probably the results would not be worth the time and cost involved.

Besides a need for improving the numerical model to simulate the carbon monoxide concentration distribution in the Tucson airshed, there is a need for more measured data to verify the predicted carbon monoxide levels from such a model. Continuous monitoring at many locations in different parts of Tucson would be helpful for confirming the spatial predictions of the carbon monoxide levels from the numerical model. This carbon monoxide data would also be useful to the Pima County Health Department in its attempt to become a subregion in the Phoenix-Tucson Intrastate Air Quality Region. Monitoring of concentration as a function of height would also be helpful.

The model developed in this study could be used to simulate the average carbon monoxide concentration distribution in the Tucson airshed for a year. This can be accomplished by running an ensemble of days representing different seasons or months of the year. The average concentration distribution for the year for each box can then be calculated by multiplying the average concentration during each hour for a typical day times the fractional number of occurrences of this day in a year and then

summing. This procedure would be repeated for each box so that an average carbon monoxide concentration could be obtained for the whole year.

The results presented in Chapter 8 have shown the limitations of the model developed in this report. However, the model is still useful and with further development a similar model employing many features of this multi-box model could be used by the Pima County Health Department in predicting the carbon monoxide levels in the Tucson airshed. Of special interest would be the model's use for prediction of levels during possible episode periods and in regulating and controlling land-use in accord with the EPA ambient standards.

APPENDIX A

FINITE DIFFERENCE EQUATIONS

The use of the Crank-Nicholson finite difference method to integrate equation (3.3) requires that the terms be expanded in a Taylor series about the point, $t+\Delta t/2$. Consider Fig. 3.2 which depicts a typical node (i,j). If a mass balance is made on the control volume, the following equation is obtained

$$\left.\frac{\partial C}{\partial t}\right|_{i,j}^{t+\frac{\Delta t}{2}} (L^2 H) = u(C_{i,j-1} - C_{i,j})^{t+\frac{\Delta t}{2}} \text{(LH)}$$

$$+ v(C_{i-1,j} - C_{i,j})^{t+\frac{\Delta t}{2}} \text{(LH)}$$

$$+ K_H \left(\left.\frac{\partial C}{\partial x}\right|_{i,j+\frac{1}{2}}^{t+\frac{\Delta t}{2}} - \left.\frac{\partial C}{\partial x}\right|_{i,j-\frac{1}{2}}^{t+\frac{\Delta t}{2}}\right) \text{(LH)} \tag{A.1}$$

$$+ K_H \left(\left.\frac{\partial C}{\partial y}\right|_{i+\frac{1}{2},j}^{t+\frac{\Delta t}{2}} - \left.\frac{\partial C}{\partial y}\right|_{i-\frac{1}{2},j}^{t+\frac{\Delta t}{2}}\right) \text{(LH)} + S_{i,j}$$

This equation (A.1) is the same equation as (3.5). The terms that appear as partial derivatives are expanded in a Taylor series in the following manner.

187

$$C_{i,j}^{t+\Delta t} = C_{i,j}^{t+\frac{\Delta t}{2}} + \left.\frac{\partial C}{\partial t}\right|_{i,j}^{t+\frac{\Delta t}{2}} \frac{\Delta t}{2} + \left.\frac{\partial^2 C}{\partial t^2}\right|_{i,j}^{t+\frac{\Delta t}{2}} \frac{\Delta t^2}{8} + O(\Delta t^3) \qquad (A.2)$$

$$C_{i,j}^{t} = C_{i,j}^{t+\frac{\Delta t}{2}} - \left.\frac{\partial C}{\partial t}\right|_{i,j}^{t+\frac{\Delta t}{2}} \frac{\Delta t}{2} + \left.\frac{\partial^2 C}{\partial t^2}\right|_{i,j}^{t+\frac{\Delta t}{2}} \frac{\Delta t^2}{8} + O(\Delta t^3) \qquad (A.3)$$

Subtracting equation (A.3) from equation (A.2) one obtains the result

$$\frac{C_{i,j}^{t+\Delta t} - C_{i,j}^{t}}{\Delta t} = \left.\frac{\partial C}{\partial t}\right|_{i,j}^{t+\frac{\Delta t}{2}} + O(\Delta t^3) \qquad (A.4)$$

This is the result for the expansion of the partial derivative with time as the independent variable. For the spatial derivative the expansions are as follows.

$$C_{i,j}^{t+\frac{\Delta t}{2}} = C_{i,j+\frac{1}{2}}^{t+\frac{\Delta t}{2}} - \left.\frac{\partial C}{\partial x}\right|_{i,j+\frac{1}{2}}^{t+\frac{\Delta t}{2}} \frac{\Delta x}{2} + \left.\frac{\partial^2 C}{\partial x^2}\right|_{i,j+\frac{1}{2}}^{t+\frac{\Delta t}{2}} \frac{\Delta x^2}{8} + O(\Delta x^3) \qquad (A.5)$$

$$C_{i,j+1}^{t+\frac{\Delta t}{2}} = C_{i,j+\frac{1}{2}}^{t+\frac{\Delta t}{2}} + \left.\frac{\partial C}{\partial x}\right|_{i,j+\frac{1}{2}}^{t+\frac{\Delta t}{2}} \frac{\Delta x}{2} + \left.\frac{\partial^2 C}{\partial x^2}\right|_{i,j+\frac{1}{2}}^{t+\frac{\Delta t}{2}} \frac{\Delta x^2}{8} + O(\Delta x^3) \qquad (A.6)$$

Subtracting equation (A.5) from equation (A.6) one obtains the result

$$\frac{C_{i,j+1}^{t+\frac{\Delta t}{2}} - C_{i,j}^{t+\frac{\Delta t}{2}}}{\Delta x} = \left.\frac{\partial C}{\partial X}\right|_{i,j+\frac{1}{2}}^{t+\frac{\Delta t}{2}} + O(\Delta x^3) \qquad (A.7)$$

Equation (A.7) is similar to the result presented in Chapter 3 except Δx is replaced by L since L is the length of the control volume, not Δx.

The results for the other three partial derivatives are obtained in a similar manner to equation (A.7) and are presented below.

$$\frac{\partial C}{\partial x}\bigg|_{i,j-\frac{1}{2}}^{t+\frac{\Delta t}{2}} = \frac{C_{i,j}^{t+\frac{\Delta t}{2}} - C_{i,j-1}^{t+\frac{\Delta t}{2}}}{\Delta x} \tag{A.8}$$

$$\frac{\partial C}{\partial y}\bigg|_{i+\frac{1}{2},j}^{t+\frac{\Delta t}{2}} = \frac{C_{i+1,j}^{t+\frac{\Delta t}{2}} - C_{i,j}^{t+\frac{\Delta t}{2}}}{\Delta y} \tag{A.9}$$

$$\frac{\partial C}{\partial y}\bigg|_{i-\frac{1}{2},j}^{t+\frac{\Delta t}{2}} = \frac{C_{i,j}^{t+\frac{\Delta t}{2}} - C_{i-1,j}^{t+\frac{\Delta t}{2}}}{\Delta y} \tag{A.10}$$

Now putting (A.4) along with (A.7), (A.8), (A.9) and (A.10),with Δx and Δy replaced with L, into equation (A.1) and multiplying by $\frac{\Delta t}{L^2 H}$, the following is obtained

$$(C_{i,j}^{t+\Delta t} - C_{i,j}^{t}) = \frac{u\Delta t}{L} (C_{i,j-1} - C_{i,j})^{t+\frac{\Delta t}{2}}$$

$$+ \frac{v\Delta t}{L} (C_{i-1,j} - C_{i,j})^{t+\frac{\Delta t}{2}}$$

$$+ \frac{K_H \Delta t}{L^2} (C_{i,j+1} + C_{i,j-1} - 2C_{i,j})^{t+\frac{\Delta t}{2}}$$

$$+ \frac{K_H \Delta t}{L^2} (C_{i+1,j} + C_{i-1,j} - 2C_{i,j})^{t+\frac{\Delta t}{2}}$$

$$+ \frac{S_{i,j}\Delta t}{L^2 H} \tag{A.11}$$

A simple averaging is now used to evaluate the concentrations C at t+Δt/2.

$$C_{i,j}^{t+\frac{\Delta t}{2}} = \frac{1}{2}(C_{i,j}^{t} + C_{i,j}^{t+\Delta t})$$

(A.12)

Putting (A.12) into (A.11) along with some algebra gives

$$C_{i,j}^{t+\Delta t}(1 + \frac{4K_H\Delta t}{2L^2} + \frac{u\Delta t}{2L} + \frac{v\Delta t}{2L}) - C_{i,j-1}^{t+\Delta t}(\frac{K_H\Delta t}{2L^2} + u\frac{\Delta t}{2L})$$

$$- C_{i-1,j}^{t+\Delta t}(\frac{K_H\Delta t}{2L^2} + \frac{v\Delta t}{2L}) - C_{i,j+1}^{t+\Delta t}(\frac{K_H\Delta t}{2L^2}) - C_{i+1,j}^{t+\Delta t}(\frac{K_H\Delta t}{2L^2})$$

$$= C_{i,j}^{t}(1 - \frac{4K_H\Delta t}{2L^2} - \frac{u\Delta t}{2L} - \frac{v\Delta t}{2L})$$

$$+ C_{i,j-1}^{t}(\frac{K_H\Delta t}{2L^2} + \frac{u\Delta t}{2L}) + C_{i-1,j}^{t}(\frac{K_H\Delta t}{2L^2} + \frac{v\Delta t}{2L})$$

$$+ C_{i,j+1}^{t}(\frac{K_H\Delta t}{2L^2}) + C_{i+1,j}^{t}(\frac{K_H\Delta t}{2L^2}) + \frac{S_{i,j}\Delta t}{L^2 H}$$

(A.13)

Equation (A.13) now contains terms at t+Δt on the left-hand side of the equation and terms at t on the right side. Defining some parameters, equation (A.13) can be simplified. A diffusion velocity can be defined such that

$$V_D = \frac{K_H}{L}$$

and two non-dimensional parameters are defined as

$$\theta = \frac{U\Delta t}{4L} \quad \text{and} \quad \beta = \frac{V_D}{U}$$

Using these ideas with the fact that

$$u = U \cos\alpha$$

and

$$v = U \sin\alpha$$

some of the terms in parentheses reduce to

$$\frac{4K_H \Delta t}{2L^2} = 2 \frac{V_D}{L} \Delta t \frac{U}{U} = 8\theta \beta$$

$$\frac{u\Delta t}{2L} = \frac{U\Delta t}{2L} \cos\alpha = 2\theta \cos\alpha$$

$$\frac{v\Delta t}{2L} = \frac{U\Delta t}{2L} \sin\alpha = 2\theta \sin\alpha$$

$$\frac{K_H \Delta t}{2L^2} = \frac{V_D}{2} \frac{\Delta t}{L} \frac{U}{U} = 2\theta \beta$$

and

$$\frac{S_{i,j} \Delta t}{L^2 H} = \frac{S_{i,j}}{L^2 H} \frac{4L\theta}{U}$$

$$= 4\theta \left[\frac{S_{i,j}}{LUH}\right] = 4\theta (C_{ss})_{i,j}$$

The term in parentheses is the steady state concentration for box (i,j) which was obtained by Smith (1961). This steady state concentration will be written as

$$C_{ss} = \frac{S}{LUH}$$

All the above expressions can be put into equation (A.13), and with further algebra along with dividing each term by θ, the final result obtained is

$$C_{i,j}^{t+\Delta t}(\frac{1}{\theta} + 8\beta + 2\cos\alpha + 2\sin\alpha)$$

$$- C_{i,j-1}^{t+\Delta t}(2\beta + 2\cos\alpha) - C_{i-1,j}^{t+\Delta t}(2\beta + 2\sin\alpha) - C_{i,j+1}^{t+\Delta t}(2\beta) - C_{i+1,j}^{t+\Delta t}(2\beta)$$

$$= C_{i,j}^{t}(\frac{1}{\theta} - 8\beta - 2\cos\alpha - 2\sin\alpha) \tag{A.14}$$

$$+ C_{i,j-1}^{t}(2\beta + 2\cos\alpha) + C_{i-1,j}^{t}(2\beta + 2\sin\alpha)$$

$$+ C_{i,j+1}^{t}(2\beta) + C_{i+1,j}^{t}(2\beta) + 4 C_{ss_{i,j}}$$

Equation (A.14) is the final equation needed to determine the concentrations at $t+\Delta t$ in terms of their values at t. The terms in parentheses are all in non-dimensional form.

For the case of zero convection the analysis begins with making a mass balance on node (i,j) using Fig. 3.2. The same result can be obtained by setting u and v equal to zero in (A.1) since they are the components of the wind speed U. The result obtained is

$$\frac{\partial C}{\partial t}\bigg|_{i,j}^{t+\frac{\Delta t}{2}}(L^2H) = K_H(\frac{\partial C}{\partial x}\bigg|_{i,j+\frac{1}{2}}^{t+\frac{\Delta t}{2}} - \frac{\partial C}{\partial x}\bigg|_{i,j-\frac{1}{2}}^{t+\frac{\Delta t}{2}})\ (LH)$$

$$+ K_H(\frac{\partial C}{\partial y}\bigg|_{i+\frac{1}{2},j}^{t+\frac{\Delta t}{2}} - \frac{\partial C}{\partial y}\bigg|_{i-\frac{1}{2},j}^{t+\frac{\Delta t}{2}})\ (LH) + S_{i,j} \tag{A.15}$$

This equation (A.15) is the same equation as (3.12). The terms that appear as partial derivatives are expanded in a Taylor series and the results are

$$\left.\frac{\partial C}{\partial t}\right|_{i,j}^{t+\frac{\Delta t}{2}} = \frac{C_{i,j}^{t+\Delta t} - C_{i,j}^{t}}{\Delta t} \qquad (A.4)$$

$$\left.\frac{\partial C}{\partial x}\right|_{i,j+\frac{1}{2}}^{t+\frac{\Delta t}{2}} = \frac{C_{i,j+1}^{t+\frac{\Delta t}{2}} - C_{i,j}^{t+\frac{\Delta t}{2}}}{\Delta x} \qquad (A.7)$$

$$\left.\frac{\partial C}{\partial x}\right|_{i,j-\frac{1}{2}}^{t+\frac{\Delta t}{2}} = \frac{C_{i,j}^{t+\frac{\Delta t}{2}} - C_{i,j-1}^{t+\frac{\Delta t}{2}}}{\Delta x} \qquad (A.8)$$

$$\left.\frac{\partial C}{\partial y}\right|_{i+\frac{1}{2},j}^{t+\frac{\Delta t}{2}} = \frac{C_{i+1,j}^{t+\frac{\Delta t}{2}} - C_{i,j}^{t+\frac{\Delta t}{2}}}{\Delta y} \qquad (A.9)$$

$$\left.\frac{\partial C}{\partial y}\right|_{i-\frac{1}{2},j}^{t+\frac{\Delta t}{2}} = \frac{C_{i,j}^{t+\frac{\Delta t}{2}} - C_{i-1,j}^{t+\frac{\Delta t}{2}}}{\Delta y} \qquad (A.10)$$

The results (A.4), (A.8), (A.9), (A.10) are repeated here for completion in reducing (A.15). Putting these results into (A.15) while replacing Δx and Δy by L and then multiplying by $\frac{\Delta t}{L^2 H}$, the following is obtained.

$$(C_{i,j}^{t+\Delta t} - C_{i,j}^{t}) = \frac{K_H \Delta t}{L^2} (C_{i,j+1} + C_{i,j-1} - 2C_{i,j})^{t+\frac{\Delta t}{2}}$$

$$+ \frac{K_H \Delta t}{L^2} (C_{i+1,j} + C_{i-1,j} - 2C_{i,j})^{t+\frac{\Delta t}{2}}$$

$$+ \frac{S_{i,j} \Delta t}{L^2 H} \qquad (A.16)$$

Note that (A.16) is similar to (A.11) with u and v equal to zero. A simple averaging is now used to evaluate the concentrations C at $t+\Delta t/2$.

$$c_{i,j}^{t+\Delta t/2} = \frac{1}{2}(c_{i,j}^{t} + c_{i,j}^{t+\Delta t}) \qquad (A.12)$$

Putting (A.12) into (A.16) with some algebra gives

$$c_{i,j}^{t+\Delta t}(1 + \frac{4K_H\Delta t}{2L^2}) - \frac{K_H\Delta t}{2L^2}(C_{i,j+1} + C_{i,j-1} + C_{i+1,j} + C_{i-1,j})^{t+\Delta t}$$

$$= c_{i,j}^{t}(1 - \frac{4K_H\Delta t}{2L^2}) + \frac{S_{i,j}\Delta t}{L^2 H} \qquad (A.17)$$

$$+ \frac{K_H\Delta t}{2L^2}(C_{i,j+1} + C_{i,j-1} + C_{i+1,j} + C_{i-1,j})^{t}$$

Equation (A.17) now contains terms at $t+\Delta t$ on the left side of the equation and terms at t on the right side. Defining a non-dimensional parameter, the equation can be simplified. The parameter is given by

$$\phi = \frac{K_H\Delta t}{2L^2} = \frac{V_D\Delta t}{2L}$$

where

$$V_D = \frac{K_H}{L}$$

Using this expression

$$\frac{4K_H\Delta t}{2L^2} = 4\phi$$

and defining a concentration for node (i,j) for the case of zero wind

$$C_{zw_{i,j}} = \frac{S_{i,j}\Delta t}{L^2 H}$$

Equation (A.18) can be put in a final form which is the following

$$c_{i,j}^{t+\Delta t}(1 + 4\phi) - \phi(C_{i,j+1} + C_{i+1,j} + C_{i,j-1} + C_{i-1,j})^{t+\Delta t}$$

$$= c_{i,j}^{t}(1-4\phi) + C_{zw_{i,j}}$$

$$+ \phi(C_{i,j+1} + C_{i+1,j} + C_{i,j-1} + C_{i-1,j})^{t}$$

(A.18)

This result is the same as (3.13) in the text of the report. This equation is used to obtain the concentrations at t+Δt in terms of their values at t for the case of zero convection.

Vertical Concentration Distribution

A distribution for the concentration is assumed in the vertical direction so a ground level concentration can be calculated. The vertical profile has a logarithmic dependence given by

$$C(z) = a + b \; \ln \frac{z}{z_o} \qquad\qquad z_o \le z \le H$$

$$C(z) = a \qquad\qquad 0 \le z \le z_o$$

(A.19)

z_o is the reference height equal to one meter. The coefficients a and b can be obtained by applying the conditions set forth in equation (3.21) and (3.22) appearing in the text of this report. Applying the relation (A.19) in equation (3.21) the following is obtained

$$\overline{C} = \frac{1}{H} \int_o^{z_o} a \; dz + \frac{1}{H} \int_{z_o}^{H} (a + b \; \ln \frac{z}{z_o}) \; dz$$

Integrating gives

$$\overline{C} = \frac{1}{H} [a \; z_o] + \frac{1}{H} \{a(H-z_o) + b \int_{z_o}^{H} \ln \frac{z}{z_o} \; dz\}$$

Applying the substitution of

$$w = \frac{z}{z_o} \qquad \text{and} \qquad dw = \frac{dz}{z_o}$$

the following is obtained

$$\overline{C} = \frac{a\,z_o}{H} + \frac{aH}{H} - \frac{a\,z_o}{H} + \frac{b\,z_o}{H} \int_1^{\frac{H}{z_o}} \ln w \, dw$$

Now integrating the last term gives

$$\overline{C} = a + \frac{b\,z_o}{H} [w \ln w - w]_1^{\frac{H}{z_o}}$$

Putting in the limits for the term in brackets and substituting for w gives

$$\overline{C} = a + \frac{b\,z_o}{H} [\frac{H}{z_o} \ln \frac{H}{z_o} - \frac{H}{z_o} - 1 \ln 1 + 1]$$

so

$$\overline{C} = a + b [\ln \frac{H}{z_o} - (1 - \frac{z_o}{H})] \qquad (A.20)$$

Now applying the relation in equation (3.22) the following is obtained

$$Q = - K_z \frac{d}{dz} (a + b \ln \frac{z}{z_o})\Big|_{z = z_o}$$

Again substituting

$$w = \frac{z}{z_o} \qquad \text{and} \qquad dw = \frac{dz}{z_o}$$

$$Q = - \frac{K_z}{z_o} \frac{d}{dw} (a + b \ln w)\Big|_{w=1}$$

Differentiating gives

$$Q = - \frac{K_z}{z_o} \left[\frac{b}{w}\right]_{w=1}$$

So

$$Q = - \frac{K_z b}{z_o}$$

or

$$b = - \frac{Q z_o}{K_z} \qquad (A.21)$$

Putting (A.21) into (A.20) and solving for a, the following is obtained

$$a = \overline{C} + \frac{Q z_o}{K_z} \left[\ln \frac{H}{z_o} - (1 - \frac{z_o}{H})\right] \qquad (A.22)$$

a is the value for the ground level concentration, given the symbol C_{GL}, and z_o is equal to 1 meter. Since $z_o << H$, the expression below can be approximated as

$$(1 - \frac{z_o}{H}) \simeq 1$$

and equation (A.22) simplifies to

$$C_{GL} = \overline{C} + \frac{S}{L^2 K_z} \left[\ln H - 1\right] \qquad (A.23)$$

with Q replaced by S/L^2 and H having the units of meters. Putting (A.23) into (A.19) along with (A.21) gives

$$C(z) = C_{GL} - \frac{S}{L^2 K_z} \ln z \qquad (A.24)$$

$$\text{for } 1 < z < H$$

Equation (A.23) and (A.24) give the value for the concentration C at any height z for any location (x,y) for the time t. Equation (A.23) is the same as (3.24) and equation (A.24) is the same as (3.25) in the report text.

APPENDIX B

LISTING OF COMPUTER PROGRAMS

Listing of the computer programs for both the macro- and micro-
model are presented here. The models are discussed in detail in
Chapter 5.

```
C              M A C R O - - M O D E L    P R O G R A M
       PROGRAM TAPBM ( INPUT,OUTPUT )
       DIMENSION TD(24),H(24),U(24),ALPHA(24),NWQ(24),RHOX(24),
      1   RHOY(24),S(156),X(156,156),CN(156),C(156),CO(50),
      2   Z(156),PPM(6,156),GLC(156)
       COMMON A1,A2,A3,A4,A5,A6,B1,B2,B3,B4,B5,B6,B7,B8,B9,
      1   B10,B11,B12,B13,B14,B15,B16,B17,B18,B19,B20,B21,B22,
      2   B23,B24,TD,H,U,ALPHA,NWQ,RHOX,RHOY,S,X,CN,Z,CO
       REAL L,KH,KZ,KM
   1   FORMAT (8E10.0)
   3   FORMAT (4I10)
  10   FORMAT (8I10)
  24   FORMAT (18X,I3,11X,F8.4,8X,F8.4,8X,F8.4,8X,F8.4,8X,
      1 F8.4,8X,F8.4,/)
  28   FORMAT (1H1,//,30X,*MIXING HEIGHT IS*,F7.1,3X,
      1 *METERS*,//,30X,*WIND SPEED IS*,F8.3,3X,*METERS/SEC*,
      2 //,30X,*WIND DIRECTION IS*,F10.1,3X,*DEGREES COUNTER
      3 CLOCKWISE W.R.T. THE EAST*,//,30X,*THIS IS HOUR *,I4,
      4 2X,*OF THE DAY*)
  29   FORMAT (////,15X,*BOX NUMBER*,33X,*CARBON MONOXIDE CON
      1 CENTRATION IN PPM*,//,33X,*INTERVAL 1*,10X,*2*,15X,
      2 *3*,15X,*4*,15X,*5*,15X,*6*,/)
  31   FORMAT (1H1,/////////////////,35X,*TUCSON   URBAN   AIR
      1 POLLUTION   BOX   MODEL   FOR   CARBON   MONOXIDE*,///,
      2 52X,*A   24   HOUR   DAY   IS   SIMULATED*,////,25X,*THE
      3 MIXING   HEIGHT,   WIND   SPEED,   AND   WIND   DIRECTION
      4 ARE   VARIED   ON   AN   HOURLY   BASIS*,////////,29X,*THE
      5 AVERAGE   CONCENTRATION   FOR   EACH   BOX   IS   PRINTED
      6 OUT*,I4,2X,*TIMES PER HOUR*)
  32   FORMAT (//////,40X,*THE SQUARE BASE DIMENSION OF EACH
      1 BOX IS*,F8.1,3X,*METERS*,//,40X,*THE HORIZONTAL EDDY
      2 DIFFUSIVITY IS*,F10.1,3X,*SQ METERS/SEC*,//,40X,*THE
      3 VERTICAL EDDY DIFFUSIVITY IS*,F10.3,3X,*SQ METERS/SEC*
      4 ,//,40X,*THE TIME STEP USED IS*,F8.1,3X,*SEC*,//,40X,
      5 *THE BACKGROUND CO CONCENTRATION IS*,F8.1,3X,*MICRO
      6 GRAMS/CUBIC METER*,//,40X,*THE EDDY DIFFUSIVITY FOR
      7 ZERO ADVECTION IS*,F10.1,3X,*SQ METERS/SEC*)
C   INPUT DATA
       READ 1,L,KH,DT,BG,KZ,KM
       READ 3,NH,NPH,NB,ND
       READ 1,(S(I),I = 1,NB)
       READ 1,(TD(I),I = 1,24)
C   INITIALIZE CONCENTRATION FOR NODES
       DO 2 I = 1,NB
       CN(I) = BG
   2   C(I) = 0.
C   LOOP FOR NUMBER OF DAYS SIMULATED
       DO 7 J = 1,ND
C   INPUT DATA
       READ 1,(H(I),I = 1,24)
       READ 1,(U(I),I = 1,24)
```

```
      READ 1,(ALPHA(I),I = 1,24)
      READ 10,(NWQ(I),I = 1,24)
      READ 1,(RHOX(I),I = 1,24)
      READ 1,(RHOY(I),I = 1,24)
      PRINT 31,NPH
      PRINT 32,L,KH,KZ,DT,BG,KM
C    INITIALIZE CONCENTRATION FOR BACKGOUND NODES
      DO 5 I = 1,50
    5 CO(I) = BG
      VD = KH/L
C    LOOP FOR NUMBER OF HOURS
      DO 4 K = 1,NH
C    CHECK FOR ZERO CONVECTION CASE
      IF (U(K) .EQ. 0.) GO TO 11
      THETA = U(K)*DT/(4.*L)
      BETA = VD/U(K)
C    DETERMINATION OF COEFFICIENTS FOR MATRIX
      CALL UPDATE (THETA,BETA,K)
      CALL CCEFF (NB,K)
      GO TO 12
   11 PHI = KM*DT/(2.*L*L)
C    DETERMINATION OF COEFFICIENTS FOR ZERO CONVECTION CASE
      CALL ADVOF (PHI,NB)
C    INVERSION OF MATRIX
   12 CALL MATRIX (10,NB,NB,1,X,NB,DX,0,0,0)
C    GROUND LEVEL CONCENTRATION CONTRIBUTION DUE TO
C    LOGARITHMIC VERTICAL DISTRIBUTION
      DO 9 I = 1,NB
      GLC(I) = S(I)*1.E6*TD(K)*(ALOG(H(K))-1.)/
    1    (L*L*KZ*3600.*1150.)
    9 CONTINUE
C    LOOP FOR NUMBER OF TIME STEPS PER HOUR
      DO 18 M = 1,NPH
      IF (U(K) .EQ. 0.) GO TO 13
      IF (K .EQ. 1) GO TO 6
C    CALCULATION OF CONCENTRATION OF BACKGROUND NODES WHEN
C    WIND DIRECTION CHANGES QUADRANTS
      CALL CCBC (BG,K)
C    CALCULATION OF CONSTANTS MATRIX
    6 CALL CONST (L,NB,K)
      GO TO 14
C    CALCULATION OF CONSTANTS MATRIX FOR ZERO CONVECTION CASE
   13 CALL CONVOF (PHI,NB,K,L,DT)
C    MULTIPLICATION OF INVERSE TIMES CONSTANTS TO GET
C     CONCENTRATIONS
   14 CALL MATRIX (20,NB,NB,1,X,NB,Z,NB,C,NB)
C    ACTUAL GROUND LEVEL CONCENTRATIONS DETERMINATION
C     FOR EACH NODE
      DO 23 I = 1,NB
      PPM(M,I) = C(I)/1150. + GLC(I)
   23 CN(I) = C(I)
```

```
18 CONTINUE
   ANGLE = 57.3*ALPHA(K)
   PRINT 28,H(K),U(K),ANGLE,K
   PRINT 29
   DO 25 I = 1,NB
   PRINT 24,I,(PPM(M,I),M=1,NPH)
25 CONTINUE
4  CONTINUE
7  CONTINUE
   STOP
   END
   SUBROUTINE UPDATE (THETA,BETA,K)
   DIMENSION TD(24),H(24),U(24),ALPHA(24),NWQ(24),RHOX(24),
  1    RHOY(24),S(156),X(156,156),CN(156),Z(156),CC(50)
   COMMON A1,A2,A3,A4,A5,A6,B1,B2,B3,B4,B5,B6,B7,B8,B9,
  1    B10,B11,B12,B13,B14,B15,B16,B17,B18,B19,B20,B21,B22,
  2    B23,B24,TD,H,U,ALPHA,NWQ,RHOX,RHOY,S,X,CN,Z,CO
   A1 = 1./THETA + 8.*BETA + (4.*RHOX(K)-2.)*COS(ALPHA(K)) +
  1    (4.*RHOY(K)-2.)*SIN(ALPHA(K))
   A2 = 1./THETA - 8.*BETA - (4.*RHOX(K)-2.)*COS(ALPHA(K)) -
  1    (4.*RHOY(K)-2.)*SIN(ALPHA(K))
   A3 = (2.-2.*RHOX(K))*COS(ALPHA(K)) - 2.*BETA
   A4 = 2.*RHOX(K)*COS(ALPHA(K)) + 2.*BETA
   A5 = (2.-2.*RHOY(K))*SIN(ALPHA(K)) - 2.*BETA
   A6 = 2.*RHOY(K)*SIN(ALPHA(K)) + 2.*BETA
   B1 = 1./THETA + 2.*SIN(ALPHA(K)) + (4.*RHOX(K)-2.)*
  1 COS(ALPHA(K))  + 6.*BETA
   B2 = 1./THETA - 2.*SIN(ALPHA(K)) - (4.*RHOX(K)-2.)*
  1 COS(ALPHA(K))  - 6.*BETA
   B3 = 1./THETA + 2.*SIN(ALPHA(K)) + 2.*COS(ALPHA(K)) +
  1 4.*BETA
   B4 = 1./THETA - 2.*SIN(ALPHA(K)) - 2.*COS(ALPHA(K)) -
  1 4.*BETA
   B5 = 1./THETA + 2.*COS(ALPHA(K)) + (4.*RHOY(K)-2.)*
  1 SIN(ALPHA(K))  + 6.*BETA
   B6 = 1./THETA - 2.*COS(ALPHA(K)) - (4.*RHOY(K)-2.)*
  1 SIN(ALPHA(K))  - 6.*BETA
   B7 = 1./THETA + 2.*SIN(ALPHA(K)) - 2.*COS(ALPHA(K)) +
  1 4.*BETA
   B8 = 1./THETA - 2.*SIN(ALPHA(K)) + 2.*COS(ALPHA(K)) -
  1 4.*BETA
   B9 = 1./THETA - 2.*COS(ALPHA(K)) + (4.*RHOY(K)-2.)*
  1 SIN(ALPHA(K))  + 6.*BETA
   B10 = 1./THETA + 2.*COS(ALPHA(K)) - (4.*RHOY(K)-2.)*
  1 SIN(ALPHA(K))  - 6.*BETA
   B11 = 1./THETA - 2.*SIN(ALPHA(K)) + (4.*RHOX(K)-2.)*
  1 COS(ALPHA(K))  + 6.*BETA
   B12 = 1./THETA + 2.*SIN(ALPHA(K)) - (4.*RHOX(K)-2.)*
  1 COS(ALPHA(K))  - 6.*BETA
   B13 = 1./THETA - 2.*SIN(ALPHA(K)) - 2.*COS(ALPHA(K)) +
  1 4.*BETA
```

```
      B14 = 1./THETA + 2.*SIN(ALPHA(K)) + 2.*COS(ALPHA(K)) -
     1   4.*BETA
      B15 = 1./THETA - 2.*SIN(ALPHA(K)) + 2.*COS(ALPHA(K)) +
     1   4.*BETA
      B16 = 1./THETA + 2.*SIN(ALPHA(K)) - 2.*COS(ALPHA(K)) -
     1   4.*BETA
      B17 = 2.*SIN(ALPHA(K)) + 2.*BETA
      B18 = 2.*SIN(ALPHA(K)) - 2.*BETA
      B19 = 2.*COS(ALPHA(K)) + 2.*BETA
      B20 = 2.*COS(ALPHA(K)) - 2.*BETA
      B21 = A4
      B22 = A3
      B23 = A6
      B24 = A5
      RETURN
      END
      SUBROUTINE COEFF (NB,K)
      DIMENSION TD(24),H(24),U(24),ALPHA(24),NWO(24),RHOX(24),
     1   RHOY(24),S(156),X(156,156),CN(156),Z(156),CO(50)
      COMMON A1,A2,A3,A4,A5,A6,B1,B2,B3,B4,B5,B6,B7,B8,B9,
     1   B10,B11,B12,B13,B14,B15,B16,B17,B18,B19,B20,B21,B22,
     2   B23,B24,TD,H,U,ALPHA,NWQ,RHOX,RHOY,S,X,CN,Z,CO
      DO 1 I = 1,NB
      DO 1 J = 1,NB
      X(I,J) = 0.
1     CONTINUE
      DO 2 I = 1,NB
2     X(I,I) = A1
      DO 3 I = 1,143
      X(I,I+13) = A3
3     X(I+13,I) = -A4
      DO 4 J = 1,144,13
      JK = J+11
      DO 5 I = J,JK
      X(I,I+1) = A5
5     X(I+1,I) = -A6
4     CONTINUE
      IF (NWO(K) .EQ. 1 .OR. NWQ(K) .EQ. 2) GO TO 6
      IF (NWQ(K) .EQ. 3 .OR. NWQ(K) .EQ. 4) GO TO 7
6     DO 8 I = 26,143,13
      X(I,I) = B1
      X(I,I-13) = -B21
      X(I,I-1) = -B17
      X(I,I+13) = B22
8     CONTINUE
      GO TO 10
7     DO 9 I = 14,131,13
      X(I,I) = B11
      X(I,I-13) = -B21
      X(I,I+1) = B18
      X(I,I+13) = B22
```

```
 9  CONTINUE
10  IF (NWQ(K) .EQ. 1 .OR. NWQ(K) .EQ. 4) GO TO 11
    IF (NWQ(K) .EQ. 2 .OR. NWQ(K) .EQ. 3) GC TO 12
11  DO 13 I = 145,155
    X(I,I) = B5
    X(I,I-1) = -B23
    X(I,I-13) = -B19
    X(I,I+1) = B24
13  CONTINUE
    GO TC 15
12  DO 14 I = 2,12
    X(I,I) = B9
    X(I,I-1) = -B23
    X(I,I+13) = B20
    X(I,I+1) = B24
14  CONTINUE
15  IF (NWQ(K) .EQ. 1) GO TO 16
    IF (NWQ(K) .EO. 2) GO TO 17
    IF (NWC(K) .EQ. 3) GO TO 18
    IF (NWQ(K) .EQ. 4) GO TC 19
16  X(13,12) = -B17
    X(13,13) = B1
    X(13,26) = B22
    X(156,143) = -B19
    X(156,155) = -B17
    X(156,156) = B3
    X(144,131) = -B19
    X(144,144) = B5
    X(144,145) = B24
    GO TO 20
17  X(1,1) = B9
    X(1,2) = B24
    X(1,14) = B20
    X(13,12) = -B17
    X(13,13) = B7
    X(13,26) = B20
    X(156,143) = -B21
    X(156,155) = -B17
    X(156,156) = B1
    GO TO 20
18  X(144,131) = -B21
    X(144,144) = B11
    X(144,145) = B18
    X(1,1) = B13
    X(1,2) = B18
    X(1,14) = B20
    X(13,12) = -B23
    X(13,13) = B9
    X(13,26) = B20
    GO TO 20
19  X(156,143) = -B19
```

```
      X(156,155) = -B23
      X(156,156) = B5
      X(144,131) = -B19
      X(144,144) = B15
      X(144,145) = B18
      X(1,1) = B11
      X(1,2) = B18
      X(1,14) = B22
  20 RETURN
     END
     SUBROUTINE ADVOF (PHI,NB)
     DIMENSION TD(24),H(24),U(24),ALPHA(24),NWQ(24),RHOX(24),
    1    RHOY(24),S(156),X(156,156),CN(156),Z(156),CO(50)
     COMMON A1,A2,A3,A4,A5,A6,B1,B2,B3,B4,B5,B6,B7,B8,B9,
    1    B10,B11,B12,B13,B14,B15,B16,B17,B18,B19,B20,B21,B22,
    2    B23,B24,TD,H,U,ALPHA,NWQ,RHOX,RHOY,S,X,CN,Z,CO
     F1 = PHI
     F2 = 1. + 2.*PHI
     F3 = 1. + 3.*PHI
     F4 = 1. + 4.*PHI
     DO 1 I = 1,NB
     DO 1 J = 1,NB
     X(I,J) = 0.
   1 CONTINUE
     DO 2 I = 1,NB
   2 X(I,I) = F4
     DO 3 I = 1,143
     X(I,I+13) = -F1
   3 X(I+13,I) = -F1
     DO 4 J = 1,144,13
     JK = J+11
     DO 5 I = J,JK
     X(I,I+1) = -F1
   5 X(I+1,I) = -F1
   4 CONTINUE
     X(1,1) = F2
     DO 6 I = 2,12
   6 X(I,I) = F3
     X(13,13) = F2
     DO 7 I = 14,131,13
   7 X(I,I) = F3
     DO 8 I = 26,143,13
   8 X(I,I) = F3
     X(144,144) = F2
     DO 9 I = 145,155
   9 X(I,I) = F3
     X(156,156) = F2
     RETURN
     END
     SUBROUTINE COBC (BG,K)
     DIMENSION TD(24),H(24),U(24),ALPHA(24),NWQ(24),RHOX(24),
```

```
1     RHOY(24),S(156),X(156,156),CN(156),CO(156),Z(156)
      COMMON A1,A2,A3,A4,A5,A6,B1,B2,B3,B4,B5,B6,B7,B8,B9,
1     B10,B11,B12,B13,B14,B15,B16,B17,B18,B19,B20,B21,B22,
2     B23,B24,TD,H,U,ALPHA,NWQ,RHOX,RHOY,S,X,CN,Z,CO
      DO 1 I = 1,50
      CO(I) = BG
1     CONTINUE
      IF (NWQ(K-1) .EQ. NWQ(K)) GO TO 2
      IF (NWQ(K-1) .EQ. 1) GO TO 3
      IF (NWQ(K-1) .EQ. 2) GO TO 4
      IF (NWQ(K-1) .EQ. 3) GO TO 5
      IF (NWQ(K-1) .EQ. 4) GO TO 6
3     IF (NWQ(K) .EQ. 2) GO TO 7
      IF (NWQ(K) .EQ. 4) GO TO 8
4     IF (NWQ(K) .EQ. 1) GO TO 9
      IF (NWQ(K) .EQ. 3) GO TO 8
5     IF (NWQ(K) .EQ. 2) GO TO 10
      IF (NWQ(K) .EQ. 4) GO TO 9
6     IF (NWQ(K) .EQ. 3) GO TO 7
      IF (NWQ(K) .EQ. 1) GO TO 10
7     DO 11 I = 38,50
      CO(I) = 2.*CN(I+106) - CN(I+93)
      IF (CO(I) .LT. BG) CO(I) = BG
11    CONTINUE
      GO TO 2
8     DO 12 I = 14,25
      MM = (I-13)*13
      CO(I) = 2.*CN(MM) - CN(MM-1)
      IF (CO(I) .LT. BG) CO(I) = BG
12    CONTINUE
      GO TO 2
9     DO 13 I = 1,13
      CO(I) = 2.*CN(I) - CN(I+13)
      IF (CO(I) .LT. BG) CO(I) = BG
13    CONTINUE
      GO TO 2
10    DO 14 I = 26,37
      MN = (I-25)*13 - 12
      CO(I) = 2.*CN(MN) - CN(MN+1)
      IF (CO(I) .LT. BG) CO(I) = BG
14    CONTINUE
2     RETURN
      END
      SUBROUTINE CONST (L,NB,K)
      DIMENSION TD(24),H(24),U(24),ALPHA(24),NWQ(24),RHOX(24),
1     RHOY(24),S(156),X(156,156),CN(156),CSS(156),Z(156),
2     CO(50)
      COMMON A1,A2,A3,A4,A5,A6,B1,B2,B3,B4,B5,B6,B7,B8,B9,
1     B10,B11,B12,B13,B14,B15,B16,B17,B18,B19,B20,B21,B22,
2     B23,B24,TD,H,U,ALPHA,NWQ,RHOX,RHOY,S,X,CN,Z,CO
      REAL L
```

```
      DO 1 I = 1,NB
      CSS(I) = S(I)*1.E6*TD(K)/(L*U(K)*H(K)*3600.)
1     CONTINUE
      Z(1) = CN(1)*A2-CN(14)*A3-CN(2)*A5+2.*CO(1)*A4
     1    +2.*CO(26)*A6+4.*CSS(1)
      DO 2 I = 2,12
2     Z(I) = CN(I)*A2-CN(I+13)*A3-CN(I+1)*A5+2.*CO(I)*A4
     1    +CN(I-1)*A6+4.*CSS(I)
      Z(13) = CN(13)*A2-CN(26)*A3-2.*CO(14)*A5+2.*CO(13)*A4
     1    +CN(12)*A6+4.*CSS(13)
      DO 3 I = 14,131,13
      LN = (I+12)/13 + 25
3     Z(I) = CN(I)*A2-CN(I+13)*A3-CN(I+1)*A5+CN(I-13)*A4
     1    +2.*CO(LN)*A6+4.*CSS(I)
      DO 4 J = 15,132,13
      JM = J+10
      DO 5 I = J,JM
5     Z(I) = CN(I)*A2-CN(I+13)*A3-CN(I+1)*A5+CN(I-13)*A4
     1    +CN(I-1)*A6+4.*CSS(I)
4     CONTINUE
      DO 6 I = 26,143,13
      LM = I/13 + 13
6     Z(I) = CN(I)*A2-CN(I+13)*A3-2.*CO(LM)*A5+CN(I-13)*A4
     1    +CN(I-1)*A6+4.*CSS(I)
      Z(144) = CN(144)*A2-2.*CO(38)*A3-CN(145)*A5+CN(131)*A4+
     1    2.*CO(37)*A6+4.*CSS(144)
      DO 7 I = 145,155
7     Z(I) = CN(I)*A2-2.*CO(I-106)*A3-CN(I+1)*A5+CN(I-13)*A4+
     1    CN(I-1)*A6+4.*CSS(I)
      Z(156) = CN(156)*A2-2.*CO(50)*A3-2.*CO(25)*A5+CN(143)*A4+
     1    CN(155)*A6+4.*CSS(156)
      IF (NWQ(K) .EQ. 1 .OR. NWQ(K) .EQ. 2) GO TO 8
      IF (NWQ(K) .EQ. 3 .OR. NWQ(K) .EQ. 4) GC TO 9
8     DO 10 I = 26,143,13
10    Z(I) = CN(I)*B2+CN(I-13)*B21+CN(I-1)*B17-CN(I+13)*B22
     1    +4.*CSS(I)
      GO TO 12
9     DO 11 I = 14,131,13
11    Z(I) = CN(I)*B12+CN(I-13)*B21-CN(I+1)*B18-CN(I+13)*B22
     1    +4.*CSS(I)
12    IF (NWQ(K) .EQ. 1 .OR. NWQ(K) .EQ. 4) GO TO 13
      IF (NWQ(K) .EQ. 2 .OR. NWQ(K) .EQ. 3) GO TO 14
13    DO 15 I = 145,155
15    Z(I) = CN(I)*B6+CN(I-1)*B23+CN(I-13)*B19-CN(I+1)*B24
     1    +4.*CSS(I)
      GO TO 17
14    DO 16 I = 2,12
16    Z(I) = CN(I)*B10+CN(I-1)*B23-CN(I+13)*B20-CN(I+1)*B24
     1    +4.*CSS(I)
17    IF (NWQ(K) .EQ. 1) GO TO 18
      IF (NWQ(K) .EQ. 2) GO TO 19
```

```
      IF (NWO(K) .EQ. 3) GO TO 20
      IF (NWQ(K) .EQ. 4) GO TO 21
 18 Z(13) = CN(13)*B2+2.*CO(13)*B21+CN(12)*B17-CN(26)*B22
    1   +4.*CSS(13)
      Z(156) = CN(156)*B4+CN(155)*B17+CN(143)*B19+4.*CSS(156)
      Z(144) = CN(144)*B6+2.*CO(37)*B23+CN(131)*B19
    1   -CN(145)*B24+4.*CSS(144)
      GO TO 22
 19 Z(1) = CN(1)*B10+2.*CO(26)*B23-CN(14)*B20-CN(2)*B24
    1   +4.*CSS(I)
      Z(13) = CN(13)*B8+CN(12)*B17-CN(26)*B20+4.*CSS(13)
      Z(156) = CN(156)*B2+CN(143)*B21+CN(155)*B17
    1   -2.*CO(50)*B22+4.*CSS(156)
      GO TO 22
 20 Z(144) = CN(144)*B12+CN(131)*B21-CN(145)*B18
    1   -2.*CO(38)*B22+4.*CSS(144)
      Z(1) = CN(1)*B14-CN(14)*B20-CN(2)*B18+4.*CSS(1)
      Z(13) = CN(13)*B10+CN(12)*B23-CN(26)*B20-2.*CO(14)*B24+
    1   4.*CSS(13)
      GO TO 22
 21 Z(156) = CN(156)*B6+CN(155)*B23+CN(143)*B19
    1   -2.*CO(25)*B24+4.*CSS(156)
      Z(144) = CN(144)*B16+CN(131)*B19-CN(145)*B18+4.*CSS(144)
      Z(1) = CN(1)*B12+2.*CO(1)*B21-CN(2)*B18-CN(14)*B22
    1   +4.*CSS(1)
 22 RETURN
      END
      SUBROUTINE CONVOF (PHI,NB,K,L,DT)
      DIMENSION TD(24),H(24),U(24),ALPHA(24),NWQ(24),RHOX(24),
    1   RHOY(24),S(156),X(156,156),CN(156),ZWS(156),Z(156),
    2   CO(50)
      COMMON A1,A2,A3,A4,A5,A6,B1,B2,B3,B4,B5,B6,B7,B8,B9,
    1   B10,B11,B12,B13,B14,B15,B16,B17,B18,B19,B20,B21,B22,
    2   B23,B24,TD,H,U,ALPHA,NWQ,RHOX,RHOY,S,X,CN,Z,CO
      REAL L
      F1 = PHI
      F5 = 1. - 2.*PHI
      F6 = 1. - 3.*PHI
      F7 = 1. - 4.*PHI
      DO 1 I = 1,NB
      ZWS(I) = S(I)*1.E6*TD(K)*DT/(L*L*H(K)*3600.)
  1 CONTINUE
      Z(1) = CN(1)*F5+F1*(CN(2)+CN(14))+ZWS(1)
      DO 2 I = 2,12
  2 Z(I) = CN(I)*F6+F1*(CN(I-1)+CN(I+1)+CN(I+13))+ZWS(I)
      Z(13) = CN(13)*F5+F1*(CN(12)+CN(26))+ZWS(13)
      DO 3 I = 14,131,13
  3 Z(I) = CN(I)*F6+F1*(CN(I-13)+CN(I+1)+CN(I+13))+ZWS(I)
      DO 4 J = 15,132,13
      JM = J+10
      DO 5 I = J,JM
```

```
5   Z(I) = CN(I)*F7+F1*(CN(I-13)+CN(I+1)+CN(I+13)+CN(I-1))
    1    +ZWS(I)
4   CONTINUE
    DO 6 I = 26,143,13
6   Z(I) = CN(I)*F6+F1*(CN(I-13)+CN(I-1)+CN(I+13))+ZWS(I)
    Z(144) = CN(144)*F5+F1*(CN(131)+CN(145))+ZWS(144)
    DO 7 I = 145,155
7   Z(I) = CN(I)*F6+F1*(CN(I-13)+CN(I-1)+CN(I+1))+ZWS(I)
    Z(156) = CN(156)*F5+F1*(CN(143)+CN(155))+ZWS(156)
    RETURN
    END
```

```
C                 M I C R O - - M O D E L     P R O G R A M
      PROGRAM SUBM ( INPUT,OUTPUT )
      DIMENSION TD(24),H(24),U(24),ALPHA(24),RHOX(24),
     1    RHOY(24),X(64,64),CN(64),C(64),Z(64),PPM(6,64),
     2    C1(24),C2(24),C3(24),C4(24),S(64),GLC(64)
      COMMON A1,A2,A3,A4,A5,A6,TD,H,U,ALPHA,RHOX,RHOY,C1,C2,
     1    C3,C4,X,CN,Z,S
      REAL L,KH,KZ,KM
    1 FORMAT (8E10.0)
    2 FORMAT (4I10)
    4 FORMAT (1H1,//////////////,35X,*TUCSON   URBAN   AIR
     1 POLLUTION    SUB-MODEL    FOR   CARBON   MONOXIDE*,///,
     2 52X,*A   24   HOUR   DAY   IS   SIMULATED*,////,25X,*THE
     3 MIXING   HEIGHT,   WIND   SPEED,   AND WIND   DIRECTION
     4 ARE   VARIED   ON   AN   HOURLY   BASIS*,////////,29X,*THE
     5 AVERAGE   CONCENTRATION   FOR   EACH   BOX   IS   PRINTED
     6 OUT*,I4,2X,*TIMES PER HOUR*)
    5 FORMAT (//////,40X,*THE   SQUARE BASE DIMENSION OF EACH
     1 BOX IS*,F8.1,3X,*METERS*,//,40X,*THE HORIZONTAL EDDY
     2 DIFFUSIVITY IS*,F10.1,3X,*SQ METERS/SEC*,//,40X,*THE
     3 VERTICAL EDDY DIFFUSIVITY IS*,F10.3,3X,*SQ METERS/SEC*
     4 ,//,40X,*THE TIME STEP USED IS*,F8.1,3X,*SEC*,//,40X,
     5 *THE BACKGROUND CO CONCENTRATION IS*,F8.1,3X,*MICRO
     6 GRAMS/CUBIC METER*,//,40X,*THE EDDY DIFFUSIVITY FOR
     7 ZERO ADVECTION IS*,F10.1,3X,*SQ METERS/SEC*)
   14 FORMAT   (1H1,//,30X,*MIXING HEIGHT IS*,F7.1,3X,
     1 *METERS*,//,30X,*WIND SPEED IS*,F8.3,3X,*METERS/SEC*,
     2 //,30X,*WIND DIRECTION IS*,F10.1,3X,*DEGREES COUNTER
     3 CLOCKWISE W.R.T. THE EAST*,//,30X,*THIS IS HOUR *,I4,
     4 2X,*OF THE DAY*)
   15 FORMAT (///,15X,*BOX NUMBER*,33X,*CARBON MONOXIDE CON
     1 CENTRATION IN PPM*,//,33X,*INTERVAL 1*,10X,*2*,15X,
     2 *3*,15X,*4*,15X,*5*,15X,*6*,/)
   17 FORMAT (18X,I3,11X,F8.4,8X,F8.4,8X,F8.4,8X,F8.4,8X,
     1    F8.4,8X,F8.4,/)
C   INPUT DATA
      READ 1,L,KH,DT,BG,KZ,KM
      READ 2,NH,NPH,NB,NR
      READ 1,(S(I),I = 1,NB)
      READ 1,(TD(I),I = 1,24)
      READ 1,(H(I),I = 1,24)
      READ 1,(U(I),I = 1,24)
      READ 1,(ALPHA(I),I = 1,24)
      READ 1,(RHOX(I),I = 1,24)
      READ 1,(RHOY(I),I = 1,24)
      READ 1,(C1(I),I = 1,24)
      READ 1,(C2(I),I = 1,24)
      READ 1,(C3(I),I = 1,24)
      READ 1,(C4(I),I = 1,24)
C   INITIALIZE CONCENTRATION FOR NODES
      DO 3 I = 1,NB
```

```
          CN(I) = BG
       3  C(I) = 0.
          NI = NPH/5
          VD = KH/L
          PRINT 4,NI
          PRINT 5,L,KH,KZ,DT,BG,KM
C    LOOP FOR NUMBER OF HOURS
          DO 6 K = 1,NH
C    CHECK FOR ZERO CONVECTION CASE
          IF (U(K) .EQ. 0.) GO TO 7
          THETA = U(K)*DT/(4.*L)
          BETA = VD/U(K)
C    DETERMINATION OF COEFFICIENTS FOR MATRIX
          CALL COEFF (NB,K,THETA,BETA,NR)
          GO TO 8
       7  PHI = KM*DT/(2.*L*L)
C    DETERMINATION OF COEFFICIENTS FOR ZERO CONVECTION CASE
          CALL ADVOF (PHI,NB,NR)
C    INVERSION OF MATRIX
       8  CALL MATRIX (10,NB,NB,1,X,NB,DX,0,0,0)
C    GROUND LEVEL CONCENTRATION CONTRIBUTION DUE TO
C    LOGARITHMIC VERTICAL DISTRIBUTION
          DO 20 I = 1,NB
          GLC(I) = S(I)*1.E6*TD(K)*(ALOG(H(K))-1.)/
         1   (L*L*KZ*3600.*1150.)
      20 CONTINUE
C    LOOP FOR NUMBER OF TIME STEPS PER HOUR
          DO 9 M = 1,NPH
C    CHECK FOR ZERO CONVECTION CASE
          IF (U(K) .EQ. 0.) GO TO 10
C    CALCULATION OF CONSTANTS MATRIX
          CALL CONST (L,NB,K,NR)
          GO TO 11
C    CALCULATION OF CONSTANTS MATRIX FOR ZERO CONVECTION CASE
      10 CALL CONVOF (PHI,NB,K,L,DT,NR)
C    MULTIPLICATION OF INVERSE TIMES CONSTANTS TO GET
C        CONCENTRATIONS
      11 CALL MATRIX (20,NB,NB,1,X,NB,Z,NB,C,NB)
          DO 12 I = 1,NB
      12 CN(I) = C(I)
          IF ( MOD(M,5) .NE. 0.) GO TO 9
          KP = M/5
C    ACTUAL GROUND LEVEL CONCENTRATIONS DETERMINATION
C        FOR EACH NODE
          DO 13 I = 1,NB
      13 PPM(KP,I) = C(I)/1150.   + GLC(I)
       9  CONTINUE
          ANGLE = 57.3*ALPHA(K)
          PRINT 14,H(K),U(K),ANGLE,K
          PRINT 15
          DO 16 I = 1,NB
```

```
      PRINT 17,I,(PPM(J,I),J = 1,NI)
16 CONTINUE
6  CONTINUE
   STOP
   END
   SUBROUTINE COEFF (NB,K,THETA,BETA,NR)
   DIMENSION TD(24),H(24),U(24),ALPHA(24),RHOX(24),
  1    RHOY(24),X(64,64),CN(64),C(64),Z(64),PPM(6,64),
  2    C1(24),C2(24),C3(24),C4(24),S(64),GLC(64)
   COMMON A1,A2,A3,A4,A5,A6,TD,H,U,ALPHA,RHOX,RHOY,C1,C2,
  1    C3,C4,X,CN,Z,S
   A1 = 1./THETA + 8.*BETA + (4.*RHOX(K)-2.)*COS(ALPHA(K))
  1  + (4.*RHOY(K)-2.)*SIN(ALPHA(K))
   A2 = 1./THETA - 8.*BETA - (4.*RHOX(K)-2.)*COS(ALPHA(K))
  1  - (4.*RHOY(K)-2.)*SIN(ALPHA(K))
   A3 = (2.-2.*RHOX(K))*COS(ALPHA(K)) - 2.*BETA
   A4 = 2.*RHOX(K)*COS(ALPHA(K)) + 2.*BETA
   A5 = (2.-2.*RHOY(K))*SIN(ALPHA(K)) - 2.*BETA
   A6 = 2.*RHOY(K)*SIN(ALPHA(K)) + 2.*BETA
   DO 1 I = 1,NB
   DO 1 J = 1,NB
   X(I,J) = 0.
1  CONTINUE
   DO 2 I = 1,NB
2  X(I,I) = A1
   KG = NB - NR
   DO 3 I = 1,KG
   X(I,I+NR) = A3
3  X(I+NR,I) = -A4
   JA = NB - (NR - 1)
   DO 4 J = 1,JA,NR
   JK = J + (NR - 2)
   DO 5 I = J,JK
   X(I,I+1) = A5
5  X(I+1,I) = -A6
4  CONTINUE
   RETURN
   END
   SUBROUTINE ADVOF (PHI,NB,NR)
   DIMENSION TD(24),H(24),U(24),ALPHA(24),RHOX(24),
  1    RHOY(24),X(64,64),CN(64),C(64),Z(64),PPM(6,64),
  2    C1(24),C2(24),C3(24),C4(24),S(64),GLC(64)
   COMMON A1,A2,A3,A4,A5,A6,TD,H,U,ALPHA,RHOX,RHOY,C1,C2,
  1    C3,C4,X,CN,Z,S
   F1 = PHI
   F2 = 1. + 4.*PHI
   DO 1 I = 1,NB
   DO 1 J = 1,NB
   X(I,J) = 0.
1  CONTINUE
   DO 2 I = 1,NB
```

```
2   X(I,I) = F2
    KG = NB - NR
    DO 3 I = 1,KG
    X(I,I+NR) = -F1
3   X(I+NR,I) = -F1
    JA = NB - (NR - 1)
    DO 4 J = 1,JA,NR
    JK = J + (NR - 2)
    DO 5 I = J,JK
    X(I,I+1) = -F1
5   X(I+1,I) = -F1
4   CONTINUE
    RETURN
    END
    SUBROUTINE CONST (L,NB,K,NR)
    DIMENSION TD(24),H(24),U(24),ALPHA(24),RHOX(24),
   1    RHOY(24),X(64,64),CN(64),C(64),Z(64),PPM(6,64),
   2    C1(24),C2(24),C3(24),C4(24),S(64),GLC(64),CSS(64)
    COMMON A1,A2,A3,A4,A5,A6,TD,H,U,ALPHA,RHOX,RHOY,C1,C2,
   1    C3,C4,X,CN,Z,S
    REAL L
    DO 7 I = 1,NB
    CSS(I) = S(I)*1.E6*TD(K)/(L*U(K)*H(K)*3600.)
7   CONTINUE
    Z(1) = CN(1)*A2-CN(1+NR)*A3-CN(2)*A5+2.*C3(K)*A6
   1    +2.*C1(K)*A4+4.*CSS(1)
    KR = NR - 1
    DO 1 I = 2,KR
    Z(I) = CN(I)*A2-CN(I+NR)*A3-CN(I+1)*A5+CN(I-1)*A6
   1    +2.*C1(K)*A4+4.*CSS(I)
1   CONTINUE
    Z(NR) = CN(NR)*A2-CN(NR+NR)*A3-2.*C2(K)*A5+CN(NR-1)*A6
   1    +2.*C1(K)*A4+4.*CSS(NR)
    KA = NR + 1
    KB = NB - (2*NR - 1)
    DO 2 I = KA,KB,NR
    Z(I) = CN(I)*A2-CN(I+NR)*A3-CN(I+1)*A5+2.*C3(K)*A6
   1    +CN(I-NR)*A4+4.*CSS(I)
2   CONTINUE
    KC = NR + 2
    KD = NB - (2*NR - 2)
    DO 3 J = KC,KD,NR
    KE = NR - 3
    JM = J + KE
    DO 4 I = J,JM
4   Z(I) = CN(I)*A2-CN(I+NR)*A3-CN(I+1)*A5+CN(I-1)*A6
   1    +CN(I-NR)*A4+4.*CSS(I)
3   CONTINUE
    KF = 2*NR
    KG = NB - NR
    DO 5 I = KF,KG,NR
```

```
 5  Z(I) = CN(I)*A2-CN(I+NR)*A3-2.*C2(K)*A5+CN(I-1)*A6
 1    +CN(I-NR)*A4+4.*CSS(I)
    JA = NB - (NR - 1)
    Z(JA) = CN(JA)*A2-2.*C4(K)*A3-CN(JA+1)*A5+2.*C3(K)*A6
 1     +CN(JA-NR)*A4+4.*CSS(JA)
    JB = NB - (NR - 2)
    JC = NB - 1
    DO 6 I = JB,JC
 6  Z(I) = CN(I)*A2-2.*C4(K)*A3-CN(I+1)*A5+CN(I-1)*A6
 1     +CN(I-NR)*A4+4.*CSS(I)
    Z(NB) = CN(NB)*A2-2.*C4(K)*A3-2.*C2(K)*A5+CN(NB-1)*A6
 1     +CN(NB-NR)*A4+4.*CSS(NB)
    RETURN
    END
    SUBROUTINE CONVOF (PHI,NB,K,L,DT,NR)
    DIMENSION TD(24),H(24),U(24),ALPHA(24),RHOX(24),
 1     RHOY(24),X(64,64),CN(64),C(64),Z(64),PPM(6,64),
 2     C1(24),C2(24),C3(24),C4(24),S(64),GLC(64),ZWS(64)
    COMMON A1,A2,A3,A4,A5,A6,TD,H,U,ALPHA,RHOX,RHOY,C1,C2,
 1     C3,C4,X,CN,Z,S
    REAL L
    F1 = PHI
    F3 = 1. - 4.*PHI
    DO 7 I = 1,NB
    ZWS(I) = S(I)*1.E6*TD(K)*DT/(L*L*H(K)*3600.)
 7  CONTINUE
    Z(1) = CN(1)*F3+F1*(CN(2)+CN(1+NR)+2.*C3(K)+2.*C1(K))
 1     +ZWS(1)
    KR = NR - 1
    DO 1 I = 2,KR
 1  Z(I) = CN(I)*F3+F1*(CN(I+1)+CN(I+NR)+CN(I-1)+2.*C1(K))
 1     +ZWS(I)
    Z(NR) = CN(NR)*F3+F1*(2.*C2(K)+CN(NR+NR)+CN(NR-1))
 1     +2.*C1(K)*F1+ZWS(NR)
    KA = NR + 1
    KB = NB - (2*NR - 1)
    DO 2 I = KA,KB,NR
    Z(I) = CN(I)*F3+F1*(CN(I+1)+CN(I+NR)+CN(I-NR)+2.*C3(K))
 1     +ZWS(I)
 2  CONTINUE
    KC = NR + 2
    KD = NB - (2*NR - 2)
    DO 3 J = KC,KD,NR
    KE = NR - 3
    JM = J + KE
    DO 4 I = J,JM
 4  Z(I) = CN(I)*F3+F1*(CN(I+1)+CN(I+NR)+CN(I-NR)+CN(I-1))
 1     +ZWS(I)
 3  CONTINUE
    KF = 2*NR
    KG = NB - NR
```

```
      DO 5 I = KF,KG,NR
5     Z(I) = CN(I)*F3+F1*(2.*C2(K)+CN(I+NR)+CN(I-NR)+CN(I-1))
1        +ZWS(I)
      JA = NB - (NR - 1)
      Z(JA) = CN(JA)*F3+F1*(2.*C4(K)+CN(JA+1)+2.*C3(K))
1        +CN(JA-NR)*F1+ZWS(JA)
      JB = NB - (NR - 2)
      JC = NB - 1
      DO 6 I = JB,JC
6     Z(I) = CN(I)*F3+F1*(2.*C4(K)+CN(I+1)+CN(I-1)+CN(I-NR))
1        +ZWS(I)
      Z(NB) = CN(NB)*F3+F1*(2.*C4(K)+2.*C2(K)+CN(NB-1))
1        +CN(NB-NR)*F1+ZWS(NB)
      RETURN
      END
```

APPENDIX C

LISTING OF MEASURED DATA

Listings of all the carbon monoxide data taken at locations 1, 2, and 3 are presented here. The CO levels at these locations were measured in the morning and evening times given in Table 7.1.

LOCATION 1

Date	CO(ppm)	Date	CO(ppm)	Date	CO(ppm)
9-10-74		9-20-74		10-3-74	
pm	1.0	am	3.5	am	1.2
9-11-74		pm	2.0	pm	1.0
am	1.0	9-23-74		10-4-74	
pm	1.2	am	0.7	am	1.8
9-12-74		pm	2.0	pm	1.0
am	1.5	9-24-74		10-7-74	
pm	1.7	am	0.5	am	2.2
9-13-74		pm	1.3	pm	2.0
am	2.1	9-25-74		10-8-74	
pm	1.8	pm	1.1	am	2.5
9-16-74		9-26-74		pm	4.1
am	1.2	pm	2.5	10-9-74	
pm	1.0	9-27-74		am	2.1
9-17-74		am	1.6	pm	0.8
am	2.5	9-30-74		10-10-74	
pm	1.8	am	2.5	am	1.1
9-18-74		pm	1.3	pm	0.5
am	3.0	10-1-74		10-11-74	
pm	1.7	am	2.2	am	0.9
9-19-74		pm	2.0	pm	1.2
am	2.5	10-2-74		10-14-74	
pm	2.1	am	3.9	am	1.3
		pm	3.0	pm	1.7
10-15-74		10-29-74		11-11-74	
am	1.2	am	2.2	am	2.1
pm	1.1	pm	1.0	pm	1.0
10-16-74		10-30-74		11-12-74	
am	2.0	am	1.1	am	6.5
pm	4.8	pm	2.0	pm	2.8
10-17-74		10-31-74		11-13-74	
am	1.4	am	2.2	am	4.0
pm	1.0	pm	1.3	pm	2.9
10-18-74		11-1-74		11-14-74	
am	1.8	am	2.8	am	1.5
pm	1.8	pm	2.0	pm	4.0
10-21-74		11-4-74		11-15-74	
am	2.1	am	2.8	am	3.3
10-22-74		pm	1.5	pm	2.5
pm	2.0	11-5-74		11-18-74	
10-23-74		am	2.1	am	1.8
am	1.8	pm	1.5	pm	2.0

Date	CO(ppm)	Date	CO(ppm)	Date	CO(ppm)
10-23-74					
pm	1.2	11-6-74		11-19-74	
10-24-74		am	2.3	am	2.2
am	2.5	pm	1.0	pm	1.3
pm	4.0	11-7-74		11-21-74	
10-25-74		am	1.2	pm	6.5
am	3.5	pm	5.3	11-22-74	
10-28-74		11-8-74		am	3.0
am	2.8	am	1.9	pm	0.5
pm	1.0	pm	3.0		
11-25-74					
am	1.5	12-9-74		12-20-74	
pm	2.8	am	0.8	am	3.2
11-26-74		pm	0.5	pm	1.0
am	2.0	12-10-74		12-23-74	
pm	1.3	am	2.0	am	0.2
11-27-74		pm	2.8	pm	0.2
am	0.8	12-11-74		12-24-74	
pm	1.0	am	1.0	am	1.5
11-29-74		pm	1.2	pm	3.8
am	1.5	12-12-74		12-26-74	
pm	5.0	am	1.5	am	0.5
12-2-74		pm	2.0	pm	1.2
am	3.2	12-13-74		12-27-74	
pm	1.5	am	2.5	am	0.7
12-3-74		pm	1.0	pm	1.0
am	3.8	12-16-74		12-30-74	
pm	4.1	am	1.7	am	2.0
12-4-74		pm	1.0	pm	2.2
am	0.5	12-17-74		12-31-74	
pm	1.5	am	6.2	am	2.2
12-5-74		12-18-74		pm	0.3
am	1.0	pm	0.8	1-2-75	
pm	0.8	12-19-74		am	2.0
12-6-74		am	2.0	pm	0.8
am	3.1	pm	1.5		
pm	0.5				
1-3-75		1-20-75		1-31-75	
am	1.0	am	3.0	am	2.3
pm	1.0	pm	1.0	pm	1.2
1-6-75		1-21-75		2-3-75	
am	3.0	am	2.5	am	2.1
pm	1.0	pm	0.8	pm	0.7

Date	CO(ppm)	Date	CO(ppm)	Date	CO(ppm)
1-7-75		1-22-75		2-4-75	
am	5.7	am	1.0	am	1.5
pm	0.5	pm	0.5	pm	1.8
1-8-75		1-23-75		2-5-75	
am	0.3	am	2.0	am	1.2
pm	4.0	pm	1.0	pm	1.0
1-9-75		1-24-75		2-6-75	
am	0.3	am	1.5	am	1.8
pm	0.5	pm	1.0	pm	1.0
1-10-75		1-27-75		2-7-75	
am	1.0	am	0.8	am	1.7
pm	1.8	pm	1.2	pm	2.0
1-13-75		1-28-75		2-10-75	
am	2.8	am	1.0	am	1.5
1-14-75		pm	0.8	pm	1.0
am	3.3	1-29-75		2-11-75	
pm	1.2	am	3.7	am	1.7
1-17-75		pm	1.7	pm	0.7
am	2.2	1-30-75		2-12-75	
		am	1.3	am	2.0
		pm	0.5	pm	0.8
2-13-75		2-26-75			
am	2.7	am	1.5		
2-14-75		pm	0.8		
pm	0.8	2-27-75			
2-17-75		am	1.0		
am	0.5	pm	1.0		
pm	1.0	2-28-75			
2-18-75		am	2.0		
am	1.0				
pm	0.7				
2-19-75					
am	1.8				
pm	0.8				
2-20-75					
am	1.0				
pm	0.7				
2-21-75					
am	1.5				
2-24-75					
am	1.2				
pm	0.9				
2-25-75					
am	1.8				
pm	0.6				

LOCATION 2

Date	CO(ppm)	Date	CO(ppm)	Date	CO(ppm)
9-10-74		9-20-74		9-30-74	
pm	1.9	am	2.1	am	1.2
9-11-74		pm	1.1	pm	2.9
am	1.3	9-23-74		10-1-74	
pm	1.5	am	0.2	am	1.9
9-12-74		pm	0.5	pm	1.2
am	2.5	9-24-74		10-2-74	
pm	2.2	am	0.5	am	2.0
9-13-74		pm	0.8	pm	1.5
am	2.0	9-25-74		10-3-74	
9-15-74		am	1.0	am	2.0
pm	1.0	pm	1.3	pm	1.9
9-16-74		9-26-74		10-4-74	
am	2.0	am	2.1	am	1.0
pm	1.2	pm	2.6	pm	2.0
9-17-74		9-27-74		10-6-74	
am	2.2	am	1.8	am	1.2
pm	1.1	pm	1.6	pm	1.1
9-18-74		9-28-74		10-7-74	
am	1.5	am	1.7	am	2.0
pm	1.8	pm	1.4	pm	4.2
9-19-74		9-29-74		10-8-74	
am	1.7	am	1.5	am	5.8
pm	1.4	pm	2.0	pm	2.0
10-9-74		10-22-74		11-4-74	
am	1.5	am	1.7	am	3.0
pm	1.0	pm	2.8	pm	2.2
10-10-74		10-23-74		11-5-74	
am	0.8	am	2.3	am	6.2
pm	1.1	pm	2.0	pm	2.1
10-11-74		10-24-74		11-6-74	
am	2.0	am	3.8	am	3.5
pm	1.1	pm	1.6	pm	2.0
10-14-74		10-25-74		11-7-74	
am	2.1	am	1.3	am	4.2
pm	2.2	pm	1.5	pm	1.0
10-15-74		10-28-74		11-8-74	
am	1.1	am	2.1	am	1.2
pm	1.0	pm	1.2	11-9-74	
10-16-74		10-29-74		am	2.0
am	1.6	am	2.1	11-10-74	
pm	1.0	10-30-74		pm	3.2
10-17-74		am	1.5	11-11-74	
am	1.1	pm	1.2	am	3.0
pm	1.3			pm	3.1

Date	CO(ppm)	Date	CO(ppm)	Date	CO(ppm)
10-18-74		10-31-74			
		am	2.8	11-12-74	
pm	1.3	pm	4.0	am	4.0
10-21-74		11-1-74		11-13-74	
am	1.0	am	2.2	am	3.0
pm	1.5	pm	3.5	pm	7.5
11-14-74		11-27-74		12-11-74	
am	1.5	am	1.8	am	2.5
pm	8.6	pm	2.0	pm	3.0
11-15-74		11-29-74		12-12-74	
am	1.0	am	1.5	am	1.8
pm	4.0	12-2-74		pm	2.8
11-18-74		am	3.0	12-16-74	
am	1.8	pm	6.0	am	3.8
pm	4.0	12-3-74		pm	3.5
11-19-74		am	4.0	12-17-74	
am	2.0	pm	8.0	am	1.1
pm	3.0	12-4-74		pm	2.5
11-20-74		am	1.0	12-18-74	
am	1.3	pm	1.5	am	1.2
pm	1.0	12-5-74		pm	3.0
11-21-74		am	2.0	12-19-74	
am	1.1	pm	2.0	am	8.8
pm	9.5	12-6-74		pm	2.7
11-22-74		am	1.7	12-20-74	
pm	1.8	pm	1.5	am	2.1
11-25-74		12-9-74		12-22-74	
am	1.0	am	0.2	pm	2.0
pm	4.0	pm	0.5	12-23-74	
11-26-74		12-10-74		am	0.5
am	2.8	am	2.0	12-26-74	
pm	4.5	pm	2.3	am	2.0
12-27-74		1-9-75		1-22-75	
am	7.2	am	0.5	am	0.8
pm	1.5	pm	0.8	pm	0.3
12-30-74		1-10-75		1-23-75	
am	1.7	am	3.5	am	1.0
pm	1.9	pm	1.9	pm	2.5
12-31-74		1-13-75		1-24-75	
am	3.2	am	2.2	am	2.8
1-1-75		pm	1.9	pm	2.0
pm	1.1	1-14-75		1-27-75	
1-2-75		am	7.0	am	1.5
am	2.6	pm	2.0	pm	1.3
pm	1.1				

Date	CO(ppm)	Date	CO(ppm)	Date	CO(ppm)
		1-15-75		1-28-75	
1-3-75		am	3.8	am	1.8
am	6.9	pm	2.5	pm	1.8
pm	3.2	1-16-75		1-29-75	
1-6-75		am	3.5	am	2.8
am	2.1	pm	2.5	pm	3.7
pm	1.8	1-17-75		1-30-75	
1-7-75		am	2.0	am	1.2
am	5.3	pm	2.0	1-31-75	
pm	3.7	1-20-75		am	2.5
1-8-75		am	1.0	pm	3.0
am	6.5	pm	2.0	2-3-75	
pm	0.8	1-21-75		am	3.7
		am	2.0	pm	1.1
		pm	1.0		
2-4-75		2-18-75			
am	2.0	am	3.1		
pm	1.0	pm	0.9		
2-5-75		2-19-75			
am	1.8	am	3.0		
pm	2.0	pm	1.2		
2-6-75		2-20-75			
am	3.5	am	3.5		
pm	1.0	pm	1.1		
2-7-75		2-21-75			
am	2.0	am	2.5		
2-10-75		pm	0.8		
pm	1.0	2-24-75			
2-11-75		am	3.2		
pm	1.3	pm	1.5		
2-12-75		2-25-75			
am	3.1	am	2.2		
pm	2.0	pm	2.0		
2-13-75		2-26-75			
am	1.7	am	2.7		
pm	1.5	pm	1.2		
2-14-75		2-27-75			
am	0.3	am	2.1		
2-17-75					
pm	1.0				

LOCATION 3

Date	CO(ppm)	Date	CO(ppm)	Date	CO(ppm)
9-17-74		9-30-74		10-10-74	
am	1.0	am	1.0	am	0.8
pm	0.8	pm	0.9	pm	0.9
9-18-74		10-1-74		10-11-74	
am	1.1	am	1.0	am	1.2
pm	9.5	pm	1.0	pm	1.6
9-19-74		10-2-74		10-14-74	
am	1.0	am	1.0	am	9.0
pm	1.0	pm	1.0	pm	1.7
9-20-74		10-3-74		10-15-74	
am	4.7	am	0.8	am	0.9
pm	1.5	pm	1.0	pm	0.9
9-23-74		10-4-74		10-16-74	
am	0.7	am	1.8	am	1.0
9-24-74		pm	1.1	pm	0.9
am	1.0	10-7-74		10-17-74	
pm	0.8	am	6.2	am	1.7
9-25-74		pm	9.7	10-18-74	
pm	0.8	10-8-74		am	0.8
9-26-74		am	1.0	pm	1.0
am	0.9	pm	1.5	10-21-74	
pm	1.0	10-9-74		am	1.2
9-27-74		am	1.5	pm	0.8
am	1.0	pm	1.8	10-22-74	
pm	1.8			am	1.0
				pm	1.2
10-24-74		11-6-74		11-19-74	
am	1.0	am	1.0	am	1.1
pm	1.2	pm	4.8	pm	4.0
10-25-74		11-7-74		11-20-74	
am	1.5	am	0.5	am	0.5
pm	1.3	pm	0.2	pm	0.8
10-28-74		11-8-74		11-21-74	
am	0.8	am	1.8	am	0.5
pm	1.1	pm	2.1	pm	2.8
10-29-74		11-12-74		11-22-74	
am	1.2	am	0.9	am	2.0
10-30-74		pm	0.5	pm	1.3
am	1.0	11-13-74		11-25-74	
pm	1.0	am	0.9	am	1.0
10-31-74		pm	1.8	pm	3.5
am	1.0	11-14-74		11-26-74	
pm	1.7	am	0.5	am	1.0
		pm	1.5	pm	3.0

Date	CO(ppm)	Date	CO(ppm)	Date	CO(ppm)
11-1-74					
am	2.0	11-15-74		11-27-74	
pm	2.8	am	1.5	am	0.8
11-4-74		pm	3.0	pm	2.2
am	2.0	11-18-74		11-29-74	
11-5-74		am	2.0	am	1.0
am	1.1	pm	1.8	pm	1.2
pm	2.2			12-2-74	
				am	1.5
				pm	2.0
12-3-74		12-19-74		1-8-75	
am	0.5	am	1.2	pm	0.5
pm	1.1	pm	3.7	1-9-75	
12-4-74		12-20-74		am	2.1
am	1.0	am	0.8	1-10-75	
pm	1.5	pm	1.2	am	1.2
12-5-74		12-26-74		pm	4.8
am	1.3	am	1.1	1-13-75	
pm	2.2	pm	1.1	am	1.1
12-11-74		12-27-74		pm	1.2
am	0.8	am	1.0	1-14-75	
pm	8.0	pm	2.3	am	1.0
12-12-74		12-30-74		pm	2.8
am	1.8	am	1.0	1-15-75	
pm	2.0	pm	6.0	am	0.5
12-13-74		1-2-75		pm	8.0
am	1.0	am	1.0	1-17-75	
pm	4.2	pm	1.8	am	2.8
12-16-74		1-3-75		pm	1.0
am	1.2	am	1.1	1-21-75	
pm	2.1	pm	1.3	am	0.5
12-17-74		1-6-75		pm	0.8
am	0.5	am	1.2	1-22-75	
pm	3.0	pm	3.0	am	0.2
12-18-74		1-7-75		pm	0.5
am	1.0	am	2.8		
pm	1.2	pm	1.4		
1-23-75		2-7-75			
am	0.5	am	0.7		
pm	4.2	pm	3.5		
1-24-75		2-10-75			
am	1.2	am	0.6		
pm	2.1	2-21-75			
1-27-75		am	2.0		
am	0.7	pm	3.5		
pm	0.9				

Date	CO(ppm)	Date	CO(ppm)	Date	CO(ppm)
		2-24-75			
1-28-75		am	2.0		
am	1.2	pm	3.3		
pm	4.8	2-25-75			
1-29-75		am	0.5		
am	1.8	pm	3.3		
pm	2.2	2-27-75			
1-30-75		pm	1.0		
am	1.0	2-28-75			
pm	1.1	am	0.8		
1-31-75		pm	1.5		
am	0.8				
pm	0.8				
2-3-75					
pm	0.8				
2-6-75					
am	1.2				
pm	0.8				

REFERENCES

Angell, J. K., P. W. Allen, and E. A. Jessup, "Mesoscale Relative Diffusion Estimates from Tetroon Flights," Journal of Appl. Met., Vol. 10, pp. 43-46, Feb. 1971.

"Automobile Exhaust Emission Surveillance," prepared by CALSPAN Corporation for EPA, Report No. APTD-1544, May 1973.

Beard, R., and G. A. Wertheim, "Behavorial Impairment Associated with Small Doses of Carbon Monoxide," Journal of Public Health, 57, 2012 (1967).

Bergstrom, R. W., and R. Viskanta, "Theoretical Study of the Thermal Structure and Dispersion in Polluted Urban Atmosphere," Dissertation of Bergstrom, Purdue University, Lafayette, Indiana, August 1972.

Bowne, N. E., "A Simulation Model for Air Pollution over Connecticut," Journal of Air Pollution Control Assoc., Vol. 19, No. 8, pp. 570-574, August, 1969.

Briley, W. R., "A Numerical Calculation of Laminar Separation Bubbles Using the Navier Stokes Equations," Report J110614-1, United Aircraft Research Laboratories, East Hartford, Connecticut, 1970.

Carson, W. W., and A. F. Emery, "Evaluation of Use of the Finite Element Method in Computation of Temperature," ASME paper #69-WA/HT 38, November 1969.

Chaudry, F. H., and J. E. Cermak, "Simulation of Flow and Diffusion Over an Urban Complex," Conference on Air Pollution Meteorology, American Met. Soc., 1971.

Clarke, J. F., "A Simple Diffusion Model for Calculating Point Concentrations from Multiple Sources," Journal of Air Pollution Control Assoc., Vol. 14, p. 347, 1964.

Cohen, S. I., M. Deane, and J. R. Goldsmith, "Carbon Monoxide and Survival from Myocardial Infarction," Arch. Environ. Health, Vol. 19, 1969.

"Compilation of Air Pollution Emission Factors," United States Environmental Protection Agency, Report No. AP-42, Section 3, April 1973.

"Controlling Emissions of Carbon Monoxide within Pima County, Arizona," prepared by the Pima County Air Pollution Control District, September 10, 1973.

Croke, E. J., J. E. Carson, F. L. Clark, A. S. Kennedy, and J. J. Roberts, "City of Chicago Air Pollution System Model," Argonne National Laboratory, Report No. ANL/ES-CC-001, February 1968.

Croke, E. J., and J. J. Roberts, "Chicago Air Pollution Systems Analysis Program," Final Report, Argonne National Laboratory, No. ANL/ES-CC-009, February 1971.

Dinman, B. D., "Palhophysiologic Determinants of Community Air Quality Standards for Carbon Monoxide," Symposium on Air Quality Criteria, University of Michigan, June 1968.

"Effects of Chronic Exposure to Low Levels of Carbon Monoxide on Human Health, Behavior, and Performance," National Academy of Sciences and National Academy of Engineering, 1969.

Eschenroeder, A. Q., and J. R. Martinez, "Concepts and Application of Photochemical Smog-Models," Photochemical Smog and Ozone Reactions, Advances in Chemistry Series, Editor, Robert J. Gould, pp. 58-100, 1972.

Federal Register, Vol. 36, No. 67, p. 6680, April 7, 1971a.

Federal Register, Vol. 36, No. 84, p. 8186, April 30, 1971b.

Federal Register, Vol. 37, No. 105, pp. 10844-10845, May 31, 1972.

Federal Register, Vol. 38, No. 53, pp. 7323-7324, March 20, 1973a.

Federal Register, Vol. 38, No. 78, p. 10119, April 24, 1973b.

Federal Register, Vol. 38, No. 120, Part II, p. 16550, June 22, 1973c.

Federal Register, Vol. 38, No. 135, Part II, p. 18942, July 16, 1973d.

Federal Register, Vol. 38, No. 206, Part I, p. 29608, October 26, 1973e.

Federal Register, Vol. 38, No. 231, p. 33373, December 3, 1973f.

Fensterstock, J. C., and R. K. Fankhauser, "Thanksgiving 1966 Air Pollution Episode in the Eastern United States," EPA Report AP-45, April 1970.

Frenkiel, F. N., "Atmospheric Pollution and Zoning in an Urban Area," Scientific Monthly, Vol. 82, No. 4, pp. 194-203, 1956.

Gilmore, T. M., and T. R. Hanna,"Regional Monitoring of Ambient Air Carbon Monoxide in Fairbanks, Alaska," Journal of Air Pollution Control Assoc., Vol. 24, No. 11, November 1974.

Heffter, J. L., "The Variation of Horizontal Diffusion Parameters with Time for Travel Periods of One Hour or Longer," Journal of Appl. Met., Vol. 4, pp. 153-156, February 1965.

Hexter, A. C., and J. R. Goldsmith, "Carbon Monoxide: Association of Community Air Pollution with Mortality," Science, Vol. 172, 1971.

Hilst, G. R., "An Air Pollution Model of Connecticut," Proceeding of the IBM Scientific Computing Symposium on Water and Air Resource Management, IBM Data Processing Div., pp. 251-274, October 1967.

Hilst, G. R., "Sensitivities of Air Quality Predictions to Input Errors and Uncertainties," Proceeding of Symposium on Multiple-Source Urban Diffusion Models, Editor, Arthur C. Stern, Publication No. AP-86, U.S. EPA, pp. 7-1 to 7-23, 1970.

Holzworth, G., "Mixing Heights, Wind Speeds, and Potential for Urban Air Pollution Throughout the Contiguous United States," EPA Report No. AP-101, January 1972.

Johnson, W. B., F. L. Ludwig, and A. E. Moon, "Development of a Practical Multipurpose Urban Diffusion Model for Carbon Monoxide," Proceeding of Symposium on Multiple-Source Urban Diffusion Models, Editor, Arthur C. Stern, Publication No. AP-86, U.S. EPA, pp. 5-1 to 5-38, 1970.

Koogler, J. B., R. S. Shottes, A. L. Davis, and C. I. Harding, "A Multivariable Model for Atmospheric Dispersion Predictions," Journal of Air Pollution Control Assoc., Vol. 17, No. 4, pp. 211-214, April 1967.

Krishnamurti, R., "A Survey of Laboratory and Theoretical Studies of Convection," notes from D. D. Gray and R. Johnson, July 28, 1972.

Leavitt, J. M., "Meteorological Considerations in Air Quality Planning," Journal of Air Pollution Control Assoc., Vol. 10, p. 246, 1960.

MacCracken, M. C., T. V. Crawford, K. R. Peterson, and J. B. Knox, "Initial Application of a Multi-box Air Pollution Model to the San Francisco Bay Area," Proc. Joint Automatic Control Conf., Stanford University, Stanford, California (1972).

Mahoney, J. R., and B. A. Egan, "A Mesoscale Numerical Model of Atmospheric Transport Phenomena in Urban Areas," Proceeding of the Second International Clean Air Congress, paper #ME 32E, 1971.

Miller, M. E., and G. C. Holzworth, "An Atmospheric Diffusion Model for Metropolitan Areas," Journal of Air Pollution Control Assoc., Vol. 17, No. 1, pp. 46-50, January 1967.

Neiburger, M., "Meteorological Aspects of Oxidation Type Air Pollution," The Atmosphere and the Sea in Motion, Bert Bolin, Editor, Rockefeller Inst. Press, pp. 158-169, 1959.

Pasquill, F., Atmospheric Diffusion, D. Van Nostrand Company Ltd., 1962.

Patankar, S. V., "Numerical Predictions of Three-dimensional Flows," Imperial College Mech. Eng. Dept., London, Report EF/TN/A/46, June 1972.

Pooler, F., "A Prediction Model of Mean Urban Pollution for Use with Standard Wind Roses," Int. Journal Air and Water Pollution, Vol. 4, pp. 199-211, 1961.

Ralston, A., A First Course in Numerical Analysis, McGraw-Hill, 1965.

Randerson, D., "Temporal Changes in Horizontal Diffusion Parameters of a Single Nuclear Debris Cloud," Journal of Appl. Met., Vol. 11, pp. 670-673, June 1972.

Reiquam, H., "An Atmospheric Transport and Accumulation Model for Airsheds," Atmos. Environment, Vol. 4, pp. 233-247, May 1970.

Reiquam, H., "Preliminary Trial of a Box Model in the Oslo Airshed," Second International Clean Air Congress Proceedings, paper #ME32A, 1971.

Roache, P. J., Computational Fluid Dynamics, Hermosa Publishers, 1972.

Robbins, R. C., K. M. Borg, and E. Robinson, "Carbon Monoxide in the Atmosphere," Journal of Air Pollution Control Assoc., Vol. 18, No. 2, February 1968.

Roberts, J. J., E. J. Croke, and A. S. Kennedy, "An Urban Dispersion Model," Proceeding of Symposium on Multi-Source Urban Diffusion Models, Arthur C. Stern, editor, U.S. EPA Publication No. AP-86, pp. 6-1 to 6-72, 1970.

Roberts, J. J., J. E. Norco, A. S. Kennedy, and E. J. Croke, "A Model for Simulation of Air Pollution Transients," Proceeding of the Second International Clean Air Congress, paper No. ME39A, 1971.

Roth, P. M., S. D. Reynolds, P. J. Roberts, and J. H. Seinfeld, "Development of a Simulation Model for Estimating Ground Level Concentrations of Photochemical Pollutants," Systems Applications, Inc., Final Report on Contract CPA70-148, 1971.

Scarborough, J. B., Numerical Mathematical Analysis, Johns Hopkins Press, 5th Edition, 1962.

Seinfeld, J. H., S. D. Reynolds, and P. M. Roth, "Simulation of Urban Air Pollution," Photochemical Smog and Ozone Reactions, Advances in Chemistry Series, Robert F. Gould, editor, pp. 58-100, 1972.

Sellars, A. L., "Prediction of Atmospheric Carbon Monoxide Concentrations from an Urban Traffic Line Source," Master's Report, University of Arizona, Tucson, May 1974.

Shieh, L. J., B. Davidson, and J. P. Friend, "A Model of Diffusion in Urban Atmospheres: SO_2 in Greater New York," Proceeding of Symposium on Multiple-Source Urban Diffusion Models, Arthur C. Stern, editor, U.S. EPA Publication No. AP-86, pp. 10-1 to 10-38, 1970.

Shir, C. C., and L. J. Shieh, "A Generalized Urban Air Pollution Model and Its Application to the Study of SO_2 Distributions in the St. Louis Metropolitan Area," Journal of Appl. Met, Vol. 13, No. 2, pp. 185-204, March 1974.

Sklarew, R. C., A. J. Fabrick, and J. E. Prager, "Mathematical Modeling of Photochemical Smog Using the PICK Method," Journal of Air Pollution Control Assoc., Vol. 22, No. 11, pp. 865-869, November 1972.

Slade, D. H., Meteorology and Atomic Energy, Atomic Energy Commission Publication TID-24190, July 1968.

Smith, M. E., Advance Papers for Intern. Symp. Chem. Reactions Lower-Upper Atmosphere, San Francisco, Stanford Research Institute, pp. 273-286, 1961.

Spalding, D. B., "A Novel Finite-Difference Formulation for Differential Expressions Involving both First and Second Derivatives," Int. J. Num. Methods in Eng., 4, 1972.

"State of Arizona Air Pollution Control Implementation Plan -- Transportation Control Strategies," prepared by the Arizona State Department of Health-Division of Air Pollution Control for EPA, September 1973.

"Tucson Area Transportation Study," prepared by City of Tucson, County of Pima, and State of Arizona, Vol. 1, 1960.

Turner, D. B., "A Diffusion Model for an Urban Area," Journal of Appl. Met., Vol. 3, pp. 83-91, February 1964

Turner, D. B., Workbook of Atmospheric Dispersion Estimates, Public Health Service Publication No. 999-AP-26, U. S. Dept. of Health, Education and Welfare, 1969.

Wayne, L. G., R. Danchich, M. Weisbund, A. Kokin, and A. Stein, "Modeling Photochemical Smog on a Computer for Decision-Making," Journal of Air Pollution Control Assoc., Vol. 21, p. 334, 1971.

Wolsko, T. D., M. T. Matthies, and R. E. Wendell, "Transportation Air Pollution Emissions Handbook," Argonne National Laboratory, Report No. ANL/ES-15, July 1972.